

# Impact of wireless link quality across communication layers

## Proefschrift

ter verkrijging van de graad van doctor  
aan de Technische Universiteit Delft,  
op gezag van de Rector Magnificus Prof.ir. K.C.A.M. Luyben,  
voorzitter van het College voor Promoties,  
in het openbaar te verdedigen op dinsdag 26 oktober 2010 om 10.00 uur

door

Jinglong Zhou  
elektrotechnisch ingenieur  
geboren te Wuhan, Hubei provincie, China.

Dit proefschrift is goedgekeurd door de promotor:  
Prof.dr.ir. I.G.M.M. Niemegeers

Samenstelling promotiecommissie:

Rector Magnificus,	Voorzitter
Prof.dr.ir. I.G.M.M. Niemegeers,	Technische Universiteit Delft, promotor
Prof.dr.ir. S.M. Heemstra de Groot	Technische Universiteit Delft
Prof.dr.ir. P. Van Mieghem	Technische Universiteit Delft
Prof.dr.ir. R.E. Kooij,	Technische Universiteit Delft
Prof.dr.ir. O.Yarovyi,	Technische Universiteit Delft
Prof.dr.ir. E.R. Fledderus,	Technische Universiteit Eindhoven

ISBN 978-94-6113-025-9

Keywords: Wireless communication, link quality estimation, rate adaptation, power saving, link quality based routing, performance evaluation.

This research was supported by the Dutch Ministry of Economic Affairs through the project PNP2008 under the Freeband Communication Impulse of the technology programme.

Copyright © 2010 by Jinglong Zhou

All rights reserved. No part of the material protected by this copyright notice may be reproduced or transmitted in any form or by any means, electronic or mechanical, including photocopying, recording or by any information storage and retrieval system, without written permission from the author.

Printed in The Netherlands

# Acknowledgements

This thesis describes the research work that I performed at Wireless and Mobile Communications group at Delft University of Technology under Prof. Ignas Niemegeers. It is his wide area knowledge, broad interest, thoughtful guidance that give me insight in the research process. It is his kind encouragement that inspire me to solve one after one problems. It is his all perspective support that give me great help in all my scientifically publications. His is the supervisor for both my M.Sc thesis work and Ph.D thesis work, his help for this thesis is invaluable. Further, I would like to thank the committee members for spending time and providing feedback to this thesis. I also would like to acknowledge Dr. Geert Heijenk for his valuable comments and discussion for this thesis.

I would like to say thanks also to all my colleagues with whom I have had many interesting and fruitful discussions, with whom I have wrote my conference and journal papers. In relation to this thesis, I am especially grateful for the cooperation with Martin Jacobson, Przemyslaw Pawelczak, Ertan Onur, Venkatesha Prasad, Vijay S. Rao, Malohat Ibrohimovna, Sonia Heemstra de Groot, Cheng Guo and Anthony Lo. I would also like to thanks Marjon Verkaik-Vonk who help me so much during this four years period. In addition, there are also a couple of M.Sc. students who contributed to this work by doing their final projects with me. I would like to acknowledge them here: Ziyuan Liu, Xin Zhang, Jiazen Hao. Last but not least, I also would like to acknowledge my good friends Vikko Smit and Emile Broesterhuizen who helped me in translating the propositions and thesis summary into Dutch. Javier Hernandez who helped me in designing the cover of the thesis.

Thanks to Freeband PNP2008 project, which gave me research funding and provided me an interesting and promising research area, I had the opportunity to work with many excellent researchers. I have gain a lot during the project meetings and discussions.

Finally, I want to thank my big family in China. Especially to my mother, who is always supportive to me. To my wife, who is always the one with

whom I would like to share all my happiness. Also to all my friends in delft, such as Sha Xia, Jie Zhong, Xueli An, Yanying Gu, Weidong Lu, SiYu Tang, Yi Wang, Dajie Liu, Qin Tang, Jing Wang and Huijuan Wang, Antonio.J.P.S.Madureira who give me a colorful life during my study in Delft.

Xiexie, Thank you, Bedankt!

Jinglong Zhou  
Delft



To the people who have helped me.





# Contents

<b>1</b>	<b>Introduction</b>	<b>5</b>
1.1	A Brief History of Wireless Communication . . . . .	5
1.1.1	Past . . . . .	5
1.1.2	Modern wireless technologies . . . . .	6
1.1.3	Wireless technology in future . . . . .	8
1.2	Motivation Scenarios . . . . .	9
1.2.1	Wireless networks . . . . .	9
1.2.2	High throughput scenario . . . . .	10
1.2.3	Power saving scenario . . . . .	11
1.2.4	Mobile hot spot scenario . . . . .	12
1.3	Problem Formulation . . . . .	13
1.3.1	Link quality estimation in wireless links . . . . .	14
1.3.2	Link quality based transmission power adaptation . . . . .	14
1.3.3	Link quality based data rate adaptation . . . . .	15
1.3.4	Link quality based route selection . . . . .	16
1.3.5	Transport layer performance with different link quality	16
1.3.6	Application layer performance with different link quality	17
1.4	Research Challenges . . . . .	18
1.4.1	Observational challenges . . . . .	18
1.4.2	Mechanism design challenges . . . . .	19
1.4.3	Performance enhancement and optimization challenges	20
1.5	Thesis Overview . . . . .	20
1.6	Chapter Summary and Discussion . . . . .	21
<b>2</b>	<b>Background on Wireless Link Quality</b>	<b>23</b>
2.1	Introduction . . . . .	23
2.2	Common Wireless Link Quality Indicators . . . . .	24
2.2.1	Hello packet . . . . .	24
2.2.2	Broadcast packet . . . . .	25
2.2.3	Unicast packet . . . . .	25
2.2.4	Data packet . . . . .	26

2.2.5	Signal to noise ratio . . . . .	26
2.3	Preliminary Measurement Result . . . . .	26
2.3.1	IEEE 802.11 channel characteristic measurement . . . . .	26
2.3.2	IEEE 802.15.4 channel characteristic measurement . . . . .	32
2.3.3	HSDPA channel quality traces . . . . .	37
2.4	Chapter Summary and Discussion . . . . .	41
<b>3</b>	<b>Wireless Link Quality Estimation</b>	<b>43</b>
3.1	Introduction . . . . .	43
3.2	Related Work . . . . .	44
3.2.1	Packet-Based LQE . . . . .	45
3.2.2	BER-Based LQE . . . . .	46
3.2.3	SNR-Based LQE . . . . .	46
3.2.4	Combined Methods of SNR- and Packet-Based LQE . . . . .	48
3.3	Our Proposed Linearization Method . . . . .	48
3.3.1	Proposed linearization LQE mechanism . . . . .	49
3.3.2	Experimental evaluation . . . . .	51
3.4	Our Proposed SNR Mapping Method . . . . .	56
3.4.1	Proposed method . . . . .	56
3.4.2	Measurement scenarios . . . . .	59
3.4.3	Properties of SNR profile . . . . .	63
3.4.4	Accuracy of proposed LQE . . . . .	70
3.5	Mathematical Analyzing . . . . .	74
3.5.1	Proposed SNR map-based LQE: General overview . . . . .	74
3.5.2	System model . . . . .	75
3.5.3	Estimation time analysis . . . . .	75
3.5.4	LQE efficiency analysis . . . . .	76
3.5.5	Overall LQE efficiency . . . . .	78
3.5.6	Numerical evaluation . . . . .	78
3.6	Chapter Summary and Discussion . . . . .	78
<b>4</b>	<b>Power Adaptation in MAC Layer</b>	<b>83</b>
4.1	Introduction . . . . .	83
4.2	Related Work . . . . .	85
4.3	Energy Emission and Consumption Measurements . . . . .	86
4.4	PDR-Based Transmission Power Control . . . . .	90
4.4.1	Initialization phase . . . . .	92
4.4.2	Updating phase . . . . .	92
4.5	Experimental Setup . . . . .	93
4.5.1	IEEE 802.11 test-bed . . . . .	93
4.5.2	IEEE 802.15.4 test-bed . . . . .	94

4.5.3	Experiment methodology . . . . .	94
4.6	Performance Evaluation . . . . .	96
4.6.1	Energy emission reduction . . . . .	96
4.6.2	Energy consumption reduction . . . . .	105
4.6.3	Trade-off between energy emission and consumption . .	108
4.7	Summary and Discussion . . . . .	110
<b>5</b>	<b>Rate Adaptation in MAC Layer</b>	<b>111</b>
5.1	Introduction . . . . .	111
5.2	Related Work . . . . .	112
5.3	Adapting the Existing Protocol . . . . .	114
5.3.1	Experiment setup . . . . .	114
5.3.2	Measurement results . . . . .	115
5.4	Novel Link Quality Based Rate Adaptation . . . . .	118
5.4.1	Improved rate selection mechanism . . . . .	118
5.4.2	New rate adaptation mechanism performance evaluation	120
5.5	Chapter Summary and Discussion . . . . .	123
<b>6</b>	<b>Link Quality Based Routing</b>	<b>125</b>
6.1	Introduction . . . . .	125
6.2	Related Work . . . . .	126
6.2.1	Routing metrics . . . . .	126
6.2.2	Routing protocol: OLSR . . . . .	127
6.2.3	Previous studies . . . . .	127
6.3	Data Rate Determined Route Selection . . . . .	128
6.4	Linearization LQE Based Routing . . . . .	130
6.4.1	Fixed data rate . . . . .	130
6.4.2	Adaptive data rate . . . . .	138
6.5	SNR Mapping Based Routing . . . . .	141
6.5.1	Implementation . . . . .	141
6.5.2	Measurement scenarios . . . . .	142
6.5.3	Measurement results . . . . .	142
6.6	Chapter Summary and Discussion . . . . .	144
<b>7</b>	<b>Transport Layer Evaluation</b>	<b>147</b>
7.1	Introduction . . . . .	147
7.2	Related Work . . . . .	148
7.3	Network Architecture and Simulation Setup . . . . .	149
7.3.1	Integrated network architecture and protocols . . . . .	149
7.3.2	TCP packet transmission procedure . . . . .	150
7.3.3	Simulation model . . . . .	152

7.4	HSDPA TCP Single Flow Throughput . . . . .	152
7.4.1	Impact of TCP window size . . . . .	152
7.4.2	TCP over integrated network . . . . .	154
7.4.3	File downloading . . . . .	158
7.5	HSDPA TCP Multiple Flow Throughput . . . . .	160
7.5.1	Unfairness in the HSDPA and IEEE 802.11 integrated network . . . . .	160
7.5.2	Proposed scheduling mechanism . . . . .	162
7.5.3	The optimal parameter selection . . . . .	162
7.5.4	Fairness index improvement . . . . .	165
7.6	Chapter Summary and Discussion . . . . .	167
<b>8</b>	<b>Application Layer Evaluation</b>	<b>169</b>
8.1	Introduction . . . . .	169
8.2	Related Work . . . . .	170
8.3	Multi-hop Cellular Networks and MPEG-4 . . . . .	171
8.3.1	System architecture . . . . .	171
8.3.2	MPEG-4 . . . . .	171
8.4	Simulation Models . . . . .	171
8.4.1	Integrated network module in ns-2 . . . . .	171
8.4.2	MPEG-4 video evaluation tool-set . . . . .	173
8.4.3	Simulation setup . . . . .	174
8.4.4	Video contents . . . . .	175
8.5	Simulation Results . . . . .	175
8.5.1	Single MPEG-4 flow . . . . .	176
8.5.2	Multiple MPEG-4 flows . . . . .	189
8.6	Chapter Summary and Discussion . . . . .	192
<b>9</b>	<b>Conclusion</b>	<b>195</b>
9.1	How Far We Have Gone . . . . .	195
9.2	Main Results and Contributions . . . . .	196
9.2.1	Link quality based optimization for the end-to-end performance . . . . .	196
9.2.2	Link quality based optimization for the power saving .	197
9.2.3	Cellular multi-hop network with different link quality .	198
9.3	Future Work . . . . .	199
<b>A</b>	<b>IEEE 802.11 Test-bed</b>	<b>203</b>
A.1	Indoor test-bed . . . . .	203
A.1.1	Hardware . . . . .	203
A.1.2	Software . . . . .	203

A.1.3 Scenarios . . . . .	206
A.2 Outdoor test-bed . . . . .	208
A.2.1 Hardware . . . . .	208
A.2.2 Software . . . . .	208
A.2.3 Scenarios . . . . .	208
<b>B IEEE 802.15.4 Test-bed</b>	<b>211</b>
B.1 Hardware . . . . .	211
B.2 Software . . . . .	211
B.3 Scenario . . . . .	212
<b>C UMTS/HSDPA Simulator Structure</b>	<b>213</b>
C.1 IEEE 802.11 Model . . . . .	214
C.2 UMTS Model . . . . .	215
C.3 New Mobile Gateway . . . . .	215
C.4 Addressing and Routing . . . . .	217
C.5 Gateway Discovery Protocol . . . . .	219
<b>D Abbreviations</b>	<b>221</b>
<b>Bibliography</b>	<b>225</b>
<b>Publications by the Author</b>	<b>237</b>
<b>Curriculum Vitae</b>	<b>241</b>



# Summary

Nowadays, wireless networks are used in most of the applications with radio technologies being used in all kinds of wireless networks. In all wireless links, the transmitted packets can be lost. How to identify the quality of a certain wireless link and achieve the best delivery performance over a certain wireless network is an open issue. In this thesis, the performance of wireless mesh network, wireless sensor network and cellular network have been investigated by the method of measurements, simulations and mathematical model. Several novel algorithms also have been proposed. We have proposed two mechanisms to estimate wireless links where better performance is achieved compared to the traditional algorithms. The achievements lead to a higher end-to-end throughput (faster information delivery) for the IEEE 802.11 networks. Meanwhile, an energy saving and interference reducing mechanism for wireless mesh and sensor networks has been proposed and validated which can dramatically save energy in those wireless networks. Impact of wireless link quality on heterogeneous cellular and ad hoc networks has been evaluated and the results could be used for Telecom operators for the cellular networks optimization. Test-beds for IEEE 802.11 and IEEE 802.15.4 have been built and the 3G cellular networks have been studied via simulations.

We looked at the impact of the wireless link quality to the MAC layer for the IEEE 802.11 and IEEE 802.15.4; the impact of the wireless link quality to the IEEE 802.11 network layer. To understand the link quality characteristics of these two radios, we carried out many measurement experiments with various indoor and outdoor scenarios. The measurement methods and results are presented in Chapter 2. To achieve accurate link quality estimation, we proposed two estimation methods for different scenarios in Chapter 3. In Chapter 4, we used accurate link quality information to determine the packet transmission power level in the IEEE 802.11 and IEEE 802.15.4's MAC layer and the measurement results show that the energy consumption and interference reduces. The accurate link quality estimation methods are further used in data rate adaptation in the IEEE 802.11's MAC

layer (Chapter 5) and route selection in the IEEE 802.11’s network layer (Chapter 6). The measurements using IEEE 802.11 devices show tremendous performance enhancement. Our algorithms and results can be useful for all kinds of protocol designs for IEEE 802.11 and IEEE 802.15.4 networks.

Furthermore, we look at the end-to-end performance of the cellular multi-hop network which comprises of two different wireless networks, 3G UMTS/HSDPA network and IEEE 802.11 network in Chapter 7. When multiple TCP flows exist in the cellular multi-hop network, different flows may not share the cellular network’s resources fairly due to the fact that each flow may have different topology and wireless link quality. We have proposed a weighted scheduling method which obviously alleviates this unfairness. In Chapter 8, a typical video streaming traffic, MPEG-4 is used to evaluate the end-to-end performance over the cellular multi-hop network. The results show that wireless link quality also has great impact on the end-to-end performance of MPEG-4 over the cellular multi-hop network. Our result can be used by the telecom operators to optimize the UMTS/HSDPA system for the cellular multi-hop scenario. We conclude our thesis and suggest the future research directions in Chapter 9.

*Jinglong Zhou*

# Samenvatting (Summary in Dutch)

Tegenwoordig worden draadloze netwerken gebruikt in de meeste toepassingen met radio-technologieën die gebruikt worden in allerlei soorten draadloze netwerken. In alle draadloze overdrachten kan pakketverlies optreden. Hoe bepaal je de kwaliteit van een bepaalde draadloze verbinding en bereik je de beste prestaties bij een bepaald draadloos netwerk is een onbeantwoorde vraag. In dit proefschrift zijn de prestaties van het draadloze mesh-netwerk, draadloze sensor netwerk en mobiele netwerk onderzocht door te meten, simuleren en een wiskundig model te formuleren. Verschillende nieuwe algoritmen zijn hieruit voorgekomen. Zo zijn we hier ook tot twee nieuwe mechanismen gekomen om te bepalen of deze draadloze verbindingen beter functioneren ten opzichte van netwerken met de traditionele algoritmen. Deze bevindingen leiden tot een hogere end-to-end doorvoer (snellere levering van informatie) voor de IEEE 802.11-netwerken. Ondertussen wordt er een energiebesparend en antistorings mechanisme gebruikt wat de verbruikte energie dramatisch kan verminderen in deze draadloze netwerken. De invloed van de kwaliteit van draadloze netwerken op heterogene mobiele en ad hoc netwerken zijn geëvalueerd en de resultaten hiervan kunnen gebruikt worden om draadloze netwerken van Telecom operators te optimalizeren. Testbedden voor IEEE 802.11 en IEEE 802.15.4 zijn gemaakt en 3G netwerken zijn bestudeerd in simulaties.

We hebben de invloed van de kwaliteit van draadloze verbindingen op de MAC laag van het IEEE 802.11 en IEEE 802.15.4 bekeken en de invloed van de kwaliteit op de IEEE 802.11 netwerk laag. Om de karakteristieken van de verbindingskwaliteit op deze twee radio's te kunnen begrijpen, hebben we verschillende metingen uitgevoerd binnen- en buitenshuis. De methoden en resultaten van deze metingen worden gepresenteerd in Hoofdstuk 2. Om een nauwkeurige schatting van de verbindingskwaliteit te verkrijgen hebben we twee bepalingsmethoden voorgesteld voor verschillende scenario's in Hoofdstuk 3. In Hoofdstuk 4 wordt deze informatie gebruikt om het vermogen van

de pakketoverdracht in IEEE 802.11 en IEEE 802.15.4's MAC laag te bepalen en uit meetresultaten blijken energieverbruik en verstoringen te verminderen. De nauwkeurige bepalings methoden worden vervolgens gebruikt voor het aanpassen van de overdrachts snelheid in IEEE 802.11's MAC laag (Hoofdstuk 5) en route bepaling in IEEE 802.11's netwerk laag (Hoofdstuk 6). De metingen met de IEEE 802.11 apparaten tonen ontzettende prestatie verbeteringen. Onze algoritmen en resultaten kunnen nuttig zijn voor alle soorten protocolontwerpen voor IEEE 802.11 en IEEE 802.15.4 netwerken.

Verder kijken we naar de end-to-end prestaties van het mobiele multi-hop netwerk dat bestaat uit twee verschillende draadloze netwerken, 3G UMTS / HSDPA-netwerk en IEEE 802.11-netwerk in Hoofdstuk 7. Als er meerdere TCP stromen voorkomen in het mobiele multi-hop netwerk, kunnen verschillende stromen mogelijk niet de middelen van het mobiele netwerk goed gebruiken door het feit dat elke stroom een andere topologie en verbindingskwaliteit kan hebben. We hebben een gewogen rooster methode die deze oneerlijkheid er uit licht. In Hoofdstuk 8, een typisch videotostream verkeer, wordt MPEG-4 gebruikt om de end-to-end prestaties te evalueren op het mobiele multi-hop netwerk. De resultaten tonen dat draadloze verbindingen kwaliteit ook een grote invloed heeft op de end-to-end prestatie van MPEG-4 over het mobiele multi-hop netwerk. Onze resultaten kunnen gebruikt worden door Telecom operators om het UMTS/HSDPA systeem voor mobiele multi-hop scenario te optimaliseren. In Hoofdstuk 9 sluiten we de stelling en geven we aanwijzingen voor toekomstig onderzoek.

# Chapter 1

## Introduction

### 1.1 A Brief History of Wireless Communication

#### 1.1.1 Past

The history of wireless communication can be traced back to more than 2000 years ago. Beginning from the Chun Qiu period (770 B.C - 476 B.C), the Chinese started to use the smoke from the fire to convey the information of enemy invasion. The fire light is used as information carrier and the light is one kind of wireless wave.

There is a famous story in China. There was a king whose wife never smiled. The king did everything he could to make her laugh, but he did not succeed. Finally, the king asked the soldiers in the capital city to fire the alarm although there were no enemies. So, the soldiers from other places came to his capital and found the information to be incorrect. They were very tired and disappointed. The King's wife sat at the castle and finally laughed to the soldiers who were fooled. One year after, when there was a real enemy invasion and the king set the fire again, no soldiers came for the second time and the kingdom was lost. We can see the importance of delivery of correct information via wireless communication.

Over the years, various means of communication have been used. Many years ago, pigeons were used as means of communication later on, humans themselves. Later on, when the industrial period started, people started to know the principle of electromagnetic waves. In 1887, Heinrich Rudolf Hertz was the first to broadcast and receive radio waves in the laboratory. He proved that there are mysterious electromagnetic waves that cannot be seen through our naked eyes and gave an interesting conclusion "It's of no

use whatsoever". Three years later, The English mathematical physicist, *Sir.OliverHeaviside*, said in 1891, "Three years ago, electromagnetic waves were nowhere. Shortly afterward, they are everywhere."

The modern usage of wireless waves started from 1895 when Marconi sent the first telegraph. With hundred years of development, the wireless communication technology has been improved in all aspects, from the connecting distance to the connecting speed. In the twentieth century, the wireless communication technology advanced more and became more popular in the civil area. Different radio technologies are used in our daily life with the fact that more and more spectrum are used.

### 1.1.2 Modern wireless technologies

After the telegraph was used for long distance communication, the radio technologies were not used in communication too much in the early twentieth century. In contrast, the wired technologies were more used in communication system. The telephony with wired lines were widely used all over the world in 19th century. In 1969, the Internet was started as an research project and grew into a world wide network in the late 1990s.

Until the 1980s, the first successful commercial mobile phone systems had started. This cellular communication system provided large area connections. About 15 years later, short range communication technologies started to develop. The free ISM band technology has been involved more and more in our daily life. In 1997, the first version of IEEE 802.11 was released and since then the Wireless Local Area Network (WLAN) has become common in our life. Few years later, the wireless technology has evolved to an even shorter range of 10m to achieve low power consumption (IEEE 802.15.4) or even higher data rate (IEEE 802.15.3).

Nowadays, more and more electronic devices use wireless technologies, such as, cell phones, Personal Digital Assistant (PDA), laptop, are now becoming the essential part of our life. Providing the best connection between the devices and delivering the data with the best quality is our concern.

In this thesis, we mainly discuss three popular wireless technologies, namely, IEEE 802.11, IEEE 802.15.4 and Universal Mobile Telecommunications System/High-Speed Downlink Packet Access (UMTS/HSDPA). They are focused due to their popularity in our current world and their important role in wireless ad hoc and mesh networks, wireless sensor networks (WSNs) and cellular networks. We introduce some basic features of these three technologies as follows:

**IEEE 802.11** IEEE 802.11 is a wireless technology for local area network that can work in the infrastructure mode or ad hoc mode. In infrastructure mode, 802.11 basically allows terminals to connect to each other just like wired Ethernet in a wireless manner. We used IEEE 802.11b/g in our experiments and simulations. The IEEE 802.11g provides gross bit rate up to 54 Mbps. Since 802.11 can operate in infrastructure or ad hoc mode, the architecture of 802.11 network can be infrastructure based or ad hoc based.

In infrastructure mode, all Mobile Nodes (MNs) can only communicate with one Access Point (AP) and can not communicate directly to each other. Hence, all communication has to go through AP. In ad hoc mode, MNs can connect to each other as long as the distance between them is within their radio coverage range and no AP is needed. Several MNs in ad hoc mode form an Independent Basic Service Set (IBSS). All MNs in the same IBSS use the same radio frequency. In this thesis, for all the measurement and simulation studies, we use ad hoc mode. The 2.4GHz and 5GHz frequency can be used for IEEE 802.11.

**IEEE 802.15.4** IEEE 802.15.4 intends to offer fundamentally lower network layers for wireless personal area network (WPAN) which focuses on low-cost, low-speed ubiquitous communication between devices. The target is to provide a low cost communication connecting nearby devices with little or no underlying infrastructure. The intention is to exploit this lower power consumption devices even more.

The basic framework conceives a 10m communication area with a transfer rate of 250 Kbps. The general communication range depends on the environment, the maximum transmission range is about 30m for indoor environment, 100m for the outdoor environment. Lower bit rate can be used to reduce power consumption further. As already mentioned, the main identifying feature of 802.15.4 among WPAN's is the importance of achieving extremely low manufacturing and operational cost with technological simplicity, without sacrificing flexibility or generality.

Important features include real-time suitability by reservation of guaranteed time slots, collision avoidance through Carrier Sense Multiple Access with Collision Avoidance (CSMA/CA) and integrated support for secure communication. Two frequencies can be used – 915MHz and 2.4GHz.

**UMTS/HSDPA** The UMTS is a third generation (3G) mobile communication system. It delivers low cost, mobile communication at data rates up to 2 Mbps. It not only provides enhanced capabilities but also has the handover capability between UMTS and Global System for Mobile Commu-

nication (GSM) networks. UMTS network supports both voice and data services. It offers teleservices (like speech or Short Message Service (SMS)) and bearer services, which provide the capability for information transfer between users. Both connection oriented and connectionless services are offered for Point-to-Point and Point-to-Multipoint communication.

The HSDPA [35] concept, which is defined by the Third Generation Partnership Project (3GPP) further improved the capacity and bandwidth for UMTS. The highest speed of 2 Mbps provided by UMTS is already very high for mobile communication but still can not satisfy some applications such as high quality video transfer or fast downloading. So the HSDPA is proposed at UMTS release 5 to increase the downlink speed. It is particularly suited for extremely asymmetrical data services, which require significantly higher data rates for the transmission from the network to the User Equipment (UE) (downlink) than they do for the transmission from the UE to the network (uplink). HSDPA aims to boost up the downlink data rate performance of UMTS. With HSDPA technology end users are going to experience obvious improvement in their throughput bit rates.

### **1.1.3 Wireless technology in future**

We can foresee that the wireless communication will be developed even faster in the future. The 4G systems have been proposed and discussed. New standard like Worldwide Interoperability for Microwave Access (WiMAX), Ultra-Wide Band (UWB) have been coming into our life. In one direction, computation capability of the devices keeps on increasing, which enables more complex protocols and algorithms. On the other hand, in one single device there could be multi radio interfaces and multiple channels could be used with a certain radio frequency. Communication system will be more complex.

From the users' perspective, the demand also keeps on increasing. With more contents necessary to be delivered between different devices, higher bandwidth will be required to provide faster information delivery. On the other hand, the size of devices will become smaller which means we can not increase the battery size in mobile devices. meanwhile the battery technology does not keep up currently.

To provide more types of services and increase the quality, a study on the performance optimization and power saving for wireless networks becomes a must. Hence, few studies have been carried out in this thesis.

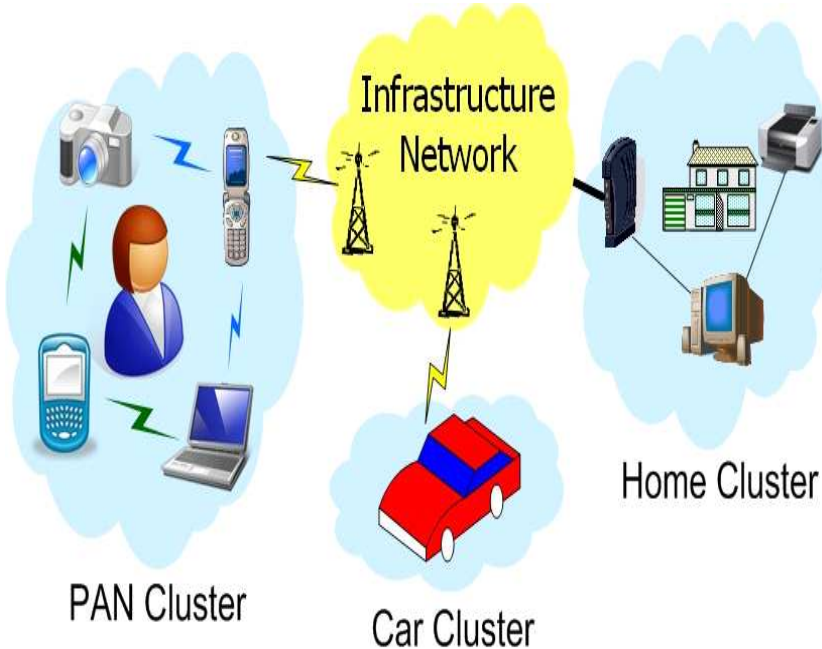


Figure 1.1: PN architecture.

## 1.2 Motivation Scenarios

Since there are so many wireless technologies and devices which are capable of sending and receiving the radio waves, there are lots of wireless connections just around us. Wireless devices can form wireless networks. Based on different radio technologies used in devices, there are plenty of wireless network types. e.g, Wireless Sensor Network (WSN), WMN. The wireless networks greatly facilitate our daily life and we use three typical scenarios to indicate the importance of our research in this thesis.

### 1.2.1 Wireless networks

This thesis starts with the Personal Networks (PN) [73]. Since all kinds of wireless radios can be used in PN. The PN can be made up of different types of wireless networks such as WLAN, Mobile and Ad hoc Network (MANET), WSN, Cellular Network and Wired Networks. Different wireless technologies can be used in this network and it will facilitate human's life tremendously. The architecture of PN is depicted in Fig. 1.1. The detail description of PN can be found in [36].

For all the wireless links, packets can be lost. It is well known that wireless links normally have much higher error rates compared to the wired links (e.g.

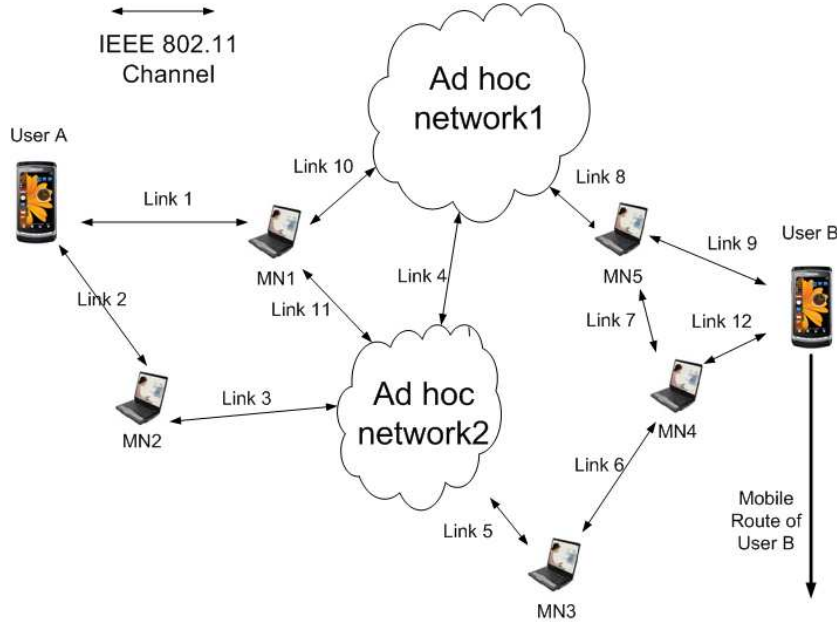


Figure 1.2: High throughput scenario.

fiber links, copper lines) and the error ratios in wireless links are dynamic. How to cope with those errors and improve the service quality of wireless networks is an open question. Let us now start to show the importance of our work through three typical scenarios in our daily life.

### 1.2.2 High throughput scenario

Our first scenario is just a common scenario in which two users want to share a file or a photo. As we can see in Fig. 1.2, between them there are lots of devices which all have the same radio interface, IEEE 802.11. Since the distance between the User A and User B are much larger than the maximum one hop connection distance, they have to use a multi-hop network to build a connection between them. There are plenty of nodes between them and some of the nodes form small ad hoc networks. Also, there are 12 links between the nodes and ad hoc networks.

For a certain link, IEEE 802.11 b/g technology can offer 12 different data rates to select. Higher data rate may offer faster packet transmission but more errors can occur during the communication process. If accurate packet delivery ratio information is known by the nodes at the two ends of a certain link, a proper data rate can be selected which can bring in the highest throughput for one-hop connection. Further, if the accurate packet

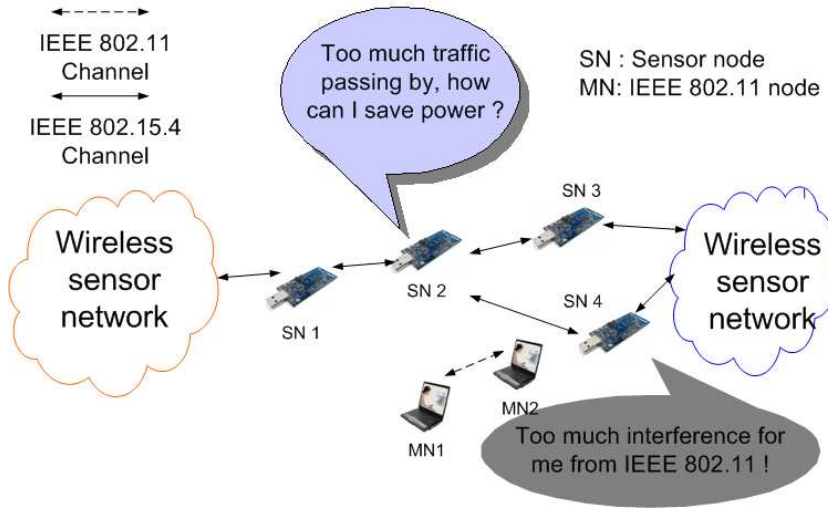


Figure 1.3: Power saving scenario.

delivery ratio information and the data rate information is known by the higher communication layer of the all the nodes, a proper route between User A and User B can be built which can result in a faster file sharing between the Users. However, the packet delivery ratio for each link may be dynamic, especially when certain nodes, e.g. User B, is mobile. How our system could always select the best connection between User A and User B is an interesting problem.

### 1.2.3 Power saving scenario

Nowadays, WSNs are also more and more popular. Lots of applications use WSNs to deliver information. The wireless sensor nodes are normally small and battery based which is designed for long lifetime. Therefore, for the wireless sensor networks, power is an important issue.

We plot a common scenario in Fig. 1.3, we assume some information required to be delivered between two wireless sensor networks. There are four wireless sensor nodes in between SN1 to SN4. Since SN2 is at an important position and all the traffic needs to be passed by, it will consume lots of power compared to other nodes. Power saving is especially important for this node. We have to use the link quality information to reduce unnecessary power consumption and meanwhile deliver the same information between the two sensor networks.

Further, it is proved that IEEE 802.11 radio links may generate interference to IEEE 802.15.4 links. Therefore, it is also interesting to investigate

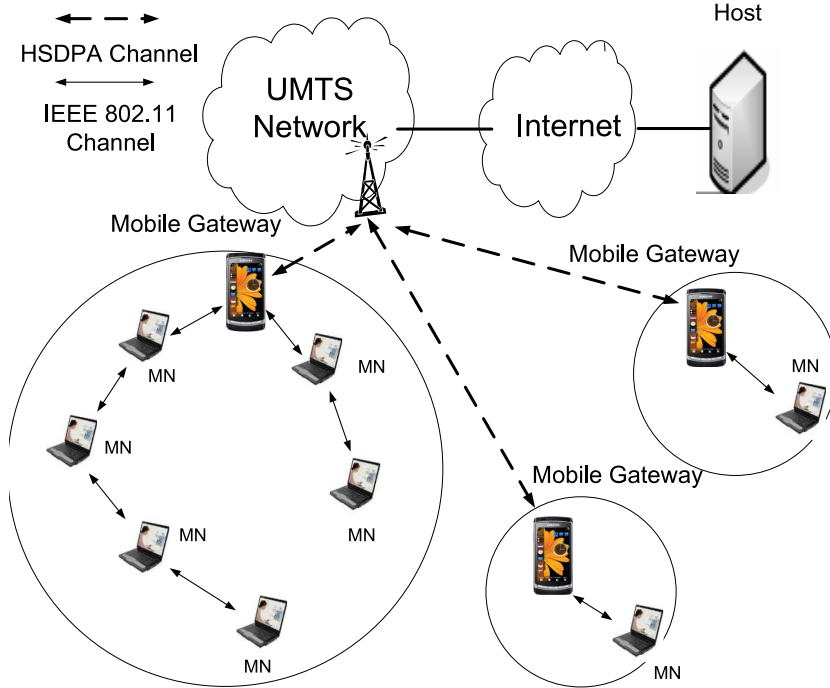


Figure 1.4: Mobile hot spot scenario.

the reduction of the interference generated by certain links. These problems can be also alleviated by using the link quality information.

#### 1.2.4 Mobile hot spot scenario

In our daily life, there can be some scenarios that in certain locations at a certain time period, the cellular networks can not be used by the certain users. The reason can be that the user's device does not have a cellular network interface, or there are suddenly too many people in an area that the local cellular base station can not support so many users since it is not designed for such large number of users.

We shall introduce one type of network which could be used for those scenarios, namely, the cellular multi-hop ad hoc network [113]. The architecture of cellular multi-hop network is depicted in Fig. 1.4.

The end users can use both IEEE 802.11 and cellular network radios to transfer information. This network is quite dynamic and useful for those scenarios. The performance of this network needs to be investigated by the service provider to provide the best service to all the users.

### 1.3 Problem Formulation

For all the scenarios described above, wireless link quality information can be greatly useful for the performance enhancement. But what is wireless link quality exactly? As we know, current communication systems use the lowest unit bit to convey information, several bits can made up of packets. Wireless link quality can be referred as Packet Delivery Ratio (PDR) or Bit Error Rate (BER) for a certain wireless link. If the bit or packet is lost or impaired during the communication process, we call it wireless errors.

The wireless channel error is always the concern of engineers and scientists. Due to multiple factors, the information transferred on the wireless channel can be impaired. The low Signal to Noise Ratio (SNR) is the fundamental cause of the wireless error and there are also other reasons such as collision. Our aim is to achieve high efficiency to deliver information over wireless links by reducing wireless errors. There are two methods to increase the information delivery efficiency over wireless links. Firstly, use higher transmitting power or different modulation and coding techniques, which can reduce the errors in a certain link. Secondly, find another neighbor which has a better link connection with the information sender and information receiver and use this neighbor as a relaying node.

In this thesis, we do not focus on the first method due to two reasons. Firstly, the government has the regulations to limit the maximum transmission power of each device. It is impossible to increase the transmission power to a level that is higher than the government regulation to reduce the errors in some systems. Secondly, in this thesis, we do not focus on the physical layer which discusses the modulation and coding, this method is for a single link information transmission. We are looking at the problem in a particular system and then try to find solutions at the network level. We mainly focus on the wireless errors at packet level instead of bit level. The PDR is the estimation target.

The main focus of this thesis is to identify the properties of wireless errors and packet losses in the wireless channels. We estimate the number of errors in time domain and use the most appropriate channel to deliver the information with best quality. The current inefficient wireless link quality estimation mechanism not only delivers the information in an inefficient way but also uses more energy than necessary. Meanwhile, for the network resource reservation and quality of service, performance evaluation of the information delivery over heterogenous wireless channels is quite important. Those facts lead us to further explore the methods that can improve the system performance.

The Open System Interconnection (OSI) Reference Model is used to de-

scribe different functional entities in modern communication system. The wireless link quality have impact on all the layers in this model. In this section, we briefly describe our problem and motivation for the research of wireless link quality in each OSI communication layer.

### 1.3.1 Link quality estimation in wireless links

Accurate and fast packet delivery ratio estimation used in evaluating wireless link quality, is a prerequisite to increase the performance of multi-hop and multi-rate wireless networks. The link quality information is highly important to the higher layer's performance. Accurate and fast response link quality estimation will enhance the wireless communication system performance. Unfortunately, contemporary PDR estimation methods, i.e., beacon-based packet counting in Estimated Transmission Time (ETT) [20] and Expected Transmission Count (ETX) [9] metrics, have unsatisfactory performances. This is because they use one type of packet to estimate the link quality for all the links which use packets that have different rates and sizes. Meanwhile, they only looked at the problem for the stationary scenarios whereas in real life, lots of communication devices can be mobile.

To accurately estimate the link quality for all the links, lots of issues need to be considered. Firstly, the dynamics of the wireless links and the estimation methods should provide accurate estimation. They should respond fast when the link quality of a certain link changes. The estimation methods need to consider the impacts from the data rates, packet size, mobility and change in the environment. All these factors make the link quality estimation a hard task.

### 1.3.2 Link quality based transmission power adaptation

Many wireless devices are mobile and battery powered nowadays [36], which means that service duration is highly dependent on the energy consumption and battery capacity. However, the fact that battery capacity is still limited (e.g, in many applications, namely, the battery of Nokia N95 normally cannot last for more than 24 hours). For IEEE 802.11 and IEEE 802.15.4, the link layer decides the transmission power in OSI model. The selected transmission power should not higher than the maximum power level indicated in the government's regulation. Some wireless technologies allow adapting the transmission power levels to achieve better system performance.

Energy saving is still an important issue in wireless communication. On the other hand, power adaptation can also reduce the interference between

different communication nodes if the appropriate transmission power levels are selected which generates the lowest energy emission to the environment.

Many methods have been proposed to save energy and reduce the interference for the IEEE 802.11 and IEEE 802.15.4 radios, such as power-aware routing and sleep mode. In this thesis, we try to solve the problem in a different perspective, we look at the transmission power control and propose a mechanism that tries to achieve minimum transmission power consumption or minimum energy emission under any circumstance.

The problem is how we can incorporate the wireless link quality information into our power saving mechanism. Despite the dynamic nature of the wireless link quality, the algorithm should try to select the appropriate transmission power level to transmit packets based on the received packet counting method, instead of using a fixed default power level for all packets, which is common in IEEE 802.11 and IEEE 802.15.4. Lower transmission power levels may result in more retransmissions, but in total, still energy can be saved in many scenarios. Moreover, interference is also reduced. The decision of appropriate transmission power level can be made via the wireless link quality information.

### 1.3.3 Link quality based data rate adaptation

Some wireless technologies also allow multiple data rates to transmit packets. The selection of appropriate data rate to achieve higher transmission efficiency is called data rate adaption. For example, some links are quite easy to lose packet with certain high data rates while they can deliver all the packets in some low data rates. It is obvious to see that there is also a trade off between the transmission speed and error rate. The selection process for the best data rate that has the best combination of transmission speed and packet error rate is rate adaptation. Successful rate adaptation can bring in the highest throughput over a certain wireless link. This adaptation needs to be adaptive also since the link quality of the channels are dynamic.

For the data rate adaptation, IEEE 802.11 networks provides multi-rate options and several rate adaptation mechanisms provide the ability to select the rate intelligently. Prior works on the rate-adaptation focus on stationary scenarios, such as mesh networks. The effect of the smoothing of the rate adaptation is not a well-studied topic in the mobile scenarios such as IEEE 802.11 mobile multi-hop networks.

In this thesis, we try to use an experimental method to evaluate the one-hop throughput performance of a wide spread rate adaptation mechanism. Our study can be divided into two steps, in the first step we investigate the performance of the traditional method, which uses the smoothing factor to

control the speed of adaption. We have performed experiments to investigate the impact of the smoothing factor on the rate adaptation. The throughput is used as metric. It is observed that smaller smoothing factors lead to larger throughput improvement and faster response when the channel is more dynamic. In the second step, we feed our accurate link quality information into the system to let the rate adaptation mechanism to act faster to link variance. The difficulty is that how to estimate the wireless link quality information accurately and use it appropriately in the rate adaptation schemes.

### 1.3.4 Link quality based route selection

The routing layer in OSI model is set to select the route for packet forwarding. A good selection will result in higher throughput, lower delay from the end-to-end point of view. Link quality information can be very useful in this process. Based on lower layer's information, the routing layer decides the route between the source and the destination node. Previous works have proved that the hop count method which is widely used in wired network is not suitable in wireless network. This is because the wireless network has a different link quality and each link has its own link quality characteristic.

Link quality based route selection will perform better than pure hop count routing metric. However, the performance enhancement in the routing layer by the introduction of the accurate and fast response link quality estimation is unknown. Therefore, in this thesis, we have investigated different link quality estimation sources to the routing layer in various scenarios. We will show the impact on the end-to-end performance due to the improved estimation on route selection using different routing metrics and configurations. The measurement results show that our accurate link quality information estimation method lead to a better route selection in the form of increased end-to-end throughput compared to the traditional method, which respond slowly to the link dynamics.

### 1.3.5 Transport layer performance with different link quality

For the transport and application layer, we mainly discuss a wireless heterogeneous network type, which we call the next-generation communication networks. It will comprise 3G cellular and multi-hop ad hoc networks as shown in Fig. 1.4. The extension of ad hoc network can bring in several benefits to the cellular network, such as higher throughput, load balancing and the nodes in ad hoc network can use two radio technologies to access the Internet. Meanwhile, ad hoc networks can increase the service range

of the cellular network, and also improves the performance for the end-user who experience bad channel conditions. This integrated network can be seen as an extension to the cellular network and use two different technologies, UMTS/HSDPA and IEEE 802.11. The performance evaluation of this network under different link quality in both types of wireless channels can help us understand the potential of the integrated network. With the performance evaluation, the service provider can provide better Internet connection to the end users. Also, this evaluation can help the providers to provide Quality of Service (QoS) services.

In this thesis, a popular traffic, Transmission Control Protocol (TCP) will be used as evaluation traffic in the transport layer and the performance of TCP over this new integrated network will be interesting. The throughput simulation results show that the bottleneck of the multi-hop cellular network shifts between the UMTS/HSDPA network and the ad hoc network based on the different channel quality and the number of hops. Moreover, the relation between UMTS/HSDPA radio channel usage and user experience under different network configurations and channel conditions can also be revealed. We try to evaluate the performance of TCP over the network with different link quality. The result can be used to select the optimal routes and system performance optimization.

Meanwhile, compared to the traditional cellular network, there is a new problem for the integrated network that nodes in IEEE 802.11 ad hoc network may not always be served fairly due to the different channel quality in the radio channels. Traditional scheduling mechanisms for HSDPA are not multi-hop aware, because it only considers the different channel conditions for cellular channel users. In this thesis, we try to use a weighted scheduling mechanism to alleviate the problem. We propose a new weight calculation method which considers the parameters in both the IEEE 802.11 ad hoc network and UMTS/HSDPA network, namely the number of hops away from the gateway, and the packet delivery error in ad hoc network.

### 1.3.6 Application layer performance with different link quality

For the application layer, the most important evaluating factor is the user satisfaction. The difficulty of our integrated network is that different traffic types could be transmitted over this resource limited channel sharing network. The HSDPA uses the shared downlink channel which may be used by lots of users with higher demand of bandwidth. Meanwhile, the link quality of HSDPA is also dynamic. Ensuring the quality of content delivery to each

user is an open question.

Video streaming is a potential application of the integrated network. Moving Picture Experts Group-4 (MPEG-4) [49] is one of video streaming encoding technologies which generates low bit rate video streams. Therefore it is suitable for bandwidth limited wireless networks. MPEG-4 is a widely used traffic to evaluate the video transmission over different wireless networks [77]. Due to its adaptive coding ability, it is suitable for the resource limited network. However, it is also a delay constraint application which has high requirement on both PDR and end-to-end delay. How to build a simulation model and use this model to evaluate the MPEG-4 over this integrated network is our problem.

We extend a simulation tool with realistic assumptions and investigate the MPEG-4 performance over the integrated network in the simulator with all kinds of configurations, such as different topology, different link quality, with single and multiple flows for the channel and so on. The result can be used for gateways selection and performance optimization for this integrated network.

## 1.4 Research Challenges

The main challenges in this thesis are: accurate wireless link and network performance observation, novel mechanism design, and system performance enhancement.

### 1.4.1 Observational challenges

There are three methods to investigate the wireless link quality and the performance of wireless networks. They are mathematical model, simulation and experimental measurements. The mathematical model can help us to investigate the fundamental limitations and bounds of the communication systems. However, for each model, there are too many assumptions, which can hardly be used directly in the current applications. The simulation method has several advantages namely controllable environment, supports large scale scenarios and is easy to implement at low cost. However, the problem for all the simulations are the same, for some applications, unrealistic channel models and some simplification assumptions can not achieve the good performance. It has been proved by the previous works [6] that the simulation results have large differences from the real world measurements. Some previously proposed protocols or solutions can not be used practically at all due to those unrealistic assumptions. The measurement method can provide us the most

accurate result which is precious for real practical mechanism's design and validity. However, the challenges are huge.

There are mainly two difficulties in the measurement of the wireless link quality. The design of software and prototype coding for the test-bed and the measurement scenario is quite difficult. To build a measurement software, coding is a tedious job for the author's experience and needs to be coded for different purposes of the experiment and the core software architecture. The software needs to be tested under several extreme situations to find the hidden bugs. Some bugs have to be discovered during the real measurement process, which means, large amount of time is spent to optimize all the factors in the experiment setting and the measurement process, then a tiny bug destroys all previous efforts. Meanwhile, the prototype software should not use too much of the system resources and the delay for packet processing should be less.

Another difficulty is in the experimental design. The scenarios have to be selected carefully. Due to the limitation of the number of available experimental nodes, we have to design the experimental scenarios which represent the most common situations and to be stable enough to prevent too much variance. Experiments need to be repeated to provide a reasonable confidential interval. Further, they need to be able to show the performance difference for different protocols. The experimental scenarios are described in each chapter. Our prototype design is described in Appendix A and Appendix B.

### 1.4.2 Mechanism design challenges

Another challenge of the research in this field is the mechanism design. After an in depth research in the previous work, we found out that several previous solutions are not capable of solving the existing problem. Therefore, we have to propose new solutions to improve the system performance. Especially, lots of previous solutions for data rate selection, power adaptation, and route selection problems have not used the wireless link quality information. How to incorporate the dynamic wireless link quality information into our solution is a challenge. The new mechanisms have to consider different impacting factors that affects the system performance. The factors depend upon the scenario, weighted combination method or other combination method which results in a different performance. Hence the way of considering these factors is a question. These mechanisms have to be carefully designed, implemented, tested and validated.

### 1.4.3 Performance enhancement and optimization challenges

After gathering huge simulation and measurement data via our wireless link and network observations, the most difficult part is the system performance enhancement. As an old saying, there is no free lunch in the world. The performance enhancement is always kind of trade off. Some aspects have to be sacrificed to trade the enhancement in other aspects. For example, accurate link quality information may introduce better performance in terms of higher throughput or less packet delay. However, the link quality estimation itself may generate some overhead. The system needs to use more power to compute all the link quality information gathered from different resources. The challenging point is that for performance enhancement and optimization, we need to consider all the factors that may impacts the performance and carefully study the trade off behind certain performance enhancement.

Meanwhile, the validation process is also not easy for the proposed solutions. The wireless link quality is dynamic in nature. How to make sure that the proposed method works in all types of combinations and environment is a complex problem. For the performance enhancement, we have to validate the variance of performance enhancement in different scenarios or over a long time observation.

## 1.5 Thesis Overview

The thesis comprises of nine chapters in total, this chapter has explained the basic introduction of the thesis. In Chapter 2 we have the basic introduction to the link quality in wireless links. All types of link quality estimation methods are described and evaluated in Chapter 3. The link quality based power saving is discussed in Chapter 4 and link quality based rate adaptation is discussed in Chapter 5. With the background from Chapter 5 we discuss Chapter 6 and we show that link quality estimation improves the system performance. In Chapter 7 and Chapter 8, various traffic is used to evaluate their performance over the cellular multi-hop network with the assumption of different link quality. The system optimization solutions are proposed in these two chapters. Chapter 9 concludes the thesis. The experimental test-beds and the simulation model are introduced in the Appendix part.

## 1.6 Chapter Summary and Discussion

Starting from the history of wireless communication, we have introduced the background of wireless communication. Due to the fundamental characteristic of the wireless communication, there can be always transmission errors during the transmission process. We look at those transmissions in a frame level and motivate our work for link quality estimation and use them to improve the performance for all the communication layers. We have described the challenges that we have met during our study. A general overview is given for the following chapters.



# Chapter 2

## Background on Wireless Link Quality

### 2.1 Introduction

For all the radio channels, packet can be lost due to several reasons, such as low SNR, collisions, or multi-path. In this thesis, wireless link quality means the packet delivery ratio. Estimation and modeling the wireless link quality is very important to improve the performance of wireless networks. However, due to channel differences, wireless link quality has different characteristics for different radio channels, which make the wireless link quality estimation not an easy task.

To successfully estimate the wireless link quality, we have to understand the wireless link quality characteristics. We use both measurement and simulation methods to understand the different wireless channel characteristics. Especially, we use the real device to carry out large scale measurement activities in both indoor and outdoor environments. Several different wireless link quality indicators are analyzed. For the cellular network, we can not carry out the real measurement due to the conditional constraints. Instead we build a channel model which allows us to generate simulation traces and evaluate the performance of different traffic over different channel condition.

In this chapter, we discuss the wireless link quality for two kinds of short range radios, namely IEEE 802.11 and IEEE 802.15.4. Also, we discuss the wireless link quality for the radio which has long transmission range, in UMTS cellular system. The chapter is organized as follows: We first describe some wireless link quality indicators in Section 2.2. Preliminary experiments have been carried out and the results are presented in Section 2.3, we give a summary at end of the chapter in Section 2.4.

## 2.2 Common Wireless Link Quality Indicators

The communication system is defined with OSI model which separate the system to a few communication layers. Each layer has its own properties and information sources for the link quality assessment and can provide their own information. We introduce the potential wireless link quality indicators from each layer. Physical layer can differentiate the link quality based on the bit level. A successfully received packet can gain more information on bit error ratio or signal strength. Link layer can provide statistical information about large number or long term level packet delivery statistics. Network Layer can provide more information based on the end-to-end view and more information on which the link is more valuable to be accessed. The indicators in each layer is shown in Fig. A.1(b). In this section, since we only perform the link quality estimation for IEEE 802.11 and IEEE 802.15.4 radio links, we will discuss five indicators which are easy to get from the WMN and WSN. The traffic in those two networks are called as data packets, we refer the data packet delivery ratio to wireless link quality in those two networks.

### 2.2.1 Hello packet

Most ad hoc networks rely on the hello packets. Usually, hello packets are small periodical broadcast packets. Neighboring nodes know the period of those packets and can count the number of successful hello packets over a given time period. By dividing the number of received hello packets by the number of transmitted hello packets, a node can estimate the hello packet delivery ratio of a link. Essentially the same, but a slight alternative is to use a Exponentially Weighted Moving Average (EWMA) filter [9,20] to calculate the hello packet delivery ratio.

$$E_t = \alpha X_t + (1 - \alpha) E_{t-1}, \quad (2.1)$$

where  $0 \leq \alpha \leq 1$ ,  $E_t$  is the estimated hello packet delivery ratio at time  $t$ ,  $X_t = 1$  represents a correctly received hello packet at time  $t$ ,  $X_t = 0$  implies an incorrectly received probing packet at time  $t$ , and  $\alpha$  is the smoothing factor. This method requires only one hello packet sent per time interval, thus it is fast and simple. The hello packet transmission interval is known by all nodes [20]. Therefore, the delivery ratio is measured on the receiver side.  $\alpha$  in Eq. 2.1 is to smooth the estimate. A larger  $\alpha$  results in the estimation reacting faster to link dynamics. However, at the same time, the estimate becomes more jittery, since it changes according to temporal

and random events as well as using less historical values. The  $\alpha$  value used in the experiments is deduced as shown by our prior experiments. Since hello packets are used by a lot of previous work, we will call it the *traditional method*. In the rest of this section and we will use  $R_H$  to denote this estimate.

### 2.2.2 Broadcast packet

The hello packet is normally very small, which is much lower than the data packet<sup>1</sup>. Meanwhile, for IEEE 802.11 radio, the hello packet use the low data rate while the data packet can use much higher data rate. The packet size and data rate difference can introduce inaccuracy when we use hello packet to predict the data packet delivery ratio. We use the packet which has the same packet size and use the same data rate as data packet to probe the link and estimate the link quality. However, the packets are sent using the broadcast method. We call this type of packet as broadcast packets. We can still use the Eq. 2.1 to compute the broadcast packet delivery ratio and use this ratio as an indicator of the wireless link quality. Same as in the previous method, the ratio is computed on the receiver side. The advantage of this method is that it is more accurate than the hello packet counting since it's packets are more similar to the data packet. The disadvantage is that it will generate more overhead, since the packet is larger and if we want to know the packet delivery ratio for different data rates, we have to send broadcast packets in all data rates.

### 2.2.3 Unicast packet

The broadcast packets are sent and no acknowledgement can be received. To probe the link, we can also use the same type of packets as the broadcast packet, while we use the unicast method to send them to the receiver. The benefit of this method is that packet delivery ratio is computed in the sender size. In a certain interval, the number of received acknowledgements divided by the number of transmissions. Compared to the broadcast packets, the advantage of unicast packets is that they can estimate the link quality even more accurately than the broadcast packets since this estimation is per neighbor. For the same reason, it will generate even more overhead to the network.

---

<sup>1</sup>For IEEE 802.15.4 links, the data packets can be around 120 Bytes while the hello packets can be around 20 Bytes. For IEEE 802.11 links, the data packets can be as large as 1500 Bytes while the hello packet can be around 40 Bytes

### 2.2.4 Data packet

The most direct way is to use the data packet to probe the link. It will be the most accurate link quality indicator since this is the most accurate information we can get. However, it is very obvious to know that this will generate the highest overhead. If we use the traffic which is passing in the link to estimate the channel, no overhead will be generated and this method can be called passive method. It will perform very badly in the dynamic links.

### 2.2.5 Signal to noise ratio

Received signal strength is another important packet delivery estimation source. Previous work claims the inaccuracy of this source due to its fluctuation, however, it has the advantage that its value is not affected by different data rate and packet sizes as we can see in Fig. 2.2. The signal strength can be obtained by any packet and usually the signal strength is read only from the hello packets [18], since the hello packets are transmitted at fixed intervals.

Some work [93] uses SNR to estimate the channel. In our observations, the noise level is constant most of time with a maximum difference in an office environment being 1 or 2 dBm. Hence, using SNR or received signal strength directly will achieve the same result.

## 2.3 Preliminary Measurement Result

To understand the basic IEEE 802.11 and IEEE 802.15.4 link characteristics, we carried out some preliminary measurement for those two types of radio links. Also, we present our generated HSDPA channel traces in this section. We will explain the measurement result in the following sections.

### 2.3.1 IEEE 802.11 channel characteristic measurement

Based on the description in the previous section, we know that lots of wireless link quality indicators can use the EWMA method to calculate packet delivery ratio. If the  $\alpha$  value can be selected properly, the indicator can reflect the link quality more accurately. We are wondering how much performance can be enhanced by selecting an optimal  $\alpha$ . Also it is interesting to know how much different, the performance can be with all possible  $\alpha$  values. We performed a group of experiments in three scenarios, S1, S2 and S3, which

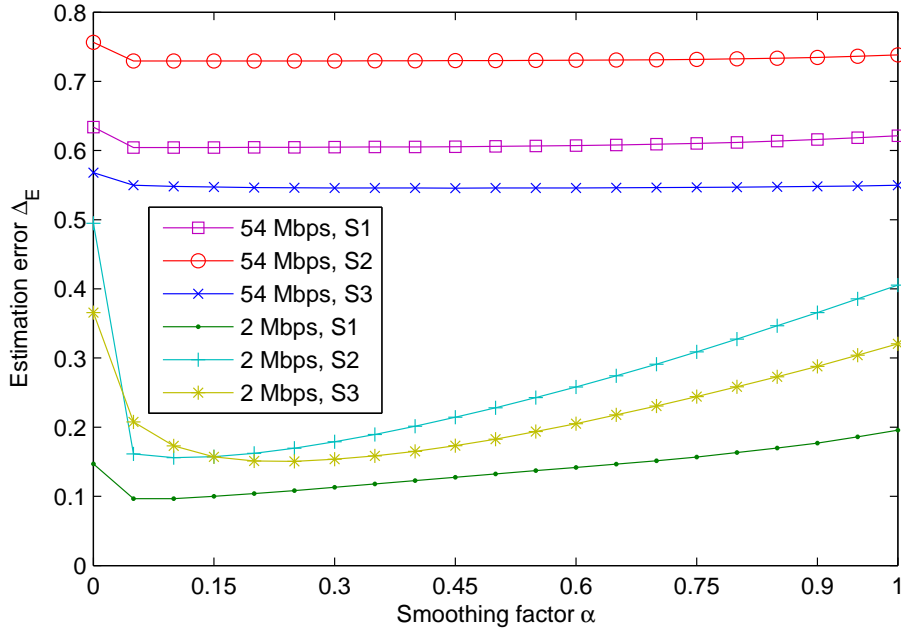


Figure 2.1: Plot of estimation error  $E_D$  as a function of  $\alpha$  for different scenarios and data rates.

are further described in Section 3.4.2. All three scenarios have different wireless channel characteristics. Therefore, all of them require different optimal smoothing factors for the EWMA filter. To measure the impact of an inaccurate  $\alpha$ , in Fig. 2.1 we show the performance for all possible smoothing factors  $\alpha$  in two different link rates and three considered scenarios. Indeed, we can see that for all scenarios with 54 Mbps, the accuracy of an EWMA estimation is very bad. This is due to the fact that even in the worst channel conditions with 54 Mbps, the hello packet sent with a 2 Mbps rate, can easily go through. Thus, the optimal  $\alpha$  has little or no impact on the result.

In order to have an in depth understanding of the correlation between signal strength and PDR, we carried out three experiments on the suitability of using signal strength to predict the link quality. See Fig. 2.2, Fig. 2.3 and Fig. 2.4. The experiments were done in an indoor environment, with only two nodes; a sender and a receiver. Both nodes recorded the beacon packet delivery ratio, data packet delivery ratio and received packet signal strength<sup>2</sup>. In the first two experiments, we changed only one particular parameter at a time to see the effect of that parameter on the correlation between the signal

<sup>2</sup>Since the noise level is quite constant in our experiments, the SNR and signal strength shows the same link quality

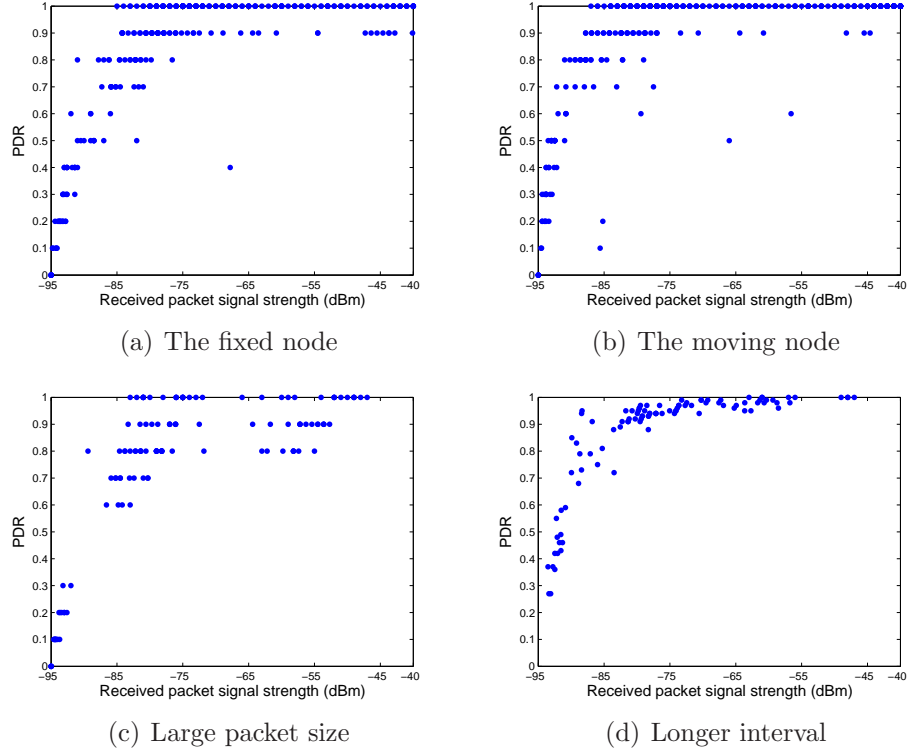


Figure 2.2: Hello packet signal strength vs. hello packet delivery ratio.

strength and PDR. In the third experiment, we experimented with two nodes moving away from each other in order to investigate the speed and accuracy of different LQE mechanisms on a degrading link.

### Experiments with hello packets

In this group of experiments, we kept one of the nodes stationary while the other node was randomly moved from one location to another in a typical indoor environment. The node was kept there for a few seconds before moving to the next location. To investigate the correlation of hello packet delivery ratio with hello packet signal strength, we let each node to broadcast 10 hello packets per second using a 2 Mbps transmission rate and a packet size of 36 bytes. In this experiment, each measurement included 10 hello packets collected over a period of 1 second. Then, we calculated the hello packet delivery ratio and average received signal strength, where a lost hello packet was assigned the minimum receivable signal strength of  $-95\text{dBm}$ .

The two nodes's hello packet delivery ratio and signal strength are plotted in the top two graphs of Fig. 2.2. Despite that the same channel was

measured; the result is a little bit different, which means that the channel is asymmetric<sup>3</sup>.

In Fig. 2.2(c), we increased the broadcast packet size to 1500 Bytes including IP headers. The result shows that a larger packet size results in worse correlation between the two variables. The packet delivery ratio fluctuates even when the signal strength is good or medium.

In Fig. 2.2(d), we extended the packet delivery ratio measurement interval to 10 s, which then included 100 hello packets. Here, we see a better result, which shows a better correlation between signal strength and packet delivery ratio. This is because for a longer interval, instantaneous channel properties are suppressed. However, a longer measurement interval has the disadvantage of slow reaction to link changes. Based on the first group of experiments, we can draw the conclusion that different configurations can result in different correlation between signal strength and packet delivery ratio. Furthermore, only one signal strength value can hardly be used to predict link quality.

### Experiments with data packets

To further investigate the correlation between received signal strength and data packet delivery ratio, we introduced the measurements of the data traffic in Fig. 2.3. We used two different data rates, 24 Mbps and 54 Mbps in the experiment, which is indicated as 24M and 54M in Fig. 2.3. The sender generated 20 User Datagram Protocol (UDP) data packets per second, each with a length of 1000 Bytes including the IP header. We fixed the WLAN rate to either 24 or 54 Mbps. Each measuring point covers a period of 1 second and includes one hello packet and 20 data packets. The number of measuring points in each of the experiments is more than 300.

As we can see in Fig. 2.3, the first row of graphs show the correlation of hello packet signal strength and data packet delivery ratio. We can clearly see that the packet delivery ratio is likely to be more than 95% when the signal strength is more than  $-60\text{ dBm}$ . When the signal strength is lower than  $-80\text{ dBm}$ , we hardly see any data packet delivery ratio higher than 5%. Compared to Fig. 2.2, it is common that the packet delivery ratio is more than 50% when the signal strength is less than  $-80\text{ dBm}$ . Furthermore, the 24 Mbps results show better performance than 54 Mbps, which shows that at a high data rate, the signal strength is even less correlated with packet delivery ratio. This result further proves that using hello packet signal strength alone can not give a good prediction of data packet delivery.

The second row of Fig. 2.3 shows the same thing except that we replaced

---

<sup>3</sup>Lorentz reciprocity theorem

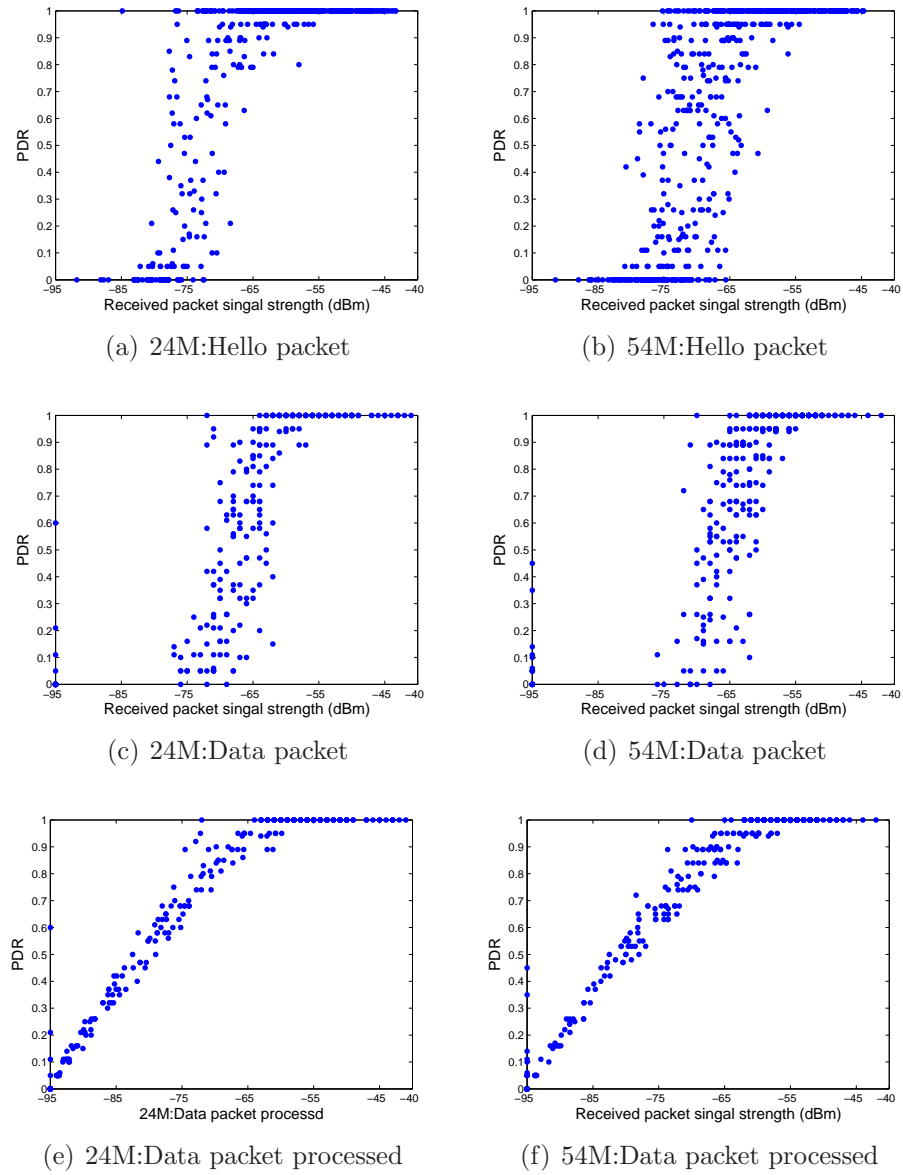


Figure 2.3: Signal strength vs. data packet delivery ratio.

the hello packet signal strength with signal strength from the data packets themselves. This signal strength is based on the average of all received data packets's signal strength which in this experiment meant twenty times more measurements per second. The correlation is slightly better than the previous one. With the same packet delivery ratio, the signal strength variance range is shorter.

In the bottom row of Fig. 2.3, the average data packet signal strength is further processed with packet loss. A lost packet's received signal strength is counted as  $-95 \text{ dBm}$  and as we expected, this gives an excellent correlation between the two variables. This is because not all packet loss is due to low SNR value. Unfortunately, this only works when we also have access to the data packet delivery ratio at the receiver and if we have that, we can use the data directly instead.

Based on these results, we conclude that we still can not use received signal strength to get an accurate link quality estimation, because neither the hello packet nor the data packet signal strength has a very good correlation with the packet delivery ratio on medium quality links (signal strength between  $-60 \text{ dBm}$  and  $-80 \text{ dBm}$ ). However, the received signal strength can give us some additional information that helps us to better estimate the link quality. Extremely high or low signal strengths can immediately indicate the link quality with a high accuracy while medium signal strength can be used to predict mobility by tracking the trend. In the experiments, we found that when the node moves away, the packet delivery ratio is likely to decrease a lot, but hello packet delivery ratio reacts very slowly to these changes, while the signal strength typically shows much faster response. Therefore, the signal strength value changes can be used to predict link changes. When the hello packet delivery ratio is unavailable (a node just joined the network), received signal strength can be a coarse indicator for predicting the link quality.

### Degrading link experiment

To have a direct view of a dynamic channel and to the problems we described earlier, we carried out one more experiment. We used a fixed IEEE 802.11 data rate of 54Mbps. One node sends UDP packets to the other one as in the previous experiment. The two nodes start at the same time and the receiver slowly moves away from the sender (around 0.5 m/s) after the program starts and stops after a very long distance from the sender. The interval for measurement was 100 ms. We plotted the measured hello packet delivery ratio (with EWMA,  $\alpha = 0.2$ )<sup>4</sup>, data packet delivery ratio ( $\alpha = 0.1$ ), hello

---

<sup>4</sup>the EWMA method is described in Eq. 2.1 in Section 3.3

packet signal strength ( $\alpha = 0.6$ ), and data packet signal strength ( $\alpha = 0.1$ ) in Fig. 2.4. For clarity reasons, we have plotted the same experiment in two graphs. The background grey graph is the same and shows the instantaneous data packet delivery ratio for each measurement interval (no EWMA). The  $\alpha$ -values we used are only examples, but do seem to fit the data well. More investigations are needed to find the optimal values.

We can clearly see that the hello packet delivery ratio in Fig. 2.4(a) has a slow start at first and then is much higher than the data packet delivery ratio most of the time. When the data packet delivery ratio changes dramatically, the hello packet delivery ratio reacts very slowly. For the signal strength in Fig. 2.4(b), we can clearly see that the hello packet signal strength is almost identical to the data packet signal strength, while the signal strength also shows similar fluctuation with data packet delivery ratio and is useful for link quality prediction. The graph also shows that when the signal strength is smaller than  $-80 \text{ dbm}$ , the hello packet delivery ratio is still high, but the data packet delivery ratio is 0. Which means the distance is too large and the data packet can hardly go through the channel between the two nodes.

### 2.3.2 IEEE 802.15.4 channel characteristic measurement

PDR metric is also used by WSNs' protocols for selecting best routes and optimum transmission power between source and destination [16, 19, 22]. Naturally, wireless link quality in WSNs is subject to environmental changes and hence the PDR may vary dramatically over time. Especially in an indoor environment, people's movement and Non Line of Sight (NLOS) connections make PDR hard to estimate. IEEE 802.15.4 does not have multiple data rates. However, the power level is much smaller than the IEEE 802.11 radio, which introduce much more interference in the channel and this makes the link quality estimation (LQE) in IEEE 802.15.4 different from the LQE in IEEE 802.11. Thus, a good method is required to timely and accurately estimate the PDR in an indoor WSN link. We carried out experiments to investigate the IEEE 802.15.4 channel characteristic.

#### Experiment Setup

The nodes used in the experiments are t-mote sky sensor motes with 2.4 GHz IEEE 802.15.4 compliant Texas Instruments CC2420 transceivers [10]. The transceiver provides Received Signal Strength Indication (RSSI) in a range of 100 dBm for every received packet, which is the received signal strength reading averaged over eight symbol periods. IEEE 802.15.4 [28] uses 2.4 GHz

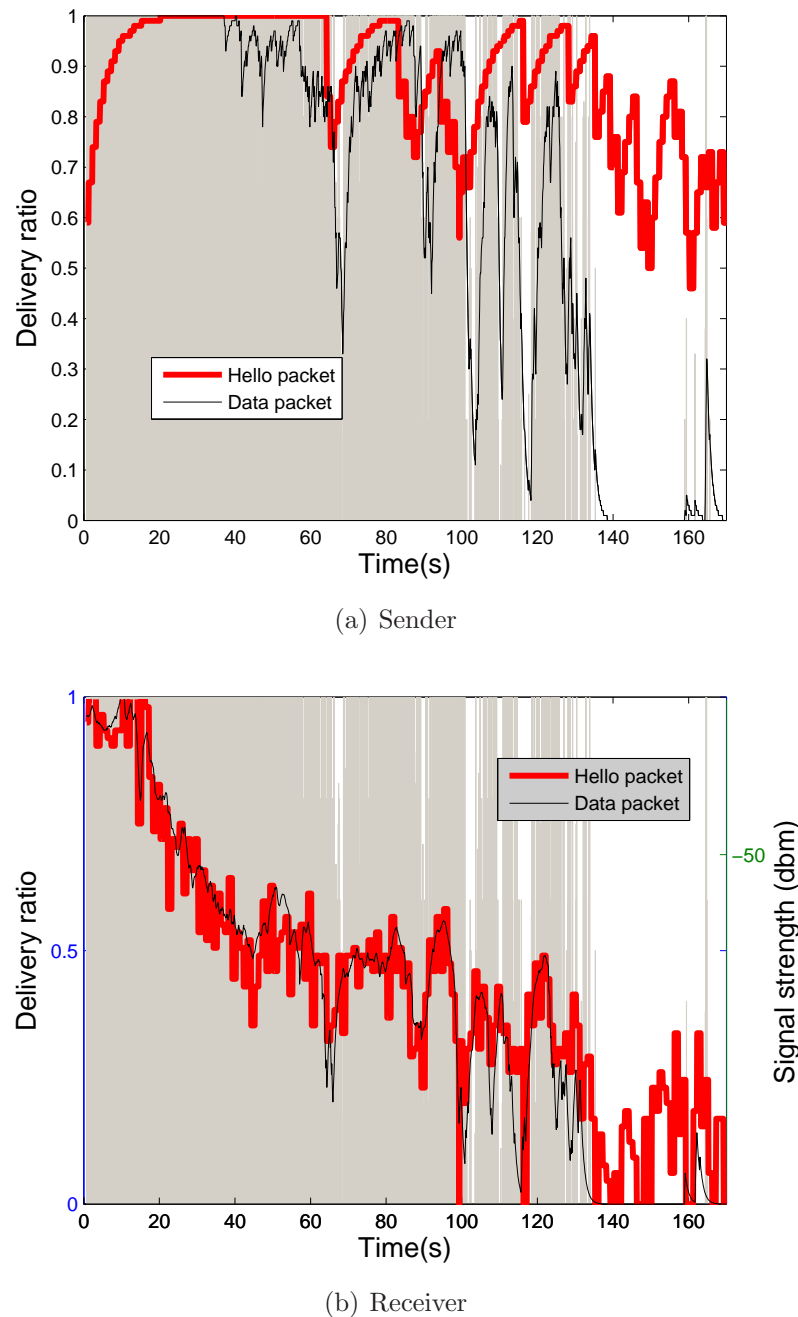


Figure 2.4: Responsiveness during changing quality.

DSSS RF modulation with a data rate of 250 kbps. In our experiments, the IEEE 802.15.4 packet header is 17 Bytes and the payload is set to 18 bytes. Thus a packet is 35 bytes long.

We connected the receivers to a PC via wire. Once a receiver received a packet, it reported to the PC an unique packet ID and the RSSI of the packet. The senders transmitted 10 packets every second and we counted how many packets were received. We expect that sending 10 packets per second should give an accurate estimation of the actual PDR. We tested the wireless links in four typical scenarios. We briefly describe them below.

1. *Strong link*: The two nodes (sender and receiver) were placed about 75 m apart in the corridor of TU Delft’s Wireless and Mobile Communications Lab, which was about 100 m long and 2 m wide with offices at either side. There was LOS so a link with high PDR was expected. The packet collection lasted for about 45 minutes.
2. *Weak link*: The experiment was performed in the same corridor as above. However, one node was kept in an office and the other in the corridor, thus no LOS existed. The distance between the nodes were deliberately tuned so that the PDR varied a lot in the link and this resulted in a distance of about 25 m. The packet collection lasted for about 2.5 hours.
3. *Mobile link*: Again, the same corridor was used as the experimental environment. The transmitter was placed on a table in an office and the receiver was carried with walking speed of approximately 1 m/s. The office door was kept open in the experiment. We started from the fixed node and walked out of the office with the mobile node to the corridor. We walked with even pace for 30 m and turned around to go back to the office. At the farthest point, the PDR was expected to drop to zero.
4. *Dynamic link*: The sender and receiver were placed in the EEMCS faculty canteen of TU Delft. The packet collection started at 11:00 AM and lasted for 2.5 hours. There was LOS between the nodes, which were placed 20 m apart. However a lot of interruptions were expected during the lunch time due to the frequent movement of people.

We emphasize that the first three experiments were conducted in a quiet period after the working hours. Thus, we expected no intensive interruption from the movement of people. Also, in all four experiments, we operated in a 2.4 GHz range absent from WLAN activity to minimize interference from other wireless systems.

Table 2.1:  $A_D$  of the PDR in the four considered experiment scenarios

Link Type	$A_D$
Strong	0.039
Dynamic	0.096
Mobile	0.120
Weak	0.135

## Observations

From the collected experimental data we draw the following observations.

1. The PDR in strong link is almost 1 for the whole observation time, except for the very beginning when the link was disturbed by people's movement. Majority of the RSSI values were between  $-72 \text{ dBm}$  and  $-74 \text{ dBm}$ . Therefore, we conclude that the transceiver can report stable RSSI there.
2. In the weak link, the PDR was unstable. The PDR varied from 1 to 0 within a couple of seconds and approximately 50% of the packets were lost.
3. The PDR in the mobile link changed in a repeating pattern. In each period there was a transition, where the PDR changed from high, above 0.9, to low, below 0.1, or vice versa within 5 s.
4. The dynamic link showed two properties. Before the lunch time, from 11:00 to 11:30AM, the PDR was near 1. However, when people were moving in the canteen during lunch, the link was distorted. From time to time, there were periods when the PDR in the dynamic link showed the same characteristics as the weak link.

For each of the links we computed the Allan deviation of PDR (see Eq. 3.8), which describes the level of fluctuation between consecutive samples. From Table 2.1 we see that  $A_D$  of the dynamic, weak and mobile links are very high compared to the strong link. We calculate the estimated PDR every second using the method described in Section 3.3.1, which we assign to each received packet. For instance, if 5 packets were received in a second, then the estimated PDR of the packets is  $5/10=0.5$ . Later, the RSSI of a received packet is mapped to its PDR. Fig. 2.5 shows the RSSI to PDR mapping in the four considered links. Note that the maximum PDR is 1 and the ranges of RSSI on the X-axis is different for each scenario. We can see that

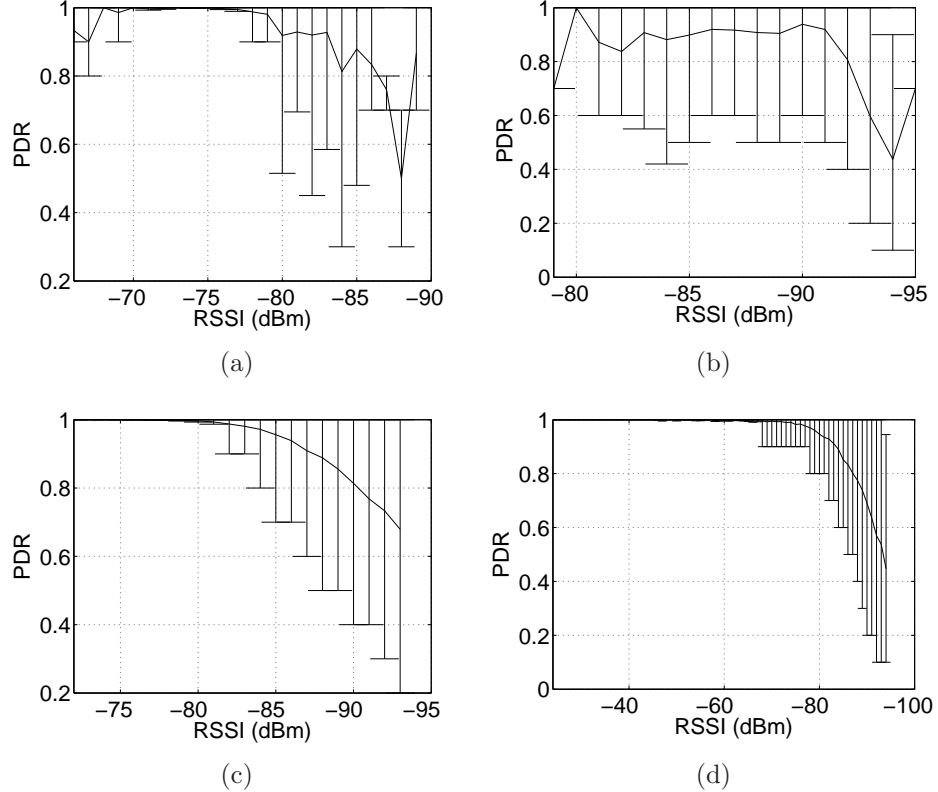


Figure 2.5: RSSI to PDR mappings for all considered links: (a) strong, (b) weak, (c) dynamic, and (d) mobile. Here a line represent the average PDR a RSSI maps to, and the bars show the dispersion of the PDRs, of which 90% PDRs are within the bars.

in the strong link, Fig. 2.5(a), RSSI from  $-72 \text{ dBm}$  to  $-74 \text{ dBm}$  has average PDR around 1 and the dispersion is very small. It is due to the fact that majority of packets in this link were received within this RSSI range. The rest of the RSSIs were rarely received, thus have large dispersion in mapping. For the weak link, Fig. 2.5(b), the range of RSSI is small. When the RSSIs are  $-91 \text{ dBm}$  or higher, the average PDR is above 0.9. The dispersion for all the RSSIs are relatively large compared to the other links due to the features explained in the second observation above. The dynamic link and mobile link, Fig. 2.5(c) and Fig. 2.5(d) respectively, show similar characteristics. In both cases, when RSSI is relatively high, the mean is close to 1 with small dispersion. However, as RSSI decreases, the correlation between RSSI and PDR decreases as well and larger dispersion can be observed.

### 2.3.3 HSDPA channel quality traces

#### HSDPA channel modeling

There are plenty of works which try to model the HSDPA channel. We can divide them into two types, network level and link level. For the network level ns-2 simulator users. [74] [100] [86]. Some physical level simulators are also published such as [26], [66], [29]. Eurane simulator [23] is a widely used simulator and we integrate the IEEE 802.11 ad hoc network to the UMTS system in this simulator. Therefore, we would like to have good simulation trace input to analyze the performance of the integrated network.

We generated the Enhanced UMTS Radio Access Network Extensions for ns-2 (EURANE) simulation input trace file by the following channel model, which is depicted in Fig.2.6. It is almost the same as EURANE. Since the intra-cell and inter-cell interference is small and changes very little compared to the propagation channel variation, constant value is used to represent them. Three major components in Path Loss (PL) are the Distance Loss (D), Shadow fading (S), and Multi-Path fading (M). We use the formula

$$\overline{D}(dB) = \overline{D}(d_0) + 10n \log \left( \frac{d}{d_0} \right), \quad (2.2)$$

and

$$S(d + \Delta d) = aS(d) + b\tilde{\sigma}N, \quad (2.3)$$

to represent the Distance loss and Shadow fading [27] in which  $d$  is the distance between mobile gateway and 3G cellular network base station. For the Multi-path Fading, we assume Rayleigh fading channel and use the Matlab function *rayleighchan* which is built based on [39] to generate trace file. The Path Loss is given by  $PL = D + S + M$  in each Transmission Time Interval (TTI) and final SNR value is generated by formula as below.

$$SNR = P_{TX} - 10 \log_{10} \left( 10^{\frac{I_{Intra}}{10}} + 10^{\frac{I_{Inter}+PL}{10}} \right), \quad (2.4)$$

The calculated SNR values are further converted to the Channel Quality Indicator (CQI) and form some trace files which depict the channel variance. Each simulation run lasts 200s and the mobile gateway circle around the base station with constant speed.

#### HSDPA channel generated traces

In this section, we use two approaches to check if the input SNR files generated by our model are close to the samples provided by EURANE which

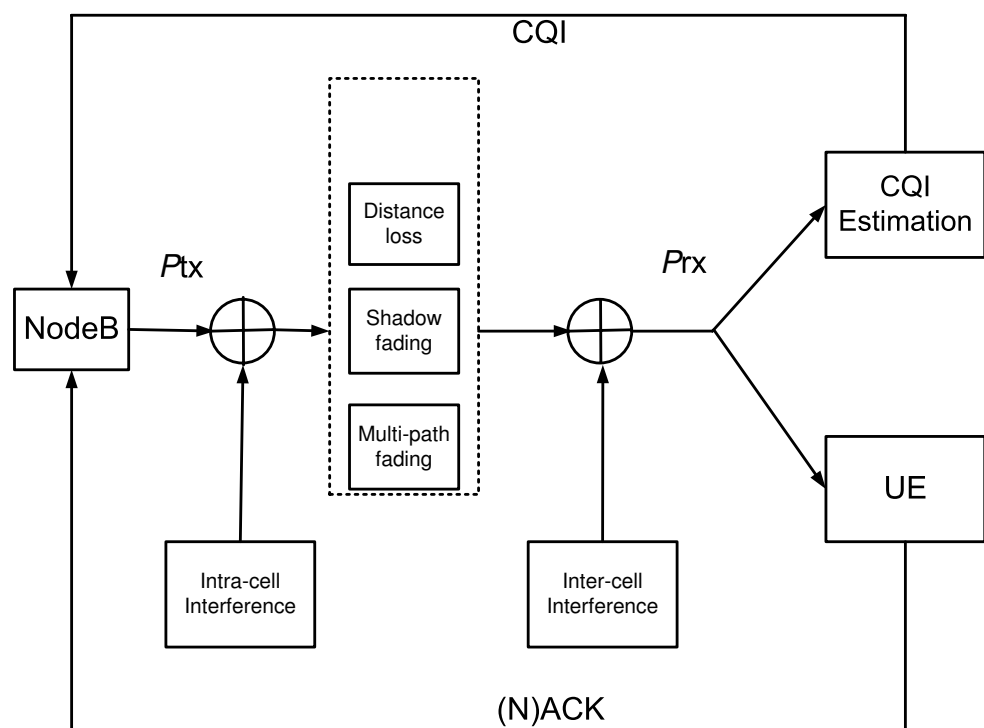


Figure 2.6: HSDPA channel model.

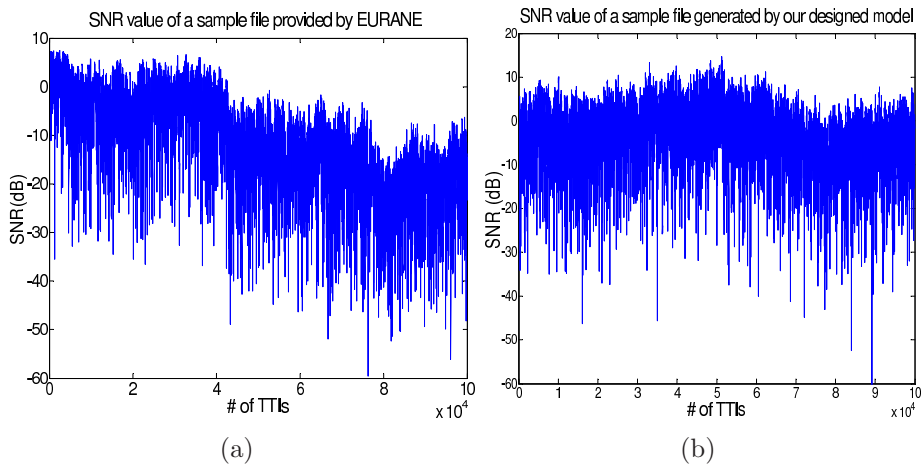


Figure 2.7: Comparison of EURANE and generated trace: (a) EURANE, and (b) Generated by our channel model.

have similar scenario as our generated traces. The first approach is to directly compare the SNR values. Here we choose the sample file provided by EURANE. This file is produced when the initial position of the UE is 700 meters away from the NodeB. For comparison, we also produced a similar file by presetting some parameters such as the initial position the moving pattern and the moving speed. The initial position is set same as in the EURANE. However, there is no information about the moving pattern of the EURANE file. So we choose to let the HSDPA node moving around the NodeB with the same distance. The SNR values of the generated and EURANE files are shown in Fig. 2.7(a) and Fig. 2.7(b), respectively.

There is one SNR value for each TTI (2 ms) and totally the trace lasts for 200 s. As we described in the Section 2.3.3, the variance of SNR values are mainly decided by three factors in our model such as path loss, slow fading (shadow fading) and fast fading. The SNR variance caused by path loss is totally decided by parameters, such as the initial position of the UE from the NodeB, the moving pattern and the moving speed during the whole simulation period. And the other two factors provide random variance for either short time or long time. From Fig. 2.7, we can find these two kinds of random variance easily. The difference between every TTI represents the instantaneous random variance caused by fast fading. Another random variance caused by shadow fading is also represented by the variance for longer period as several thousand TTIs. By presetting those three parameters which can make very accurate decision on variance caused by path loss, we can make our generator good enough.

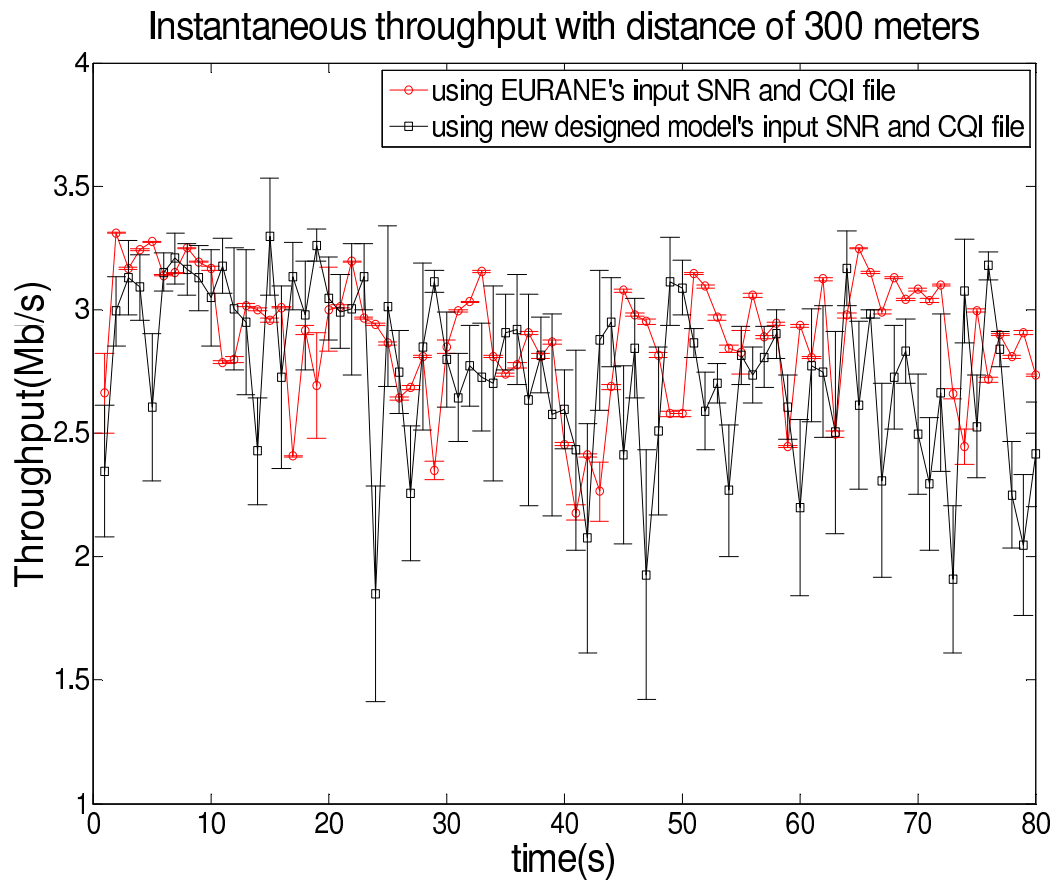


Figure 2.8: TCP over HSDPA channel.

After checking the SNR values, we also evaluate the instantaneous TCP throughput of the HSDPA channel using the SNR values generated by our designed model. In this test, we use the EURANE's file which the UE is 300 meters away from the NodeB as our comparison object. Then we generate 10 files using our SNR generator under almost the same condition as in EURANE's file. Using these files, we carried out the simulation 10 times to get the average values and their 95% confidential interval. In Fig. 2.8, we can see that generally the TCP behavior with these two simulation traces are also similar. We can see that the average TCP throughput values are almost in the same level. Further, the average TCP throughput values and the varying range of black line have similar characteristics and are close enough to the red line.

From these two testing results, we can conclude that our model is close enough to the EURANE's propagation model. In future it can be used to produce more SNR trace files to analyze the average TCP throughput performance or other characteristics of the HSDPA channel.

## 2.4 Chapter Summary and Discussion

In this chapter, we first introduce the basic concept of wireless link quality. We briefly introduced the three relevant radio technologies discussed in this thesis. Especially, we presented five common wireless link quality indicators and analyzed their advantages and disadvantages. Based on the experimental results and simulation, we investigated the three types of wireless channel's characteristics. Based on our measurement result, we conclude that the wireless link quality in WMN and WSN is very dynamic based on different environment and link settings. Better link quality estimation methods need to be proposed for estimating the wireless links.



# Chapter 3

## Wireless Link Quality Estimation

### 3.1 Introduction

In the previous chapter, we discussed wireless link quality for three popular radio technologies. In this chapter, we will focus on how to estimate the wireless link quality using the available wireless link quality indicators. The methods that are used to estimate a certain wireless channel quality are called wireless link LQE methods.

Due to the broadcast nature of the wireless medium in IEEE 802.11b/g-based mesh networks and IEEE 802.15.4-based sensor networks, each node may form many links with its neighbors in a large network. Varied data rates and data packet sizes result in different link setups. To achieve high connectivity and end-to-end throughput, nodes must intelligently select link data rates and efficient routes. Wireless link quality, usually measured by PDR, is the fundamental metric by which data rate and route selection are optimized [8,9]. Therefore efficient and accurate LQE methods are pivotal to the effective operation of wireless networks. However, there are multiple factors that affect PDR, predominantly SNR, shadowing, multi-path, interference, and packet collisions, which make effective LQE challenging. Previous results indicate that link quality can differ significantly with different propagation environments [115]. Nevertheless, even in the same propagation environment, different radio receivers react differently to the packet loss, which makes it even harder to accurately measure the link quality. Therefore, the LQE method must be able to adapt to the network environment to maintain accuracy. Unfortunately, our investigation shows that all known LQE methods do not meet the required objectives such as:

- (i) efficient measurement of the link quality
- (ii) adaptation of measurement result to a new environment, and
- (iii) remaining efficient.

The most popular LQE methods are based on the received packet count. Usually beacon [9] or unicast [45, 48] packets are sent periodically over each link. Later, transmitters count the number of acknowledged packets from each receiver. Due to the difference between data packets and probing packets<sup>1</sup> and inefficient neighbor discovery, previous methods for estimation results will not be accurate enough. Among the newer LQE methods, a promising approach is based on the correlating SNR levels with PDRs, as proposed independently in [93, 109, 111]. However, the evaluation of this method is very limited and its potential is still unknown.

The issue of LQE adaptation to a new network environment is not well discussed in the literature. Most of the LQE methods, that we are aware of, are evaluated using limited network scenarios, e.g. with limited transmission rates, and in limited propagation environments [85, 95]. The impact of the rate and route selection by the different LQE methods are unknown. Most importantly these methods have not been evaluated in real-world scenarios. Finally, some proposed LQE methods require additional hardware to work, like location information [107], which are not usually available in IEEE 802.11 devices and introduce low overhead.

Therefore, the *objective* is to propose a highly efficient LQE method that is accurate, rapidly adaptable, environment aware, easily implementable in IEEE 802.11 or IEEE 802.15.4 devices, which imposes no additional requirements on the hardware.

This chapter is organized as follows, in Section 3.2, we introduce the related work about all kinds of current LQE methods. In the following sections, we introduce two types of our proposed LQE methods and their performances. In Section 3.3, we introduce our linearization method. In Section 3.4, we introduce another method which is called SNR mapping LQE method. We have also done a mathematical analysis for most of the LQE methods in Section 3.5. Finally, we summarize the chapter in Section 3.6.

## 3.2 Related Work

In Section 3.1 we have briefly explained the existing LQE methods. In this section, we look at the LQE methods closely and compare them with our proposed LQE method in Section 3.3 and Section 3.4.

---

<sup>1</sup>By probing packets we mean a packet that has been sent separately from regular data packet to assess the link quality.

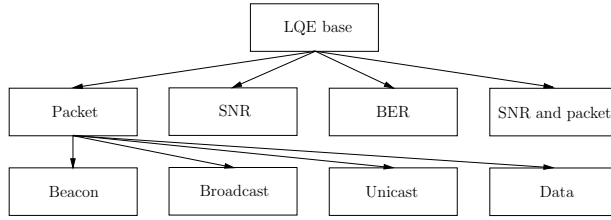


Figure 3.1: Classification of LQE methods.

LQE in IEEE 802.11 wireless networks can be categorized into four major types, based on the information sources for the estimation: packet-, SNR-, BER-based and the combination of those methods, see Fig. 3.1.

### 3.2.1 Packet-Based LQE

The direct method to assess wireless link quality is to count the number of packets received over each link in the network for a predefined unit of time. For the results of PDR properties in wireless network, see [4, 38]. Since different types of packets are used, packet-based LQE can itself be categorized into four methods: beacon packet-, broadcast packet-, unicast packet- and data packet.

**Beacon Packet-Based** The first LQE method used beacon packets (40 B broadcast packets sent at 2 Mbps rate, also known as “hello” packets) to probe the link. ETX [20] and ETT [9] are two beacon-based metrics. Several papers have reported the inefficiency of this method due to the fundamental difference between beacon packets and data packets [45, 48, 110].

**Broadcast Packet-Based** To resolve the problem of beacon packet-based probing, nodes assessing PDR can broadcast packets equal in length to data packets, transmitted at any desired data rate<sup>2</sup>. The overhead of this method is much higher than the beacon packet-based probing. This is because rate adaptation requires the link quality for all data rates and packet lengths. Thus many test packets must be broadcasted to cover all cases.

**Unicast Packet-Based** An approach to solve the difference between broadcast probe packets and data packets transmitted with various data rates and sizes was to use unicast packets to probe the links [45]. In [25], a combination

---

<sup>2</sup>Interestingly, we were unable to find any studies that proposed and evaluated such a method in isolation.

of broadcast and unicast packet probing were used. When no unicast traffic was passing through the link, broadcast packets were transmitted and used for LQE. A method for very short term LQE with unicast packets was proposed in [3], while in [43], a mathematical model was developed to account for packet retransmissions within a single coherence time of time varying channel, which could be used to predict the state of the link. We note that the short term LQE is of limited use in real networks, since frequent LQE messages would saturate the routing process. In [106], the authors use spatial correlation and unicast packet to predict the link quality and find that different PDR is observed for different locations. To implement this method in a real network, localization hardware would have to be supported by all devices. The most significant drawback of this method in this approach is detrimental effect on the network connectivity.

**Data Traffic-Based** To alleviate the problems of probing with broadcast or unicast packets, authors in [107] have proposed to use the latest data packets flowing through the link generated by the users, for estimation of PDR. Better performance in terms of throughput has been observed compared to broadcast-based probing. However, this LQE method considers only heavily loaded links. For lightly loaded links, this method is ineffective and results in an incomplete link state information for the network.

### 3.2.2 BER-Based LQE

Yet another approach to estimate the link quality is to utilize BER information [7, 51]. The estimation of accuracy in this method is better than the packet-based LQE since it conveys more information on the link quality and is retrieved directly from the physical layer. It will not introduce communication overhead. However, as indicated in [94], this method causes significant processing overhead since it requires processing of a large amount of data. Primarily, BER information is not reported by commodity wireless cards which makes this method hard to implement on standard IEEE 802.11 devices.

### 3.2.3 SNR-Based LQE

This LQE method is of high relevance in the context of this chapter. The authors of [20] have noted a low correlation between the SNR observed over the packet counting interval and measured PDR. This incorrect conclusion was a result of combining data measurements from different environments,

receivers and links. It was later found that SNR can actually be a good indicator of wireless link quality [30, 54, 85, 87, 115]. The SNR-based LQE method was evaluated independently by the authors of [109, 111] and [41, 80, 93, 108]. However, the accuracy of these methods except [41, 108], were not compared to any other estimation method. Moreover, except for [80], a static SNR to PDR mapping profile was used. Thus adaptation to different environments was not considered. Authors in [95] have proposed different metrics that correlate with packet delivery probability and have used machine learning techniques to select the best metric in the LQE process. Nevertheless, the fact that different rates in IEEE 802.11 have different SNR profiles, as pointed out in [108, 111], was not taken into account in the analysis.

A separate discussion is required for [108]. Although a correlation between SNR and PDR has been well discussed, a piecewise linear approximation of this relation has been used in rate adaptation process, see [108, Fig. 7], which loses throughput gain in transitional regions of SNR map [115, Fig. 3]. Also, to obtain the SNR map, the authors required a calibration process in which, an unrealistic interference-free channel was assumed. Further, the profiles have been obtained by probing the link with very high intensity, i.e. every second for 20 ms, which creates huge overhead for the device. But the most significant drawback of this method is the usage of beacon packets of with sizes different from that of the data packets to obtain SNR profiles, which as we pointed out earlier, results in inaccurate rate adaptation.

The work from Dmitri Moltchanov is also related to this chapter, especially for the mathematical modeling part in Section. 3.5. In work [67–69], the authors model the channel using the Markov process and have good description of distributional and autocorrelational properties of empirical data. In the work [67], the frame error traces are modeled and in the work [68], the SNR process have been modeled. The work [69] modeled the relation between SNR to bit error rate, then a cross layer approach is used to further use this relation to predict higher layer packet loss. However, those works are focused on the autocorrelational properties for the packet errors and SNR values. While our work look at the SNR value series in a one dimensional view and we are more focused on the impacts of several factors to the SNR and PDR mapping. Those factors include the types of packets, different environment, different estimation intervals and so on.

Table 3.1: Qualitative Comparison of LQE Methods (Desired Performance: Update Ability–High, Accuracy–High, Overhead–Low)

Information Source	Update Ability	Accuracy	Overhead
Packet (beacon) [9, 20]	Low	Low	Low
Packet (broadcast)	Low	Medium	High
Packet (unicast) [3, 45, 48, 106]	Low	Medium	High
Packet (data) [107]	High	High	High
SNR [41, 80, 93, 108, 109, 111]	High	Medium	Low
BER [7, 51]	Medium	High	High
Packet and SNR [110]	Low	Medium	Low

### 3.2.4 Combined Methods of SNR- and Packet-Based LQE

Since, individually, SNR- and packet-based LQE have advantages and disadvantages, authors in [94] have remarked to use the combination depending on the environment and LQE accuracy. Works in which such combined methods were proposed and evaluated independently are [25, 109, 110]. The estimator was a weighted function of the individual packet- and SNR-based LQEs. However, the metric had limited practical application, since the weight needed to be set individually for each environment and data rate, among others, and the learning process for the optimal weight involved the entire history of network operation. This combined method has been described further in detail in Section 3.3.

A qualitative comparison of all existing LQE methods is given in Table 3.1. We compare different methods in three aspects i.e., update ability, accuracy and overhead.

## 3.3 Our Proposed Linearization Method

Various information sources can be used to estimate the link quality, such as counting the received hello packets, observing the amount of Media Access Control (MAC)-level retransmissions, or using received packet signal strength [109]. In this section, we describe our proposed linearization method with best performance in a stable environment.

### 3.3.1 Proposed linearization LQE mechanism

In this section, we combine the hello packet delivery ratio,  $R_H$  and received hello packet signal strength,  $S_H$  to estimate the packet delivery ratio,  $\hat{R}$  and compare it with the actual data packet delivery ratio,  $R_D$ . The measurements of  $R_H$ ,  $S_H$ , and  $R_D$  are described in Section A.

Each LQE source has its own advantage. For example,  $R_H$  is simple and stable, while  $S_H$  need not to inject new packets into the network, and hence, it is costless.  $S_H$  is fast and does not depend on the packet type and data rate.  $R_D$  is the most accurate one. However, in real networks, always there will not be data traffic on each potential link. Therefore,  $R_D$  is always not available.

To leverage the advantages of all LQE sources, we propose the following method to estimate the packet delivery ratio based on different situations:

1. When there is enough data traffic on the link, we use the feedback about the MAC-level retransmissions,  $R_D$ ,
2. When a node first joins the network, we use  $S_H$  to estimate the packet delivery ratio,
3. Otherwise, we use the  $S_H$  to adapt fast to link dynamics and compensate the difference of transmission rate and packet size between hello and data packets.

For situation 3, we propose packet delivery ratio estimation as follows:

$$\hat{R} = C \left( 1 - \frac{S_H}{S_{min}} \right) R_H, \quad (3.1)$$

where  $C$  is a constant multiplier and  $S_H$  is normalized with the minimum signal strength level,  $S_{min} = -95$  dBm. Two extra rules to this formula are: (1) If the resulting  $\hat{R}$  is larger than 1, then the packet delivery ratio is estimated to be 1. (2) If the signal strength is larger than  $-50$  dBm, the  $\hat{R}$  is also estimated to be 1, no matter what the  $R_H$  value is. The multiplier  $C$  is a constant that may depend on different conditions, such as transmission rate and packet size. To find the proper value for  $C$ , we made a set of measurements on a real test-bed, which has been discussed in Section 3.3.2. In this section, this formula with the two extra rules is called as the *proposed method*.

Moreover, the  $C$  value can also be adjusted when there is huge amount of traffic over the link. A machine learning technique can be used to decide when the nodes need to adjust each  $C$  value towards the neighbors. To find

a proper value of  $C$  in our experiments, we made a set of measurements on a real test-bed, which are presented in Section 3.3.2.

[93] uses SNR to estimate the channel. If the SNR is used instead of signal strength, there will be a different  $C$  value<sup>3</sup>. In our experiments, the noise level is constant most of the time and the maximum difference in an office environment is 1 or 2 dbm. Hence, using SNR or signal strength directly will achieve the same result. Therefore, we may just as well use the SNR value in the place of  $S_H$  in our method. We can directly change the formula as follows:

$$\widehat{R}_{SNR} = C \cdot SNR_{current} \cdot R_H, \quad (3.2)$$

$$\widehat{R} = \min(1, \widehat{R}_{SNR}); \quad (3.3)$$

The  $C$  value in Eq. 3.1 and Eq. 3.2 is a linearization of the correlation between the  $S_H$ ,  $R_H$  and  $R_D$  or between  $SNR_H$ ,  $R_H$  and  $R_D$ . We show this approximation for SNR in Fig. 3.2 with some different values of  $C$ . We can see that a  $C$  between 0.06 and 0.07 best approximates the measurements.

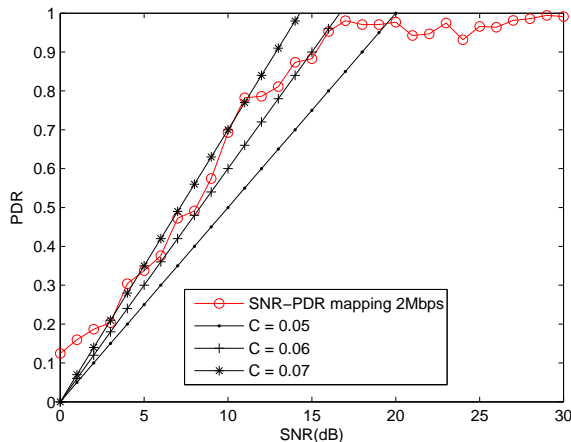


Figure 3.2: The  $C$  value for SNR formula.

To get this result, we carried out an experiment in which we collected 1800 SNR and PDR correlation points during a communication process. For a certain SNR value, we averaged all its PDR values. We plotted each SNR value and its average PDR value in Fig. 3.2. During the communication process, the  $R_H$  does not change much and is mostly the  $SNR_H$  or  $S_H$

---

<sup>3</sup>When a node has neighbors, it can gather information of the  $S_H$ ,  $R_H$  and  $R_D$  via the initial communication with its neighbors or by overhearing the communication of its neighbors

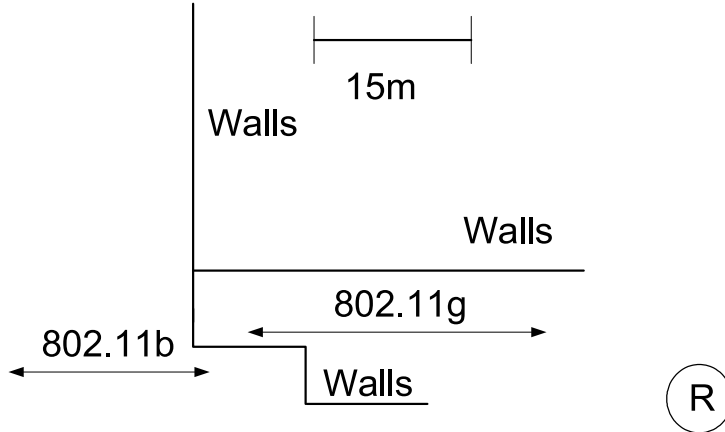


Figure 3.3: Experiment topology.

that actually determines the estimation. The  $C$  value is the slope of the approximation lines, which we have used to describe the  $SNR_H$  or  $S_H$ 's correlation with  $R_D$ . Different input values, such as  $SNR_H$  or  $S_H$ , or different data rates, environments and other impacting factors will affect the  $C$  value. Hence, our aim is to find a  $C$  value that brings the estimation line close to the actual correlation.

### 3.3.2 Experimental evaluation

To show the effectiveness of the proposed estimation method, we carried out real measurements. The experimental scenario is shown in Fig. 3.3 and is in an indoor environment. Depending on the maximum range that can be achieved by a specific data rate, the experiments are grouped into two scenarios based on modulation differences. One of the nodes was stationary (R in Fig. 3.3) and the other was mobile (the mobile node's moving range is marked as an arrow and other lines are the walls in the figure). The path is designed so that the mobile node moves from the point where it starts to drop packets until it reaches the point where it can not receive any more data packets from the stationary node. This means that the sender tries to experience a link with a PDR variance from 0 to 1 and back again. The speed of the mobile node was one meter per second. Both nodes constantly sent hello and data packets at the same time. Samples were collected for a period of 300 seconds. The PDR will change from 0 to 1 or vice versa in about 60s. Therefore, we have 5 rounds in our experiment.

For performance comparison, we defined the average absolute percentage

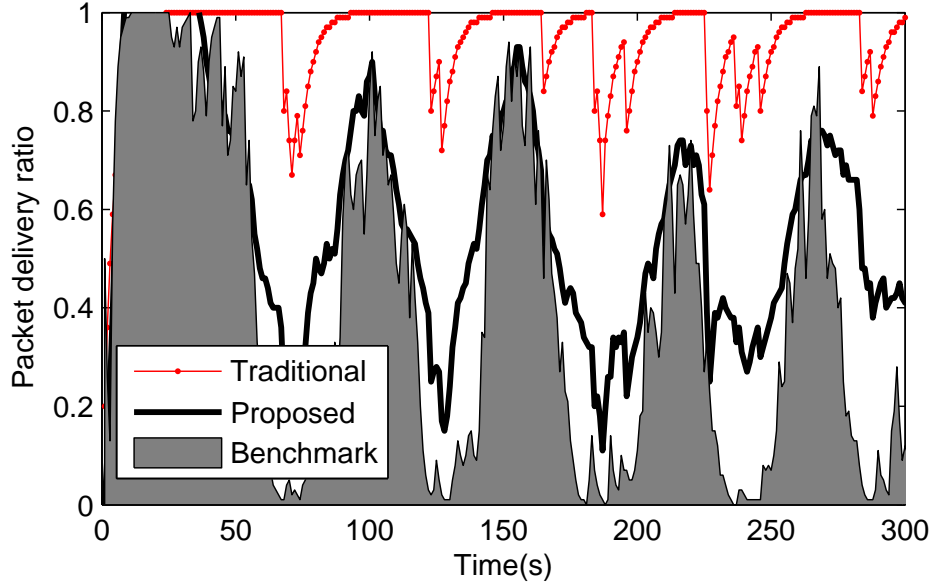


Figure 3.4: The effectiveness of the estimation. (Rate is 36 Mbps,  $C^* = 2.3$ )

deviation  $D$  as:

$$D^{\text{method}} = \frac{100}{M} \sum_{i=1}^M |r_{d_i} - r_i^{\text{method}}|, \quad (3.4)$$

where  $M$  is the number of samples,  $r_{d_i}$  is the sampled data packet delivery ratio,  $r_i^{\text{method}}$  is the estimated sample delivery ratio, where `method` is either the traditional hello packet estimation,  $R_H$  or, our proposed  $\hat{R}$ .

In this experiment, we used a fixed transmission rate of 36 Mbps. Based on the measurements, we could find the  $C$  constant that minimizes the error according to Eq. 3.4 as  $C^* = 2.3$ . As can be seen in Fig. 3.4, our proposed  $\hat{R}$  with  $C^* = 2.3$  estimates  $R_D$  better than the traditional hello packet-based method  $R_H$ .  $R_H$  hardly predicts the link quality variance in this scenario. The errors, according to Eq. 3.4, are  $D^{\hat{R}} = 18\%$  and  $D^{R_H} = 50\%$  respectively. Hence, our method estimates the link quality much better than the traditional  $R_H$ .

The main reason that  $D^{\hat{R}}$  is more accurate is that there is some correlation between the signal strength and  $R_D$ . When the channel changes very fast, signal strength adapts quickly. However, signal strength tends to fluctuate more. Therefore  $R_H$  is multiplied in Eq. 3.1 to generate more stable predictions.

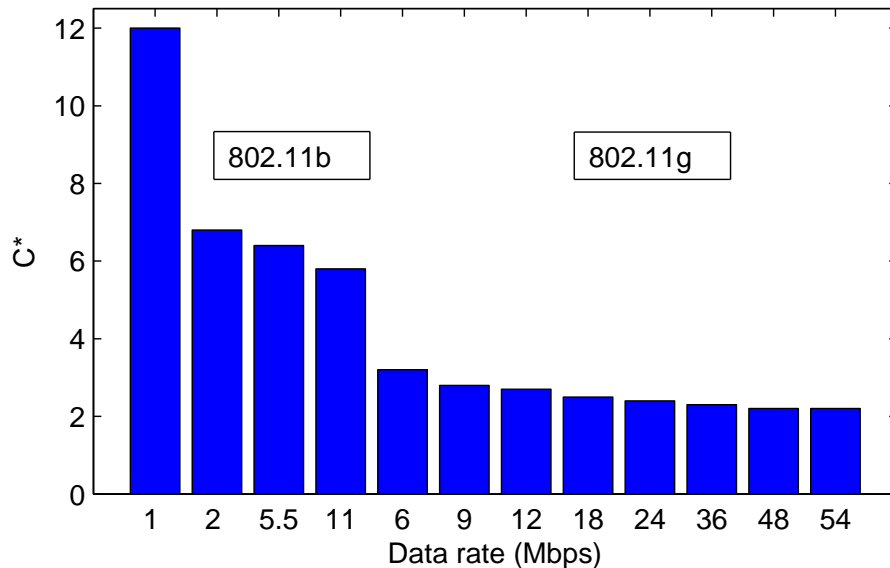


Figure 3.5: The best constant value for the 12 data rates.

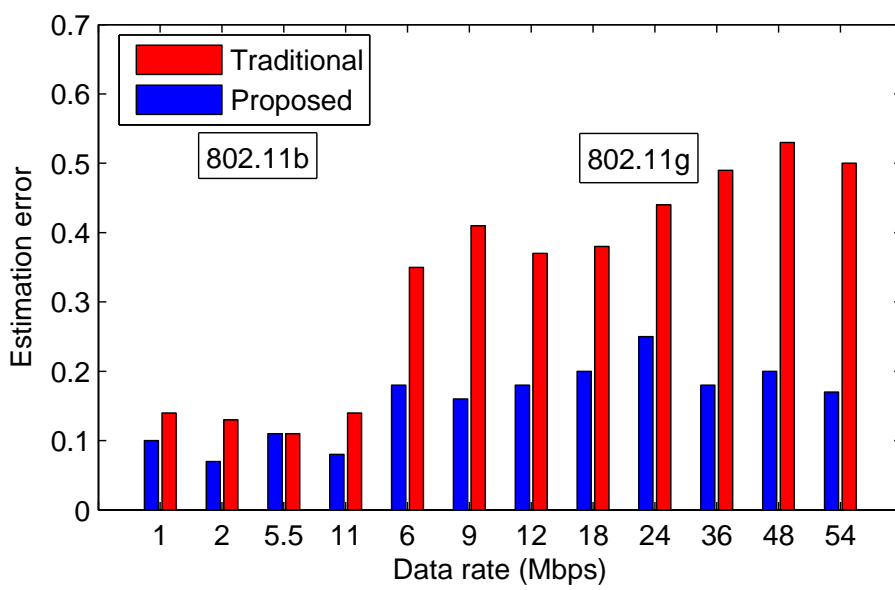


Figure 3.6: The estimation error of the two methods.

### Different data rates

One question that remains is the determination of the variation of  $C^*$  with the situation. The most obvious quantity is the variation in transmission rate. In this paragraph, we analyze how different transmissions rates affect  $C^*$ .

To analyze this, we carried out the same experiment, but with different transmission rates. The optimal multiplier value  $C^*$  for all twelve IEEE 802.11 transmission rates are shown in Fig. 3.5. We can see that when higher data rates are used, smaller  $C^*$  produces more accurate estimates. The data rate does not affect the delivery ratio of hello packets because the hello packets use the lowest data rate and a fixed small packet size. For the same experimental conditions, the data packet delivery ratio decreases when the data rate is increased and  $C^*$  is decreased. Notice that  $C^*$  converges to a value around 2.0, as the rate increases.

In Fig. 3.6, we plot the error made by the proposed method and the traditional method. The improvement is very obvious for high data rates (36, 48, 54 Mbps). This improvement decreases with the data rate, which is due to the smaller difference between data packets and hello packets. An interesting effect is that for the IEEE 802.11b data rates, the traditional method causes a much smaller error while our proposed method still outperforms it.

### Other impacting factors

In our experiments, we found that the transmission rate impacts the optimal  $C^*$  value. To analyze if other factors impact also the estimation method, we carried out experiments with different configurations, such as, different packet sizes, traffic loads, speeds, and mobile patterns.

First, we conducted an experiment with four different packet sizes using the same data rate, 54 Mbps in the setup as before. We use the dot to indicate the optimal  $C^*$  value in each situation in Fig. 3.7. Fig. 3.7(a) shows that as the packet size increases, the optimal  $C^*$  value decreases. Larger packet sizes lead to larger packet loss ratios. For all packet sizes, the input parameters  $S_H$  and  $R_H$  are almost the same, since they are only affected by the channel conditions. Therefore,  $C^*$  is generally smaller for larger packet sizes. When the data packet size becomes small, the difference between the hello and data packets becomes less and the estimate becomes less accurate.

Second, the data traffic between the two testing nodes used in previous experiments had a rate of 50 UDP packets per second. Based on Fig. 3.7(b), we can see that more traffic load leads to a larger  $C^*$ , because of larger collision probability between the data and hello packets. Meanwhile, the

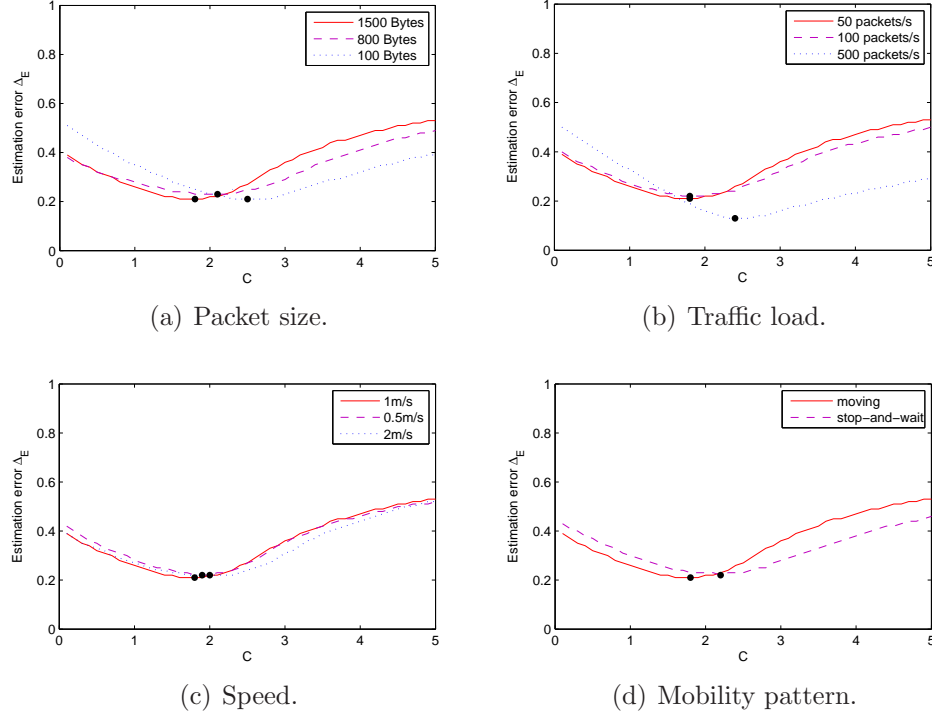


Figure 3.7: Different impacting factors for the estimation method.

data packet delivery ratio is not affected when the traffic load increases. The right side of Eq. 3.1 becomes smaller and hence a larger  $C^*$  is required.

Third, another potential impacting factor is the speed of the nodes. Previously, we assumed a constant speed of one meter per second for the moving node. In Fig. 3.7(c), we show the effect of double node speed. There is almost no impact of the speed on the optimal  $C$  value. The small difference in pedestrian speed will not lead to a variance in any of the components of Eq. 3.1.

Fourth, in all our previous experiments, we assumed a node moving with a constant speed and trajectory. In these experiments, we used the stop and wait scheme. That is, the node stops at every 4 meters for a period of 5 seconds and then walks for another 5 seconds. Based on the results in Fig. 3.7(d), we can see that the mobility pattern does not have a large effect on Eq. 3.1 due to the same reason as we observed for speed.

These experiments show that the transmission rate, packet size, and traffic load have a large impact on  $C^*$ . Thus, for an optimal implementation of our packet delivery ratio estimation method in a real protocol stack, the effects of the transmission rate, packet size, and data traffic intensity should also be

considered. We draw the conclusion that, these factors does affect, however, the performance degradation caused by a sub-optimal  $C^*$  is not large. To obtain the optimal  $C^*$  for all scenarios, a machine-learning mechanism can be used to adapt all impacting factors and select the optimal  $C^*$  for a certain combination of the impacting factors.

## 3.4 Our Proposed SNR Mapping Method

### 3.4.1 Proposed method

In the approach described in this section, we also used a combined method to estimate the link quality. However, instead of signal strength, we used the SNR profile based mechanism and the SNR profile estimation is the dominant factor for the estimation method. We measure link quality with PDR. The proposed SNR profile based LQE is based on two independent methods of evaluating PDR: (i) SNR profile and (ii) received packet counts. Depending on the environment and the required LQE efficiency the appropriate method will be chosen. The proposed LQE flow graph is depicted in Fig. 3.8. We will describe and discuss each method in detail. However, due to the condition constraint currently, this selection of estimation source based on the context is not used in the measurement and most of our proposed LQE measurement results are refer to SNR profile method.

#### Broadcast packet counting

Every second we transmit a fixed size broadcast packet of 1.5 kB for each supported data rate. For each data rate, every receiver calculates the PDR using an EWMA filter as Eq. 2.1. However, in this formula, we do not count the hello packet, instead we count the broadcast packet.

It is important to note the differences between our packet counting LQE approach and the LQE used in calculating ETX [20, Eq. (1)] and ETT [9] metrics. Firstly, our method requires only one packet sent per time interval to obtain a PDR estimate, while the LQE in ETX requires  $w$  broadcasting intervals (in [9, 20]  $w = 10$ ) to calculate the delivery ratio. Secondly, our method continuously updates the PDR, while the LQE of ETX discards previous measurements for every  $w$  broadcasts. Finally, in contrast to [9, 20] we assume a reciprocal link, i.e., the same PDR is experienced in the forward and reverse links<sup>4</sup>. Our assumption is supported by recent measurements,

---

<sup>4</sup>For a LQE method using unicast packet-based probing assuming non-symmetric links please refer to [48].

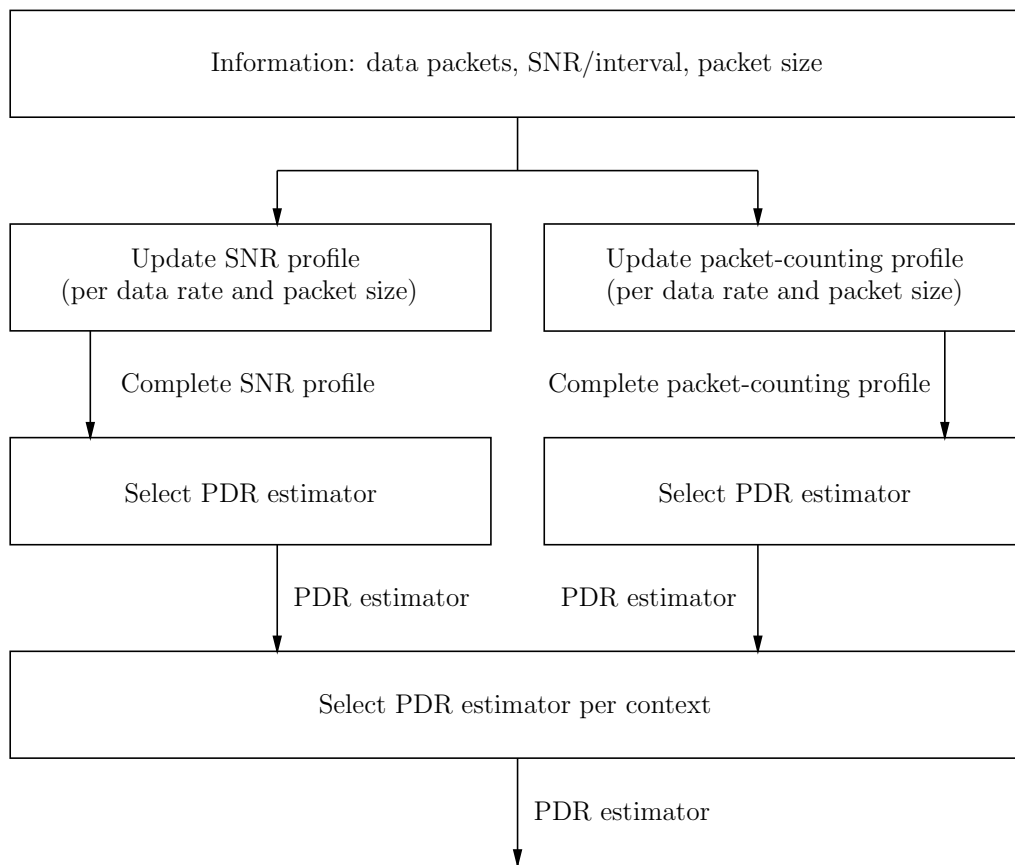


Figure 3.8: Proposed IEEE 802.11b/g LQE system (PDR block).

e.g. [88, Fig. 5] and simplifies the implementation significantly, since it does not require separate broadcast packets (in this case 60 B sent in  $R(2)$  rate) to account for the lost acknowledgement packets on the reverse link.

### SNR profile

After an initial node bootstrap, a node sends unicast packets of 1.5 kB at 10 packets per second, and at every IEEE 802.11b/g data rate in  $R$  over every link. During the period  $t$ , each node is able to send  $w(t)$  successfully transmitted packets, while the sender counts for every acknowledgment before new unicast packet is transmitted. For a certain period of link probing, we calculate the PDR as:

$$E_{R(k),\Psi} = \frac{1}{w(t)} \sum_{i=1}^{w(t)} X_{R(k),i,\Psi}, \quad (3.5)$$

where  $E_{R(k),\Psi}$  is the mean PDR for discrete SNR value  $\Psi$  and data rate  $R(k)$ ,  $X_{R(k),i,\Psi} = 1$  when a packet transmission was received at discrete instants of time  $i$ , SNR  $\Psi$  and rate  $R(k)$ , and  $X_{R(k),i,\Psi} = 0$ , otherwise. This way we create a mapping relation between SNR and PDR, which we refer to as SNR map or SNR profile, for all IEEE 802.11b/g rates. This procedure is needed for devices that have no SNR maps, such that device deployed elsewhere will be able to easily update its existing map without necessary probing. SNR values  $\Psi$  are registered once per second, i.e., once per 10 transmitted unicast packets. Ideally, a profile should be created for each packet size. It is important to note however, that in the current Internet approximately 50% of the traffic is sent with the Maximum Transmit Unit (MTU) size, where the MTU for IPv6 is 1.268 kB, for IEEE 802.3 1.492 kB, for Ethernet II 1.5 kB, and for IEEE 802.11 2.272 kB [101]<sup>5</sup>. In our implementation we chose 1.5 kB packets, since the majority of Internet traffic is from wired network and wireless network gateways relay packets unaltered from the wired domain.

Due to the constant changes in the propagation conditions, as well as possible changes in the network environment, results of the initial measurements must be updated. The measurement result is updated as:,

$$E_{R(k),i,\Psi} = \frac{\alpha_s}{w(t+1)} \sum_{l=1}^{w(t+1)} X_{R(k),l,j} + (1 - \alpha_s) E_{R(k),i-1,\Psi}, \quad (3.6)$$

---

<sup>5</sup>It was also noted in [101] that about 40% of packets are 40 B long, which accounts for TCP ACK packets. The remaining 10% of packets are scattered between two extremes, i.e ACK and MTU.

if and only if a node sends data traffic with a given packet size. In the above equation,  $E_{R(k),i,\Psi}$  is the estimated SNR profile mapping point for SNR  $\Psi$  at discrete time instant  $i$  and rate  $R(k)$  and  $\alpha_s$  is the smoothing factor, which is specific to the network environment. Eq. 3.6 smoothens the incoming measurements of  $E_{R(k),i,\Psi}$  with a EWMA filter, just as in (2.1). The complete SNR profile for one node and one data rate is then a  $n$ -tuple

$$E_{R(k),\Psi} = \{E_{R(k),i,\Psi(1)}, \dots, E_{R(k),i,\Psi(n)}\}, \quad (3.7)$$

where  $\Psi = \{\Psi_1, \dots, \Psi_n\}$  is a  $n$ -tuple of all SNR values reported by the physical layer. Note that due to the link reciprocity the same profile has been assumed for both the reverse and forward directions of a link. The profile occupies  $S = P|R|\bar{N}$  B of uncompressed disk space, where  $P$  is the size in Bytes of individual SNR profile for each packet size (in our case  $P = 8$  kB). For example, in the case of  $\bar{N} = 10$ ,  $S = 960$  kB.

### Method selection based on network environment and required LQE accuracy

Environment (or more generally context) awareness can indeed improve the LQE process. Context encompasses operating state of a device: whether it is indoor or outdoor, moving or not, whether the communication has LOS or not, and what level of LQE accuracy is required by the applications. Information about the environment can be manually entered by the user or automatically detected by the device itself. In the latter case, the node must be location aware, which may require an additional hardware. In the proposed LQE system in Fig. 3.8, context is needed to decide which PDR method to use at a given moment. We show in next section that in very limited scenarios packet based counting achieves better performance than SNR profile-based LQE. Context, however, is not absolutely necessary, since the SNR profile can be updated, which leads to a comparably accurate LQE after some learning time. This will also be shown in next section.

#### 3.4.2 Measurement scenarios

The experimental test-bed is described in Appendix A in detail. Here, we only describe the experimental scenarios for the indoor and outdoor results.

##### Indoor

The proposed SNR based LQE method has been evaluated for different measurement scenarios using five nodes in the indoor scenario. We have evaluated

the LQE process, rate adaptation and routing independently for different scenarios. The LQE result is presented in this section as described below.

In evaluating the proposed link quality aware IEEE 802.11b/g network we have set up six different scenarios referred as T1–T6. Scenarios T1–T5 were setup at the cafeteria of Electrical Engineering, Mathematics and Computer Science department of Delft University of Technology. This environment was chosen purposefully, since it contained many walls, pillars, doors, etc., which presents a challenging propagation environment. In all except for one scenario, described below in Fig. 3.9, one pair communicated on channel 7 of IEEE 802.11g spectrum, which was least affected by other transmissions in our indoor environment. Finally, all the experiments were performed during late afternoon and night to reduce the probability of interference on that channel.

- T1 The sender was located at L1 while the mobile node moved along path 1 with the speed of  $\approx 1$  m/s. The experiment lasted 1 hour. This scenario was needed to evaluate the proposed method in a mobile environment and to observe the SNR mapping table for a broad range of SNR values. For 80% of path 1, the link had LOS and the remaining 20% was shadowed by a wall. The shadowed portion of the path was needed to obtain very low values of SNR. In LOS portion we could not obtain a SNR lower than 15 dB.
- T2 The sender was located at L1 while the receiver moved along path 2, in a stop-and-go fashion, i.e., the receiver resides in one location for 1 min and then moves 1 m away from the sender (in the case of LQE measurements), and waits 3 min, then moves 4 meters away from the sender (in the case of rate adaptation measurements). The whole process took about 50 min.
- T3 The same as T2, except the sender moved along path 2 and the receiver was located at L2.
- T4 The same as T3, with a third node located at F separated 20 cm from L2 and not involved in the same network. Node F broadcasted a large amount of traffic, i.e., 500 packets/s, at the same data rate and packet size as the sender at L1, but on a channel two slots away from that of the sender and receiver. This scenario served the purpose of evaluating the impact of non-overlapping channel interference on the proposed LQE method.
- T5 The same as T4, except the interfering node transmitted packets on the same channel as the sender and receiver. This scenario served

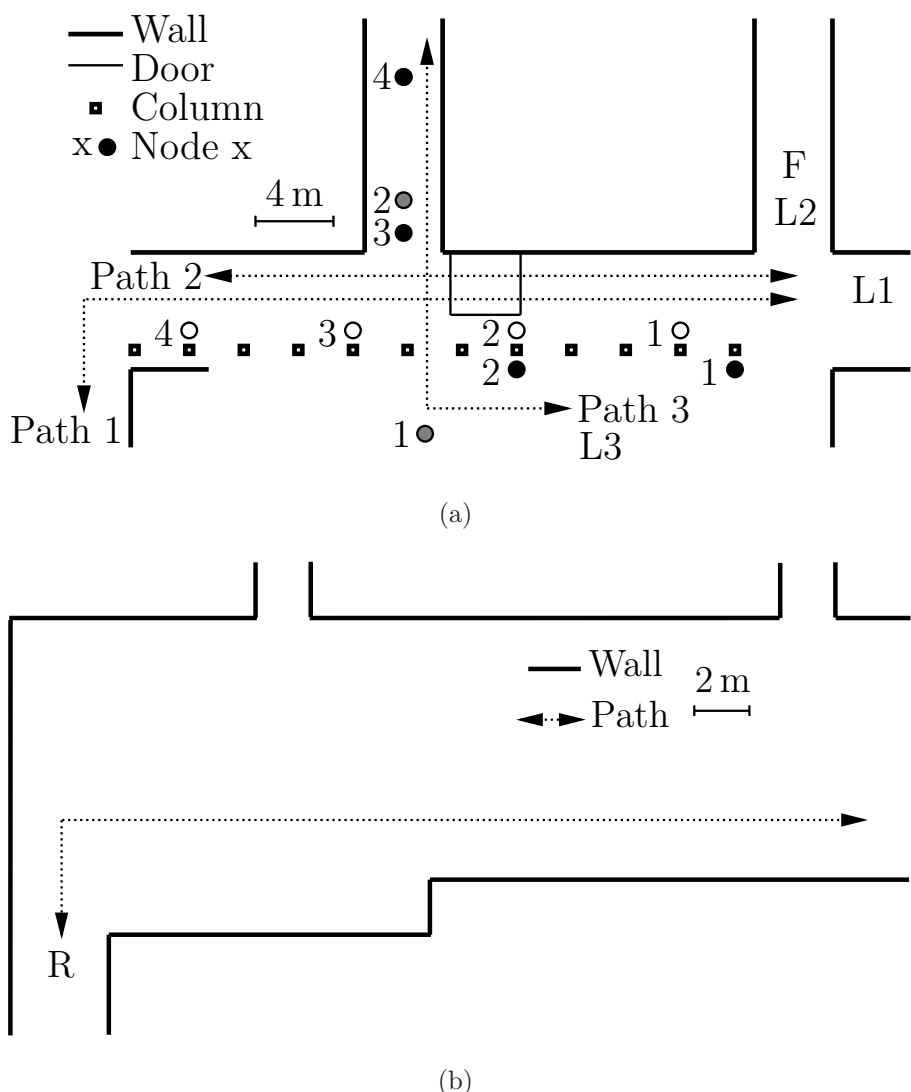


Figure 3.9: Different topologies used in the evaluation of the proposed network for experiments T1–T6 in (a) cafeteria, and (b) aula.

the purpose of evaluating the impact of co-channel interference on the proposed LQE method.

### **Outdoor**

The outdoor experiments were performed on the Quail Ridge Wireless Mesh Network [103]. The network was located in Napa County, California, on a southern peninsula of Lake Berryessa and consisted of hilly and densely forested terrain. There were 34 nodes at the time of testing, all placed at varying elevations due to the terrain spanning 2000 acres. Distances between nodes ranged from one kilometer to a few hundred meters. Directional antennas were used for point-to-point links on top of the hills, while omnidirectional antennas were used for lower elevations. The following experiment was performed.

- T6 A randomly selected sender sent data to a randomly selected receiver for about 30 minutes in all available data rates. This experiment was needed to obtain an SNR profile for an outdoor scenario.

### **Dynamic environment**

In order to evaluate the impact of the optimal  $\alpha$  in the broadcast packet counting based estimation and the variation of the SNR profile, we performed four more groups of experiments in four different environments: three indoor and one outdoor. In each scenario, several experiments were done to evaluate different impacting factors based on different configurations and environments. The distance between two laptops was chosen such that the channel has the medium link quality, just like in, [20]. The nodes were stationary during the experiments. In detail, the scenarios were as follows:

- S1 Scenario 1: Two laptops, with no line of sight wireless link were placed in an indoor narrow passage, where activity of people moving was limited;
- S2 Scenario 2: Two laptops were located at the ground floor of the Electrical Engineering, Mathematics and Computer Science department of Delft University of Technology. The wireless link between the two laptops was frequently obstructed by people entering and leaving the building, thus link quality was quite dynamic;
- S3 Scenario 3: The location was the same as S1, however one laptop was mobile and the other was stationary. The mobile laptop moved back

Table 3.2: Allan deviation  $A_D$  for different scenarios considered.

Rate [Mbps]	S1	S2	S3	S4
2	0.11	0.16	0.15	0.10
54	0.13	0.13	0.19	0.10

and forth from the stationary node with constant speed of  $\approx 0.8 \text{ m/s}$  to create link quality variance between 0 and 1;

- S4 Scenario 4: Two laptops were placed in a public park where no people's presence was observed and no WiFi transmissions were present. This scenario represented a rural area. The distance between two laptops was about 30 m.

To be able to evaluate the link quality variation difference of these four scenarios, many authors used a simple metric called Allan deviation which we define here as

$$A_D = \sqrt{\frac{1}{2y} \sum_{t=2}^y (p_t - p_{t-1})^2}, \quad (3.8)$$

where  $p_t$  represents the data packet delivery ratio at time  $t$  and  $y$  represents the number of time intervals. The result of  $A_D$  calculations for our considered scenarios is presented in Table 3.2. We can see that the S3 has the almost highest link variance for two different data rates, followed by S1, S2 and S4.

### 3.4.3 Properties of SNR profile

#### Data rate versus SNR profile

We have obtained SNR maps for all IEEE 802.11b/g data rates in scenario T1 and have shown the results in Fig. 3.10(a). We can see that there is a clear difference between IEEE 802.11 b and g data rates. However, it is not clear that for a certain SNR, a higher data rate will result in lower packet delivery rate.

The IEEE 802.11b rates have higher PDR even at lower SNR than IEEE 802.11g rates. This is due to the modulation used by each system. IEEE 802.11b uses DS-SS and CCK modulation whereas the higher data rates of 802.11g uses OFDM. This results in two distinct groups of curves visible in Fig. 3.10(a).

The SNR maps of IEEE 802.11g rates show more fluctuations, which can be attributed to the propagation environment, narrowband interference, Inter

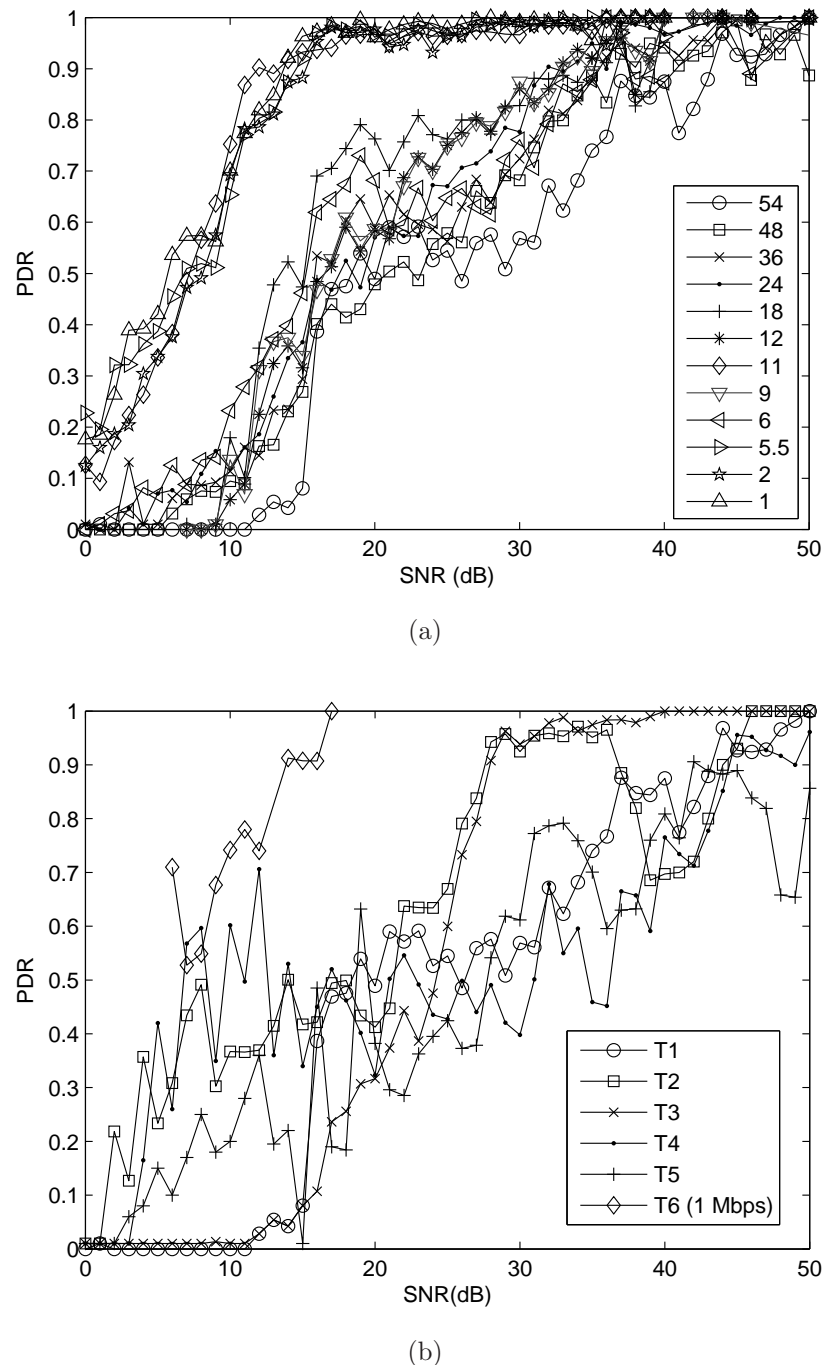


Figure 3.10: Examples of SNR profiles: (a) profiles for all data rates of IEEE 802.11b/g in T1, and (b) SNR profile for 54 Mbps data rate in T1-T5 and for 1 Mbps in T6 and different measurement scenarios, as described in Section 3.4.2.

Symbol Interference (ISI) and vulnerability of modulation to bit errors<sup>6</sup>. To achieve higher bit-rates, IEEE 802.11g uses BPSK, QPSK, 16-QAM, and 64-QAM with different code rates. Higher rates have higher vulnerabilities to bit errors than lower rates. Hence, higher SNR is required by IEEE 802.11g rates to achieve a PDR of 1. From Fig. 3.10(a), it can be seen that a  $\text{SNR} > 40 \text{ dB}$  is required to achieve a  $\text{PDR} \geq 0.9$  reliably by 64-QAM and code-rate 3/4 (54 Mbps).

In order to understand the SNR mapping properties in depth, we did more measurements in the dynamic environments described in Section 3.4.2 and the different impacting factors that can effect the best SNR mapping profile were analyzed. In this section, we will discuss which impacting factors can affect the mapping relation between  $S_H$  and  $R_D$  based on single link measurement. As we described in previous section, the difference between SNR and signal strength is not much due to the low noise fluctuation in our measurement environment. We just use the signal strength instead of SNR in the following graphs. Therefore, the phenomenon shown as below also indicate the properties of the SNR mapping.

#### Impact of Data Rate on LQE

The first experiment is preformed in S2. Three IEEE 802.11 rates were used and the mapping relation is shown in Fig. 3.11<sup>7</sup>.

IEEE 802.11 use different modulation methods for different data rates, i.e., in general, with the same power level, higher data rate will have shorter transmission range. Thus, the mapping relation for different data rate will also be different. As we can see, for the fixed data packet size, the average values of mapping in Fig. 3.11(a)–Fig. 3.11(c) obviously confirms that higher signal strength results in better LQE and there is a shift in LQE for each data rate. If we set some  $S_H$  range, say from -75 dBm to -80 dBm, we can see that 54 Mbps has a  $R_D$  around 0.25, while 24 Mbps and 11 Mbps can reach with  $R_D$  0.9. When the  $S_H$  further decreases to -85 dBm, the 24 Mbps rate link has only  $R_D$  of 0.2 and 11 Mbps still can have a  $R_D$  of 0.8.

#### Impact of Packet Size on LQE

---

<sup>6</sup>We note that even with minimized interference on the considered measurement channel and very long measurement times, i.e. longer than ten hours. We were not able to reproduce such smooth SNR profiles as in [108, Fig. 2, Fig. 5].

<sup>7</sup>We note, that in the reminder of this section, if not specified, the measurement for each scenario lasts 1 hour, resulting in 3600 sample mapping relations. Also, for each signal strength value, if the sampling point is less than 20, we do not plot them in the figure.

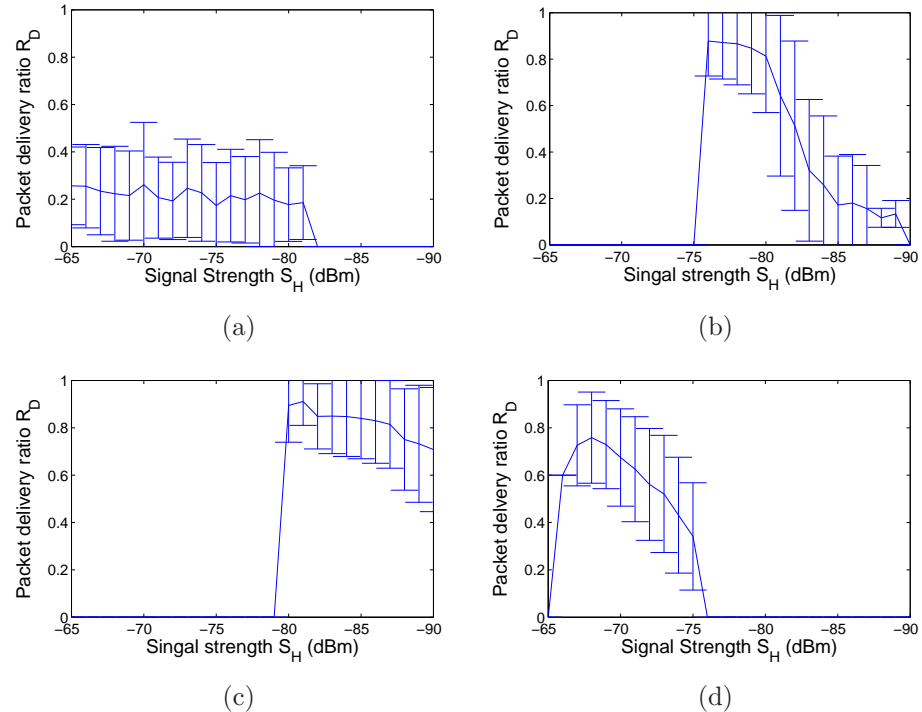


Figure 3.11:  $S_H$  to  $R_D$  mappings for three data rates and two packet sizes: (a) 54 Mbps, 1500 Bytes of data packet, (b) 24 Mbps and 1500 Bytes data packet, (c) 11 Mbps, 1500 Bytes data packet, and (d) 54 Mbps, 100 Bytes data packet. Here a line represents the average  $R_D$  a  $S_H$  maps to, and the bars show the standard deviation. The PDR for the signal strength value which has less than 20 samples is set to 0.

Packet size can also impact the packet delivery ratio, thus we conducted another experiment with two different data packet sizes of 100 and 1500 Bytes. By using the same data rate of 54 Mbps, in Fig. 3.11(a) and Fig. 3.11(d) we show that with the increase in packet size, the medium link quality corresponds to lower signal strength value. For example, with 1500 Bytes, the  $R_D$  is 0.3, when the  $S_H$  is -70 dBm. For the 100 Bytes packet size -70 dBm correspond to  $R_D$  of 0.6, which demonstrates quite different mapping relation for different packet sizes.

#### Impact of Environment on LQE

As described in Section 3.4.2, four scenarios were selected such that they have the so called medium link quality [20]. As we can see in Fig. 3.12, in all environments, a certain  $S_H$  corresponds to similar  $R_D$  in all scenarios. However, there is no obvious result to show that lower  $S_H$  corresponds to larger standard deviation in medium links. The received  $S_H$  range in Fig. 3.12(d) is less than the range in other scenarios. This is because the S4 experiment is done in the park which does not have any 2.4 GHz radio in the area and there is no interruption between the two laptops, while other factors like multipath influence the result.

#### Impact of cumulation duration on LQE

Another interesting question is how long the LQE processing should be done to give an accurate LQE. The S2 experiment with 54 Mbps and 1500 Bytes data packet was used.

In Fig. 3.13, we can see that the mapping relation for a shorter time period is less linear than for longer observation time. For example, we can clearly see that for  $S_H$  value around -70 dBm,  $R_D$  first decreases and then increases, see Fig. 3.13(a) and Fig. 3.13(b). This is due to insufficient number of samples in the mapping relation. When we increase the sample source to 2 hours, we can clearly see that the mapping relation becomes linear again, see Fig. 3.13(c). For the 3 hour mapping relation, see Fig. 3.13(d), we can see that it becomes even more linear, combined with the increased standard deviation value due to the increase in the number of samples. This mapping relation can be self learned also when there is data traffic passing the link. The number of  $S_H$  values is 1 packet per second. If each data packet is also used for signal strength value learning, the duration of learning can be much shorter.

We also calculate the average estimation error  $\Delta_E$  (compared with  $R_D$ ) for different intervals. The result is shown in Fig. 3.14. The mapping

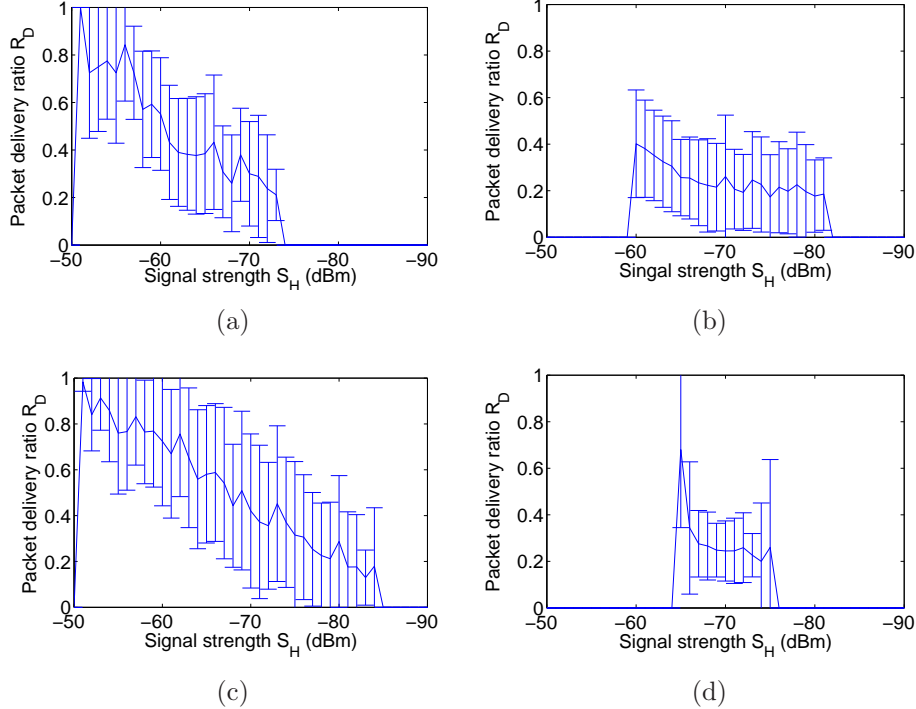


Figure 3.12:  $S_H$  to  $R_D$  mappings for different environment: (a) S1, (b) S2, (c) S3, and (d) S4. The line represents the average  $R_D$  a  $S_H$  maps to and the bars show the standard deviation of the  $R_D$ .

table built by the 3 hour experiment achieves the  $\Delta_E$  with 0.17. We can see that the 60 minutes interval can achieve very similar result as the optimal one. However, the 30 minutes result shows some deviation and the 15 minutes can result in larger  $\Delta_E$ , which suggest that 60 minutes or 3600 samples is the appropriate number for building the table for the considered network setup.

### General Remarks

In a real system, the mapping tables can be built based on different data rate, and some packet sizes. When the data traffic passes by the link, the mapping table can be updated based on self-learning to improve the performance. In our experiments, the mapping relation is built based on the post process of recorded statistical data. In real system, the mapping table can be built by the system itself.

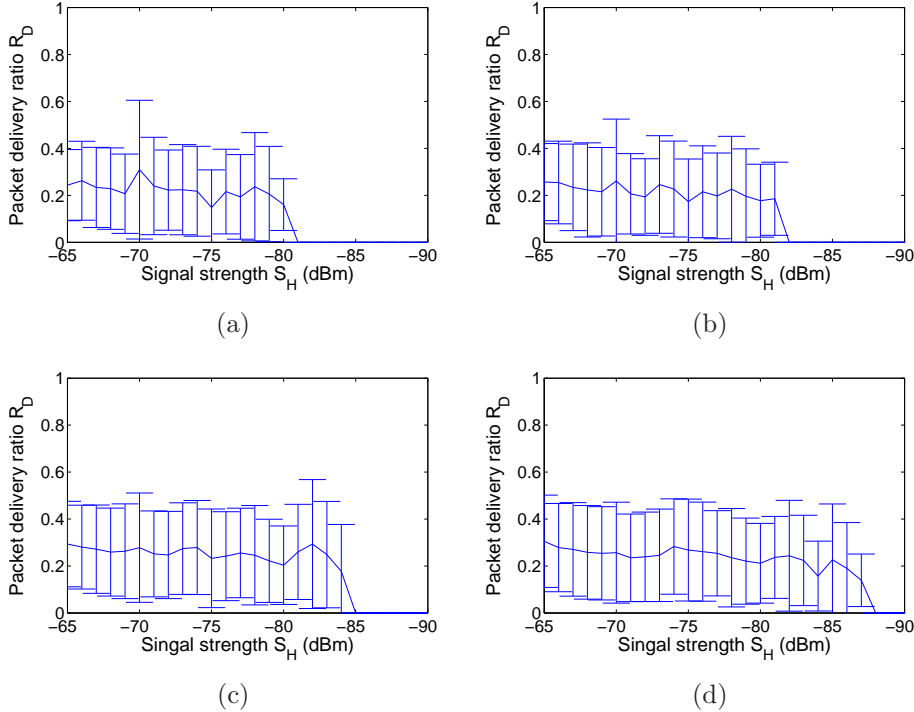


Figure 3.13:  $S_H$  to  $R_D$  mappings for different measurement duration: (a) 0.5 hour, (b) 1 hour, (c) 2 hours, and (d) 3 hours. Here a line represents the average  $R_D$  and  $S_H$  maps and the bars show the standard deviation of the  $R_D$ .

### Environment versus SNR profile

Apart from the data rate and packet size, different environments influence the SNR profile. We have created SNR profiles for the 54 Mbps data rate from the experiments in scenarios T1–T6, and present our results in Fig. 3.10(b). The received SNR is higher for LOS communication (T1 and T2) and hence the PDR is higher. However, in T1 the sender moves continuously and the decoding of the signal depends on the propagation environment causing fluctuations in the graph. Similar arguments follow for other scenarios.

The SNR profiles of T2 and T3 (stationary sender in quasi-LOS and non-LOS, respectively) are different in the low SNR region, i.e.  $\approx [0, 25]$  dB and similar in the high SNR region. The PDR from T1 is not perfect even at high SNR and is much lower than that in scenario T2 and T3. For T4 interference caused by the independent transmitter increased the noise level on the desired channel. Finally, for T5 we can see that for high SNR, the PDR is not as high as from the pure non-LOS stationary scenario T3. For

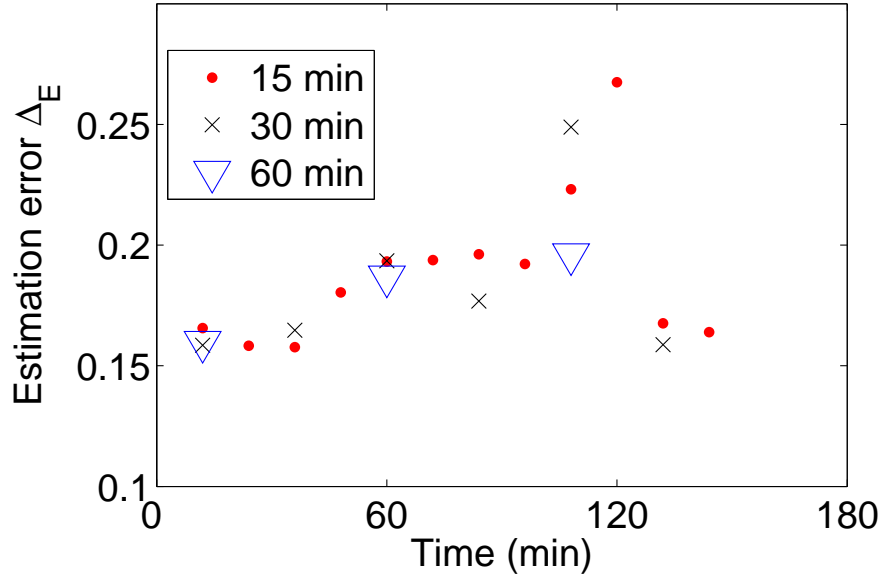


Figure 3.14: Impact of learning interval on LQE accuracy: fluctuation of signal strength mapping  $\Delta_E$ , 54 Mbps in S2 scenario.

low SNR values, due to large variance of the channel, the PDR varies largely and sometimes can achieve high PDR.

In T6, due to the outdoor test-bed constraint, we could not obtain mapping at high data rates, including 54 Mbps, since SNR was too low for high data rate packets to go through the selected link. To show how the mapping looks like in outdoor links, we plot mapping relation for 1 Mbps. Moreover, for the outdoor test-bed, since nodes are fixed and largely separated, the channel is far more stable than the indoor channels seen in T1-T5. So single link cannot provide a wide range of SNRs as seen in the indoor environment. Therefore we combined SNR maps from three links to obtain the mapping.

### 3.4.4 Accuracy of proposed LQE

To compare the accuracy of SNR profile-based and packet counting-based LQE, we use data packet counting method as our benchmark, which was used in [107]. For a given data rate and scenario we compute the estimation error using the mean absolute error metric, widely used in evaluating time series forecasting accuracy, as

$$\Delta = \frac{1}{m} \sum_{i=1}^m |E_{R(k),i,d} - E_{R(k),i}|, \quad (3.9)$$

where  $m$  is the total number of collected packet sampling intervals, which contains  $E_{R(k),i}$ , both for SNR profile estimation and broadcast packet based estimation, beacon based LQE, and  $E_{R(k),i,d}$ , which is the LQE obtained using data packet counting.

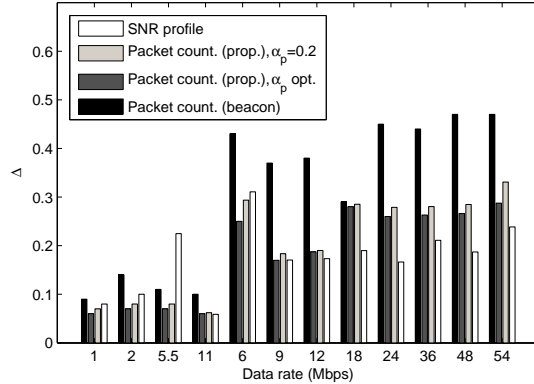
Our results are split into two parts. First we analyze a static profile where one SNR profile is used in all measurement scenarios. Later we analyze the on-line updated SNR profile.

### Static SNR profile

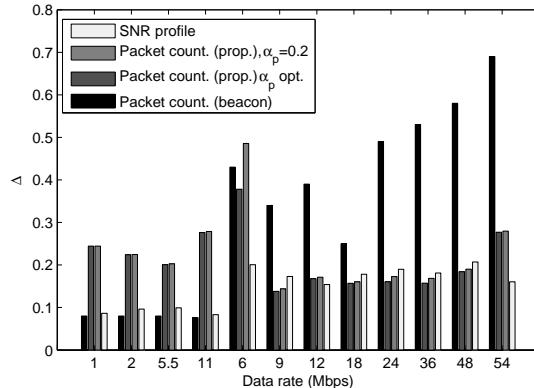
Here we focus only on scenario T1, T2 and T6. The experimental results for the T1, T2 and T6 scenarios are shown in Fig. 3.15(a), Fig. 3.15(b), and Fig. 3.15(c), respectively. In case of the proposed broadcast packet based LQE, we have separately measured link quality with  $\alpha_p = 0.2$ , which is an arbitrary but still a reasonable value for the EWMA filter, and for the optimal value of  $\alpha_p$ , which gives the lowest  $\Delta$ .

In T1, the beacon based estimation has the highest error for all data rates except 5.5 Mbps. In T2, the method under performs for all IEEE 802.11g data rates in T2, mostly because of the difference between probing packets and data packets and the higher channel variance. For the proposed broadcast packet based probing, the error is much less because the probing packet is the same as the data packet. Still, the SNR profile based LQE for the majority of rates in T1 (except for 1, 2 and 5.5 Mbps) outperforms the two methods. For T2 it achieves comparable performance as the proposed broadcast based packet counting. Interesting conclusions can be drawn for low data rates, primarily over IEEE 802.11b, in scenario T2. Since these data rates have much larger transmission range, evidently more robust modulation schemes compared to IEEE 802.11g, beacon based LQE have similar or less estimation error than the SNR profile. In both environments, optimized broadcast packet based LQE has almost the same performance as the one with  $\alpha_p = 0.2$ , which proves that the chosen smoothing factor is sufficient.

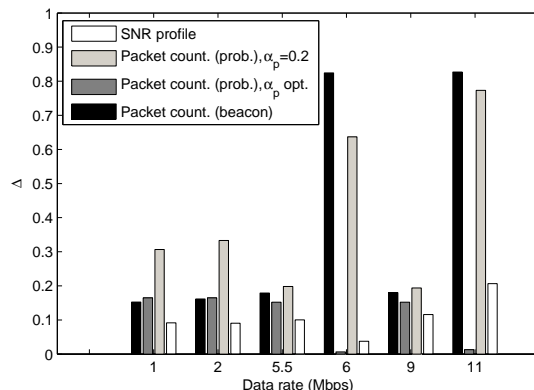
Using the same processing methods for Fig. 3.15(a) and Fig. 3.15(b), we plot estimation error  $\Delta$  for different data rates obtained in T6. Due to the phenomena described in Section 3.4.3, we use only eight lower data rates to calculate LQE accuracy in the outdoor links, instead of all twelve. The conclusions are in line with the ones obtained for T1 and T2. The SNR mapping is the best LQE method, being worse only for optimal packet counting-based LQE for 6 Mbps and 11 Mbps. This can be explained as follows. Because for the selected link in T6, the number of data packets that were successfully passed through was very low. So if we start with a PDR of zero in the estimation, the optimal  $\alpha_p$  is zero. Then the estimated



(a)



(b)



(c)

Figure 3.15: LQE error  $\Delta$  given by (3.9) in (a) T1 scenario, (b) T2 scenario and (c) T6 scenario. Data rates of  $R$  are sorted in the figure such that first left four are IEEE 802.11b data rates and the remaining ones are IEEE 802.11g.

PDR is good, since it also takes zero for the estimation. Needless to say that the selection of optimal  $\alpha_p$  is just a benchmark instead of real practical LQE method, since in reality the optimal  $\alpha_p$  can never be used due to huge number of neighbors and dynamic links. This means that if we use the optimal  $\alpha_p$ , computation for the optimal value has to be performed for each neighbor frequently and not all nodes have enough processing power to do so. Finally, this method still performs worse than SNR mapping in most scenarios, as seen in Fig. 3.15(a) and Fig. 3.15(b).

It is important to note that since in the IEEE 802.11g data rates, data packets are rarely transmitted most of the time the PDR estimation for those data rates is almost zero, but beacon still can pass through easily, so that beacon packet-based LQE makes a huge error when it tries to estimate the IEEE 802.11g data rates. The error for the broadcast packet-based LQE is due to the fact that broadcast packets are not retransmitted while the unicast packets are transmitted.

Based on the results from the above scenarios, we conclude that the SNR profile based or broadcast packet counting based methods perform better than methods based on beacon packet counting. In some scenarios, the proposed broadcast based method performs slightly better than the SNR based method. However, due to the facts described in Section 3.2.1 probing all data rates and packet sizes will cause huge overhead for the network. Therefore, the SNR profile based method is the only method that maintains both accuracy and efficiency for all scenarios.

### **Dynamic SNR profile: mitigating the need for context awareness**

As we have discussed in Section 3.4.1, it is possible to mitigate the need for a context aware system to obtain the required accuracy in a certain scenario by optimizing parameters of the SNR profile based LQE as the data traffic passes through the node.

We will use the SNR profile generated in T1 at 54 Mbps in a different scenario. The results for the other data rates will behave similarly. Scenario T1 is used as the initial one, and with SNR profile-based LQE, the speed of the update in new environment is controlled by  $\alpha_s$ . The result is presented in Fig. 3.16. We conclude that in all scenarios, indoor and outdoor, updating the SNR profile at the optimal rate achieves better estimation than the static profile, i.e. static profile (when  $\alpha_s = 0$ ).

Although for the outdoor scenario  $\Delta$  is the smallest when the  $\alpha_s$  is zero, however  $\Delta$  is very small for all  $\alpha_s$  which still shows that our method can be effectively used in different scenarios.

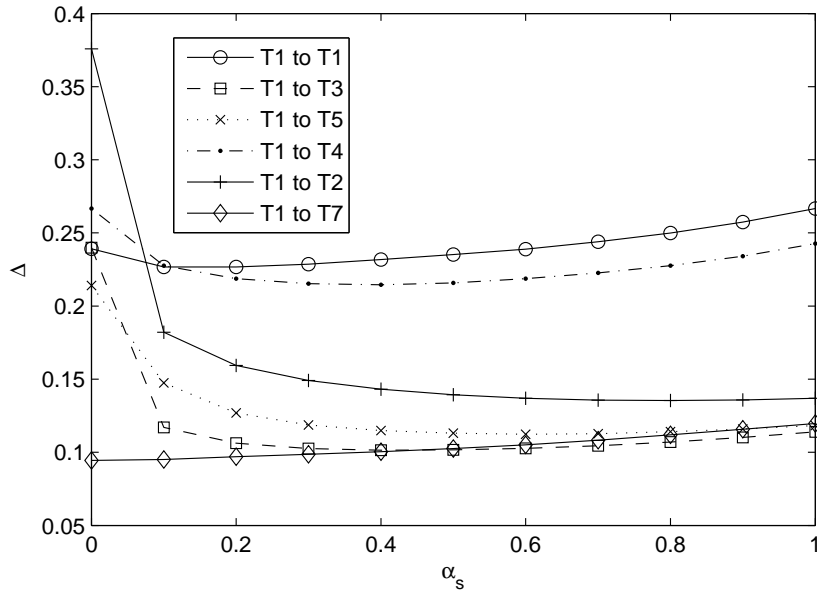


Figure 3.16: Estimation error  $\Delta$  for all values of  $\alpha_s$  and changes in measurement environments.

## 3.5 Mathematical Analyzing

While broadcast packet-based LQE generally conforms to the well described process of LQE based on counting acknowledged unicast packets, the novelty of our proposed SNR profile based LQE method (see Section 3.4) lies in the way of selecting these methods, their update, as well as in different approach of generating SNR maps. We will briefly describe here the idea behind creating novel SNR maps and their usage in LQE.

### 3.5.1 Proposed SNR map-based LQE: General overview

In our implementation of SNR maps-based LQE, each node counts the number of acknowledged data packets from the intended receivers for each SNR value and the data rate it reads from the packet. Based on these counts, each node creates a map, i.e. a relation between all observed SNR values and the associated number of successfully received packets. In our method, the map is updated whenever new data traffic passes between the considered transmitter and the receiver. Please note that we do not transmit any probing packets, perform any calibrations initially or linearize SNR maps, as other methods do, see Section 3.4. We constantly update the maps whenever traffic

passes and use the actual data packets (not probing packets) to create maps. In this way there is no impairment between maps and the actual SNR to PDR relation and the mapping is always updated. For the packet counting method, we used the ETX's calculation method.

We will now compare our proposed SNR map-based LQE method with other methods listed in the previous section. Specifically, we will compare unicast, beacon, broadcast, and data packet-based LQE, against proposed LQE based on SNR maps, referred with the variable subscripts  $u$ ,  $b$ ,  $r$ ,  $d$  and  $s$ , respectively. We will not compare combined LQE methods, since we focus on each method individually, or methods based on BER, due to their impracticality, as remarked in Section 3.2.4.

### 3.5.2 System model

We assume that each node in the network is located at a fixed position. The statistical process behind signal strength (given in linear scale)  $\psi \sim \mathcal{N}(\Psi, \sigma)$  is stationary. Each node has  $\bar{N} = g_t(N)$  number of neighbors, where  $N$  is the number of nodes in the network and  $g_t(\cdot)$  is the network topology. Nodes can transmit at any rate  $R = \{1, 2, 5.5, 6, 9, 11, 12, 18, 24, 36, 48, 54\}$  Mbps for IEEE 802.11b/g. Nodes send data packets of  $A_d$  Bytes transmitted at any rate  $R$  and beacon packets of  $A_b$  Bytes are sent at rate  $R(2)$ . During each link estimation interval for all LQE methods, except for data packet-based and SNR profile-based LQE,  $w$  packets are sent in equal intervals. On the contrary data packets are sent randomly at an average rate of  $w_d$  per estimation interval per node neighbor.

We will use two metrics to compare the LQE methods: (i) time it takes to estimate the link quality and (ii) efficiency defined as a distance from actual relation between SNR and PDR. We will not take update ability into consideration, which is qualitatively assessed in Table 3.1. All variables used in this section, as well as in the remaining parts of the chapter, are summarized in Table 3.3.

### 3.5.3 Estimation time analysis

The time spent to transmit packets in one estimation interval for unicast packet-based LQE is [93, Sec. II-A]:

$$\tau_u = \left( \sum_{i=1}^{|R|} \frac{A_d}{R(i)} + \left[ t_{di} + t_{si} + t_{bt} + \frac{A_b}{R(2)} \right] |R| \right) w \bar{N}, \quad (3.10)$$

where  $t_{di}$  is the length of IEEE 802.11b/g Distributed Inter-Frame Space (DIFS),  $t_{si}$  is the length of IEEE 802.11b/g Short Inter-Frame Space (SIFS),  $t_{bt} = \frac{c_m}{2} t_l$  is the average backoff time<sup>8</sup>. With a uniformly distributed contention window size with minimum value of  $c_m$  and slot size  $t_l$ , and  $|R| = 12$  is the size of vector  $R$ .

For a beacon packet-based LQE, the average time consumed in one estimation interval is

$$\tau_b = \left( \frac{A_b}{R(2)} + t_{si} + t_{bt} \right) w \bar{N}, \quad (3.11)$$

and in the case of broadcast packet-based LQE consumed time for the estimation is

$$\tau_r = \left( \sum_{i=1}^{|R|} \frac{A_d}{R(i)} + [t_{si} + t_{bt}] |R| \right) w \bar{N}. \quad (3.12)$$

Finally for the data packet-based LQE and SNR profile-based LQE, the consumed time is

$$\tau_d = \tau_s = \left( \bar{T}_d + t_{di} + t_{si} + t_{bt} + \frac{A_b}{R(2)} \right) w_d \bar{N}_p, \quad (3.13)$$

where  $\bar{T}_d = \frac{1}{|R|} \sum_{i=1}^{|R|} \frac{A_d}{R(i)}$  is the mean data packet transmission time across all data rates, and  $\bar{N}_p = \bar{N} p_a$  is the mean number of neighbors to whom each node transmits, with the probability  $p_a$  to any of the  $\bar{N}$  neighbors.

We finally define the inverse time consumption metric normalized to  $\tau_d$  for each LQE method

$$\epsilon_{t,x} = \frac{\tau_d}{\tau_c} \in [0, 1], \quad (3.14)$$

where

$$\tau_c = \begin{cases} \tau_d, & \text{data packet and SNR profile,} \\ \tau_{x=\{u,b,r\}} + \tau_d, & \text{otherwise.} \end{cases} \quad (3.15)$$

### 3.5.4 LQE efficiency analysis

There are three essential factors that influence LQE efficiency: (i) SNR estimation accuracy, (ii) validity of the mapping between SNR and link quality, and (iii) the difference between the probing and data packets. We can therefore construct the link quality estimation efficiency metric,  $\delta_x$  for each LQE

---

<sup>8</sup>In the implementation of SNR maps-based LQE, described in Section 3.4, we will take PDR into account while evaluating  $t_{bt}$ .

method as

$$\delta_x = \sum_{k=1}^{|R|} \left| \underbrace{(1 - f_{e,k}(\Psi_x))^{A_e}}_{M_x} - \underbrace{(1 - f_k(\Psi))^A_d}_{M_y} \right|, \quad (3.16)$$

where  $x = \{d, u, b, r, s\}$ ,  $f_k(\cdot)$  is the actual mapping function between SNR and link quality for a data packet,  $f_{e,k}(\cdot)$  is the mapping used by LQE method  $x$ ,  $\Psi_x$  is the mean estimated SNR by LQE method  $x$ , and  $A_e$  is the size of the probing packet used by the LQE process  $x$ .

For unicast and broadcast packet-based LQE

$$M_{x=u} = M_{x=r} = (1 - f_k(\Psi_c))^{A_d} \quad (3.17)$$

and for beacon packet-based LQE

$$M_{x=b} = (1 - f_2(\Psi_c))^{A_b}. \quad (3.18)$$

Please note that in (3.17) and (3.18) the same estimated SNR  $\Psi_c = \Psi_{\{u,r,b\}}$  is observed, since each method uses the same number of packets from which the SNR  $\psi$  is extracted and averaged. In case of data packet-based LQE

$$M_{x=d} = (1 - f_k(\Psi_d))^{A_b}. \quad (3.19)$$

Before we compute  $M_{x=s}$  for the SNR profile-based LQE, we introduce the following proposition:

**Proposition 1** *For SNR profile-based LQE  $M_{x=s} = M_y$  asymptotically. For all but the SNR profile-based LQE method minimum squared error of the SNR estimate is,*

$$\Psi_{e,x} = \begin{cases} \mathbb{E}[(\Psi - \Psi_d)^2] = \frac{\sigma}{\bar{w}R}, & \text{data packet-based LQE,} \\ \mathbb{E}[(\Psi - \Psi_c)^2] = \frac{\sigma}{w}, & \text{otherwise.} \end{cases} \quad (3.20)$$

Again, note that  $\Psi_{e,x}$  is always constant for every estimation interval. Since with every interval each LQE method, except for SNR profile-based, will discard previous measurements and estimate current SNR based on recently received packets. However, in the case of the SNR profile the measurements are never discarded. The profile is always updated after every new interval of measurement. The estimation error in this case is

$$\Psi_{e,x} = \mathbb{E}[(\Psi - \Psi_s)^2] = \lim_{\bar{w} \rightarrow \infty} \frac{\sigma}{\bar{w}R} = 0 \quad (3.21)$$

which results in estimated SNR value for SNR profile-based LQE  $\Psi_s = \Psi$ . Since  $M_s$  is constructed in the same way as (3.19) but replaced with accurate SNR, it completes the proof.

Finally, the normalized estimation efficiency metric for method  $x$  is

$$\epsilon_{e,x} = 1 - \frac{\delta_x}{\sum_{x=\{d,u,b,r,s\}} \delta_x} \in [0, 1]. \quad (3.22)$$

### 3.5.5 Overall LQE efficiency

Having  $\epsilon_{t,x}$  and  $\epsilon_{e,x}$  we define an overall efficiency metric as

$$\epsilon_x = \epsilon_{e,x} + \epsilon_{t,x} \in [0, 2]. \quad (3.23)$$

This metric allows us to assess each method and obtain the information on which the features i.e., time or efficiency were more dominant in the estimation process. In the next section, we present some numerical results and comparison.

### 3.5.6 Numerical evaluation

We will focus on a tandem network in which  $\bar{N} = \frac{2(N-1)}{N}$  [32, Ch. 3]. Results are given in Fig. 3.17 with the assumed parameters therein. We remark that, without loss of generality, we have focused only on  $R = \{1, 2\}$  Mbps for which  $f_k(\cdot)$  in AWGN channel, used in this evaluation, are given as  $f_1(\Psi) = Q(\Psi)$ , for BPSK, and  $f_2(\Psi) = Q(\Psi/2)$ , for QPSK, respectively, where  $Q(\cdot) = 1 - \Phi(\cdot)$  and  $\Phi(\cdot)$  is a CDF of a Normal distribution. In the numerical evaluation we have assumed that  $\Psi_x = \Psi - \Psi_{e,x}$ . Note that both sets of  $w$  and  $w_d$  are chosen such that one sending rate is greater than the other.

We see that the SNR profile-based LQE performs best irrespective of  $w$  and  $w_d$ . The beacon packet-based LQE has the worst performance. Also note that the unicast and broadcast packet-based LQE perform equally well, irrespective of  $w$  and  $w_d$  value. The difference in  $\epsilon_x$  between data packet-based and SNR profile based LQE is greater when  $w_d \gg w$ .

## 3.6 Chapter Summary and Discussion

In this chapter, we have discussed wireless link quality estimation for two types of radio channels, IEEE 802.11 and IEEE 802.15.4. We have done a comprehensive investigation on the IEEE 802.11 LQE methods and have proposed two different LQE methods for IEEE 802.11 radio.

Based on the preliminary measurement results for IEEE 802.11, we found that the SNR and PDR have strong correlation and can be a good indicator for the link quality estimation, while other indicators also have some advantages. Therefore, we proposed two different link quality estimation methods

Table 3.3: Summary of Used Variables

Value	Description	Unit
$c_m$	minimum window size	$\mu\text{s}$
$g_t(\cdot)$	neighbor function	—
$f_{k,e}(\cdot), f_k(\cdot)$	estimated and actual BER function	—
$k, i$	rate index, time instant	—
$p_a$	probability of connecting to neighbor	—
$r_k$	index of the selected rate	—
$t_l$	slot length	$\mu\text{s}$
$t_{si}, t_{di}$	distributed and long interframe space	$\mu\text{s}$
$t_{p,R(k)}$	packet transmission time in lossless condition	$\mu\text{s}$
$t_{b,R(k),i,\Psi}$	backoff time given retransmissions	$\mu\text{s}$
$w, w_d$	number of probes and data packets	—
$w(t)$	number of acknowledged packets in time $t$	—
$A_d, A_b$	size of data and beacon packets per interval	kB
$K$	Rician factor	dB
$M_x, M_y$	probe and actual SNR to PDR function	—
$N, \bar{N}, \bar{N}_p$	number of nodes, neighbors and connected neighbors	—
$P, S$	size of one and complete SNR profile	Bytes
$\mathcal{R}$	routing metric	—
$R(x)$	IEEE 802.11b/g rate $x$	Mbps
$\bar{T}_d$	mean transmission time of $A_d$	$\mu\text{s}$
$E_{R(k),(i)},$ $E_{R(k),(i),d},$ $E_{R(k),(i),\Psi}$	estimated PDR using broadcast packets, data traffic and SNR map	—
$F_{(i-1,i),R(k)}$	number of retransmissions	—
$G_{R(k),i,\Psi}$	rate metric	—
$X_{R(k),(i),\Psi}$	packet reception indicators	—
$\mathbf{E}_{\Psi}$	vector of PDRs	—
$M_{\Psi,k,D_m}$	data structure with $tx$ and $t_{ack}$ for $\Psi, k, D_m$	—
$\alpha_p, \alpha_s, \alpha_r$	packet, SNR and rate smoothing factors	—
$\sigma$	SNR variance	dBm
$\epsilon_{t,x}, \epsilon_{e,x}, \epsilon_x$	normalized time, estimation and total efficiency	—
$\tau_x, \delta_x$	time and estimation efficiency of metric $x$	—
$\Delta$	PDR estimation accuracy	—
$\psi, \Psi, \Psi_{x=\{d,s,c\}},$ $\Psi_{e,x}$	SNR: instantaneous, mean, individual ( $d$ data packet, $s$ SNR profile, $c$ rest), error vector of SNRs	dBm
$\Phi(\cdot)$	Normal distribution CDF	—

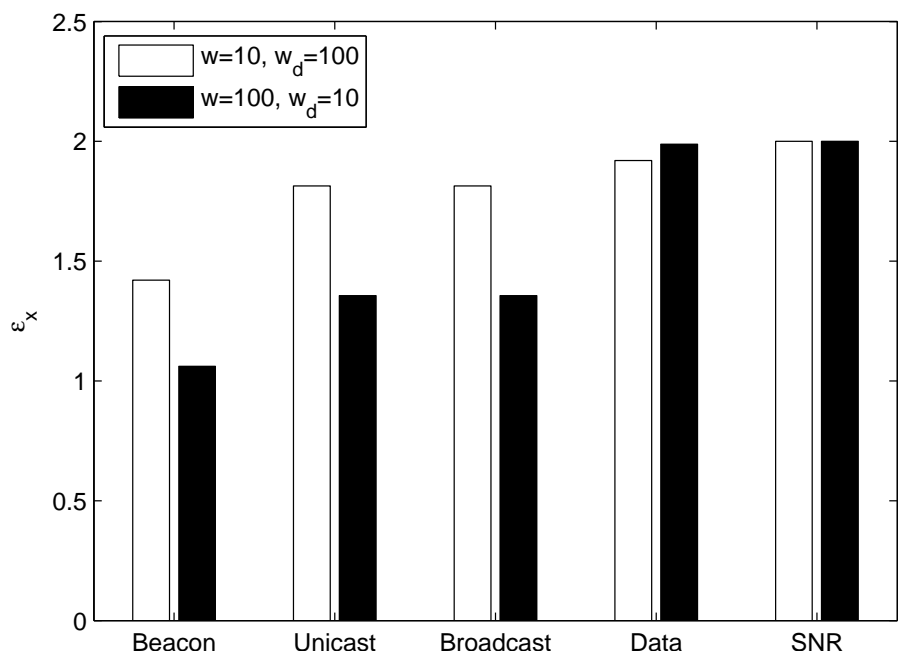


Figure 3.17: Numerical comparison of available LQE methods for two different sets of  $w$  and  $w_d$  in AWGN channel. Assumed parameters:  $A_d = 1500 \text{ kB}$ ,  $A_b = 40 \text{ B}$ ,  $N = 40$ ,  $t_{si} = 10 \mu\text{s}$ ,  $c_m = 32$ ,  $t_l = 20 \mu\text{s}$ ,  $p_a = 0.3$ ,  $\Psi = 10 \text{ dBm}$ ,  $\delta = 1 \text{ dBm}$ ,  $R = \{1, 2\} \text{ Mbps}$ .

for IEEE 802.11. They are the linearization method and mapping method of using the SNR values. The linearization method can provide accurate estimation in a certain environment while the mapping methods are much easier to be updated and hence is more adaptive to different environments. The real test-bed's measurement results indicate that our proposed methods can achieve performance enhancement up to 100%.

Further, we compare those methods by using an analytical framework and measurement results. The framework shows the LQE capability for all different methods.

The next chapters will use the proposed methods and results of this chapter and investigate further performance improvement in higher layers enhanced by accurate LQE method.



# Chapter 4

## Power Adaptation in MAC Layer

### 4.1 Introduction

Plenty of wireless devices use battery-based power, but the battery technology does not keep up. To increase device service duration, saving power is crucial. Power saving in communication can be achieved by different methods at different communication layers. Power-aware routing selects routes that together consume less energy or use devices that have more energy [59]. In the MAC layer, the receiver can turn off the receiver function periodically to save energy [13]. Another way of saving energy is to adapt the transmission power for the transmission of packets. Power transmission adaptation can achieve two benefits; save energy and reduce interference. Interference is becoming an increasing problem due to the enormously growing number of wireless devices. One way to alleviate this problem is to reduce the emitted transmission power.

The motivation for transmission power adaptation for energy saving and interference reduction stems from the fact that many of the current wireless communication systems (e.g., IEEE 802.11 and IEEE 802.15.4) usually use a fixed default transmission power level for all transmissions. However, when two nodes are very close to each other, the default power level is much higher than required to successfully deliver all packets. This both wastes energy and creates unnecessary interference. A lower transmission power level may require a larger number of retransmissions, but overall less energy will be emitted or consumed for each transmission and in total, there may be less waste. Therefore, a trade-off is possible between the number of retransmissions and energy consumption for each packet delivery. This trade-off

requires the knowledge of the PDR for each transmission power level, that is, the link quality information. We call this the *PDR-table*. The PDR-table differs between different links and different environments. To always select the transmission power level that consumes the least energy or have lowest energy emission, a self-adaptive transmission power adaptation mechanism is required that accurately observes the PDRs. In this thesis, we focus on IEEE 802.11 and IEEE 802.15.4 as our experiment technology. However, our methods can be used in other radio technologies as well.

Energy consumption for IEEE 802.11 is not so crucial as for IEEE 802.15.4, since IEEE 802.11 is normally used with larger devices, such as laptops, PDAs, mobile phones, which can be recharged easily. However, minimizing energy emission is more important because of the interference. For IEEE 802.15.4, energy consumption is critical due to its use in wireless sensor networks. Therefore, we mainly discuss interference reduction for IEEE 802.11 and energy saving for IEEE 802.15.4.

In this chapter, we propose a power transmission control mechanism that is based on gathering PDRs for every transmission power level (the PDR-table). It consists of two phases: initialization and updating. It can be used both as an interference reducing mechanism and an energy saving mechanism depending on the energy model. We propose five different methods for the initialization phase. In the updating phase, we use an exponential weighted moving average (EWMA) method to update the PDR for each transmission power level and use the result to select the optimal level. Our work focused on one-hop communication scenario, however, we think our mechanism can be extended to more complex scenarios. To the best of our knowledge, we are the first to select the transmission power that achieves the minimum energy consumption or emission for delivering a certain amount of information based on link PDR-tables. We explore the maximum potential reduction of energy emission and consumption by an investigation of all relevant parameter combinations in our mechanism. The proposed mechanism is evaluated based on measurement data and the results indicate that significant savings can be achieved in many scenarios compared to always using the default transmission power level. We also compare our PDR-based mechanism with one that uses signal strength. Also there, the results indicate a significant improvement.

The rest of this chapter is organized as follow: Section 4.2 introduces related work and Section 4.3 presents our measurement results and shows the potential reduction of energy consumption and emission. Our PDR-based transmission power adaptation mechanism is introduced in Section 4.4. In Section 4.5, our experimental system is described and in Section 4.6, the measurement results are presented. The chapter is concluded in Section 4.7.

## 4.2 Related Work

Transmission power control requires good knowledge of the correlation between link quality and transmission power levels. This correlation has been studied before via measurement activities. In [54,83], the correlation of transmit power level and packet delivery probability was analyzed in different indoor scenarios. Based on their observations, small adaptations in the power level do not change the packet delivery ratio in any measurable way. Some work also discussed combinations of power and rate adaptation to achieve good performance. In [46], it was proposed to select data rate and transmission power based on link quality. The method was applied in an indoor environment and achieved higher throughput than traditional mechanism. However, energy consumption was not calculated.

Most previous work on applying transmission power adaptation schemes was more focused on reducing interference, maintain connectivity, and topology control, such as [17,63,78,96]. Paper [84] discusses the use of transmission power control to select reliable links and disable unreliable links via a blacklisting method in order to improve the system performance. Paper [70] discusses the use of transmission power control to reduce interference and simulation results reveal that throughput can be increased by adapting the transmission power in an ad hoc network. This shows the benefit of reducing energy emission. However, the aim of these papers were to maintain the link quality at a certain level, control the topology, and increase throughput by using transmission power adaptation. Energy was not their main focus and the selected transmission power level does not always result in the minimum energy consumption or emission level.

A few papers address energy saving explicitly. The authors of [40] proposed to use a RTS-CTS handshake in the highest power level to discover the channel quality and then use the lowest possible power level for the data packet. Simulation results show that the proposed power mechanisms can achieve energy savings without degrading the throughput. However, in their proposal, a separate channel is used for controlling, which means that adaptations to the IEEE 802.11 standard are necessary. Meanwhile, a theoretical model does not reflect the real channel situation accurately. In [5], a loop-based mechanism is used to adapt the transmission power level to achieve the minimum required power level for message delivering. Simulation results show that energy can be saved and throughput can be increased. However, this work also assumes that a RTS-CTS handshake is used. Moreover, a mechanism that adapts the transmission power level one level at the time will be too slow for fast channel variances. It may take several periods for the system to choose the appropriate power level.

In [50], the authors propose a power saving algorithm that adjusts the transmission power and extends the network lifetime. Again, only simulations are used to validate the proposed protocol. Paper [105] is the most similar work to ours; transmission power adaptation was used for power saving in different scenarios. However, the optimal transmission power level is set by the received signal strength. We use PDR information for two reasons. First of all, the mapping between PDR and RSSI is not straight forward and noise and interference have a large impact on the mapping. Second, different receivers have different sensitivity levels and using RSSI may require different thresholds for different devices. A PDR-table method is affected by different devices. We compare this mechanism with our mechanism in Section 4.6.

### 4.3 Energy Emission and Consumption Measurements

To minimize the energy consumption or emission for successfully delivering a fixed amount of information, such as a certain number of packets, we turn to the expected energy consumption or emission. We calculate the expected total energy consumption or emission for one packet delivery as follows,

$$E = P \cdot N \cdot T, \quad (4.1)$$

where  $E$  is the total energy consumption or emission for successfully delivering one packet (in Joules).  $P$  is either the energy emission or the energy consumption (in Watt),  $N$  is the expected required number of transmissions to successfully deliver a packet (i.e.,  $N = 1/\text{PDR}$ ), and  $T$  is the duration (in seconds) for one packet transmission including headers and preambles. We can see that if we use a single data rate and packet size,  $T$  will be a constant value.  $E$  can be calculated for each transmission power level and the result can be used to find the optimal level, i.e., the one with the lowest  $E$ . Depending on what  $P$  value we use, we will optimize for different things. For instance, if we are interested in minimizing energy emission we use the following formula:

$$P = P_{RF}; \quad (4.2)$$

where  $P_{RF}$  is the energy emission created by the transmission power level. For IEEE 802.11, the transmission power range is from 0 to 15 dBm and for IEEE 802.15.4, it is from -25 to 0 dBm [10]. Our 802.15.4 device has 31 different power levels, but we used only 15 of them, which we calculate in this simplified way: level 3 corresponds to -23 dBm and level 31 corresponds

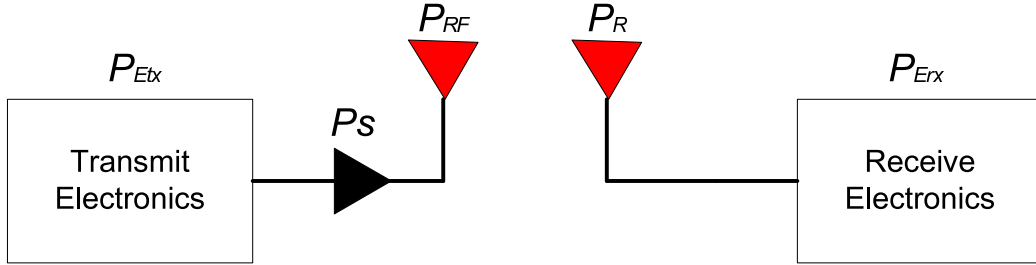


Figure 4.1: The high level block model of an RF link

to 0 dBm and then we assume a linear correlation to map the transmission power levels in between to the different energy emission levels.

For minimizing the energy consumption, we also need to consider the energy consumption of the wireless device circuit, the energy consumption ( $P_{E_{TX}}$ ) of other parts, and the wireless card amplifier energy consumption ( $P_S$ ) as shown in Fig. 4.1. While  $P_S$  is dependent on the transmission power level,  $P_{E_{TX}}$  is not.

For calculating the total energy consumption, we refer to the results in [61, Fig.5]. Since measuring the PDR introduces a lot of inaccuracies, we do not need a perfect approximation of the energy consumption. Hence, we can simply use the following linear equations for approximating the energy consumption:

$$P = 10 \cdot P_{RF} + 1400; \quad (\text{for IEEE 802.11}) \quad (4.3)$$

$$P = 35 \cdot P_{RF} + 30; \quad (\text{for IEEE 802.15.4}) \quad (4.4)$$

If we only calculate the energy emission to the environment, Eq. 4.1 and Eq. 4.2 are used. If we calculate the total energy consumption of the whole transmitter, Eq. 4.1 and either Eq. 4.3 or Eq. 4.4 are used.

To capture the accurate correlation between transmission power and PDR, a measurement-based method has to be used. For this reason, we carried out measurements in an indoor environment with different radios and configurations. For all experiments, the same number of packets (2000) were sent with 15 different transmission power levels. Two different radio technologies were used, IEEE 802.11 and IEEE 802.15.4. Let us first start with IEEE 802.11. We used UDP with a fixed packet size of 1500 Bytes including the IP header due to the fact that this packet size is common in the Internet traffic [99]. We ran some indoor scenarios with different locations, but with a fixed data rate. Then we tried different data rates in the same location. The results are presented in Fig. 4.2. The first group of experiments were done with 2 Mbps

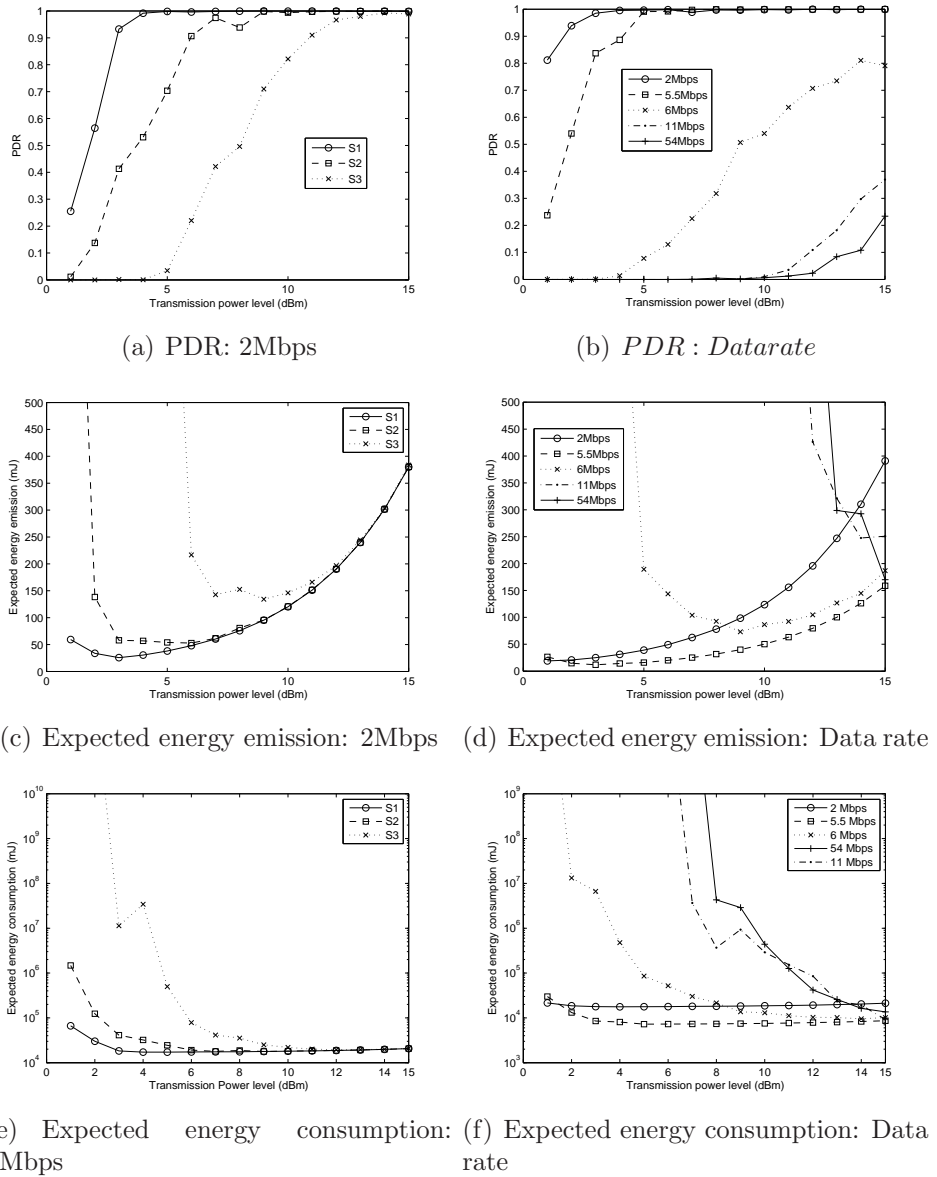


Figure 4.2: The PDR-table and expected energy emission and consumption for IEEE 802.11

data rate in three different scenarios, using different distances between the sender and the receiver. The measurement PDR-table of the three stationary scenarios is plotted in Fig. 4.2(a). The second group of experiments were with different data rates and are presented in Fig. 4.2(b). All scenarios and the experiment setup details are further described in Section 4.5.

At the receiver side, we recorded the PDR for each transmission power level. When doing this for our scenarios, we obtained the results in Fig. 4.2(c) and Fig. 4.2(e). We can see that a certain transmit power level achieves the minimum energy emission or consumption and they are different for different links. The minimum energy emission level for each link in Fig. 4.2(c) is 3, 6 and 9 for each link, respectively. For the energy consumption, we use log scale to show the results due to the large differences. We can still see that there is a level which results in the lowest energy consumption for the transmitter, and this level is not the highest power level.

To show that this phenomenon not only exists for IEEE 802.11 with 2 Mbps data rate, we carried out measurements for many data rates. The power trade-off for IEEE 802.11 with different rates is presented in Fig. 4.2(d) and Fig. 4.2(f). It is interesting to see that for higher data rates, e.g. 54 Mbps, the level that results in minimum energy consumption and emission is 15. This is caused by the fact that the link quality is so poor and struggles even with full power.

In Fig. 4.3(a), the PDR-table with different transmission power levels but with a fixed packet size in IEEE 802.15.4 is presented. We can see that although the power level is different from IEEE 802.11, the results are similar to Fig. 4.2(a). For IEEE 802.15.4, only one data rate is possible, but we can change the packet size. When we change the packet size in Fig. 4.3(b), we can see some PDR changes. However, the PDR difference is not very obvious. We also calculated the expected energy emission and consumption for IEEE 802.15.4 and present the results in Fig. 4.3(c) and Fig. 4.3(e). The power trade-off for IEEE 802.15.4 with different packet sizes is presented in Fig. 4.3(d) and Fig. 4.3(f). The expected energy emission and consumption are calculated and compared with the case where we assume that every link had to deliver the same amount of bytes. We used 100 Byte as assumed payload, which means for a 20 Byte packet payload, one needs to deliver five packets to reach the same information delivery. In the same way, one needs two 50 Byte packets.

Based on the four groups of results shown in Fig. 4.2 and Fig. 4.3, we can see that almost all the links have a PDR from 0 to 1 within a 10 dBm transmission power difference. In almost all situations, the PDR is higher for larger transmission power levels. From Fig. 4.2(c) and Fig. 4.3(c), we can see that given a data rate and packet size, links with better PDR always

requires less energy emission and consumption to deliver the same number of packets. However, if we are also able to change the data rate and packet size, it is possible to further lower the energy emission and consumption.

## 4.4 PDR-Based Transmission Power Control

For a certain channel, if the correlation between  $P$ ,  $N$ , and  $T$  is known and constant, the best combination can be selected easily. However, the actual channel PDR-table can be quite different from link to link as shown in Fig. 4.2 and Fig. 4.3 and this is also indicated in [83]. Therefore, to have an efficient transmission power control, we need a good mechanism of learning this PDR-table in real time. Meanwhile, the PDR-table may change due to several reasons, such as mobility, environmental changes, and interference. Hence, a self-adapting mechanism is required.

For each link, we need to keep a PDR-table that contains all the  $N$  values for the different transmission power levels. The PDR-table may contain values for all possible transmission levels or only a subset of them. The  $P$  values are not dynamic and can be calculated beforehand for each of the transmission power level based on the chosen energy model. Since Eq. 4.1 will be used for both the energy emission and consumption calculation, we can use the same transmission power control mechanism for both.

We divided the mechanism into two phases; the initialization phase and the updating phase. The initialization phase tries to quickly learn or “guess” the correlation between the transmit power level and the PDR once a new communication link is established. The updating phase keeps on updating this PDR-table and adapts the transmission power during the whole communication period. The initialization phase should be very short compared to the updating phase. Hence, the initialization phase is more useful for small amounts of traffic and the updating phase is more useful for large amounts of traffic. We describe the two phases in detail in the following two sections.

For neither phase, we do not generate any extra packets to probe the PDR-table. Instead, we use the normal data packets to “learn” the channel and select the appropriate transmission power level. If acknowledgments are being used, which is the case for most wireless links, including 802.11 and 802.15.4, the sender can use them to find out about the packet losses. Otherwise, this information needs to be passed back to the sender in another way. The energy emission or consumption calculation for all methods have the same prerequisite, the same amount of information need to be delivered.

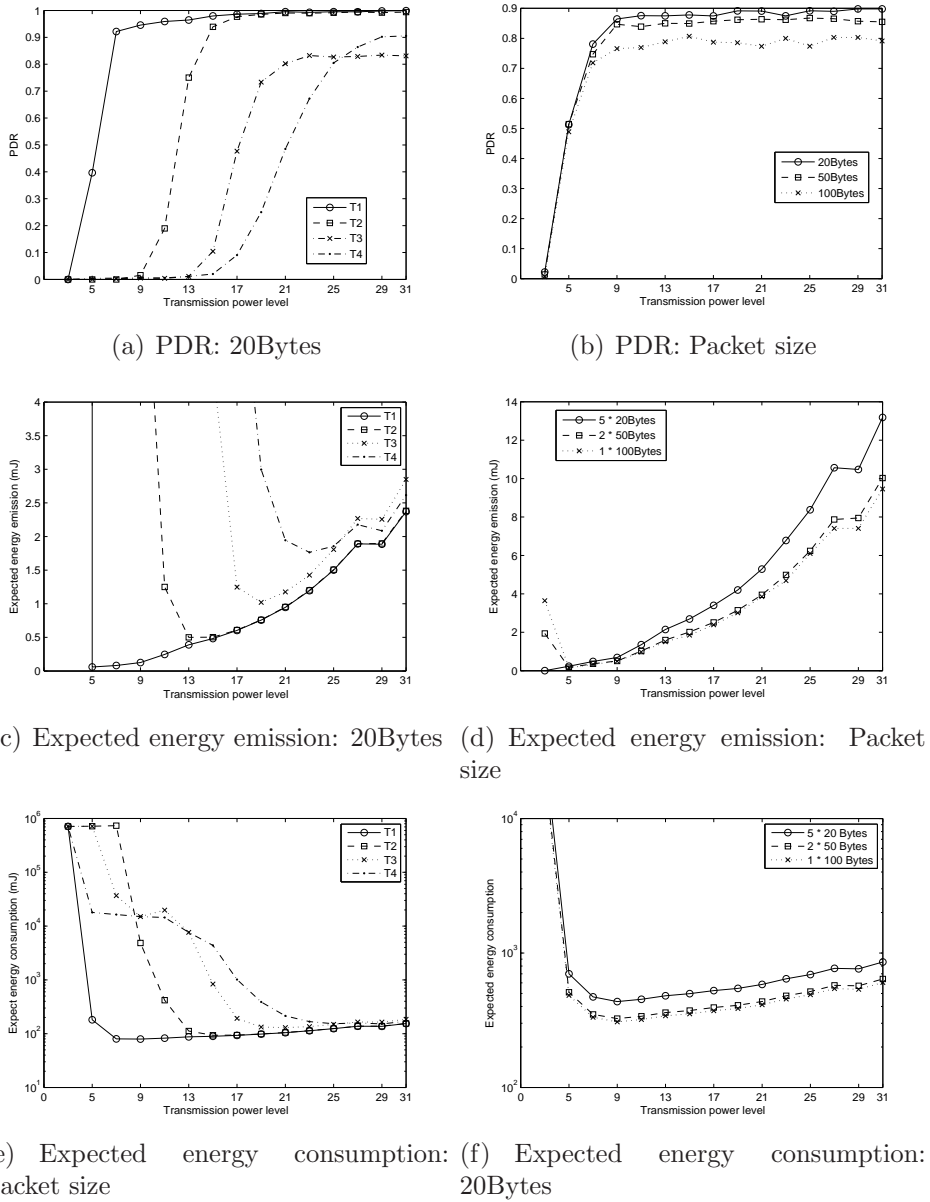


Figure 4.3: The PDR-table and expected energy emission and consumption for IEEE 802.15.4

#### 4.4.1 Initialization phase

In the initialization phase, different methods can be used to learn or “guess” the correlation between PDR and transmission power level and populate the PDR-table. We propose four initialization methods and compare them with the default method that always transmits with 15 dBm, which we call ”Fixed”. We introduce all four methods as follow:

Default start: Start using the default power level (15 dBm in 802.11 or 0 dBm in 802.15.4) and then immediately move on to the updating phase. This means only one packet is transmitted and depending on whether it was received or not  $N = 0$  or  $\infty$  for the default power level. The remaining  $N$ s in the PDR-table are set to  $\infty$ .

Sampling: Send 10 packets in all transmission levels to probe the channel and then use the obtained measurements to build the initial PDR-table and then move on to the updating phase.

Historical: Use the last recorded PDR-table (recorded based on the latest communication record between two nodes). The sender sends 10 small packets (40 Bytes) with full transmission power and the receiver reads and sends back the received signal strength. The sender then compares this with the received signal strength recorded last time. The original table is shifted left or right with the difference value based on the signal strength difference and forms the new PDR-table.

Combined: First collect the received signal strength as in the Historical method. If the signal strength between now and the previous communication are similar (within 2 dBm difference), the Historical method is used. Otherwise, the Sampling method is used.

A better initialization method starts closer and converges faster to the optimal transmit power. In Section 4.6.1, we will compare all these methods with the Fixed method, which sends all packets with default power level during both the initialization and updating phases and hence makes no use of the PDR knowledge.

#### 4.4.2 Updating phase

In the updating phase, most packets are transmitted with the transmission power level that minimizes Eq. 4.1. If two levels have the same power consumption, then the higher transmission power level will be used.

The estimated PDR for the other power levels also needs to be updated, since the whole PDR-table is dynamic if the link changes. Therefore, we propose to send a certain percentage of packets using a randomly selected power level other than the current one. In this way, the estimated PDR for all power levels can be updated. Periodically, we calculate the PDR for each level by dividing the number of received packets with the number of sent packets during that period. To have a controllable smooth updating process for all the information, we use an EWMA method as in Eq. 4.5,

$$E_{t+1} = \alpha X_t + (1 - \alpha)E_t, \quad (4.5)$$

where the  $E_t$  means the current estimation of PDR for a certain transmission power level in interval  $t$ ,  $X_t$  is the calculation of PDR for this power level in interval  $t$ , and the smoothing factor  $\alpha$  is used to tune the speed of updating. This is only done for  $N$  values that had a transmission in the PDR-table during the interval. We used an interval of 10 packets.

We defined another parameter which controls the probability that a packet will use another level than the selected optimal level. This probability is defined as  $\beta$ . The level to probe is selected uniformly among the other levels in the PDR-table. The performance of the updating phase with different  $\alpha$  and  $\beta$  is investigated in Section 4.6.1.

## 4.5 Experimental Setup

All experiments were carried out in a typical indoor office environment. They were done at night when there were very few people walking around. For each scenario, we collected a packet trace and used a post processing approach to compare every method and parameter. In this way, every parameter combination could be compared based on the same actual link in a fair way.

### 4.5.1 IEEE 802.11 test-bed

For all our IEEE 802.11 experiments, we used two HP laptops (HP7400) equipped with 3Com 108Mbps 11g XJACK PC wireless cards. Linux 2.6 and the Madwifi driver version 0.9.4 were used. We specially wrote a one-hop communication program, which had a sender and a receiver part. The node running the sender program controlled the transmission power level for each packet transmission. A fixed packet size (1500 Bytes) was used during all experiments. We used broadcast packets to avoid MAC level retransmissions and the receiver side recorded the number of received packets. In a real system, feedback from the retransmission mechanism can be used instead.

We used channel 7 during the experiments. Long duration observations were done of the noise level for this channel and the value was around  $-96$  dBm with a maximum variance of  $2$  dBm. Different distances ( $8$ ,  $16$ , and  $20$  meters respectively) were used in the experiments to generate different channel conditions, but always non-line of sight (NLOS). We name these scenarios as S1, S2, and S3. For the experiments with different data rates, we used a distance of  $20$ m with another NLOS channel. Therefore, we call it S4.

#### 4.5.2 IEEE 802.15.4 test-bed

We used a IEEE 802.15.4 compliant device in the  $2.4$ GHz ISM band from Moteiv, called Tmote sky that uses the CC2420 wireless chip [10]. During the experiment, the USB was used as power supply. As in IEEE 802.11, we also wrote a one-hop communication program for these devices. We used three different payload sizes. They were  $20$ ,  $50$  and  $100$  Bytes. IEEE 802.15.4 has a packet header, which consists of  $11$  Bytes of PHY header and  $6$  Bytes MAC header. The standard data rate ( $250$  kbps) was used during all experiments. We used only  $15$  different transmission power levels for the Tmote to be more comparable with our 802.11 experiments. Since there are  $31$  possible levels, we only used the odd levels between  $3$  and  $31$ . Based on [10], they correspond to dBm as follows: Level  $3$  corresponds to  $-23$  dBm, level  $31$  to  $0$  dBm and the levels in between are mapped in an almost linear fashion.

All the experiments were done in a channel that did not interfere with any IEEE 802.11 radio. We also did experiments in a channel that was impacted by IEEE 802.11 radio interference and found that the result was not much influenced. We used broadcast packets in the same way as in IEEE 802.11. We recorded the number of received packets and the used transmission power levels.

The IEEE 802.15.4 experiments were done in the same location as for IEEE 802.11, however, different distances were used. All channel were NLOS and the distances were  $12$ ,  $14$ ,  $16$ ,  $18$ m respectively. We call these experiment scenarios T1 to T4. The experiments with different packet sizes were done with  $17$ m between the sender and receiver with a NLOS channel.

#### 4.5.3 Experiment methodology

For each scenario, we collected a data trace by sending  $30000$  packets with different power levels during a period of  $20$  minutes. To be able to compare fairly between different methods and parameters, we used a post processing approach. In this approach, we took the trace and divided it into  $200$  batches.

Each batch contained 150 packets, 10 packets of each power level. For each method and parameter combination, we emulated the process. This was done by assuming that only 10 packets were sent from each batch and it was up to the method to decide which power levels to pick. That is, for each emulation, only a fraction of the trace was used.

For the updating phase,  $(1 - \beta)\%$  of the 10 packets were assumed to be transmitted with the currently selected best power level and  $\beta\%$  were assumed to be sent for probing the other power levels. These assumed packets were randomly selected from the trace, based on the power level and the batch it belonged to. From the trace, we checked whether the selected packets were received or not and used this information in the method. An important issue is that, due to the limited number of packets on each non-best transmission power level (e.g., 10 · 10% for each interval is only 1 packet), the PDR for each transmission power level is only updated when there is a packet transmission in this interval. Since this random selection introduces variance, we repeated this process 300 times and calculated the mean and 95% confidence interval.

Parts of the packets are sent in the initialization phase and parts are in the updating phase. Each transmission was done with a certain transmission power level and took a certain duration. Therefore, the total energy emission or consumption was the sum of all energy emitted or consumed for all the transmissions. We processed the data using this method several times and due to some random factors in the processing, the total energy emission from each processing are hardly exactly the same. However, they are quite similar and the confidence intervals are very small, so we did not plot them and only plotted the average expected energy emission for a certain method and parameter combination. We did the same processing for the updating phase as well.

Since our IEEE 802.11 card did not support fast power variation<sup>1</sup>. We divided the time into intervals, each of 8 seconds long. In each interval, we first transmitted 200 packets with one transmission power level and then paused for two seconds. Right after the pause, we modified the power level to the next level and waited two seconds, which was necessary because the wireless card we used took some time to change the transmission power. The power level was changed in a round robin fashion between all 15 levels. For IEEE 802.15.4, we changed the power level per packet, which caused no problems.

---

<sup>1</sup>Based on measurements, we could conclude that it took our card about 1 second to change from the highest to the lowest transmission power level

## 4.6 Performance Evaluation

In this section, we evaluate the performance of our PDR-based mechanism. The energy emission and energy consumption are discussed in the following two sections, starting with the energy emission. In Section 4.6.3, we look at strategies to optimize both.

### 4.6.1 Energy emission reduction

First, we present the emission reduction results for both the initialization and updating phases.

#### Initialization phase

The target of the initialization phase is to quickly populate the PDR-table and select a good transmission power level to start with and then enter the updating phase as explained in Section 4.4.1. In this comparison, a fixed  $\alpha$  value of 0.2 and a fixed percent of probing packets of  $\beta = 10\%$  were used in the updating phase. We tried different  $\alpha$  and  $\beta$  values in Section 4.6.1. For the Historical method, we used the PDR-table learned from the same location one day earlier. In Fig. 4.4, we present an example of how each initialization phase selects the best transmission power level in each batch for 802.11. We can see that all methods, except Fixed, converge to the best transmit power level after no more than 50 batches (corresponding to 500s or 500 transmitted packets).

We calculated the total expected energy emission for the first 60 batches of each method and present the results in Fig. 4.5. The number of 60 batches is selected due to the reason that after this time, all the methods definitely go to the updating phase. The expected energy emission means the required energy needed to be generated to the environment to deliver a certain amount of information, that is, to successfully transmit all 2000 packets. We can see that all our proposed initialization methods can reduce the energy emission compared to the Fixed method. The Historical and Sampling methods can further reduce the energy emission compared to Default start. The Combined method achieved the best performance, which indicates that using an accurate PDR-table is essential for a good initialization phase.

#### Updating phase

**IEEE 802.11** For the updating phase, we need to find the optimal  $\alpha$  to use in Eq. 4.5. To have a fair comparison of all different  $\alpha$  values, we fixed all

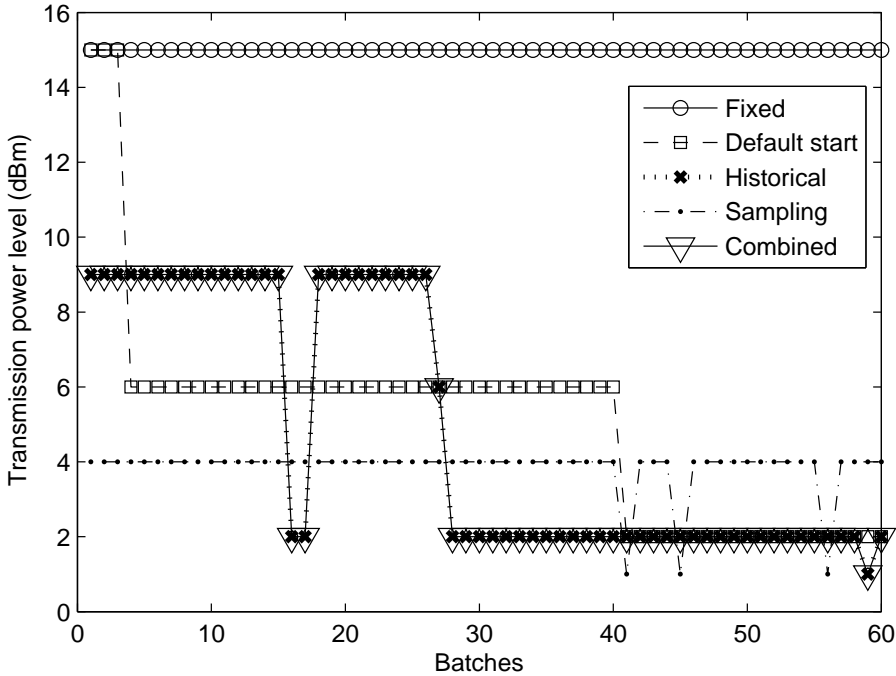


Figure 4.4: The selected best power level in each time interval by different methods in scenario 1 (802.11)

the other parameters. The percentage of probing packets,  $\beta$ , was set to 10% and we used the Default start method. For each  $\alpha$  value, we calculated the average expected energy emission of 300 experiments and show the result in Fig. 4.6(a) based on all 200 batches from the trace. We can see that when  $\alpha > 0$ , the energy emission decreases compared to when no updating is done ( $\alpha = 0$ , always using 15 dBm) and that different links have different optimal  $\alpha$ . We can also see that when  $\alpha > 0.2$ , no major improvements can be seen. Since a smaller  $\alpha$  is better for mobile scenarios, we propose to use  $\alpha = 0.2$ .

Another parameter to investigate is  $\beta$ . Fig. 4.6(b) shows the results of using  $\alpha = 0.5$  and different amounts of probing packets. We can see that for each scenario, the optimal  $\beta$  values for each link are all between 5 to 10%, which suggests that we should not send too many packets to probe other transmission power levels. However, the optimal  $\beta$  is different for each link. The general rule is that, when the link is worse (PDR is lower for most power levels), the optimal  $\beta$  is larger, which suggest that for lossy links, more probing should be done. However, a value of 10% performs well enough for all scenarios.

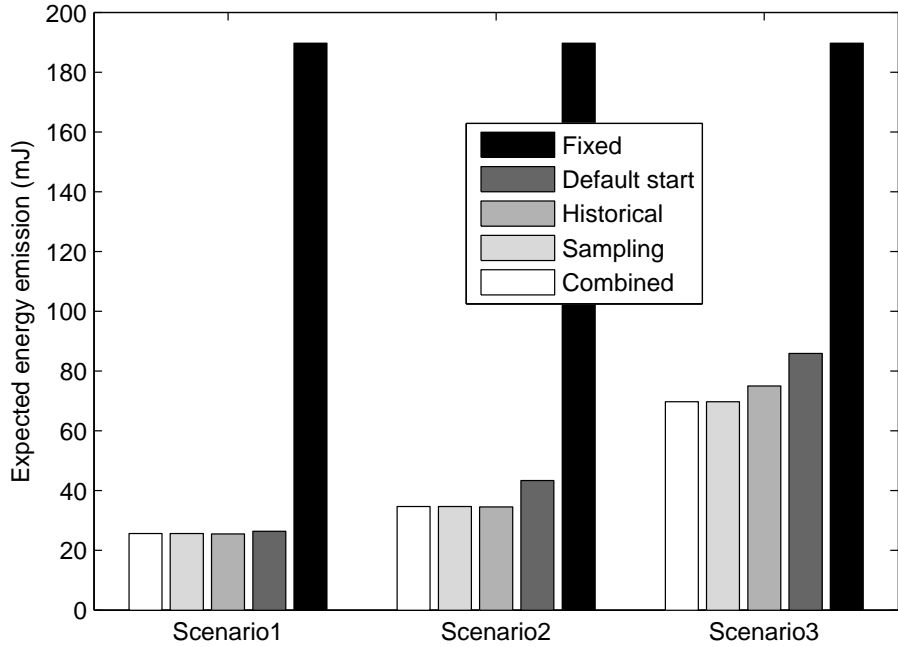


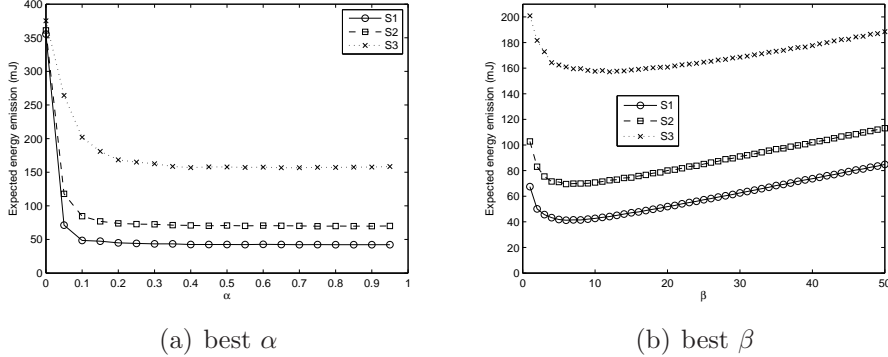
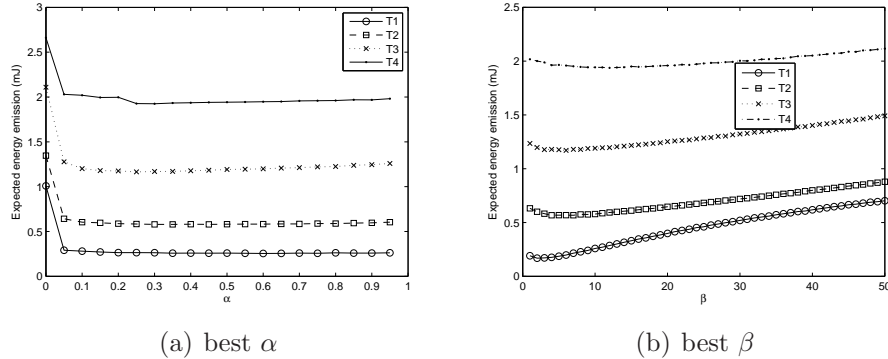
Figure 4.5: The initialization phase performance comparison (802.11)

Using  $\alpha = 0.2$  and  $\beta = 10\%$ , we made a general comparison in Table 4.1 between the PDR-based method and the Fixed method of always using 15 dBm. Default start was used in the initialization phase. We can see that for each scenario, the energy emission is much less than for the Fixed method.

**IEEE 802.15.4** We used the same processing code to process the results for IEEE 802.15.4, but with the traces from scenario T1 to T4. To have a fair comparison of all different  $\alpha$  values, we fixed  $\beta$  at 10%. We used the maximum transmission power level (31) to start. Based on Fig. 4.7(a), we

Table 4.1: Quantitative comparison of expected energy emission for the updating phase: IEEE 802.11

Scenario	S1	S2	S3
Fixed (mJ)	379.44	379.44	379.44
PDR-based (mJ)	41.87	67.78	161.42
Reduction	-89%	-84%	-57%

Figure 4.6: The best  $\alpha$  and  $\beta$  for IEEE 802.11, 2 MbpsFigure 4.7: The best  $\alpha$  and  $\beta$  for IEEE 802.15.4, 20Bytes

can see that we got similar results as in Fig. 4.6(a). When  $\alpha$  is larger than 0.1, the expected energy consumption is much smaller than the expected energy consumption when  $\alpha$  equal to 0. There is not much difference when  $\alpha$  is larger than 0.1.

We further processed the measurement results with the assumption that  $\alpha$  is equal to 0.5 and we compared the expected energy emission with different  $\beta$  values, from 1 to 50. The results are shown in Fig. 4.7(b). The optimal  $\beta$  value for  $\alpha = 0.5$  is around 5% and more probes will result in more energy emission.

To have a better comparison between different  $\alpha$  and  $\beta$  in each scenario, we calculated all the combinations for  $\alpha$  values from 0 to 1 in steps of 0.05 and  $\beta$  values from 1 to 50 in steps of 1.0. In Fig. 4.8, we use a 3D graph to show the expected energy emission for all combinations. A common trend is that when  $\alpha = 0$ , which means no update at all and always use the highest transmission power level, the energy emission is much larger compared to

when  $\alpha > 0$ . In Fig. 4.8(a), we can see that it is very obvious that larger  $\beta$  values will result in more energy emission. This is because the optimal transmission power level is 5 and higher power levels will cost more energy for each transmission. Most power levels are not worth to be probed, therefore, a larger  $\beta$  results in more energy waste. When the channel becomes worse, the expected energy emission with different  $\beta$  is less, which is most obvious in Fig. 4.8(d). Another interesting result is that there are more fluctuations when  $\alpha$  or  $\beta$  increase in scenarios with worse channels, which can be seen in Fig. 4.8(d).

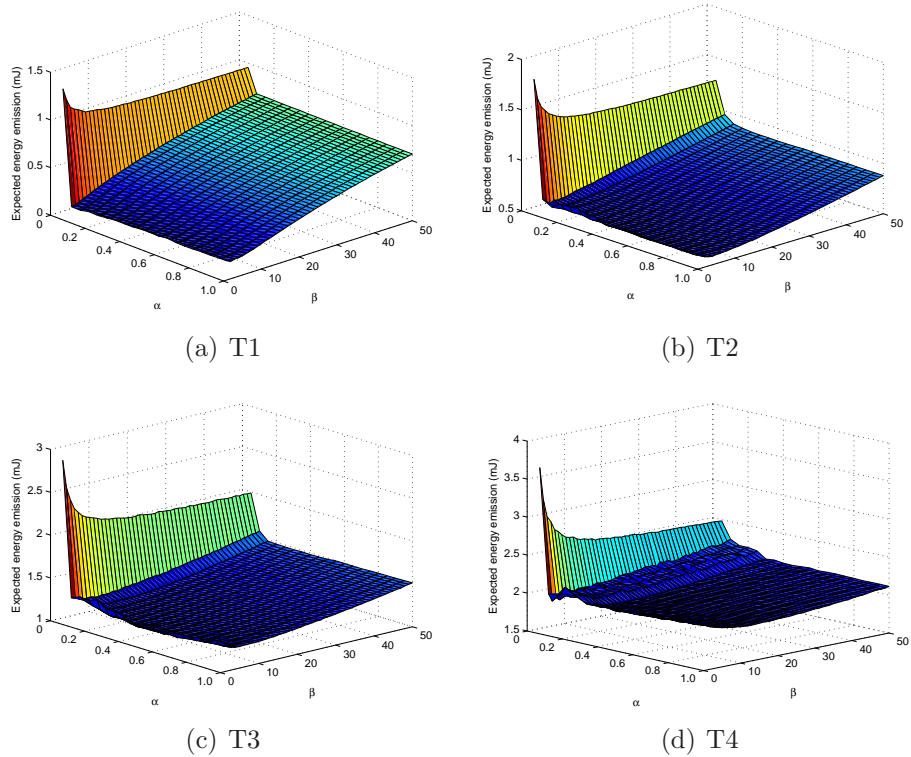


Figure 4.8: 3D  $\alpha$  and  $\beta$  combinations for different Scenarios (802.15.4)

Similar to Table 4.1, we calculated the total energy emission for each scenario with  $\alpha = 0.2$  and  $\beta = 10\%$  and present the results in Table 4.2. The best  $\alpha$  and  $\beta$  values are also included in the table. We can see that the PDR-based method only emits about 20% to 53% percent of the energy compared to the Fixed method. We also present the values based on the optimal  $\alpha$  and  $\beta$  selection from Fig. 4.8. We can see that in most cases, we are very close to the optimum simply by using  $\alpha = 0.2$  and  $\beta = 10\%$ , which means we can use this combination for almost all the scenarios.

Table 4.2: Quantitative comparison of expected energy emission for the updating phase: IEEE 802.15.4

Scenario	T1	T2	T3	T4
Fixed (mJ)	1.3496	1.8223	2.8932	3.6682
PDR-based (mJ)	0.2735	0.5865	1.1863	1.9430
Reduction	-80%	-68%	-59%	-47%
PDR-based (optimal) (mJ)	0.1428	0.5621	1.11572	1.9118
Optimal $\alpha$	0.15	0.5	0.35	0.35
Optimal $\beta$	2%	10%	14%	28%

### Impacting factors for the updating phase

The results presented in Section 4.6.1 are all with the same configuration for different scenarios. To make it more practical to the real world, we further evaluated the performance of the updating phase by studying factors that may influence the performance, such as transmission data rate, packet size, mobility, and time dependence.

**Data rate** IEEE 802.11 offers multiple data rates. Based on different channel conditions, different modulation and coding schemes can be used to achieve the highest throughput. The main question is whether the results in Section 4.6.1 are valid for other data rates or not. Moreover, from the energy emission perspective, the highest throughput data rate may not be the one that saves the most energy. We post processed the measurement traces shown in Fig. 4.2(b) to see the impact of  $\alpha$  and  $\beta$  and display it in Fig. 4.9(a).

We can see that for the three experiments with lower data rates (2, 5.5, 6 Mbps), the effect is the same as in Fig. 4.6(a). However, for the high rates (11, 54 Mbps), due to the lower PDR at almost all the transmission power levels, the updating phase can not do much to reduce energy emission and 15 dBm is optimal. Therefore,  $\alpha$  does not have much impact on the performance. Since these experiments were done in the same location, we can see that 5.5 Mbps is the most power saving data rate. However, if we change to another location with another distance, another data rate may be optimal, which suggests that not only the transmission power level, but also the data rate can be selected to save power.

Concerning  $\beta$ , low data rates need more probe packets to update the PDR information. For the higher data rates in this experiment, most other power levels will directly result in packet drops. Therefore, probing more on other power levels increases the expected energy emission. In other scenarios, this

may not be the case.

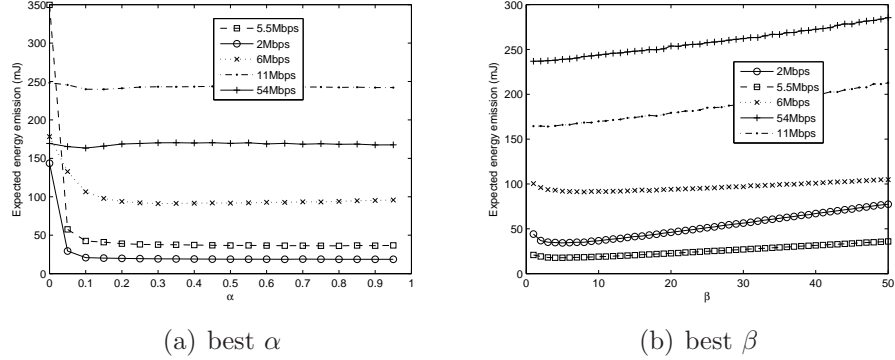


Figure 4.9: The best  $\alpha$  and  $\beta$  for IEEE 802.11 with difference data rates

**Packet size** It is also important to know the performance with different packet sizes. In order to experiment with different packet sizes over a similar link, we used 802.15.4 and changed the packet sending method. For each packet size, we will send 30000 packets in 200 batches. We split each of the three different packet size experiments into 10 equal-sized parts and we interleave the parts of the experiments in a round robin fashion. In this way, the three packet sizes experiment are experiencing very similar channel conditions. By interleaving, we mitigate unfairness caused by slowly changing link conditions.

We again calculated the best  $\alpha$  and  $\beta$  using our post processing method and got the results in Fig. 4.10. For the best  $\beta$ , the conclusion is similar as previously. However, it is interesting to see the result for the best  $\alpha$ . When  $\alpha = 0$ , the energy emission is still very high. However, a larger  $\alpha$  will have less energy emission. To deliver the same amount of information, a larger packet size emits less energy in this scenario.

**Mobility** Since all the scenarios are stationary, we still need to investigate the performance in a mobile environment. Instead of moving the devices around, which is time consuming and difficult to replicate between experiments, we emulated a mobile channel by stitching together the traces from scenario T1, T2, and T3. The way we generate mobility is not ideal, but it still gives us some insights. It shows how channel variance can affect the selection of  $\alpha$  and  $\beta$ , which is our interest.

The measurement results were segmented into different numbers of batches based on different mobility level assumptions. The mobile channel went from

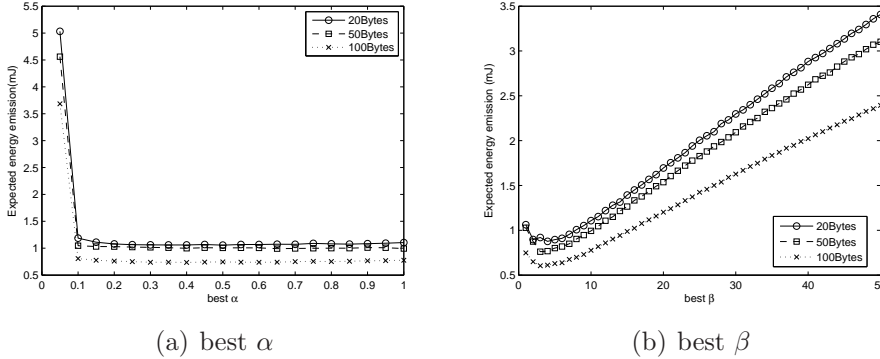


Figure 4.10: The best  $\alpha$  and  $\beta$  for IEEE 802.15.4 with difference packet sizes

good (T1), to medium (T2), to bad quality (T3). To emulate different amount of mobility, we stayed with the same scenario data for different amount of time before changing to the next scenario trace. We used four different PDR change speeds, which we measured in number of batches. A mobility scenario which changes trace every 10 batches, i.e. Mobility-10, is more mobile than one which changes only every 100 batches, i.e. Mobility-100.

We plot the performance of different  $\alpha$  for different mobility levels in Fig. 4.11. We can see that for low mobility levels, e.g. Mobility-100, the best  $\alpha$  is not big. When the mobility level increases, the best  $\alpha$  also increase. This conclusion does not hold for the situation with Mobility-10, in which the mobility is quite high. It is interesting to note that despite different mobility levels, the expected minimum energy emission remains similar. Less mobility will decrease the minimum expected energy emission, but not significant.

We also plotted all the combinations of the  $\alpha$  and  $\beta$  for different mobility levels with 3D graphs in Fig. 4.12. The results are similar to the previous 3D results in Fig. 4.8. However, it is obvious that with higher mobility, the best  $\alpha$  value gradually increases, except for Fig. 4.12(a). Perhaps somewhat surprising, different mobility levels do not cause too much impact on the optimal  $\beta$  value. Furthermore, the minimum expected energy emission is similar for all levels of mobility. Hence, mobility does not affect  $\alpha$  and  $\beta$  very much.

**Variance over time** To study the change of the optimal  $\alpha$  value over time, we segmented the experiments into 5 different pieces in the time domain and used the same method as previously to select the best  $\alpha$  for each piece. The results for both IEEE 802.11 and 802.15.4 are shown in Fig. 4.13. We found that the optimal selection for  $\alpha$  changes over time for all links. However, the

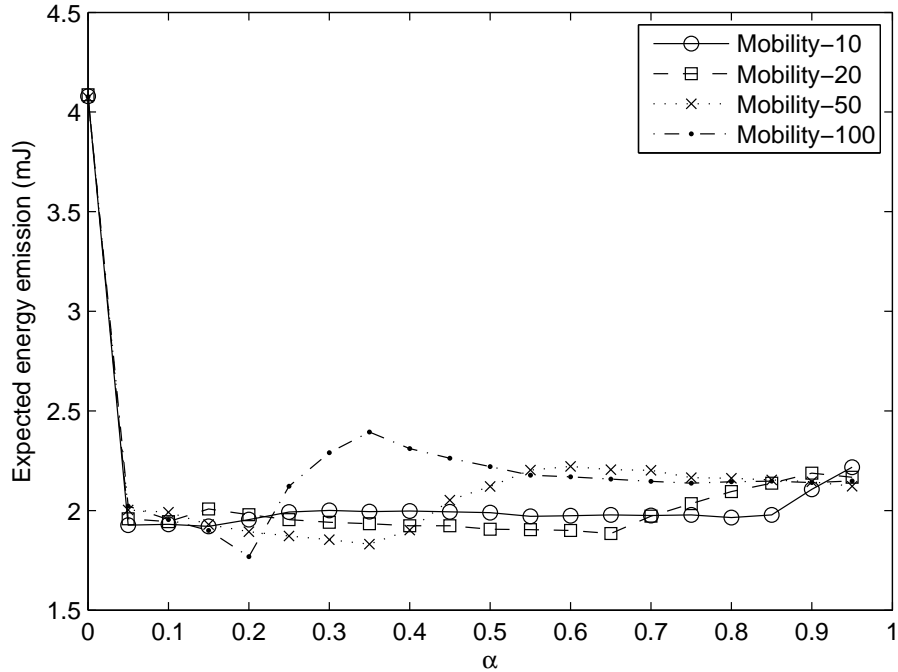


Figure 4.11: The best alpha value with different levels of mobility

difference in energy emission between the different  $\alpha$  values is not significant, given the results in Fig. 4.6(a). Therefore, in practice, one should just stick to one fixed  $\alpha$  as long as  $\alpha \geq 0.1$ . For IEEE 802.15.4, the variance of the optimal  $\alpha$  is larger over time, but still the energy emission difference is small as shown in Fig. 4.7(a).

### Discussion

Although all experiments were done with only changing the transmission power levels, our PDR-based method can also be applied to multi-factor environments. For example, we can keep records of three different data rates (or packet sizes) but only five different power levels instead of all 15. The selection would then involve finding the most optimal rate (packet size) and power level combination. It is also obvious to see that if proper  $\alpha$  and  $\beta$  values are selected, the energy emission can be reduced in most scenarios.

One concerned may be arisen when we use the power adaptation mechanisms. Since lower transmission power levels may cause the communication nodes not working well in the CSMA/CA mechanism. We have several further solutions for this concern. For the IEEE 802.11 radio, the RTS/CTS

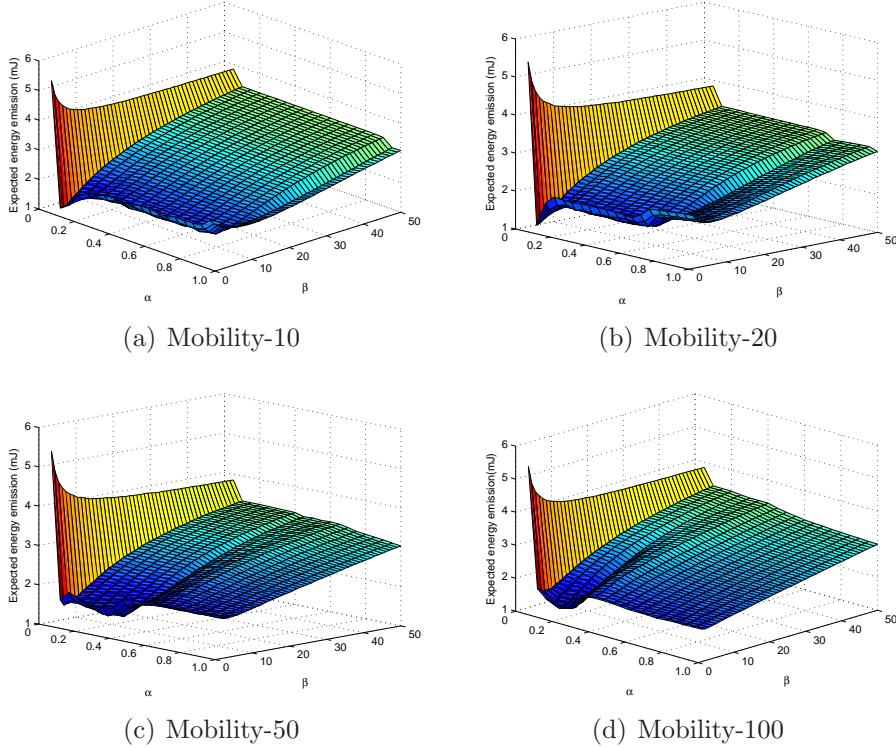


Figure 4.12:  $\alpha$  and  $\beta$  combinations for different mobility levels

mechanism can be used and we transmit the RTS/CTS packets in full power, we use the selected power to transmit the data packets. For the IEEE 802.15.4 radio, a special optional frame structure can be used and modified. In this structure's contention access period, all nodes can use full power to get the access to channel. After that, the nodes who get the access to channel can select the special power level by the algorithm to transmit the data packets. Another direct way is to transmit the packet header with full power and transmit the payload in the selected power level. Those two methods can alleviate the hidden terminal problem in CSMC/CA and our result will not be effected much since the packet headers or RTS/CTS packets are quite small compared to the data packets or payload.

#### 4.6.2 Energy consumption reduction

Since energy saving is more important for IEEE 802.15.4 devices, we also need to look at reducing the energy consumption by means of selecting the transmission power level. To do this, we used the trace files of the IEEE 802.15.4 radios from scenario T1, T2, and T4. However, we replaced the

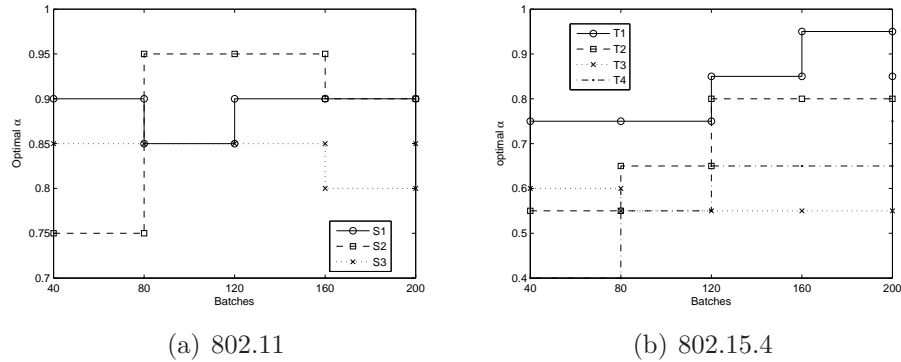


Figure 4.13: The best  $\alpha$  with time for 802.11 and 802.15.4

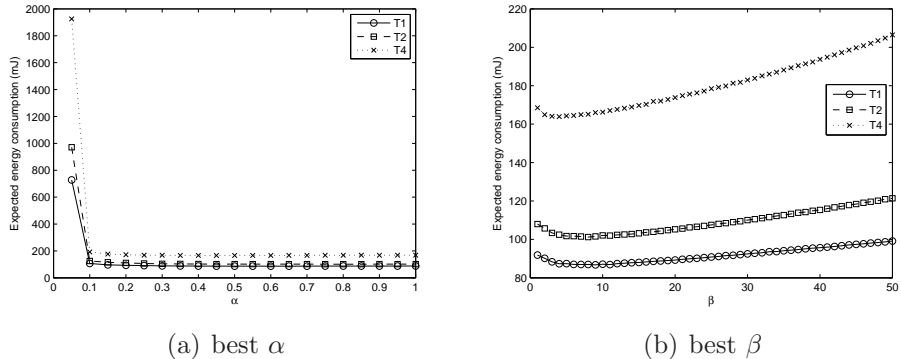


Figure 4.14: The best  $\alpha$  and  $\beta$  for IEEE 802.15.4 energy consumption, 20Bytes

energy model and used  $P = 35 \cdot P_{RF} + 30$  instead. Then we did the same experiments as in the previous section. We show the results in Fig. 4.14 and we can see that we got similar conclusions with respect to  $\alpha$  and  $\beta$  as the results in Fig. 4.7. The main difference is that the expected energy consumption is much larger than the expected energy emission due to the fact that most consumed energy is not emitted. Due to the similarity of the results, we do not present more results for the energy consumption calculation for other situations. Instead, to better demonstrate the effectiveness of our mechanism, we compare it with a typical signal strength-based algorithm proposed in [105]. We used their *aggressive method* in our comparison, since it was claimed by the authors to have better performance. We briefly introduce this mechanism as follows.

The mechanism uses the received packets' signal strength to adapt the transmission power level. This received signal strength is denoted as  $R$ . An

EWMA method (see Eq. 4.5) is used to smooth  $R$  with  $\alpha = 0.8$  and then denoted as  $\hat{R}$ . Every time a packet is received,  $\hat{R}$  is updated and then one of the following is done:

- if  $\hat{R} < T_L$ , double the transmit power.
- if  $T_L < \hat{R} < T_H$ , keep the same transmit power.
- if  $\hat{R} > T_H$ , reduce the transmit power by a constant.

where  $T_L = -85$  dBm and  $T_H = -80$  dBm for our wireless chip CC2420 according to [105].

During the implementation, we found that there is a logical error in the mechanism. If a packet is lost, no new signal strength value will be read and  $\hat{R}$  will not be updated. If, at the same time,  $\hat{R} > T_L$ , the transmission power will not be increased and this can lead to a deadlock. This situation could be quite possible, especially in mobile scenarios. Therefore, we adapted their method by letting a lost packet have an assumed received signal strength of  $-95$  dBm, the lowest receivable signal strength for CC2420.

Furthermore, the authors do not specify the constant used when decreasing the transmission power level. In our implementation, we decrease the power by one level (corresponding to a decrease between 1 dBm and 3 dBm depending on the levels) when  $\hat{R} > T_H$ .

To compare the two mechanisms, we used scenario T1, T2, and T4. The same trace data was used, since we also recorded the received signal strength. The results are shown in Table 4.3. We can see that the PDR-based method outperformed both the Fixed method and the signal strength method. Our PDR-based method always saves energy compared to the Fixed method, meanwhile, the signal strength-based method sometimes performs worse. This is because it only focuses on signal strength and ignores packet loss and at the same time, packet loss increases so much that the increased number of retransmissions cancels out the lower power consumption of using a lower transmission power level.

The reason why the PDR-based method performs better is its direct use of the PDR to power level correlation. The signal strength-based method uses fixed thresholds for all the scenarios, which may work in some cases, but not in others, such as T1 and T2. The correlation between received signal strength and packet loss is simply too weak.

To show the reason behind the good performance of the PDR-based method, we show in Fig. 4.15 the transmission power level distribution for both methods in scenario T1 and T2 as examples. Also compare these results with the PDRs for these levels shown in Fig. 4.3(a) and the energy consumption shown in Fig. 4.3(e). We can clearly see that the signal strength method

Table 4.3: Quantitative comparison for the energy consumption of IEEE 802.15.4

Scenario	T1	T2	T4
Fixed (mJ)	154.0	154.8	169.9
Signal strength-based (mJ)	121.6	154.8	169.9
PDR-based (mJ)	79.9	130.2	164.1

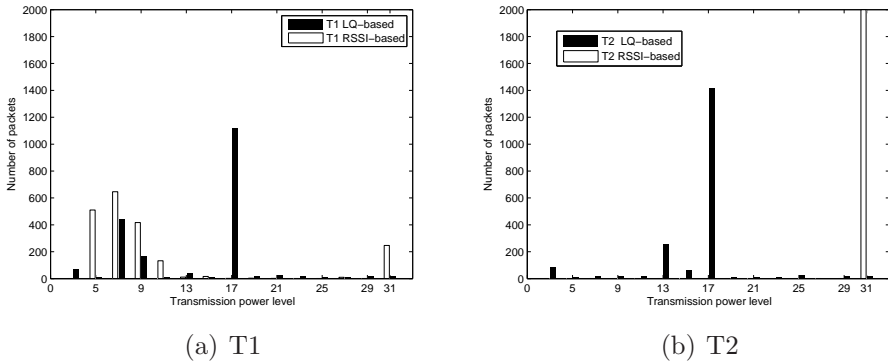


Figure 4.15: The transmission power levels distribution for the proposed and RSSI algorithms in the two scenarios

always use the maximum power level in scenario T2, which is the same as the Fixed method. The same happens in scenario T4 (not shown). Only in scenario T1, it shows some "smarter" selection. For the PDR-based method, we can clearly see that the transmission power level used for most packets are close to the optimal level 7 ( see Fig. 4.3(e)).

#### 4.6.3 Trade-off between energy emission and consumption

In some cases, a trade-off between minimizing the energy emission and the energy consumption may be sought. To allow for this, we introduce a tunable parameter  $\omega$  as follows.

When comparing Eq. 4.2 with Eq. 4.3 or Eq. 4.4 and given that a multiplicative scalar does not affect the end result, we may capture all optimization functions with the following equation:

$$P = P_{RF} + \omega; \quad (4.6)$$

where  $\omega \in [0, \frac{1400}{10}]$  for 802.11 or  $\omega \in [0, \frac{30}{35}]$  for 802.15.4. If we set  $\omega = 0$ , we get Eq. 4.2 and will optimize for energy emission. If we set  $\omega = \frac{1400}{10}$  for 802.11

(or  $\omega = \frac{30}{35}$  for 802.15.4), we optimize for energy consumption. However, it is also possible to set  $\omega$  to a value in between and that would mean that we get a trade-off between energy emission and energy consumption.

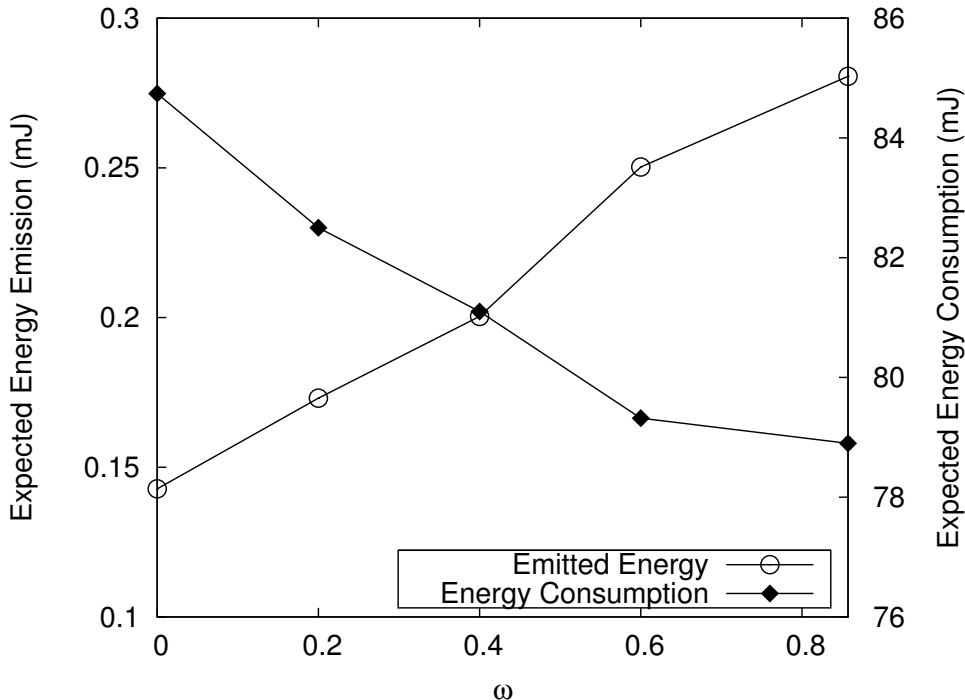


Figure 4.16: Trade off between minimum energy consumption and energy emission

To demonstrate how this tuning works, we used the T1 scenario as an example and calculated the expected energy consumption and emission with different  $\omega$  values. The result is plotted in Fig. 4.16. We can see how different  $\omega$  values affect the energy emission and energy consumption for this scenario. By making  $\omega$  smaller, we reduce the energy emission, while the energy consumption increases and by making  $\omega$  larger, we reduce the energy consumption, while the energy emission increases. Hence, we can use  $\omega$  as a tuning parameter.

We can also use  $\omega$  to control the expected delay. A larger  $\omega$  will penalize a lost packet more and this causes a higher power level to be chosen. The effect is fewer packet losses, fewer retransmissions, and thereby less delay.

## **4.7 Summary and Discussion**

Energy emission and consumption reduction are key challenges for wireless networks. In this chapter, we proposed to select the appropriate transmission power level using accurate link quality information in order to reduce the energy emission and/or consumption. We proposed to use an EWMA method to update the PDR and transmission power level correlation and use this to adapt the transmission power. We proposed five methods for the best transmission power level selection for the initialization phase to get a good transmission power level to start with. Furthermore, we investigated the optimal parameters for this correlation in order to achieve minimum energy emission or consumption. Different impacting factors were also analyzed. We carried out measurements in two types of real test-beds and showed that significant energy can be saved for the transmitter in typical scenarios. We also compared our mechanism with a signal strength-based mechanism and showed an increased performance. Finally, we demonstrated that our mechanism can be tuned to achieve a balance between the minimum energy consumption and emission, which enables the user to adaptively set the desired target.

# Chapter 5

## Rate Adaptation in MAC Layer

### 5.1 Introduction

The IEEE 802.11 technology plays an important role in wireless mesh network, wireless ad hoc network. Radio channel conditions and the mobility of the devices impact the throughput performance of those networks. The negative effects of the radio channel conditions may be suppressed with an appropriate rate adaptation mechanism. Hence, to be able to select a good data rate that maximizes the one-hop throughput and to react fast enough for link quality based route selection, the rate-adaptation mechanism need to be very "smart".

Previous work use one of two information sources to determine the IEEE 802.11 link quality for proper rate selection. One type is to use the packet delivery ratio to make decisions on the proper data rate selection [53], [47], [102]. Another type is to use the signal strength [33], [79], [41]. In all of those methods, smoothing techniques, such as EWMA, are used to combine the past and current link quality information. However, the smoothing techniques and their parameters are designed for stationary networks which may not be optimal for mobile networks. Most rate adaptation mechanisms are designed for stationary wireless networks without node mobility (e.g. mesh networks). Thus, there is a need to evaluate the impact of the smoothing factors to the responsiveness of the rate adaptation mechanisms for mobile scenarios. Moreover, as we described in Chapter 2, LQE can improve the higher layers' performance. We also propose to use our proposed LQE methods in the rate adaption mechanism.

In this chapter, we will first focus on the responsiveness of the rate adaptation mechanism in both mobile and stationary scenarios. To improve the performance of current rate adaptation mechanisms, our first attempt is to

tune a current widely used rate adaptation mechanism, SampleRate [8]. We carried out experiments in our test-bed, using SampleRate as our experimental protocol. The improvement by this approach is still limited due to the special designing of the SampleRate. To improve its performance fundamentally, we feed in our link quality estimation result into the rate adaptation mechanism and designed a new rate adaptation protocol. The experiment results show that we achieve better performance compared to SampleRate in all our scenarios.

This chapter is organized as follows. Section 5.2 will introduce some background technologies and related work, in Section 5.3, we will present our measurement results of tuning the performance of SampleRate. Our new proposed rate adaption mechanism is described in Section 5.4. A summary is given in Section 5.5.

## 5.2 Related Work

Earliest works like [33, 53] proposed to use a basic packet counting method to decide the data rate, which, as we have explained in Section 3.2, is very problematic. The packet size and data rate of the probing packets are different from that of the real data packets. The work [8] propose to record the packet delivery ratio for all data rates to determine the optimal data rate. This resulted in stale and inaccurate link quality information for all types of packets due to insufficient number of packets transmitted for all data rates. Authors in [102] claimed that they achieved better performance than [8], however the problem of packet based LQE has not been solved. The SNR value was used for rate adaptation first in [41, 108]. However, in [41] SNR was estimated per packet level which is not suitable for routing algorithms, while in [108] due to the inefficiency of the SNR profile creation, as pointed out in Chapter 2, the proposed rate adaptation can easily be outperformed. Also, rate adaptation in [108] was evaluated in indoor environments only and no mobility was taken into account. It is interesting to note, however, that even with a rather inefficient rate adaptation process it performed better than other well known rate adaptation algorithms [14].

SampleRate is quite related to our work and we use it as a comparing protocol, therefore, we introduce it in detail as follows. SampleRate was proposed in [8]. It stores the packet delivery ratio information for all IEEE 802.11 data rates. Based on history and current packet delivery ratio information, it calculates the packet delivery ratio for all data rates to estimate the link quality. A smoothing technique is used to decide how much current information is taken into the packet delivery ratio calculation. Then, it se-

lects the data rate that will occupy the minimum medium time including the expect number of retransmissions, for a successful packet transmission. A certain amount of packets are sent not on the currently selected data rate to probe the channel's performance on other possible data rates. SampleRate is implemented in a widely known IEEE 802.11 open source driver, namely Madwifi [57], which we used in our test-bed.

We describe SampleRate in mathematical equations as follow. For a given packet size, every node picks a link with a data rate such that

$$\arg \min_{R(k)} \left\{ \frac{A_d}{P_{R(1),i} R(1)}, \dots, \frac{A_d}{P_{R(12),i} R(12)} \right\}, \quad (5.1)$$

where  $A_d$  is packet size and  $P_{R(k),i}$  is the PDR for data rate  $R(k)$  at discrete time instant  $i$  defined as

$$P_{R(k),i} = \frac{\alpha_r}{1 + F_{(i-1,i),R(k)}} + (1 - \alpha_r) P_{R(k),i-1}. \quad (5.2)$$

where  $F_{(i-1,i),R(k)}$  is the number of retransmissions that occurred for one packet during the  $(i-1, i)$  interval at data rate  $R(k)$  and  $\alpha_r$  is the EWMA smoothing factor optimized for a given environment. In SampleRate, 10% of packets sent per link are transmitted at a data rate other than the selected rate (see [8, Ch. 5]) to increase the channel's probing performance and improve rate selection. The rate selection process using the SampleRate algorithm is effective only when enough traffic passes through the link since in (5.2),  $F_{(i-1,i),R(k)}$  is computed only with the acknowledgments of the transmitted packets. If for a certain rate  $i$ , the  $F_{(i-1,i)}$  is 0, this rate is temperately not considered.

The SampleRate implementation in Madwifi [57] uses EWMA [102] to calculate the medium occupying time instead of using a 10s window as described in [8]. In EWMA, the smoothing process can be modeled as  $E_{t+1} = \alpha E_t + (1 - \alpha) S_t$ , where  $\alpha$  is the smoothing factor and  $E_t$  is the previously calculated medium occupying time, and  $S_t$  is the medium occupying time for the last packet. The smoothing factor represents the percentage of the last packet transmission time in the expected medium occupying time calculation. A smaller smoothing factor value produces larger weight for the new sample. Hence, reducing the smoothing factor speeds up adaptation to the channel conditions. For example,  $\alpha = 95\%$  means the new sample's medium occupying time will be counted as 5 percent in the total calculation.

## 5.3 Adapting the Existing Protocol

Our first approach to enhance the rate adaptation performance is to tune the parameters of an existing protocol and investigate how much performance enhancement can be introduced .

### 5.3.1 Experiment setup

To evaluate the impact of smoothing factors to the rate-adaptation mechanism and routing, we use an experimental method to evaluate the throughput performance of different smoothing factors in the same scenario. The details of the experimental test-bed is described in Appendix A and the scenarios are presented as follow.

To have a clear comparison of the effects of different smoothing factors on the rate adaptation decisions, we conducted indoor experiments with the same configuration in a large place. The laptops were placed in the positions shown in Fig. 5.1. To maintain a stable link, all the stationary laptops were placed on tables one meter above the floor.

In the one hop scenarios, we have three scenarios: stationary, slow mobility and fast mobility. For the slow scenario, the sender moved away from the receiver and then moved back to the starting point, with each process lasting 30s. For the fast scenario, the process was covered in 30s. Due to the different path lengths, we got different walking speeds. All the mobile experiments were repeated with exact time control for ten times to reflect the result's statistical aspect. All the stationary experiments lasted 300s. The sender and the receiver have fixed distances, one node acted as receiver node, which record the number of received packets.

The throughput was calculated to evaluate and compare the performance. The sender generated UDP traffic as fast as possible to saturate the channel. That is, in an infinite loop, a new packet was generated as soon as the previous packet was sent out. The UDP packet length was 800 bytes. The RTS/CTS mechanism was not used and the number of packets sent in one second is depend on the channel quality. All the 12 data rates from IEEE 802.11b/g standard can be selected during the process. To evaluate the impact of the smoothing factor, several experiments were done under various conditions including different mobility patterns, with or without a contention node or background traffic.

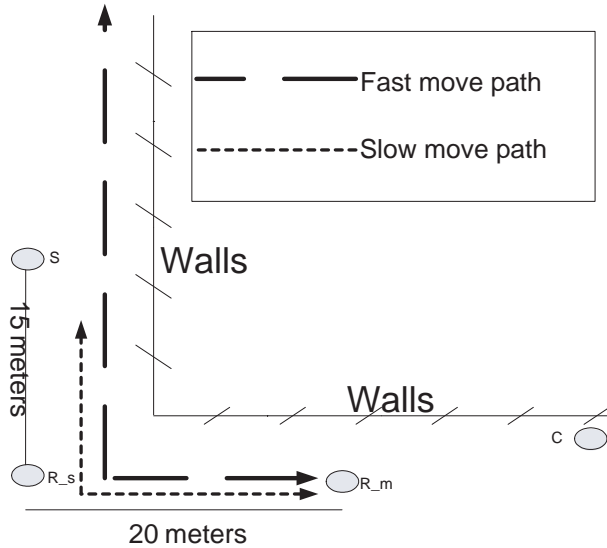


Figure 5.1: Experiment topology.

### 5.3.2 Measurement results

We discuss the effect of the different smoothing factors of the SampleRate on one-hop throughput for the stationary and mobile scenarios.

#### One-hop stationary scenarios

In this scenario, both nodes were stationary with the receiver node located at R<sub>m</sub> and the sender at S in Fig. 5.1. In the contending scenario, a node referred as contending node was placed at location C. The contending node produced a constant traffic of 0.32 Mbps to the sender (with UDP 800 Bytes packets), which communicated with the receiver. We evaluated the performance of SampleRate for different smoothing factors. The stationary experiments lasted 15 minutes for each smoothing factor and each scenario. The mean throughput of each 30 second intervals is seen as a sample. Hence, the results are the averages of 30 experiment samples with a 95 percent statistical confidence interval.

The stationary experiment results in Fig. 5.2 show that smaller values of the smoothing factor (SampleRate uses less history information) lead to increased throughput. This is because when the distance is close, there are many packets going through the link. Packet loss can easily cause rate selection decision variance [102]. In our experiment, we discovered that a smaller smoothing factor can achieve higher throughput in this large traffic load sce-

nario. This is also the case for the contention scenario.

When the contending traffic was present, the throughput was greatly reduced. The contention traffic impacts the throughput in two aspects. Firstly, the contending traffic will consume wireless medium, which reduce the transmission for the sending node in location S. Secondly, collisions can cause the rate-adaptation mechanism to make the wrong estimation of channel quality, which leads to the unnecessary selection of smaller data rate [47]. Our experiment demonstrates this effect and also shows that smaller smoothing factors can lead to faster response to channel variance and hence improve the throughput in a small scale.

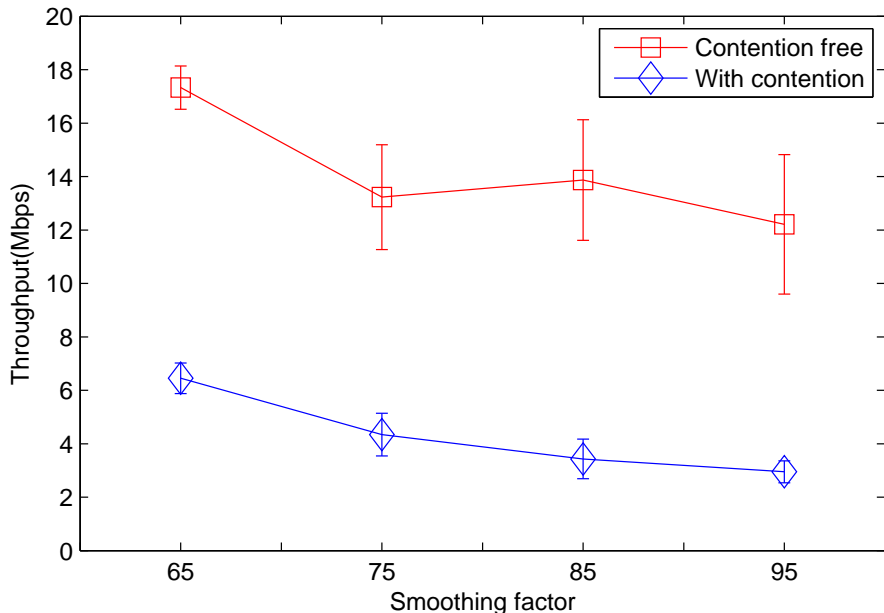


Figure 5.2: One hop throughput comparisons in stationary scenario.

### One-hop mobile scenarios

A mobile scenario will cause larger link quality variance in the channel. Thus, we designed the following mobile experiment to investigate the performance of rate adaptation in the mobile scenarios. We still use the same traffic as stated previously with the receiver always fixed at location Rm. The mobile node was set to be the sender. The sender walked based on the slow and fast mobile path as depicted in Fig. 5.1. The walking speed of the sender was around 1 and 2 m/s in the slow- and fast-moving scenarios, respectively.

Since the SampleRate first need some samples to make the initial selection of the data rate, we set up a warm-up period at 60s for each experiment. The warm-up period between the experiments ensures that the history about the channel in the previous rounds is stabilized with a large number of new packets.

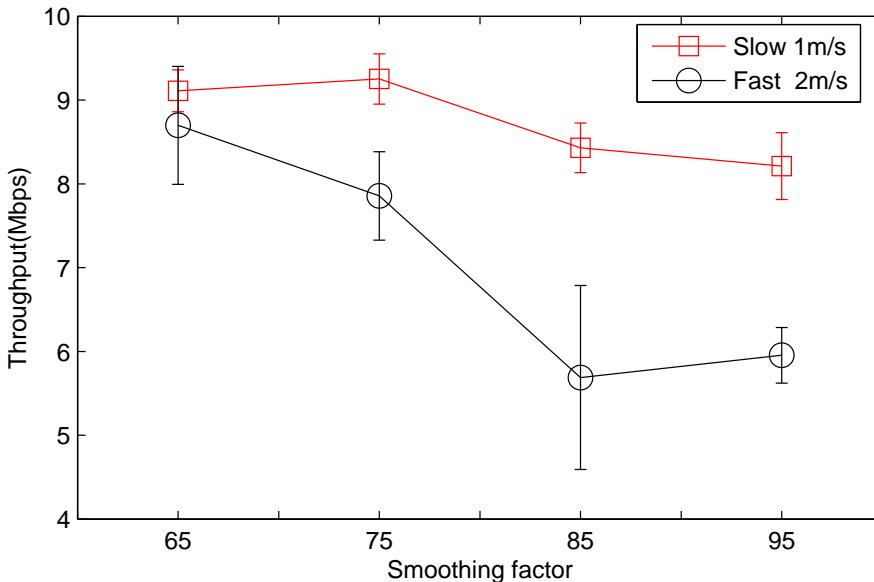


Figure 5.3: The average throughput of the mobile scenario.

The results in Fig. 5.3 show that the smoothing factor influences the responsiveness of the rate adaptation mechanism. A smaller smoothing factor leads to better performance due to faster response to link dynamics. As can be seen in Fig. 5.3, the smoothing factor impacts the throughput more significantly in the fast scenario than in the slow scenario. This indicates that when the link quality changes faster, less history information should be used in the rate-adaptation mechanism.

To clearly understand when smaller smoothing factor leads to better performance, we plotted in Fig. 5.4 the average throughput over time for the slow scenario in which the Smoothing factors are 65 and 95, with 95 confidential interval for 10 times experiments. That is, for each second we calculate one throughput and we average the 10 times experiment result for each second. In the figure we can observe that when the sender was getting apart from the receiver (0 - 30s), the results are almost the same for both values of the smoothing factor. However, when the sender was approaching the receiver (30 to 60s), rate adaptation was faster with a smaller smoothing factor.

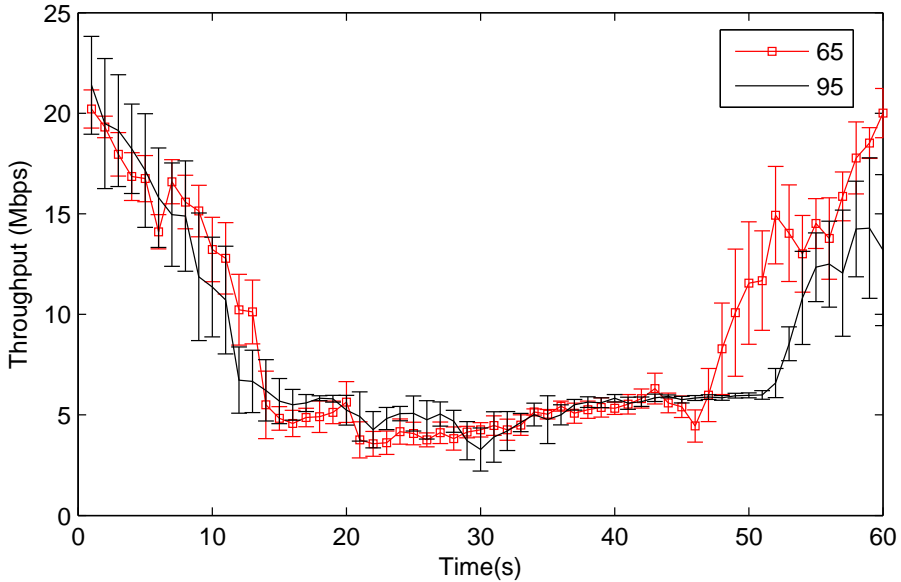


Figure 5.4: Throughput over time comparison (slow scenario).

Hence, the throughput increases.

To clearly compare the responsiveness of the rate adaptation mechanism under those two smoothing factors, we plot in Fig. 5.5 the variation of the rate in an experiment for the fast scenario. As expected, if less history is used (when the smoothing factor is 65), the rate adapts faster. This explains the throughput difference in all mobile experiments. The variation of rate is large for both values. The sharp alterations of the rate may introduce larger variance and the rate can vary between 48 and 54 Mbps even when the sender and receiver are close to each other. Perhaps better performance can be achieved if the rate adaptation mechanism can adapt a more accurate link quality estimation as described in Chapter 3.

## 5.4 Novel Link Quality Based Rate Adaptation

### 5.4.1 Improved rate selection mechanism

Due to the problem of slow reaction to link variance as shown in previous section, we would like to improve the rate selection algorithm's performance fundamentally. We think that the data rate selection mechanism in SampleR-

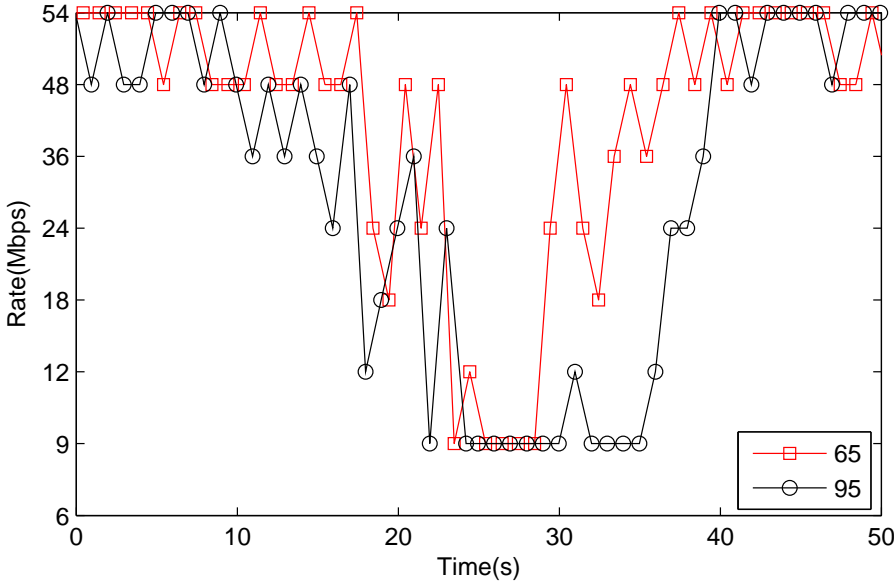


Figure 5.5: Selected rates comparison (fast scenario).

ate actually is quite good. The problem is from the link quality estimation sources. The SampleRate rely on packet counting to learn the channel quality for different data rates. Due to that the number of packets on each rate is very limited and the fast channel variance, the LQE from SampleRate is not accurate. Therefore, we propose to augment the classic SampleRate rate adaptation protocol [8] with our proposed LQE method in Section 3.4.

In the proposed rate selection process during each time instant  $i$ , given SNR  $j$  for a certain neighbor, we compute the following rate metric

$$G_{R(k),i,j} = \frac{1}{E_{R(k),i,j}} t_{p,R(k)} + t_{b,R(k),i,j}, \quad (5.3)$$

where  $t_{p,R(k)} = \frac{A_d}{R(k)}$  is the time required to transmit a packet of  $A_d$  under lossless conditions and

$$t_{b,R(k),i,j} = \frac{c_m}{2} \left( 1 + \sum_{i=0}^{10} 2^i [1 - E_{R(k),i,j}] \right) \quad (5.4)$$

is the backoff time for rate  $R(k)$ , SNR  $j$ , and time instant  $i$  which takes link quality into consideration [22, Eq. 17]. We assume a maximum 11 retransmissions. Finally our proposed algorithm chooses the rate such that

$$\arg \min_{R(k)} \{ G_{R(1),i}, \dots, G_{R(12),i} \}. \quad (5.5)$$

The complete implementation of our rate adaptation process is given in Algorithm 1. Please note that we omitted index  $i$  for clarity and we present the algorithm for SNR map only when the initial SNR profile for all data rates is available, i.e., we omit the initial phase to compute (3.6).

It is important to note that, like the original SampleRate, we deviate randomly from the chosen data rate to increase link probing efficiency. For each interval, 0.5% of packets are sent at data rate  $R(k-1)$  and 0.5% at data rate  $R(k+1)$ , where the chosen rate is  $R(k)$ . In case  $k = 1$  only  $R(2)$  is used while in case  $k = 12$  only  $R(11)$  is used. The percentage of packets sent at adjacent rates was selected empirically such that protocol performance was maximized. Any increase of the probing rate resulted in significant decrease in network throughput. Also, we decided to probe only adjacent data rates, since probing more data rates caused instabilities in the routing process.

#### 5.4.2 New rate adaptation mechanism performance evaluation

We now look at the adaptability of the proposed LQE process in rate adaptation mechanism, from the perspective of rate adaptation and focus on SNR profile based LQE only. Just like in Section 3.4, we split the discussion focusing first on static SNR profile and later on its updating.

##### Static SNR profile

We test the performance of the proposed rate adaptation mechanism in three scenarios, T1 T2 and T6, which is introduced in Chapter. 3 and compare it against the SampleRate protocol, where in contrary to our approach, a constant traffic flow was used for rate adaptation. For T1, we have tested how the amount of data traffic affects the rate adaptation efficiency. In four different experiments, we varied the amount of traffic flowing between nodes over a period of 400 s such that, on average, the network was loaded  $\{100, 80, 50, 20\}\%$  of the time with UDP traffic (fully loaded for a certain amount of time). The results are presented in Fig. 5.6. We can see that our proposed rate adaptation method outperforms SampleRate, especially in low data traffic scenarios (almost two times the throughput of SampleRate with 20% loading). In the T2 scenario (stationary, LOS), the proposed rate adaptation mechanism is again better than SampleRate, in this case by 0.5 Mbps. For T6, we clearly see that, starting with the SNR profile created in the cafeteria, nodes were able to update the profile and increase throughput by  $\approx 23\%$  for 100% loading and  $\approx 33\%$  for 20% loading. This proves the statement that the initial SNR profile can be created only once in the entire lifetime of a

**Algorithm 1:** Rate selection

---

**Input:**  $\Psi$ ,  $\alpha_s$ ,  $D_m$  (neighbor MAC address),  $t_{p,R(k)}$ ;

**Output:**  $r_k$  (selected rate);

1  $t_{b,R(k),\Psi} \leftarrow \infty$ ,  $\mathbf{E}_\Psi \leftarrow \text{GetPdr}(\Psi)$ ,  $\mathbf{E}'_\Psi \leftarrow \text{ReadPdr}(\Psi)$ ;

2 **for**  $k = (1, \dots, 12)$  **do**

3    $E''_{R(k),\Psi} \leftarrow \alpha_s E'_{R(k),\Psi} + (1 - \alpha_s) E_{R(k),\Psi}$ ;

4    $M_{\Psi,k,D_m} \leftarrow E''_{R(k),\Psi}$  (assign PDR to file);

5    $G_{R(k),\Psi} \leftarrow \frac{t_{p,R(k)}}{E''_{R(k),\Psi}} + \text{GetBot}(E''_{R(k),\Psi})$ ;

6   **if**  $t_{b,R(k),\Psi} > G_{R(k),\Psi}$  **then**

7      $t_{b,R(k),\Psi} \leftarrow G_{R(k),\Psi}$ ,  $r_k \leftarrow k$ ;

8 **Procedure**  $\text{GetPdr } (\Psi)$  (read new PDR);

**Input:**  $\Psi$ ,  $D_m$ ;

**Output:**  $\mathbf{E}_\Psi = \{E_{R(1),\Psi}, \dots, E_{R(12),\Psi}\}$ ;

9 **for**  $k = (1, \dots, 12)$  **do**

10    $E_{R(k),\Psi} \leftarrow M_{\Psi,k,D_m}$  (read PDR from file);

11 **Procedure**  $\text{GetBot } (E_{R(k),\Psi})$  (get backoff time);

**Input:**  $E_{R(k),\Psi}$ ;

**Output:**  $t_{b,R(k),\Psi}$ ;

12  $c_m \leftarrow 31$  (contention window size used),  $t \leftarrow 0$ ;

13 **for**  $i = (0, \dots, 10)$  **do**

14    $t \leftarrow t + 2^i (1 - E_{R(k),\Psi})^{i+1}$ ;

15  $t_{b,R(k),\Psi} \leftarrow \frac{c_m}{2} \frac{t+1}{E_{R(k),\Psi}}$  (see [22, Eq. 17]);

16 **Procedure**  $\text{ReadPdr } (M_{\Psi,k,D_m})$  (PDR from the driver);

**Input:**  $M_{\Psi,k,D_m}$   
    (transmitted and acknowledged packets for  $\Psi$ ,  $D_m$  and all  $k$ );

**Output:**  $\mathbf{E}_\Psi = \{E_{R(1),\Psi}, \dots, E_{R(12),\Psi}\}$ ;

17 **for**  $k = (1, \dots, 12)$  **do**

18    $t_x \leftarrow$  number of transmitted packets from  $M_{\Psi,k,D_m}$ ;

19    $t_{ack} \leftarrow$  number of acknowledged packets from  $M_{\Psi,k,D_m}$ ;

20    $E_{R(k),\Psi} \leftarrow \frac{t_x}{t_{ack}}$ ;

---

device (see Section 3.4.1), allowing for easy update every time it operates in a new environment.

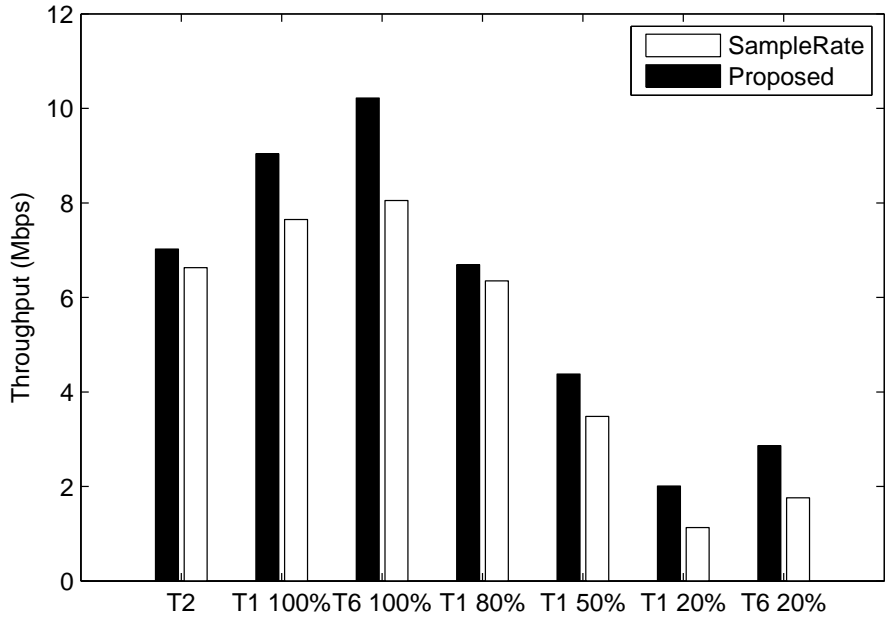


Figure 5.6: The performance of proposed rate adaptation mechanism in comparison to SampleRate in T1 and T2 scenarios. Percentage values represent average amount of traffic flowing between sender and receiver.

In Fig. 5.7 we plot the instantaneous throughput versus time for the T1 scenario. We observe that when the transmitter is closest from the receiver (around 0s and 80s), the proposed rate adaptation mechanism is better than SampleRate. However, in the middle of the range, the performance is not significantly better. In fact there are cases when SampleRate performs better, see Fig. 5.7 for [50, 65] s. This is because during the experiment the receiver, passing through the corridor, received packets with SNR in the range of 9 to 15 dB. Within this range, our algorithm often switches between 802.11b and g rates, whichever has the lowest total instantaneous transmission time. This causes our algorithm to achieve a range of throughput values. SampleRate, however, plays safe by sticking to rate of 11 Mbps and achieves a constant throughput. The same as previous chapters, the experiments are repeated 10 times and we show the average mean value and 95% confidence interval.

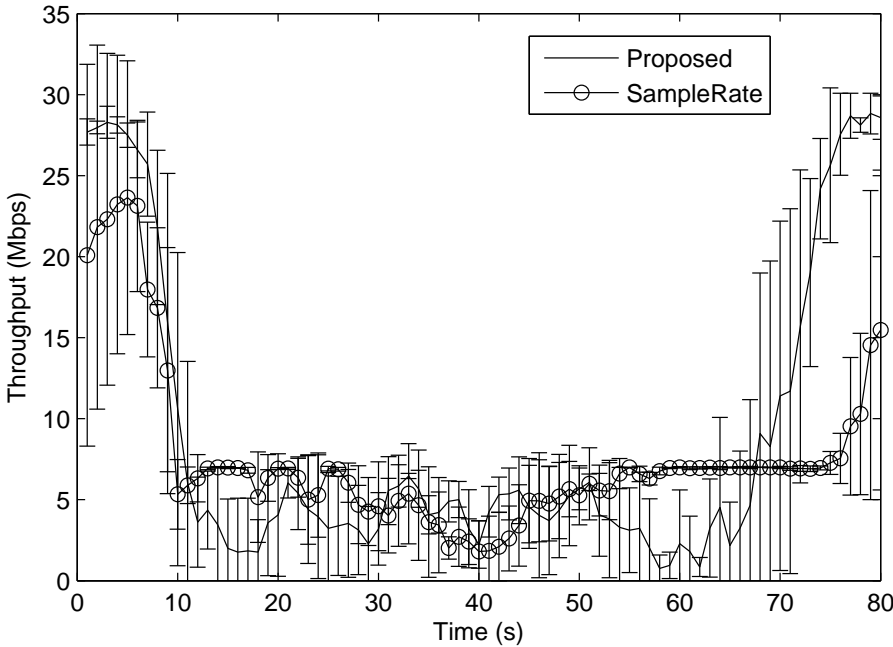


Figure 5.7: The performance of the proposed rate adaptation mechanism in relation to SampleRate in T1 scenario.

### Updating process in rate adaptation

It is important to evaluate the impact of  $\alpha_s$  on the rate adaptation process. We used scenario T1 to do this. We use a different  $\alpha_s$  each experiment and measure the achieved throughput, repeating the experiment for one  $\alpha_s$  in the same scenario at three different times. In Table 5.1, we use the same  $\alpha_s$  as in Fig. 3.16, which is used for updating the SNR profile based on new data traffic. However, it is important to note that the optimal  $\alpha_s$  is not necessarily the same in these two cases, since in Fig. 3.16, we only update the SNR profile for one data rate, and in Table 5.1, we update the SNR profile for several data rates. Nevertheless, we can see that if  $\alpha_s > 0$ , the performance is quite similar in both cases for different  $\alpha_s$  values.

## 5.5 Chapter Summary and Discussion

In this chapter, we first analyzed the effect of the smoothing factor used in SampleRate to the channel conditions and the impact on the routing layer. Smaller smoothing factors lead to better performance when the channel is

Table 5.1: The proposed rate adaptation performance for different  $\alpha_s$  values

$\alpha_s$	Throughput [Mbps]
0	[6.80, 8.55]
0.05	[8.30, 9.63]
0.1	[8.77, 9.59]
0.2	[8.20, 9.48]
0.3	[7.64, 9.11]
0.5	[8.14, 8.67]
0.9	[7.63, 8.39]

dynamic or traffic load is large. Slow rate adaptation is not suitable for mobile ad hoc networks. Moreover, when there is no background traffic, the rate adaptation mechanism performs worse. Thus, smaller smoothing factors should be used in the IEEE 802.11 mobile ad hoc network. If some context can be provided (such as the device's speed), better rate selection can be done.

Further, we also used our proposed LQE method in the data rate selection. A new rate adaption mechanism, which based on our advanced LQE method was proposed. Our measurements indicate that our proposed system improves per-link throughput in both static and dynamic environments.

These results may not only be helpful for the SampleRate mechanism, but also for other rate-adaptation mechanisms that utilize history information to make rate decisions. The new rate adaption mechanism is also used in Chapter 6 to have faster and smarter route selection.

# Chapter 6

## Link Quality Based Routing

### 6.1 Introduction

A high layer application of wireless link quality is found in routing. Hop count based routing may produce routes with poor links, because using long links generally implies fewer hops but longer links also generally means poorer link qualities. Therefore, some prior proposals by De Couto *et al.* [20] have suggested to minimize the number of transmissions necessary to reach the destination, such as the ETX. However, ETX needs the packet delivery ratio for each link and to acquire that, the authors used simple hello packets. Because of the limitations of using hello packets, ETX will benefit from an accurate packet delivery estimation. The ETT routing metric also considers the expected time for delivering one packet, which means not only the packet delivery ratio but also the data rate are the factors for route selection. Both ETX and ETT can benefit by feeding higher accuracy and faster response LQE information.

Our idea is that we evaluate the impact of the data rate in route selection along at first, then we evaluate the impact of the LQE in the route selection. We implemented our proposed LQE methods in the route selection algorithms in our IEEE 802.11 test-bed (see Appendix A) and compared their performance with the traditional route selection mechanism, such as hop count method and hello packet counting route selection. Two types of IEEE 802.11 link quality estimation sources described in Chapter 2 were fed into the route selection. Finally, one of the LQE method is also used in the rate adaptation mechanism and this rate adaption mechanism is also used together with the routing protocol. Using different test-beds in diverse scenarios, compared to the traditional beacon packet-based route selection, we show over 50% improvement end-to-end throughput obtained at the routing

layer.

This chapter is organized as follows, the related work has been introduced in Section 6.2. Our combined method based routing is introduced in Section 6.4 and SNR based routing is introduced in Section 6.5. The chapter is concluded in Section 6.6.

## 6.2 Related Work

In this section, we first describe the basic routing metrics and routing protocols.

### 6.2.1 Routing metrics

ETX is proposed in [20] as a routing metric that leads to a routing path requiring a minimum amount of transmissions, including retransmissions. Having the packet delivery ratio from both sides of the link, ETX becomes

$$ETX = \frac{1}{P_f \times P_r}, \quad (6.1)$$

where  $P_f$  and  $P_r$  are forward and reverse packet delivery ratios of the link as estimated by the packet delivery ratio estimation method, respectively.

The ETX metric is computed for each link. The previous work [20] has proved that it achieves better performance compared to the traditional hop count route selection method. To be able to consider both packet delivery ratio and data rate of a link in the route computation, ETT is proposed in [9] and tries to find the route with the minimum end-to-end medium occupying time. The ETT routing metric in [9] is computed as:

$$ETT = ETX \times \frac{L}{B}, \quad (6.2)$$

where  $L$  and  $B$  are the packet size and the current transmission rate, respectively.

The link quality estimation used in the ETX formula proposed in [20] still uses the traditional hello packet-based method. If we use our LQE method, which is more accurate and responds faster to link dynamics, the route selection will be more accurate and faster, which can introduce higher throughput. The improvement of throughput in routing is investigated in Section 6.4 and Section 6.5.

### 6.2.2 Routing protocol: OLSR

Optimized Link State Routing Protocol (OLSR) [15] is a proactive ad hoc routing protocol. We select the proactive protocol. Since we have mobile scenarios, faster reaction routing protocol is required. We used the open source routing daemon implementation of OLSR [90] (version 4.10.0). The protocol is an optimization of the classical link state algorithm. The key concept used in the protocol is that of the multipoint relays (MPRs), which are selected nodes that forward broadcast messages during a flooding process. OLSR uses Topology Control (TC) messages to propagate the link state information for non one-hop neighbors to realize the optimal route calculation. A packet delivery ratio aware extension [110] is made in the routing daemon that makes the route decisions based on the packet delivery ratio instead of hop count.

Even though we chose the OLSR protocol in our test-bed, the results obtained in our experiments should be applied to other routing protocols also, as this work is about the route selection and not about route signaling.

### 6.2.3 Previous studies

As in rate adaptation, most of the previous link quality-based routing methods are based on link probing with broadcast packets [9, 20]. In those methods, authors show that the routing performance is better than the hop-count based route selection, where the degree of improvement differs depending on the propagation environment. The authors of [51] proposed two metrics called modified ETX (mETX) and Effective Number of Transmissions (ENT), which represent the variability of steady state packet error probability and effective bandwidth (in the network sense), respectively. The metrics are designed to enable lower layers to reduce the loss rates visible to the upper layer protocols like TCP. A single data rate is considered in [51] and the metrics are evaluated in simulation environments only.

The Authors of [92] modified the traditional Ad Hoc On-Demand Distance Vector (AODV) routing protocol and used SNR to select the routes directly. The proposed method decide whether particular links should be eliminated at the routing layer, based on the selected SNR threshold. Again, the protocol was evaluated only via computer simulation. In [42], broadcast packet-based traffic was used to evaluate the link quality and select a route. Obviously, the problems of the packet counting-based methods remained the same. The method presented in [95] does not give a comparison to other known route selection methods and the routing itself is performed in a single data rate. Finally, we note that the rate adaptation method based on SNR maps of [108] was not evaluated in the routing layer.

In addition to the aforementioned issues, none of the above papers discussed a mechanism to update the estimation parameters of the used LQE method, which is of utmost importance for large scale ad hoc and mesh networks.

### 6.3 Data Rate Determined Route Selection

Rate adaptation can be important not only in one-hop throughput optimization, but also in the link quality based route selection. In this section, we use the ETT routing metric, but we set the LQE input in Eq. 6.2 to be a constant value 1 in all the links. Therefore, only the data rate will be used to select the route. We can evaluate the impact of the data rate in the link quality aware route selection method.

As shown in the section 5.3, the responsiveness of the rate adaptation mechanisms is affected by the percentage of the history information taken into account for the rate decision. For our one hop scenarios, there is always traffic between the sender and the receiver. However, for multi-hop scenarios, there is not always traffic on every link. IEEE 802.11g has 12 rates. If there is no intentionally generated traffic, there will be only one or two hello packets among the nodes for each second. Hence, SampleRate would not have adequate number of samples to decide the optimal rate of a link that is currently not used. Moreover, the failure of several packets severely impacts the expected transmission time calculation [102]. Thus, the rate adaptation performance will be very dynamic. The effect on the routing decisions when the selected data rate is taken into the calculation have not been carefully investigated in the previous literature. The rate not only affects the one hop throughput, but also the route selection.

We conducted two-hop experiments in the node movement pattern shown in Fig. 6.1. Two nodes were stationary located at N1, N2; the receiver was located at N1 and another intermediate node located at N2. The sender started walking from N1 and then passed N2 until N3 in 30 seconds, and then walked backward in the opposite trajectory as indicated in Fig. 6.1. The warm-up period was of 60 seconds.

Each node's program maintained two values for each link, the packet delivery ratio and data rate. Based on Eq. 6.2, both metrics change ETT and thereby influence the routing decision. Since we want to evaluate the effect of the rate adaptation on routing alone, the quality of each link is set to be identical and constant in these experiments. Thus, the impact of responsiveness of rate adaptation to the ETT routing decisions is analyzed independently. To demonstrate how the ETT routing works based on only

the data rate information, we plot a graph as shown in Fig. 6.1. This shows when the sender at N3 prefers a two-hop route towards the receiver node located at N1 (based on the data rates indicated in figure, we can get the following calculation as,  $0.04 + 0.08 = 0.12 < 0.3$ ). If node N3 approaches the intermediate node located at N2, the rates between the sender and the receiver will increase and the one-hop route will be selected again.

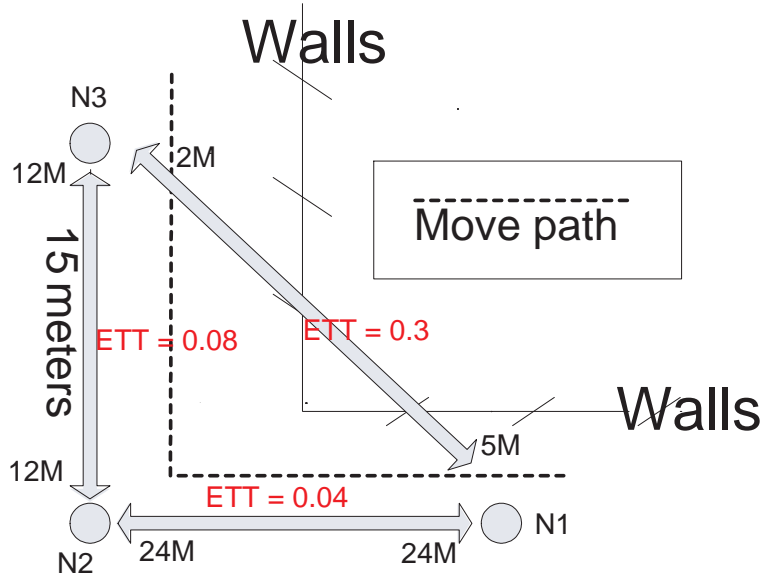


Figure 6.1: Route selection based on ETT.

Two types of experiments were done: with and without background traffic. 10 UDP packets per second were generated by the node in the location point C as background traffic. Different smoothing factors impact the throughput performance as can be seen in Fig. 6.2. As less history information is utilized, the throughput increases. When there is no background traffic between nodes, our program record shows that the data rate between two nodes changes very slow and randomly. This causes a slow response in the routing and therefore decreases the overall throughput. Two effects cause worse performance when background traffic is not present. Firstly, the sender prefers one-hop communication because the rate between the sender, the receiver and the intermediate node changes very slowly. Once the rate drops to lower values, it takes longer time to increase it because of the mobility of the sender. Another effect is that the rate-adaptation decision is quite random. The throughput variation is quite high. Secondly, when there is traffic on every link, the nodes can adapt to the link quality dynamics much

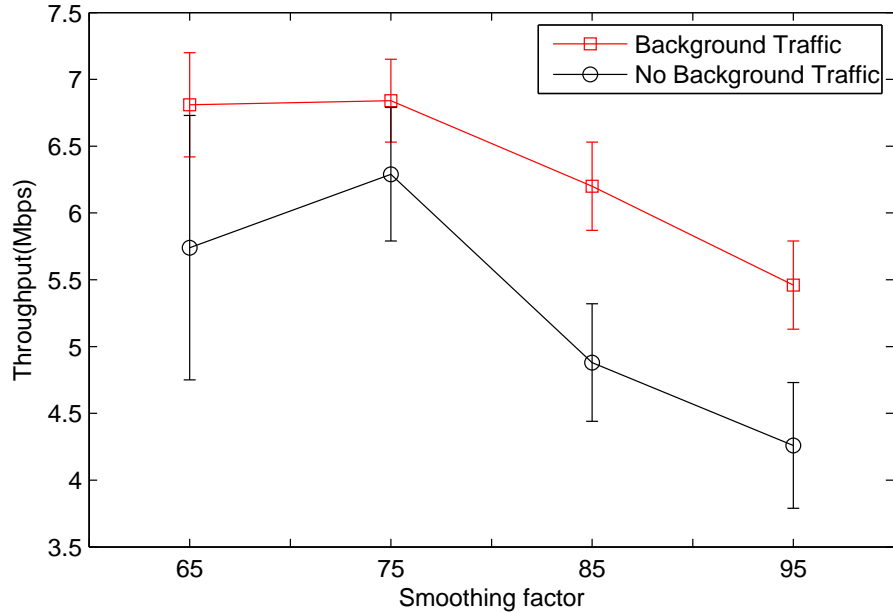


Figure 6.2: Two hop throughput comparison.

faster. When the sender loses the receiver's line-of-sight, it can communicate to the receiver through an intermediate node with a line-of-sight. Smaller smoothing factors lead to higher throughput in each experiment due to fast rate adaptation.

## 6.4 Linearization LQE Based Routing

In this section, we used our linearization LQE method (see Section 3.3.1) for estimating the link quality and use this link quality information in the routing layer and compared the performance with traditional route selection methods. We used two different configurations. Firstly, the data rate is fixed to evaluate the pure LQE's effect to the routing layer. Secondly, we allowed the data rate to be adaptive and see how much improvement can be achieved in total. The test-bed implementation is described in detail in Appendix A. In this section, we only present the measurement scenarios and results.

### 6.4.1 Fixed data rate

In this experiment, we fixed the data rate to 54 Mbps. Several routing metrics and LQE methods are tested in different scenarios.

The link quality (LQ) can be measured by different methods; those methods are discussed in previous Chapter 2. Hello packet delivery ratio provides the simplest link quality information, while measurement of the data traffic provides the most accurate link quality information. Signal strength can also give some indication on the link quality variance. For short, we use the following abbreviations:

Hello packet delivery ratio:  $LQ_{HR}$

Data packet delivery ratio:  $LQ_{DR}$

Hello packet signal strength:  $SS_{HR}$ .

The EWMA mechanism was used in calculating the  $LQ_{HR}$  and  $LQ_{DR}$  and they can adapt different  $\alpha$  in the mechanism. A larger smoothing factor  $\alpha$  achieves faster adaptation to link changes, but will also result in more frequent route changes and the accuracy of the link estimation will be lower. On the contrary, a small  $\alpha$  will calculate the link quality based on longer history record, thus will react slowly to fast link changes. Since all our link quality sources use the EWMA mechanism, to differentiate the  $\alpha$ 's for different link information sources, we use  $\alpha_{HPSS}$ ,  $\alpha_{HRSS}$  and  $\alpha_{DPDR}$  for the smoothing factors of  $SS_{HR}$ ,  $LQ_{HR}$  and  $LQ_{DR}$ , respectively.

We use the data packet delivery ratio as our benchmark for evaluating the performance. However, the data packet delivery ratio also uses the EWMA (see Chapter 2) equation for updating. We need to find out the optimal  $\alpha$  value for updating the data packet delivery ratio first. We used seven different mechanisms in total to compare their performance.

To get a clear view of the effect of different link quality information to the routing layer, we designed the following experimental scenario in a large open space as shown in Fig. 6.3. To maintain a stable link, all the laptops were placed on tables with the height of the antenna above 1m from the floor. Two laptops (Node1 and Node2) were placed about 15m away from each other such that the ETX was in the range of 1.0 – 1.2.

For each link quality assessment scheme an experiment was performed which lasted 400s. Node3 was the traffic source and Node1 was the traffic destination. Node3 gradually moved away as shown in Fig. 6.3. The ETX between Node3 and Node1 was increasing and at a certain point, Node3 chose the 2-hop route via Node 2 to Node1 instead of the 1-hop route directly to Node1. Node3 took 20s to move away and then 20s to move back. This process was repeated with exact time control ten times and each process of experiment can be assumed as independent of each other. We calculated the average throughput with confidential interval for each mechanism's experiment.

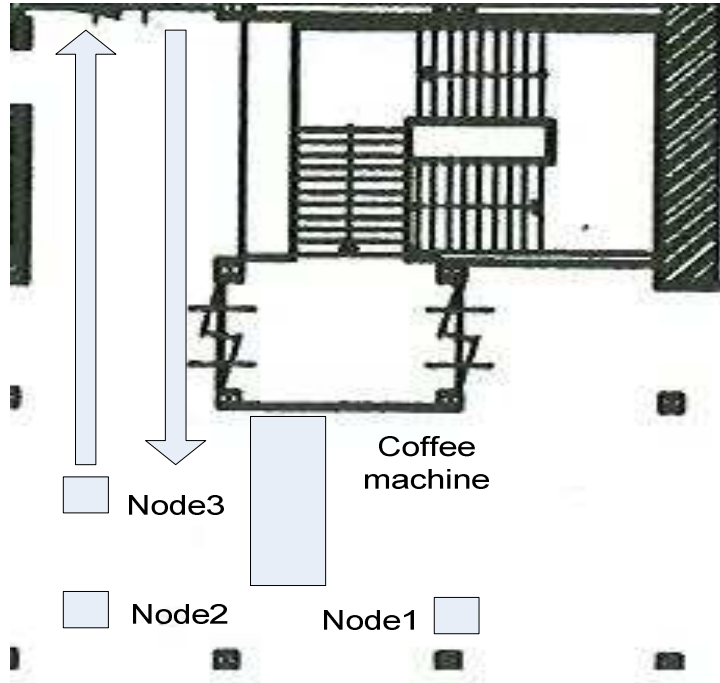


Figure 6.3: Single rate routing experiment topology.

### Selecting good $\alpha$ values

For the  $LQ_{HR}$ , due to a small number of hello packets, a large  $\alpha_{HPDR}$  will cause the prediction of link quality to be very inaccurate and instable. Therefore we use  $\alpha = 0.2$  for  $LQ_{HR}$ .  $LQ_{DR}$  can provide the most accurate link quality information. We feed in the link quality calculated to the routing layer in experiment to have a comparison.

We conduct the experiment with a mobile source node. Due to experimental equipment limitations, the mobile node was carried by the author of this book and with the intention to walk smoothly; the speed of movement and little shaking of the laptop could not be eliminated and can result in fast link quality changes. In this case, a higher  $\alpha_{HPDR}$  generally turned out to be better for the network. We tested four different  $\alpha_{DPDR}$  for  $LQ_{DR}$ ; 0.1, 0.2, 0.5 and 0.9. However,  $\alpha_{HPDR}$  can be chosen for matching mobility.

Fig. 6.4 shows UDP throughput for 7 different experiments. One hop and Two hop represent the experiments done with static routing of which the routing tables in Node3 and Node1 were fixed to one hop and two hop routes.  $LQ_{HR}$  represents the result that the link quality information is only provided by  $LQ_{HR}$ . The four results at the right side represent the throughput while using the  $LQ_{DR}$  with different  $\alpha_{DPDR}$ . The throughput is represented with

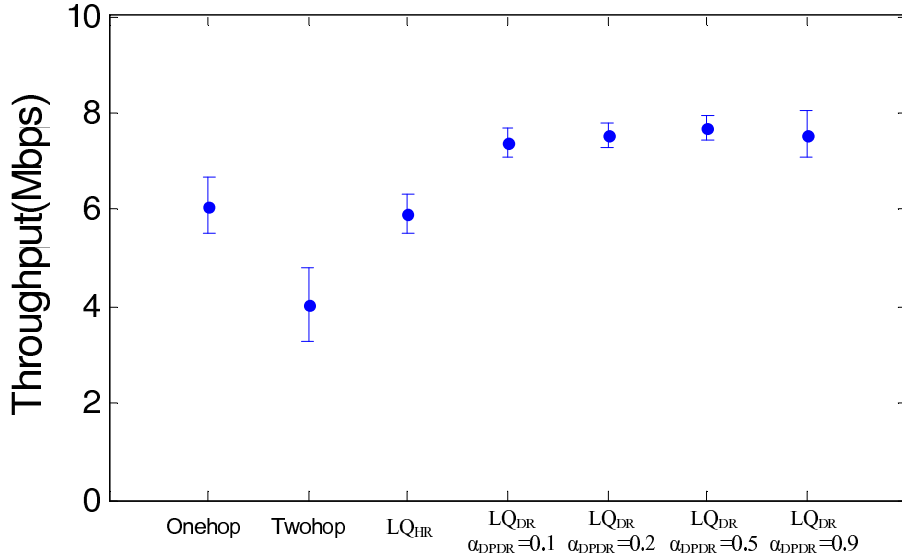


Figure 6.4: Routing throughput comparison (UDP traffic without combined LQE)

an average value and the 95% confidential interval. We can see that the  $LQ_{DR}$  indeed results in higher UDP throughput than static routing and  $LQ_{HR}$ . The difference among the different  $\alpha_{DPDR}$  is not much but with  $\alpha_{DPDR} = 0.5$  the average throughput was the highest. The Twohop experiment does not change the route, so the throughput is much more stable and the confidential interval is much less compared to the others while  $LQ_{DR}$  also resulted in small confidential intervals except  $\alpha_{DPDR} = 0.9$ .

The difference of each mechanism is caused by different routing change time. As showed in Fig. 6.3, the source node moved away from Node1 and the line of sight channel became non-line of sight. The link quality between Node1 and Node3 degraded dramatically and ETX between Node1 and Node3 became more than the ETX sum of the Node1 to Node2 and Node2 to Node3. So at a particular location, there was an optimal point for route change. Node3 was carried back and forth 10 times from Node1 and thus we had 20 times to change the route. Due to the movement limitation, this turning point may not be exactly the same location for every round, but the better link quality assessment mechanisms will result in route changing closer to the optimal changing point. However, more link quality fluctuations commonly resulted in multiple route changes during one movement.

One hop static routing achieved very high throughput at the line of sight area but almost no throughout at the other end, while the two hop static

routing achieved lower but constant throughput. During the experiment, we found that the  $LQ_{HR}$  mechanism almost always chose the one hop route and thus got almost the same throughput as the Onehop result. This is because of the differences between the hello packet and the data packet and also the slow reaction of the  $LQ_{HR}$  to link changes. While obviously the  $LQ_{DR}$  got very accurate estimation of the link, this more accurate LQE leaded to more frequent optimal route selection. Thus  $LQ_{DR}$  achieved higher throughput.

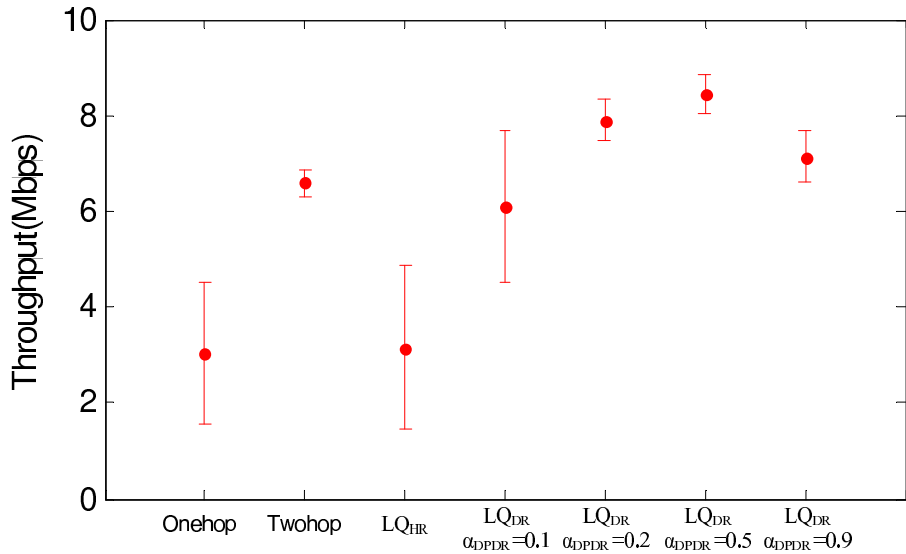


Figure 6.5: Routing throughput comparison (TCP traffic without combined LQE)

In the next experiment, we changed the traffic to use TCP. From Fig. 6.5, we can see almost similar results but with larger differences. Since the TCP traffic has the slow start problem and uses bidirectional traffic, it suffered more from the route change and low delivery ratios. The Twohop static routing had higher throughput than the Onehop showed the importance of the stable route and link quality. The hello packet delivery's throughput was almost 30% of the highest throughput of the data traffic. This showed the  $LQ_{HR}$ 's weakness in handling the fast link changes and difference between  $LQ_{DR}$ . The UDP traffic we used had less maximum throughput than the TCP traffic, so we can not directly compare the throughput of TCP and UDP.

From Fig. 6.5, we can also find out that different  $\alpha_{DPDR}$  can result in different throughput for the TCP traffic. When the  $\alpha_{DPDR}$  was 0.5, the throughput was the highest. The reason is that this value makes fewer route

changes than  $\alpha_{DPDR} = 0.9$  and got faster response than  $\alpha_{DPDR} = 0.1$  and 0.2. Better link quality information not only results in higher average throughput, but also gets more stable throughput and smaller confidential interval. Based on this part of the experiment, we can draw the conclusion that  $LQ_{HR}$  indeed performs worse than  $LQ_{DR}$  and 0.5 is the optimal  $\alpha_{DPDR}$  value.

### Performance enhancement with linearization LQE

With our new Eq. 3.1 and constant value C, we carried out an experiment with the other two LQE mechanisms. To investigate the effect of using combined LQE algorithms, we implemented an alternative version of OLSR that only uses combined algorithm to calculate  $LQ_{EST}$  (see Appendix A). The traditional hop count routing metric which only uses received hello messages to determine the existence of the neighbors is also added to evaluate the throughput performance of both UDP and TCP traffic.

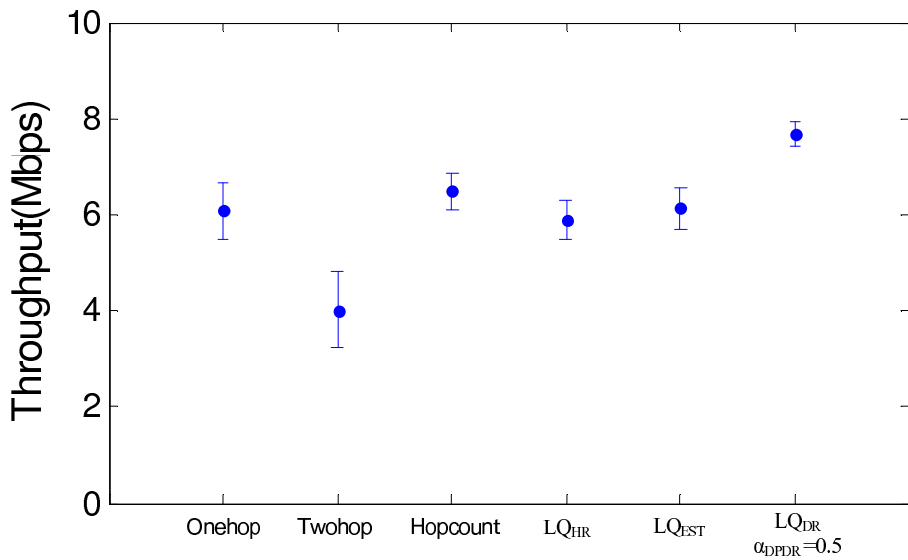


Figure 6.6: Routing throughput comparison (UDP traffic with combined LQE)

Fig. 6.6 shows the UDP throughput of these experiments. The difference between the different algorithms is not much. This is because, for UDP traffic, even Onehop static routing can achieve very good performance most of the time. When the channel turns to be non line of sight,  $LQ_{HR}$  reacts much slower than the  $LQ_{DR}$ , so the gain of the mechanisms based on  $LQ_{HR}$  and  $LQ_{EST}$  is not very obvious. On the contrary, since the  $LQ_{HR}$  and  $LQ_{EST}$  also

did some route changes, sometimes bad routes may be chosen and this results in even less throughput than one hop route. During the experiment, we found that the hop count method hardly changed to the two hop route, since in the scenario, the hello packets seldom lost three consequent packets and thus the Hop count had almost the same result as in the Onehop experiment.

One problem we found is that with very high traffic density, the hello packets sent by the traffic sender are more probable to be lost at other nodes while traffic source does not have much problem on receiving hello packets. This difference may cause link asymmetrical and fluctuation in estimation, but it is not a severe problem in reality since in the real scenario, the sender can send the  $LQ_{DR}$  directly to the receiver.

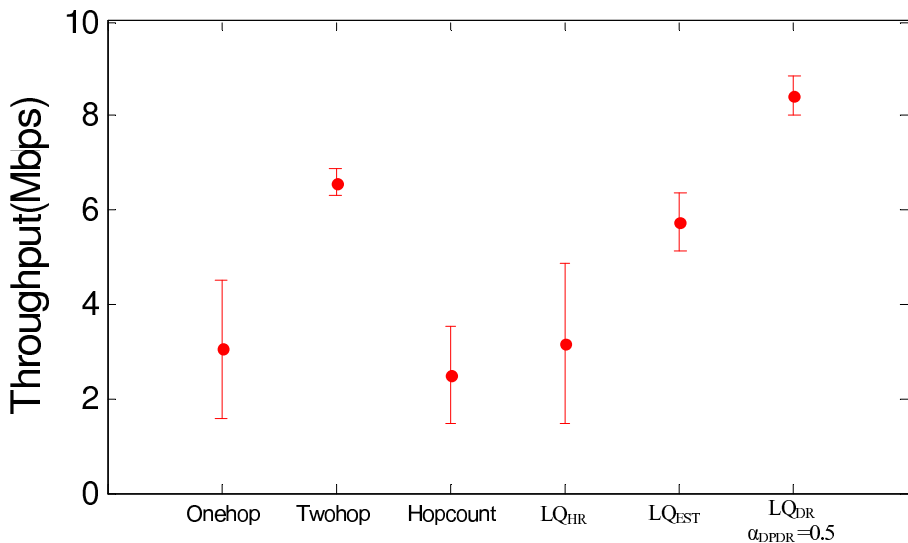


Figure 6.7: Routing throughput comparison (TCP traffic with combined LQE)

The throughput of TCP is shown in Fig. 6.7. We can see that the TCP throughput further shows benefit of  $LQ_{EST}$ . In this experiment, staying in one hop route will result in bad performance due to the slow start effect of TCP and bidirectional traffic of TCP. The Hop count performed as bad as the Onehop experiment since both of them hardly changed the route. The  $LQ_{HR}$  performs better than the Hop count, since when the channel turned bad, it changed the route to the two-hop and got better throughput. Our estimation mechanism performed much better than Hopcount and  $LQ_{HR}$  due to faster detection of the link changes and more accurate estimation. The better performance refers to higher average throughput and smaller variation.

The reason why it did not perform better than the Twohop static route was because the route change resulted in loss of packets, which greatly reduced the speed of TCP.

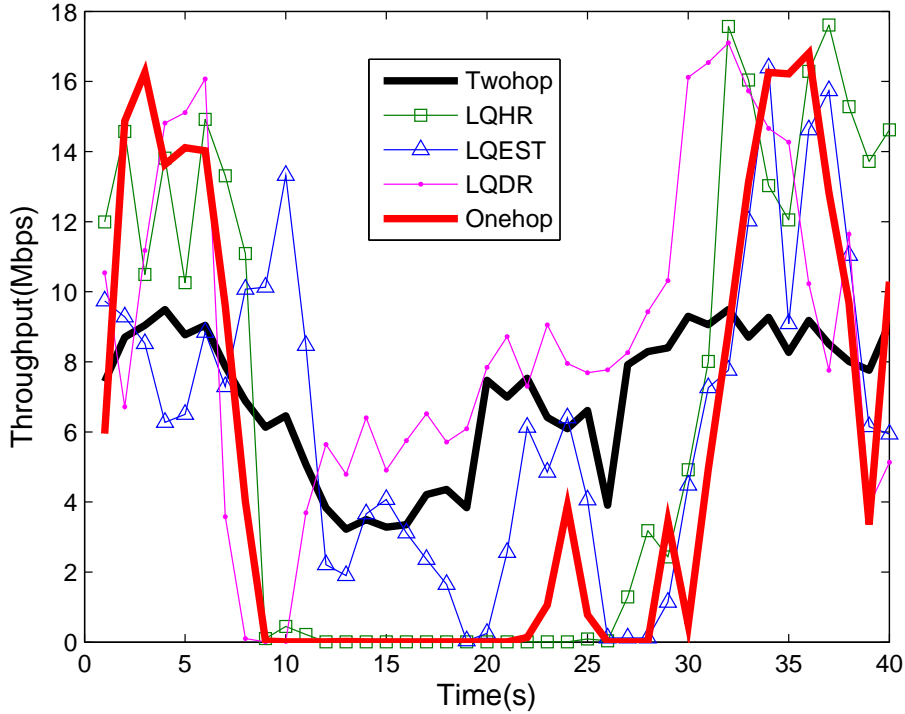


Figure 6.8: Instantaneous TCP throughput

To demonstrate the effectiveness of our mechanism better, we plot the instantaneous TCP throughput of five experiments of a 40s round in Fig. 6.8. The throughput is calculated every second. We can clearly see that at the beginning and the end of the experiment, one hop routing got higher throughput and in the middle of the experiment, the two-hop route was better. The  $LQ_{DR}$  ( $\alpha_{DPDR} = 0.5$ ) almost selected the best route and  $LQ_{HR}$  almost did not change the route.  $LQ_{EST}$  changed the route, but was later than  $LQ_{DR}$ .

The TCP traffic suffered a lot due to route changes, even the  $LQ_{DR}$  case shows this between 8 and 11 seconds. Bad route decision caused worst performance (26-29s for  $LQ_{EST}$ ). Different traffic types may require different optimal route decision criteria which are based on link quality information. The experiments together showed better performance of  $LQ_{DR}$  and  $LQ_{EST}$  compared to  $LQ_{HR}$ . Thus, the performance in reality will be even better than  $LQ_{EST}$  if the four algorithms are applied together.

### 6.4.2 Adaptive data rate

We also turned on the rate adaptation mechanism (the SampleRate implemented in Madwifi driver) to let the system decide the data rate based on the channel variance. In every interval (1s), the system checked the new data rate used in the MAC layer and sent this information to the routing layer for route selection.

#### Measurement scenario

To compare the impact on the routing layer of different LQE methods as well as the rate adaptation response to link dynamics, we carried out experiments with the scenario shown in Fig. 6.9. To maintain a stable link, three stationary laptops were placed on tables one meter above the floor at positions R, I1, I2. Two of them (I1, I2) were the intermediate nodes, while R was the receiver node. The mobile node is referred to as the sender. The sender followed the trajectory shown as an arrow in Fig. 6.9. It waited 30 seconds (warmup period) to stabilize the SampleRate mechanism, then made a movement of 45 seconds following the trajectory. This process was repeated ten times with almost exact time control. We can assume that each walk is independent. The sender kept sending UDP packets as fast as it could via the routing table provided by OLSRD. Experiments with three different configurations were carried out using the scenario described above. The three experiments used ETX (with one-rate), ETX (multi-rate), and ETT (multi-rate).

#### Measurement result

In the first experiment, all nodes used a fixed data rate of 36 Mbps. Two link quality metrics were used separately, our proposed  $LQ_{EST}$  and the traditional  $LQ_{HR}$ .

We plot the average throughput obtained in ten runs with a 95% confidence interval in Fig. 6.10. To analyze the route choice influenced by the two mechanisms, we also plot the number of hops taken to reach the receiver. At the beginning of the experiments, the two mechanisms made the same choice: the one-hop route. Thus, in the first 15 seconds, the performance is almost the same, so we do not plot this period and the performance comparison is only based on the period from 15 to 45 s for all experiments. From 25 to 35 s, the throughput achieved by our proposed  $\hat{R}$  is higher than traditional  $R_H$ , because our proposed packet delivery ratio estimation influenced the routing layer to use the interim nodes (multi-hop paths) while the estimation of the traditional packet delivery ratio continued to suggest the routing layer to use

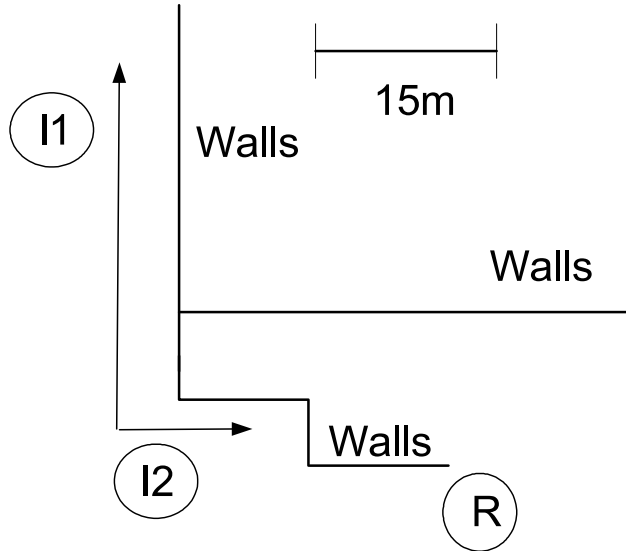


Figure 6.9: Routing experiment topology.

the low throughput one-hop route. Even though the receiver and sender did not have a line of sight and the link quality had almost dropped to zero for 36 Mbps data packets, hello packets (2 Mbps) still had good delivery ratio and this caused a slow reaction to the link dynamics. After the 35<sup>th</sup> second, the  $LQ_{EST}$  chose the three-hop route, while the  $LQ_{HR}$  chose the two-hop route. Therefore, the throughput of the  $LQ_{HR}$  is still poor. We calculate the average throughput for these two methods in Table 6.1.

In the second experiment, we turned on the rate adaptation mechanism. Hence, the data rate between each link was determined by the SampleRate algorithm. We still used the ETX routing metric to decide the route. Since the procedure is the same as the first one, we do not plot the throughput with time for this scenario, but only provide the average throughput for different packet delivery ratio estimation methods in Table 6.1. As can be seen in Table 6.1, our  $LQ_{EST}$  still has better performance than the  $LQ_{HR}$  due to the selection of the better path. The three hop selection in the later part of the experiments can not have very high throughput since all the links at that time selects the low data rate and performs much worse than the fixed 36 Mbps. It is also shown in previous work that rate adaptation does not outperform the fixed data rate in some scenarios [102]. This explains why the second experiment for the  $LQ_{EST}$  performs slightly worse than the first experiment, which used a fixed data rate of 36 Mbps. However, for the  $LQ_{HR}$ , one-hop was selected for a long time. Rate adaptation can select some lower data rate that is more suitable for long distance and non line of sight

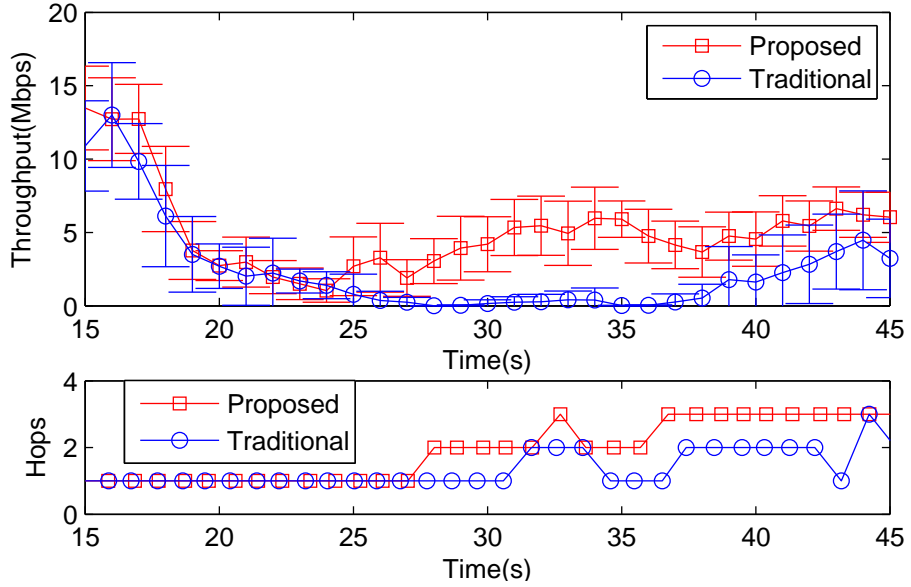


Figure 6.10: The throughput with time (ETX, constant 36Mbps).

transmission, which results in higher end-to-end throughput. The result from experiment 1 and 2 indicate that, for the ETX metric, if the route selection is fast and proper, rate adaptation may degrade the end-to-end performance due to improper rate selection. On the contrary, if the route selection is not so suitable, rate adaptation can improve erroneous links by using the lower data rate in bad links, which increases the end-to-end throughput.

In the third experiment, the rate adaptation mechanism was also turned on, and both packet delivery ratio estimation and data rate were used in the route selection by using ETT. Due to SampleRate's problems in our scenario as described in Section 5.2, we sent background traffic between each nodes in this experiment to let the SampleRate update faster<sup>1</sup>. The result which is shown in Table 6.1 is similar to the second experiment and  $LQ_{EST}$  still outperforms  $LQ_{HR}$ . When using ETT, the slow reaction of rate adaptation also affects the route decision and that is why the throughput is lower than the other two experiments. Further, the background traffic also causes the multi-hop throughput (2 and 3 hop) to be lower.

Based on these experiments, it can be concluded that our proposed packet delivery ratio estimation achieved better performance than traditional packet delivery ratio estimation with a faster response to link dynamics. The rate

---

<sup>1</sup>Based on trial experiments, without background traffic, the rate selection is very slow which causes the experiment results to be quite random.

Table 6.1: Routing throughput performance comparison.

Experiment	1	2	3
Routing Metric	ETX	ETX	ETT
Rate (Mbps)	36	adaptive	adaptive
Rate Adaptation	—	SampleRate	SampleRate
$LQ_{EST}$ (Mbps)	4.87	4.40	1.23
$LQ_{HR}$ (Mbps)	2.20	3.99	0.89
Improvement	121%	10%	38%

adaptation that we used is not so good for mobile scenarios. In fact it does not always improve the end-to-end throughput compared to a fixed data rate. Moreover, while using the selected rate in the ETT route selection metric, performance degraded even further. However, instead of looking for a better rate adaptation scheme, we propose to also use the  $LQ_{EST}$  method for rate adaptation, which is described in the following section.

## 6.5 SNR Mapping Based Routing

In the previous section, the combined LQE method is used. However, the data rate selection is still decided by hello packet link quality information. In this section, we feed our SNR based link quality information to the new rate adaptation scheme (see Section 5.4.2) and evaluate the overall performance enhancement introduced by the SNR based link quality estimation.

### 6.5.1 Implementation

By using a better LQE technique in the route selection process, it is possible to gain throughput over the links. With link-state routing protocols, which we consider in the implementation process described in Appendix A, the ETX per link is calculated using [20, Eq. 1] for which the PDRs per neighbor link are collected through topology control (TC) messages. We propose the following routing metric per link in the TC

$$\mathcal{R} = \frac{1}{E_{R(j),i}\sqrt{R(j)}} \frac{1}{E_{R(k),i}\sqrt{R(k)}}, \quad (6.3)$$

which replaces ETX and is very similar to ETT.

Using  $\mathcal{R}$ , the link with the highest throughput and PDR is always selected. To balance the accuracy of LQE and the number of route update messages, we execute one LQE interval per routing update interval.

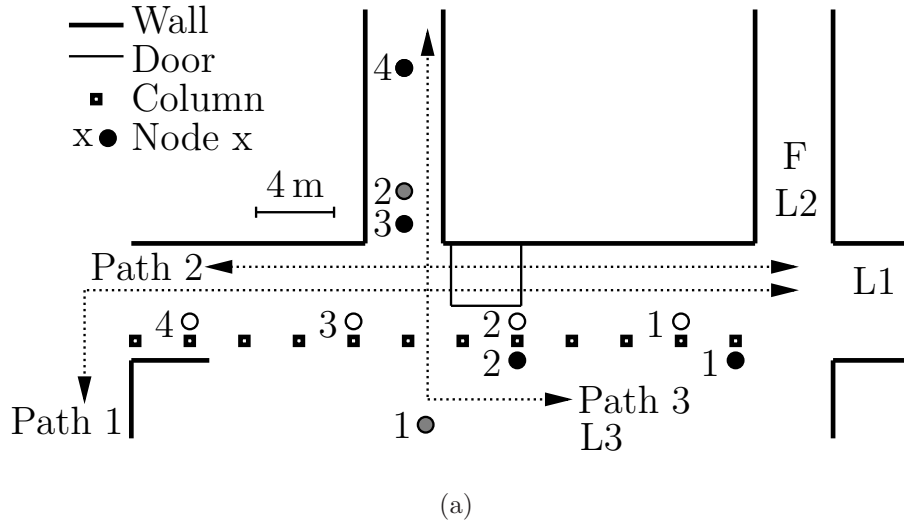


Figure 6.11: Routing experiment scenario.

### 6.5.2 Measurement scenarios

We have set up the following three scenarios, called as R1–R3. We show the scenarios in Fig. 6.11.

- R1 The sender and the receiver were located close to each other at L3, see Fig. 6.11(a). The sender followed path 3 away from receiver and returned. For this path, two nodes, marked as grey circles in Fig. 6.11, forwarded the traffic. The movement was repeated 10 times and lasted 90 s. Before each movement along path 3, the sender waited 30 s at L3. to let the rate adaptation mechanism stabilize and to de-correlate each movement from the previous.
- R2 The sender located at L1 (see Fig. 6.11), sent traffic to each of its four neighbors one by one, marked as white circles in Fig. 6.11. The sender sent a constant flow of UDP traffic for 5 min to one receiver before it targeted the next node. Nodes were allowed to forward the traffic.
- R3 The same as R2, but the receiving nodes were located differently, marked as the black circles in Fig. 6.11. This was the non-LOS communication scenario in an ad hoc network.

### 6.5.3 Measurement results

Experiments at the routing layer need to evaluate the overall efficiency of a link quality aware system. First, in Fig. 6.12, we plot the throughput

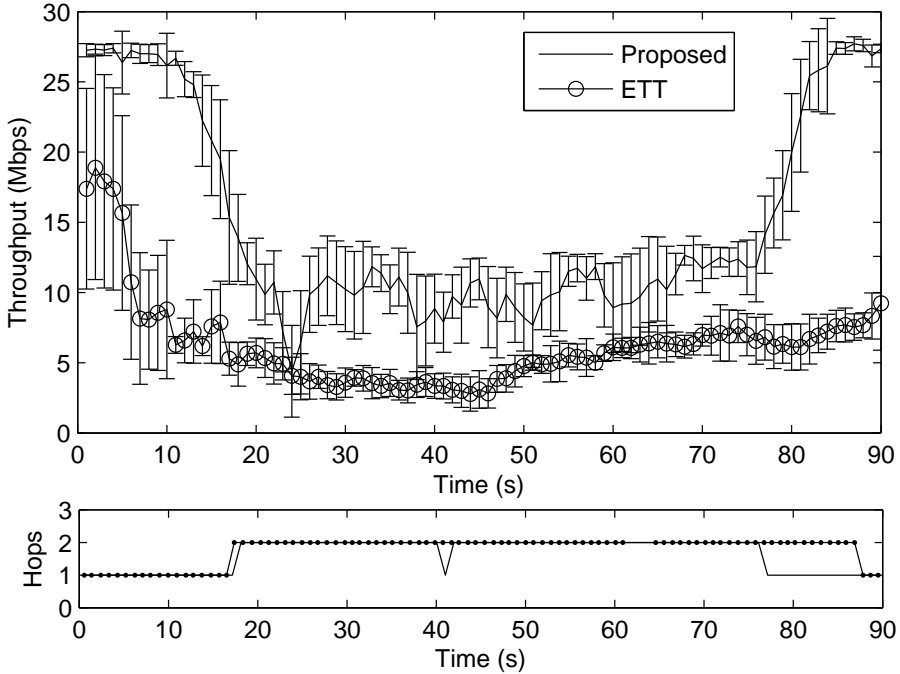


Figure 6.12: The OLSR throughput obtained for scenario R1 with proposed system and ETT metric. Please note missing information on hop count starting at 61 s, which is due to TC messages being lost.

versus time for the rate adaptive scenario R1. We can see that our proposed mechanism can outperform the current OLSR implementation using ETT. In the initial phase, our mechanism tends to select better data rates which achieves greater single hop throughput. We can see from the hop chart (bottom of Fig. 6.12) that after 20 s, both mechanisms start to use the two-hop route. As observed previously, due to better selection of data rate, the throughput with our method is also much higher than the packet counting based system. This can be seen as the transmitter moves towards the receiver (between 60 s and 80 s). This is due to the slow reaction time of SampleRate and the inaccurate LQE of ETT. The packet counting based system still chose a 2-hop route even when the distance between the transmitter and receiver is less than that between the transmitter and intermediate node. This results in more worse performance than our proposed link quality aware system.

The results of experiments in R2 are given in Fig. 6.13(a). We can see that in this situation, our proposed mechanism performs better than OLSR with ETT. When the receiver was node 2 or node 3, only one or two hops were traversed. Due to the fact that the connection between node 1 and the

sender is not satisfactory, either a one or two hop route between the receiver and the sender will result in decreased throughput. An interesting behavior is seen for node 4, which is supposed to achieve the lowest throughput due to its greatest distance from the sender. In this case, the SampleRate-based OLSR performs better than our proposed system while both of them outperform node 3 and node 2 in terms of throughput. This is presumably due to sudden link breaks that temporarily decreases the throughput to zero, which results in fixed routing outperforming our proposed LQE-based routing.

The results of the experiments for the scenario R3 are shown in Fig. 6.13(b). Similar to the results in R2, the first node uses a one hop route to the sender and the performance of our algorithm is a little better than the classic OLSR due to the same reason as described for R2. However, when the receiver was moved further away from the sender (nodes 2, 3, and 4, respectively), our method performs even better and the throughput is much higher than in the SampleRate based OLSR. Based on the results for the stationary scenarios, R2 and R3, our proposed system generally selects a better data rate and route based on more accurate link quality information and achieves higher end-to-end throughput.

## 6.6 Chapter Summary and Discussion

In this chapter, we evaluated the link quality based routing. The problem of existing routing systems are that they still use the traditional LQE method, which leads to bad performance. Meanwhile, low performance of the rate adaptation can also degrade the end-to-end throughput. We implemented two of our proposed LQE methods into the routing layer and evaluated the performance via tremendous measurements in different scenarios and with different configurations. The result reveals that the end-to-end performance can be improved even as high as 100% in certain scenarios (see Fig. 6.12), which indicate that better LQE can bring in dramatically system performance enhancements.

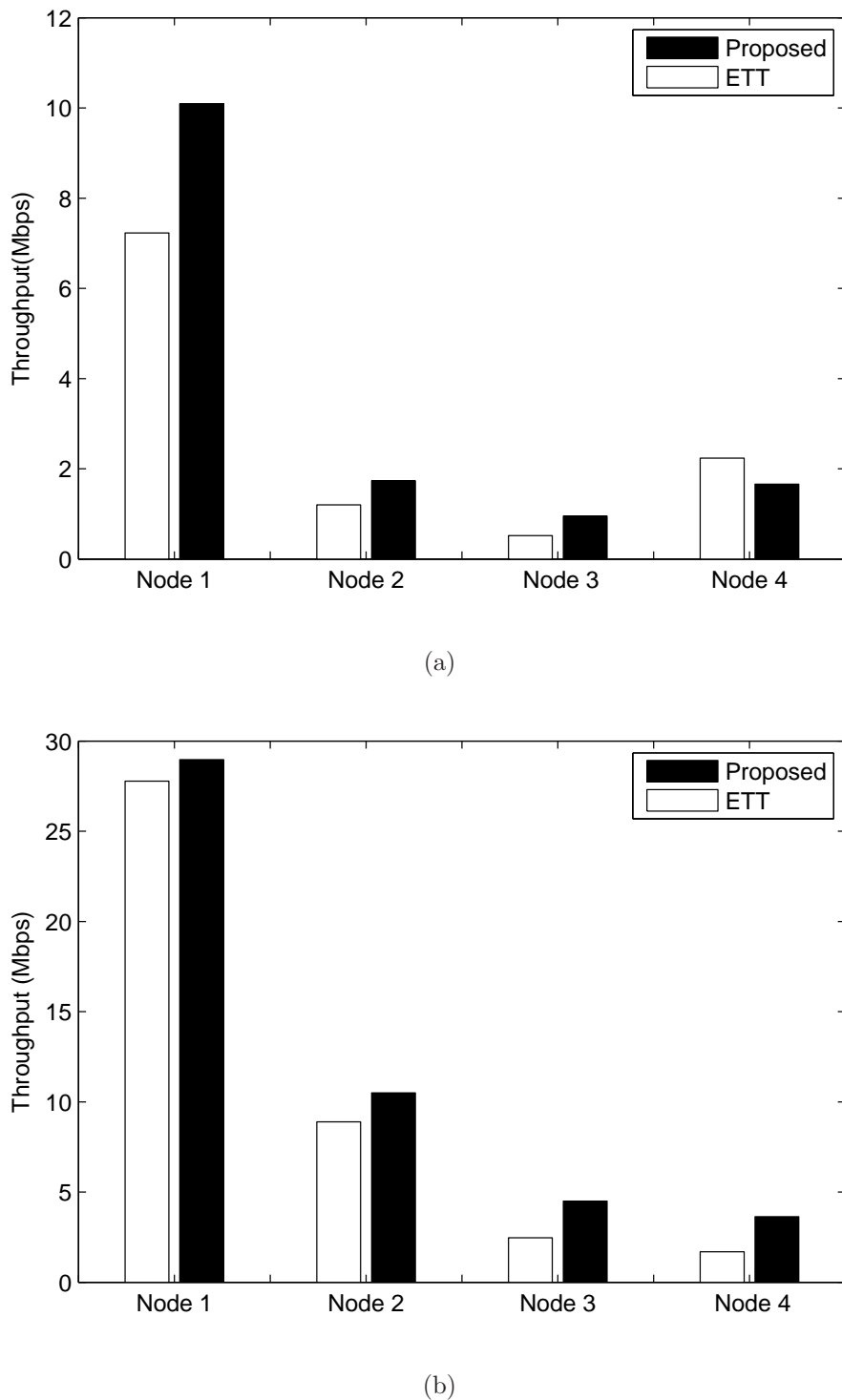


Figure 6.13: The throughput for each receiver in topology (a) R2 and (b) R3.



# Chapter 7

## Transport Layer Evaluation

### 7.1 Introduction

In the previous chapters, we have discussed the wireless link quality issues in the link and route layer. The ad hoc network has been investigated in previous study. In this chapter, the infrastructure wireless network is investigated and we evaluate the performance of wireless network in the transport layer. In particular, we shall evaluate the performance of the TCP traffic over the integrated network.

As described in Chapter 1, integration of the IEEE 802.11 and UMTS/HSDPA technologies can provide Internet access to those devices that do not have 3G cellular network interface. Meanwhile, the integrated network can leverage the advantage of these two technologies and gain some benefit, for example, load balancing for 3G cellular network, relaying traffic for the device in bad channel condition, enabling the mobile mesh network and mobile hot spots. Our new proposed integrated network can have some special performance characteristics [113]. However, the simulations for the HSDPA channel in the integrated network is still missing. Therefore in this chapter we present more simulation results for HSDPA and IEEE 802.11 integrated network.

Further, if more than one TCP flow exists in the integrated network, new problem will emerge. That is, some nodes in the ad hoc network may be poorly served due to several reasons, namely bad HSDPA channel quality, large number of hops away from the hybrid gateway, and bad channel quality on IEEE 802.11 links. Moreover, TCP will aggravate this unfairness due to its characteristics. This unfairness will make the radio resources sharing by different users highly dependent on the link quality in both channels and IEEE 802.11 network topologies. Users that are far away from the gateway can hardly access the Internet. However, this unfairness problem is not well

addressed in previous work and a good solution has not been proposed yet. In this chapter, we propose a fairness-oriented weighted scheduling mechanism which is multi-hop aware for determining the weights. The scheduling mechanism takes into account the HSDPA channel quality, number of hops away from the gateway, and the IEEE 802.11 link quality. We use the weighted method to schedule the incoming packet from the Internet to improve the fairness between different flows for different destination in ad hoc network. The weight for each TCP flow is decided by both channel qualities.

This chapter is organized as follows: In Section 7.2 we describe all the related work for the transport layer traffic over the integrated network. Our proposed integrated network is described in Section 7.3. In Section 7.4 the TCP throughput over HSDPA and IEEE 802.11 integrated network will be presented and the fairness of all the TCP flows in this integrated network is discussed in Section 7.5. The chapter is summarized in Section 7.6.

## 7.2 Related Work

The integrated network architecture described in this thesis is first proposed in [113]. Several previous works have also proposed some architectures for integrating the 3G cellular network and ad hoc network. In [98], the authors have proposed a hybrid cellular and IEEE 802.11 ad hoc network architecture. Instead of multi-hop, their work were focused on one-hop relay in the ad hoc network. The rationale behind their design was to reduce the system complexity, avoid inefficient ad hoc routing, and the impact of inefficient medium access mechanism. The authors in [64] have also proposed a hybrid cellular and ad hoc network architecture namely, UCAN, to increase cell throughput without sacrificing the fairness. The proposed architecture required every mobile station to have both cellular and IEEE 802.11 ad hoc links. The authors of [34] have described an integrated ad hoc and cellular network architecture wherein the base stations are involved in coordinating peer-to-peer communications in order to increase cell throughput and coverage. However, none of them discuss the end-to-end performance over this new integrated network.

A great deal of effort was expended to analyze the performance of transport protocols (TCP and UDP) over these two networks separately by means of mathematical models, simulation and measurement. Mathematical models for the TCP performance over UMTS/HSDPA network and IEEE 802.11 network can be found in [2, 24] and [58, 75], respectively. The paper [2] analyzed the throughput of TCP over UMTS and HSDPA. However, only low data rate downlink speed is modeled, also, there is no model of the RLC

packet average delay. The paper [11] analyzed the TCP/IP performance over 3G network and the TCP packet delay was analyzed using simulations. The paper [24] built a good analytical model which revealed the detailed delay composition of the CDMA2000 system, however, the UMTS system described in this thesis has a different transmission mechanism. Some effort was also put in modeling and optimization of the Radio Link Control (RLC) layer in UMTS/HSDPA system [12, 21, 31, 55]. The performance of the RLC layer is analyzed using the simulations and the mathematical model. However, to the best of our knowledge, there is no literature to have analyzed the integrated network bottleneck effect. This is the first work which tackles the end-to-end performance of the novel integrated network with single and multiple traffic flows using simulations.

## 7.3 Network Architecture and Simulation Setup

In this section, we introduce the architecture of the integrated network and the protocol stacks used in this architecture. Specially, we decompose the TCP round trip time.

### 7.3.1 Integrated network architecture and protocols

The integrated network architecture is as shown in Fig. 1.4. A host is connected to the Internet through IEEE 802.11 radio and the UMTS network. A node that has both UMTS radio interface and IEEE 802.11 radio interface acts as a gateway to connect to the UMTS network and the ad-hoc network. The node in the IEEE 802.11 ad-hoc network can use the gateway to relay the TCP packets and to access the Internet. We can see that both these wireless networks can affect the performance of TCP flows. Based on the bottleneck link, the end-to-end TCP throughput is determined by one of the subnetworks.

In order to realize the integrated network, we use the following network protocol stacks as depicted in Fig. 7.1. The IEEE 802.11 ad-hoc network may have different topologies, like star, mesh etc. We use the chain topology to study the impact of the number of hops on the end-to-end throughput. We only study the performance up to four hops, since the connection with more than 5 hops will have very small throughput. We can see that the right side of the stack is the UMTS core network, which consists of NodeB, Radio Network Controller(RNC), Serving GPRS Support Node(SGSN) and Gateway GPRS Support Node(GGSN). The UMTS network and the IEEE 802.11 ad-hoc networks are interconnected via a hybrid device called UMTS-802.11 Ad-hoc

gateway (referred to as the mobile gateway now onwards), which has two different network interfaces as depicted in Fig. 7.1. To enable the nodes in the ad-hoc network to find and select the mobile gateway, gateway discovery protocol is implemented over the IP layer in the mobile gateway. The mobile gateway implements the ad-hoc routing protocol to relay the TCP packets to support the ad-hoc network to connect to the Internet.

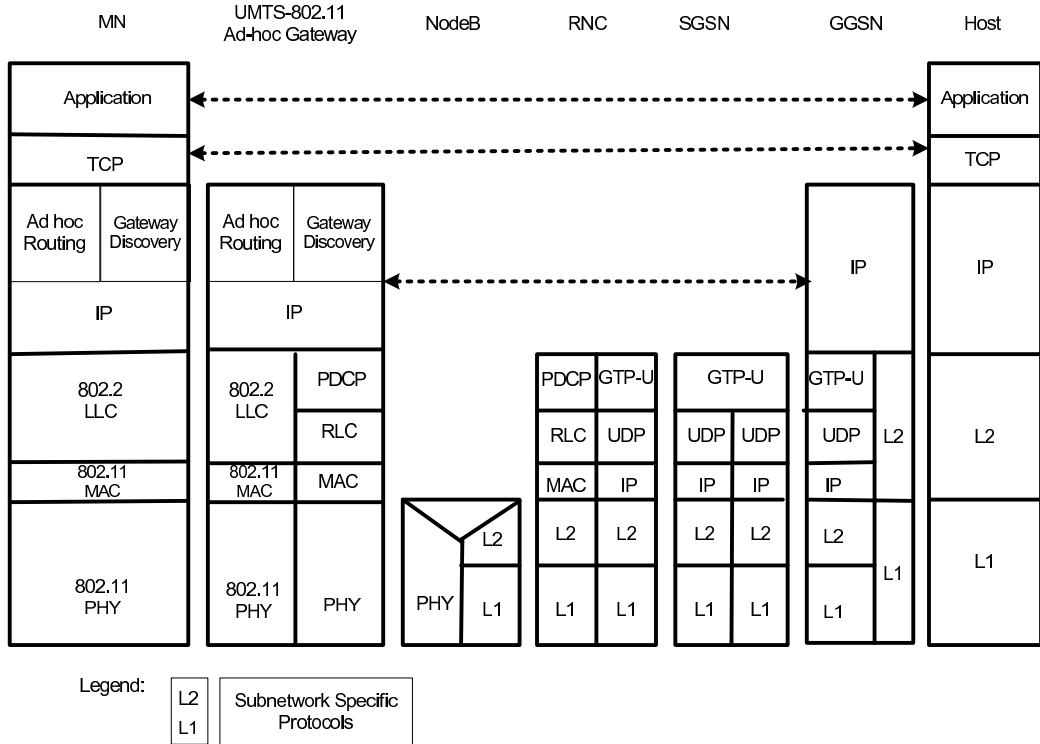


Figure 7.1: Protocol Stack across the Integrated Network. [113]

### 7.3.2 TCP packet transmission procedure

Due to the high loss of probability in UMTS links, the lower layer segmentation and retransmission scheme is used. We assume that most of the traffic is on the downlink. It means that the TCP packets are sent from the Internet to the cellular network and then to the IEEE 802.11 network. The TCP packet is segmented into small RLC packets, see Fig. 7.2. The RLC packets can be lost during the transmission over UMTS downlink channel. The receiver side of the RLC packet (the gateway) will send an acknowledgement consisting of the bitmap of packets that were lost to the RLC sender. This triggers the retransmission process of RLC packets. The RLC packets have to wait for

some time before retransmission. Once all the RLC packets within the TCP packets are correctly received, the TCP packet can be further forwarded. In the simulation, we have not set a limit on the number of retransmissions of RLC packets to enable the comparison with the mathematical analysis<sup>1</sup>. This means, that every RLC packet will be transmitted successfully. For the uplink, we assume that there are no errors, which means the TCP acknowledgements will be transmitted only once through the uplink channel. Also, since no packets are really lost, the TCP will work in steady state which allows us to use the bandwidth delay product to model the TCP throughput.

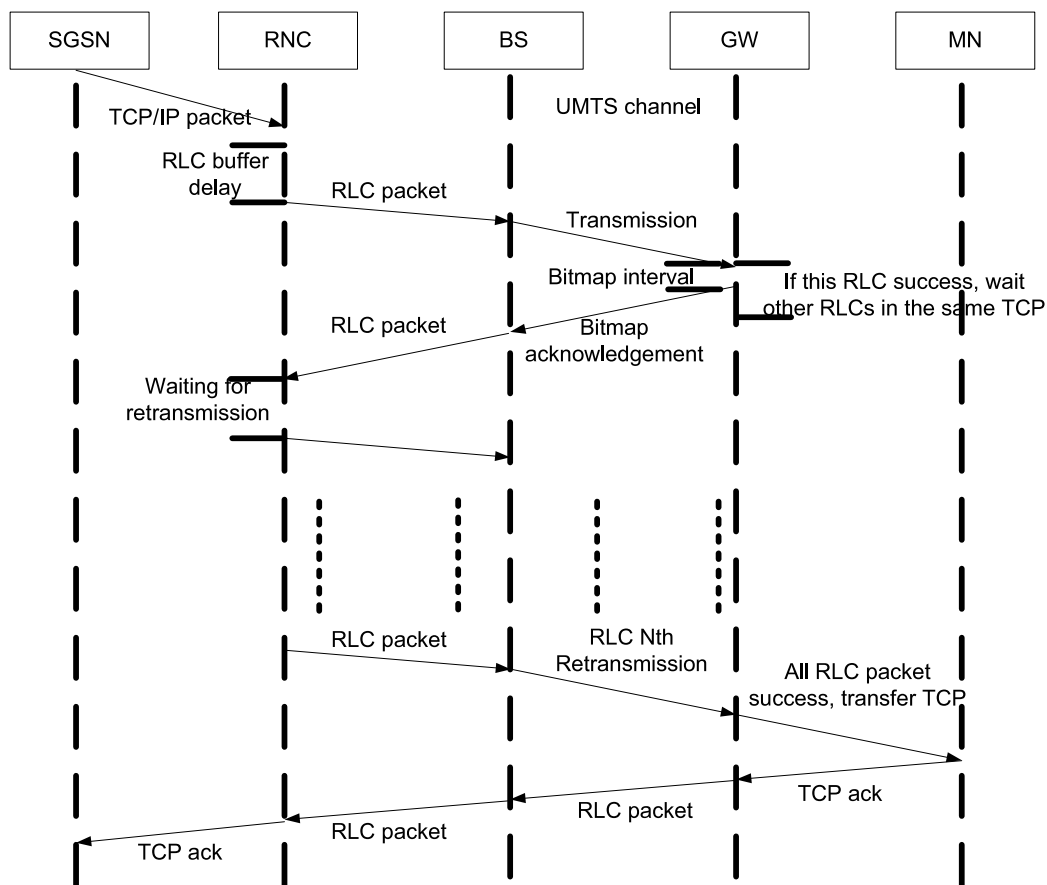


Figure 7.2: Decomposition of Round trip time of TCP packets.

---

<sup>1</sup>The real UMTS system normally sets the maximum number of retransmission to 10, with the RLC packet error rate used in this thesis, the probability that a RLC packet really lost is quite small and thus can be neglected.

### 7.3.3 Simulation model

The simulation setup and the topology is as shown in Fig. 7.3. Our main focus in this article is on UMTS network and since there are many studies that have discussed the modeling of the IEEE 802.11 ad-hoc network in depth, we do not further model the throughput in IEEE 802.11 ad-hoc network explicitly. An extensive research has been reported in [58, 75]. Here we have used multi-hop connection in our simulation topology, that means we can chose TCP receiver at 1-hop, 2-hop, 3-hop and 4-hop mobile node. The delay and connection bandwidth for the UMTS network is as shown in Fig. 7.3. We also list all our simulation parameters in the Table 7.1.

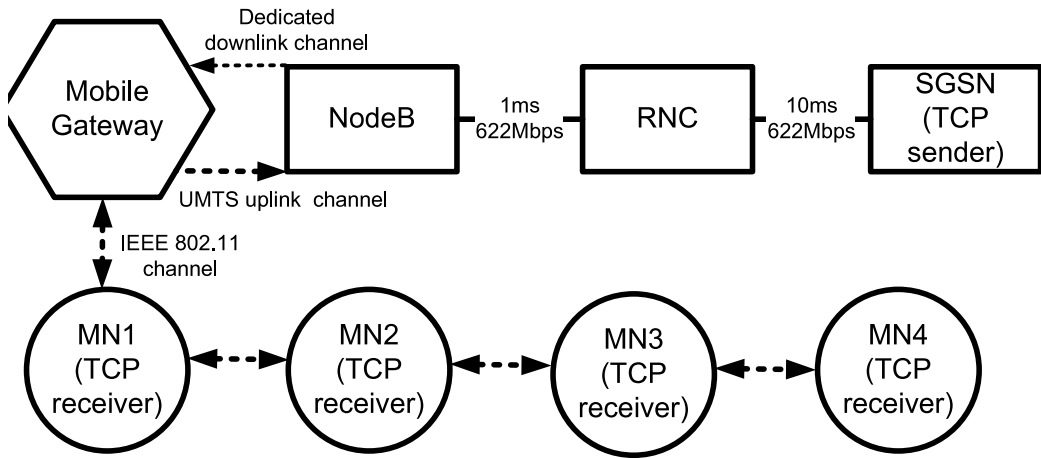


Figure 7.3: Simulation topology.

## 7.4 HSDPA TCP Single Flow Throughput

In this section, we evaluate the end-to-end TCP throughput over the HSDPA and IEEE 802.11 ad hoc network. TCP traffic has been used to evaluate the end-to-end performance. Based on the bandwidth and the delay product we have calculated the optimal window size to fully utilize the HSDPA channel, and use the configuration shown in Table 7.1 to evaluate the performance. The description of HSDPA channel model is in Section 2.3.3.

### 7.4.1 Impact of TCP window size

Compared to the UMTS module in ns-2, the HSDPA extension module simulates the real channel variance (Fig. 2.3.3) and enables this variance to affect

Table 7.1: Parameters for Simulation

HSDPA	Values
Distance from NodeB	0-700m
Path loss component (n)	3.52
Mobile gateway speed	3km/h
Mobile gateway move pattern	circle
Standard deviation in shadow fading (N)	8dB
Maximum buffer size at NodeB	1000kbytes
Downlink TTI	2ms
Uplink bandwidth	384Kbps
UPlink TTI	10ms
UMTS	Values
RLC block error rate	0 – 50
Poll timer	40 – 100ms
Status prohibit timer	20 – 60ms
Uplink bandwidth	384, 2048 kbps
Downlink TTI	10 ms
Uplink bandwidth	384 kbps
UPlink TTI	10 ms
RLC window size	4096
IEEE 802.11	Values
IEEE 802.11 bandwidth	11 Mbps
RTS\CTS Threshold	3000 Bytes
TCP Reno	Values
TCP window size	128-256 segments
TCP packet size	512 Bytes

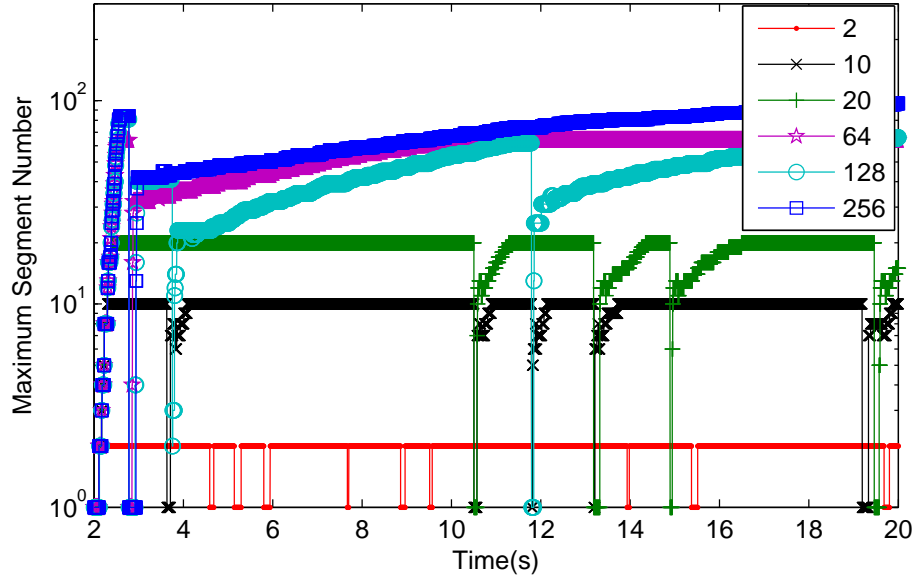


Figure 7.4: The impact of window size to number of timeout.

the packet loss ratio during the simulation instead of the fixed packet loss in the UMTS module. With bad channel conditions, the channel quality can be changed within few TTIs. Thus, timeout can happen easily due to the variance of Round Trip Time (RTT). We have investigated the relation between TCP window size and the number of timeouts. We carried out simulation with 0-hop topology with the TCP sender located at SGSN and the receiver being located at the mobile gateway. To show the most serious case, we used worst channel condition (700m away from NodeB, average SNR value is 0.18 dB). In Fig. 7.4, we can see that with smaller window size, timeout occurs more often. This is because smaller window size may cause more spurious RTT value which easily causes timeout. Thus, to fully utilize the HSDPA radio channel in our simulation, the window size 128 has been chosen because it has the smallest number of timeouts.

#### 7.4.2 TCP over integrated network

The integrated network's end-to-end TCP performance has been analyzed in this section. We used the configuration as shown in Table 7.1 and topology as in Fig. 7.3 to evaluate not only the TCP throughput and also lower high speed MAC layer transmissions' throughput. We used MAC throughput in the following for short. In Fig. 7.5, we depict the result from 0-hop to 2-hops.

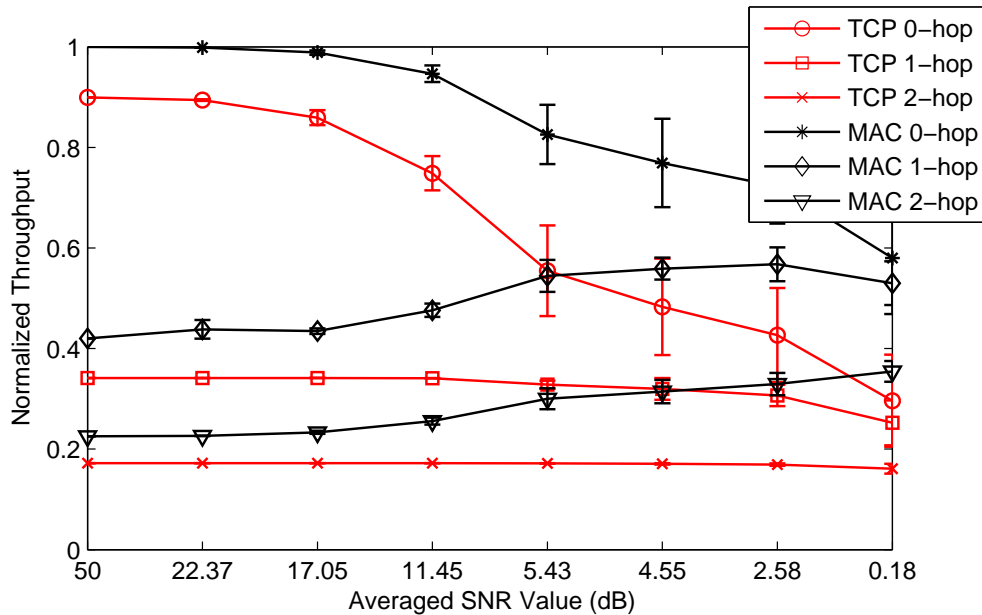


Figure 7.5: The TCP and MAC throughput (RTS/CTS).

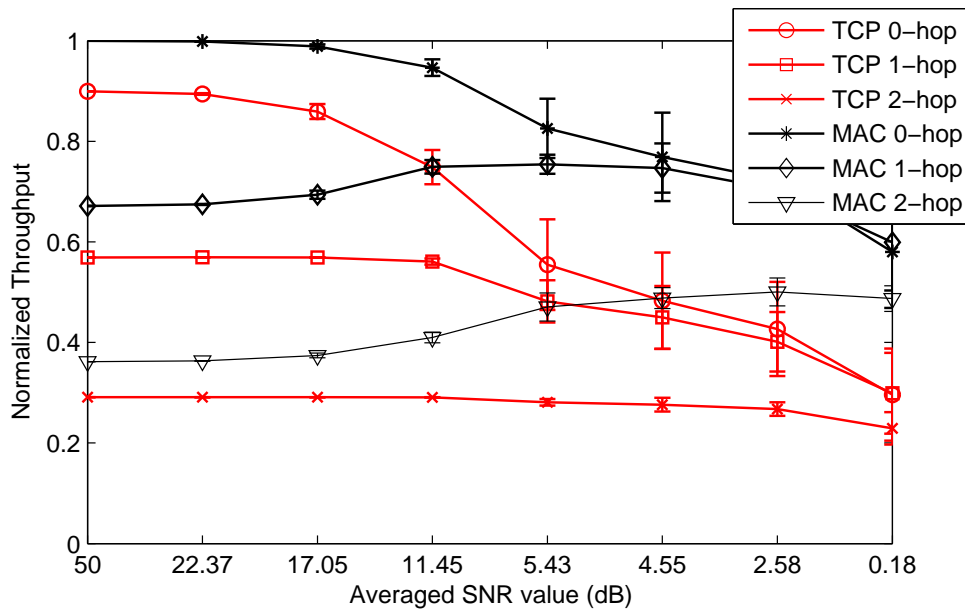


Figure 7.6: The TCP and MAC throughput (CSMA/CA).

Table 7.2: Maximum TCP Throughput for IEEE 802.11b with and without RTS/CTS mechanism [113]

Number of hops	1-hop	2-hop	3-hop	4-hop
CSMA/CA	2.26Mbps	1.08Mbps	0.75Mbps	0.56Mbps
RTS/CTS	1.31Mbps	0.66Mbps	0.41Mbps	0.32Mbps

We increase the distance between mobile gateway and NodeB from 0-700m and generate 10 different input trace files. For every distance, we calculate the average SNR for the whole simulation period. We know that with longer distance, the channel quality will become worse, the best channel condition is the ideal trace which means channel quality is always the best. In the y-axis, the normalized throughput, i.e., the ideal trace in 0-hop's MAC throughput (3.584Mbps) is our maximum value. For each channel quality trace file, we generate 10 different input trace files and every simulation uses a different file, the result is averaged and 95 percent of confidence interval is plotted in the figure.

There are six lines which represent the end-to-end TCP throughput and the HSDPA MAC throughput from 0-hop to 2-hop. We can observe that the 0-hop TCP throughput mean value decreases while its confidence interval increases, which shows that worse channel condition will dramatically decrease the end user performance and cause the performance more variable. The MAC throughput also decreases as the distance increases, but less severely than TCP. This is because bad channel condition causes more retransmissions in HSDPA radio channel and more TCP timeout. Lots of lower layer transmissions are wasted in MAC layer and redundant TCP packet retransmissions.

We can observe that for the 1-hop ad hoc extension, which means the TCP receiver shifts from the mobile gateway to the first mobile node, the TCP throughput is almost flat when the HSDPA radio channel is good (average SNR larger than 4.55), and decreases a little when channel becomes worse. To understand this result, we carried out the experiment with only IEEE 802.11 nodes connected in chain topology. In Table 7.2, we can see the maximum throughput that 1-hop ad hoc node connection can be 1.31Mbps with RTS/CTS. Thus, the network bottleneck located in the IEEE 802.11 network when the HSDPA radio channel is good. An interesting result is that the MAC throughput also increases when the channel becomes bad. Which means the end user may experience the same performance while the HSDPA radio channel consumes much more bandwidth when the mobile gateway is far away. In Fig. 7.6, we can see that the integrated network bottleneck shifts to UMTS/HSDPA network again for the 1-hop extension in some channel

conditions.

For the 700m (SNR=0.18dB) HSDPA radio channel, we can see that the TCP throughput for 0-hop, 1-hop, and 2-hop are more or less the same, in CSMA/CA situation, 0-hop and 1-hop TCP throughput are almost the same when channel is bad, which means IEEE 802.11 can improve the UMTS/HSDPA system performance via relaying traffic. However, 0-hop consumes much more cellular network channel bandwidth. This result can be used in route selection in our integrated network to optimize the performance. In both RTS/CTS and CSMA/CA situation, the 2-hop TCP throughput is flat with all channel quality, which means the bottleneck is totally shifted to the ad hoc network. The same as 1-hop simulation, the MAC throughput increases as the distance increases. In 3-hop and 4-hop experiments, we also observed similar effects so we have not plot them in the figure.

In the HSDPA' MAC transmission, there are totally three transmission chances. If the first transmission is failed, UE will send a NACK to the NodeB to trigger the second transmission. Chase combining is used so that the SNR of the two times' transmission is combined [23]. We use the 1-hop experiment's result to analyze the detailed throughput for each transmission in Fig. 7.7. We can observe that the ratio of first transmission's throughput to the TCP throughput is almost the same for all channel conditions. Meanwhile, the second transmission's throughput increases a lot when the channel becomes worse, which means the worse channel condition causes lots of first retransmissions.

We further calculate the ratio of first transmission's throughput to the TCP throughput in 2-hop, 3-hop and 4-hop, the result is 0.71, 0.70 and 0.68 respectively for each hop which seems to be almost constant for all channel conditions. Two effects cause this result, first is that the HSDPA radio channel's CQI is designed for the NodeB to select the lower layer modulation and packet size to have around 10 percent loss ratio. If the HSDPA radio channel is fully utilized, the TCP throughput will just be 90 percent of the first transmission's throughput. When the channel is not fully utilized, since the TCP throughput is fixed by the ad hoc network throughput, better HSDPA radio channel prefers larger MAC packet size [23] and the TCP packet triggers less first transmission. Thus, the first transmission's throughput will be the same for all the channel conditions. The second reason is that with number hops extension, the HSDPA radio channel is less utilized and MAC layer packet is not full by the payload which wastes the channel bandwidth. This result can also be used in the integrated network system performance optimization.

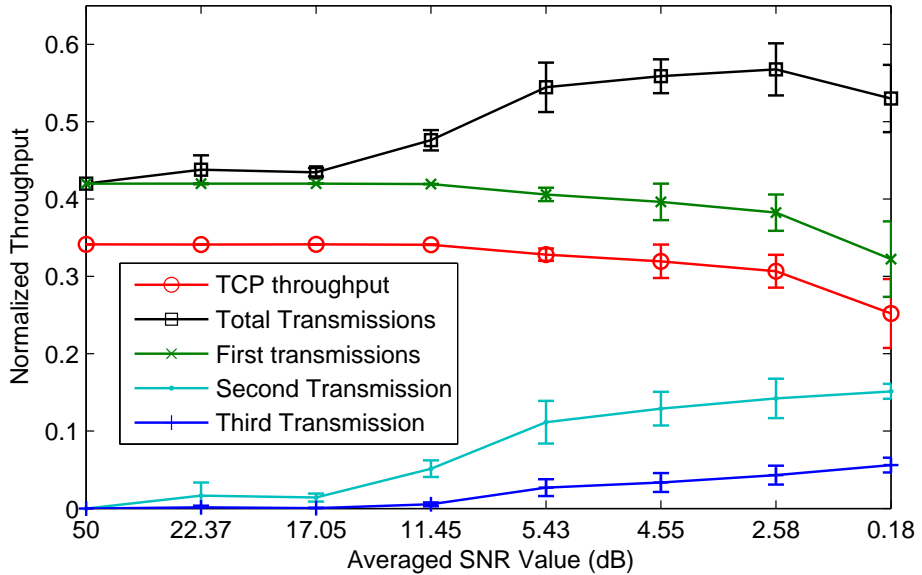


Figure 7.7: The 1-hop Throughput.

### 7.4.3 File downloading

Some applications do not need the integrated network to fully utilize the channel for long duration. Instead, it only demands the network to deliver some payload in fast transmission speed (e.g. http application). We carried out experiments using different payload sizes and different channel conditions to investigate the hop extensions' impact. At first, we present the result when all the simulations are done with 300m distance (SNR=11.45dB) between NodeB and the mobile gateway. We use goodput in the result to represent the pure payload throughput, excluding the TCP and IP header. The average goodput is plotted in Fig. 7.8. All the goodput is still normalized to the 0-hop's total MAC transmissions' throughput (3.584Mbps). It is obvious to see that with number of hop extensions, the goodput difference between large payload size and small payload size is less. Also, for the smaller payload size, the goodput between different hops extension is less. This result can be used for the route selection in the integrated network.

The channel quality difference can also effect the end user performance experience. In Fig. 7.9, we can see that for the 0-hop, different channel condition can cause very different performance with larger payload size, while for the 4-hop situation, the performance difference between better channel condition (SNR=11.45dB) and worst channel condition (SNR=0.18dB) is almost negligible.

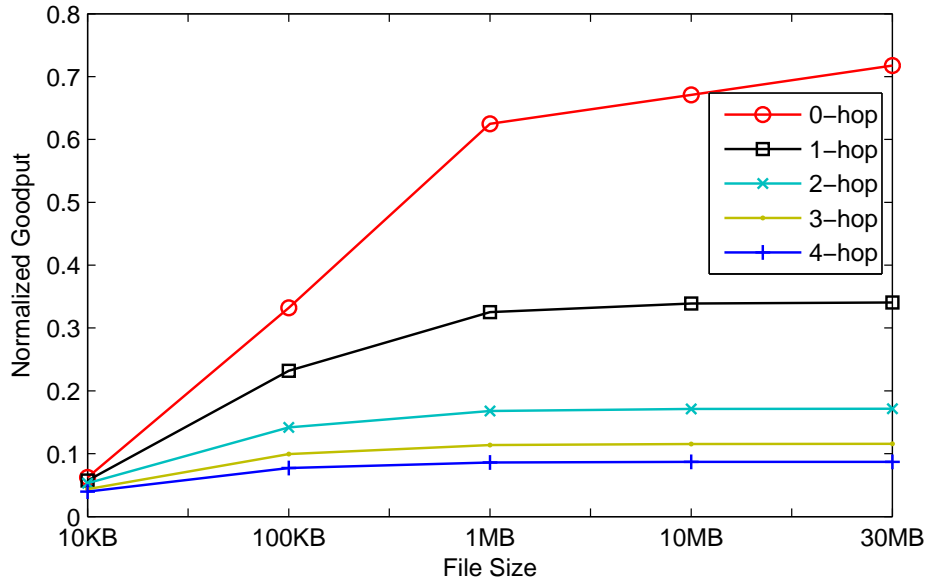


Figure 7.8: File download experiment with 300m distance with NodeB.

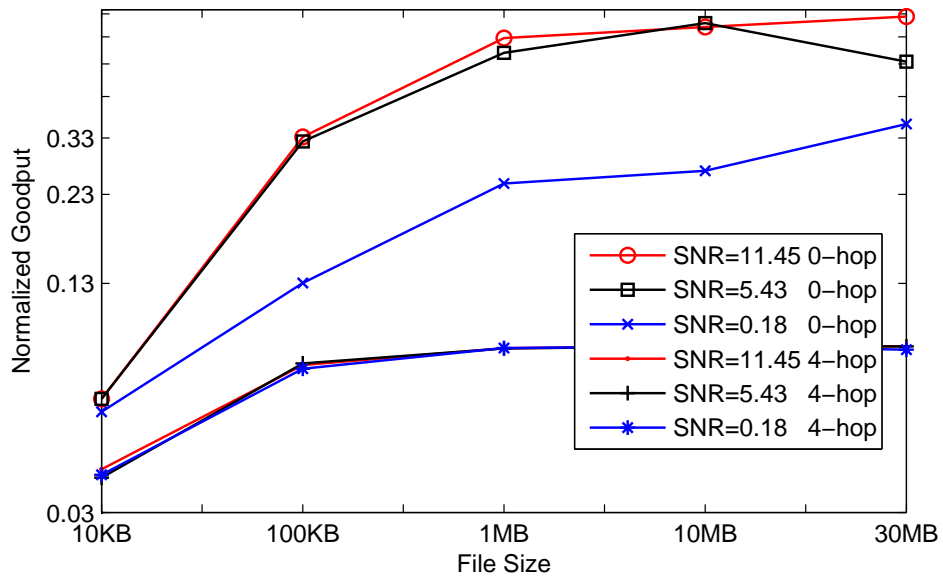


Figure 7.9: File download experiment 0-hop and 4-hop extension comparison.

## 7.5 HSDPA TCP Multiple Flow Throughput

In previous section, we have analyzed the TCP throughput for a single flow, in this section, we will analyze the system performance when multiple TCP flows exist in system. We first use the simulation results to indicate the unfairness among different TCP flows in Section 7.5.1, then we propose to use a weighted scheduling mechanism for this unfairness in Section 7.5.2 and we use the simulations to reveal the optimal parameter settings in this mechanism in Section 7.5.3. Finally, we apply this mechanism in the simulations again to evaluate its performance in Section 7.5.4.

### 7.5.1 Unfairness in the HSDPA and IEEE 802.11 integrated network

In Fig. 1.4, we can see that the nodes in ad hoc network may access the Internet via the same or different HSDPA channel. The link quality in different ad hoc networks and the link quality in between different nodes may be different. The node in the ad hoc network may be several hops away from the gateway or just one hop connection with the gateway. The HSDPA system uses scheduling mechanism to allocate transmission resources among different UEs. However, there is no scheduling algorithm to control the resource allocation between different traffic flows whose receivers are the nodes in the IEEE 802.11 ad hoc network. The nodes which are trying to access the Internet have different configurations will have different performance. The TCP throughput for each flow is used to evaluate the fairness between each flow. We carried out simulations to investigate this unfairness. To numerically compare fairness of the HSDPA radio resources allocation, we use the fairness index [37], which is defined as

$$f = \frac{(\sum_{i=1}^n x_i)^2}{n \sum_{i=1}^n x_i^2}, \quad (7.1)$$

where  $n$  is the number of concurrent FTP flows and  $x_i$  denotes the throughput achieved by the  $i$ th flow. The result ranges from  $1/n$  (worst case) to 1 (best case). We use this metric as our system fairness performance evaluation metric.

In the simulation, we used four flows and three of them used the same topology configuration, the destinations of those flows in IEEE 802.11 ad hoc network were one hop away from the gateway. We call it Flow 2, Flow 3 and Flow 4. Another flow which is called Flow 1 was configured differently, the destination of this flow in IEEE 802.11 ad hoc network can be 1, 2, 3 or 4 hops

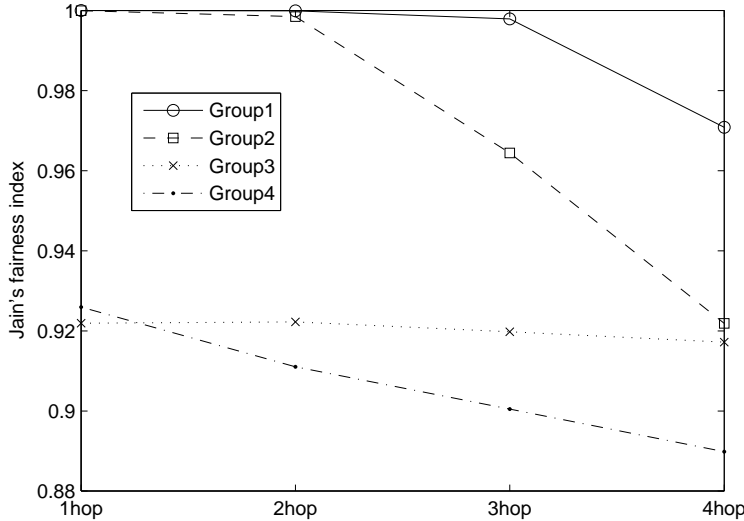


Figure 7.10: Fairness index with round robin scheduling.

away from the gateway. The gateway HSDPA channel quality of this flow can also be different from other flows' channel. We assume that the error rate for all IEEE 802.11 links are the same. The default round robin scheduling mechanism was used. The detailed description of simulation configuration can be found in Section 7.3.3. We divide the simulations into four groups, they are:

- 1: The mobile gateways with the same HSDPA channel condition (average SNR 50dB), no error in IEEE 802.11 links.
- 2: The mobile gateways with the same HSDPA channel condition, (average SNR 50dB), 5% error in IEEE 802.11 links.
- 3: The mobile gateways with different HSDPA channel condition, (flow 1 with average SNR 0.18dB and other flows still with 50dB). No error in IEEE 802.11 links.
- 4: The mobile gateways with different HSDPA channel condition, (flow 1 with average SNR 0.18dB and other flows still with 50dB). 5% error in IEEE 802.11 links.

The simulation result is shown in Fig. 7.10. We see that with number of hops increases for the Flow 1, the fairness index decreases in all groups. It is very obvious to see that when both conditions are worse for the Flow 1 in Group4, the fairness index decreases the more compared to the other groups. We also show the throughput values in Table 7.3. We can see that for the most serious situation, the Flow 1 only gets 31% of throughput compared to

Table 7.3: Throughput for all the flows in Group4 simulation.

	1hop	2hop	3hop	4hop
Flow1 (Mbps)	0.302254	0.267396	0.258655	0.236356
Flow2 (Mbps)	0.691216	0.689961	0.713423	0.732889
Flow3 (Mbps)	0.689207	0.687961	0.733722	0.724923
Flow4 (Mbps)	0.687228	0.686334	0.730843	0.725637

other flows.

### 7.5.2 Proposed scheduling mechanism

To overcome the unfairness caused by different configurations, we decided to use the weighted scheduling method to schedule the packets in HSDPA base station. Flows that are treated unfairly by the base station will get more chances to transmit data. The weight for each flow is decided based on three factors, the HSDPA channel quality, which is indicated by the Channel Quality Indicator (CQI), number of hops away from the mobile gateway ( $H_N$ ) and the IEEE 802.11 error rate ( $E_{80211}$ ). For a certain flow  $i$ , we use the following formula to decide the weights,

$$w_i = CQI_i * (H_{N_i})^\alpha * (E_{80211})^{H_{N_i}\beta}, \quad (7.2)$$

where  $\alpha$  and  $\beta$  are the parameters which control  $H_N$  and  $E_{80211}$ . In this method, the topology and link quality in IEEE 802.11 is also considered in the HSDPA base station scheduling for the HSDPA shared channel. After each flow achieves its own weight  $w_i$ , the ratio of service chances for each flow in the HSDPA base station scheduler is determined as  $R_i = \frac{w_i}{\sum_{i=1}^n w_i}$ . In this way, the flows that are further away from the gateway and suffers more packet loss will get more chance to transmit the packet from the scheduler. Therefore, the RTT for those TCP flows can be reduced. The difference in RTT between each flow can be smaller and different flows will share the resources more fairly. The interesting question for this new scheduler is that how we can select the best  $\alpha$  and  $\beta$ , and how much improvement on the fairness can be achieved. We use the simulation method to investigate this.

### 7.5.3 The optimal parameter selection

The  $\alpha$  and  $\beta$  in Eq. 7.2 can increase the transmission probability for certain flows that suffers the most. However, larger  $\alpha$  or  $\beta$  values will get too many resources for the "weak" flows and reduce the transmission chances for other

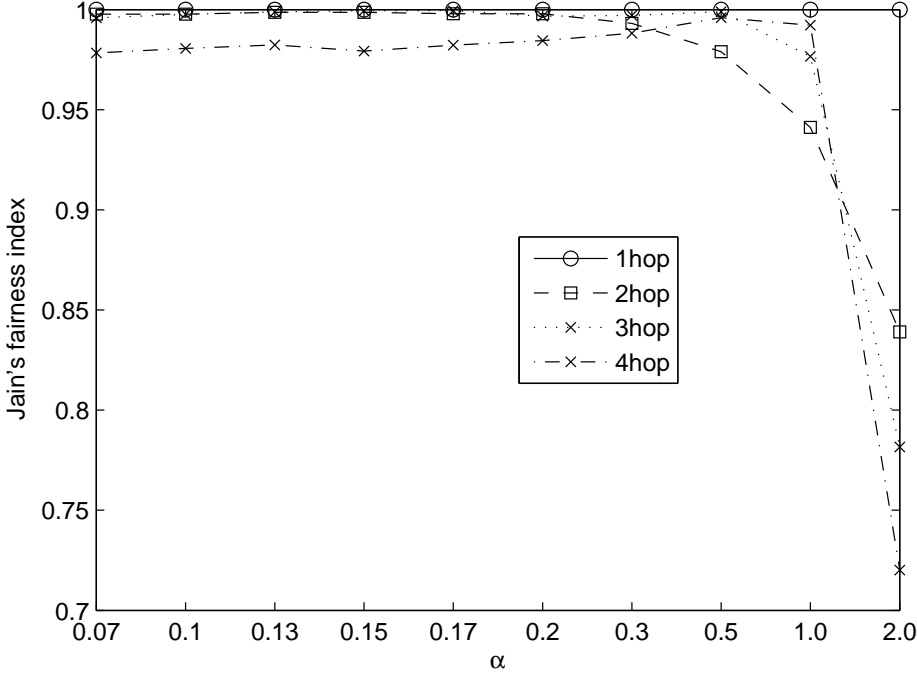


Figure 7.11: The  $\alpha$  selection in Group1.

flows, which introduce unfairness for other flows. To determine the best parameter to be used in Eq. 7.2, we carried out extensive simulations. In this section, we first present the results of optimal  $\alpha$  and  $\beta$  selection in different groups. Then, we present the improvement these parameters can be achieved compared to the round robin scheduling scheme.

For the simulation Group1 and Group3, since there is no error in the IEEE 802.11 links, the  $\beta$  value in Eq. 7.2 will not be affected. Therefore, we only use different  $\alpha$  values to tune the system. We use some preliminary simulation to decide the suitable range of  $\alpha$  and then select ten values for the simulation. The results for Group1 and Group3 is shown in Fig. 7.11 and Fig. 7.12. For Group1, we can see that if we use the  $\alpha$  value smaller than 0.2, the 1, 2 and 3-hop scenarios will result in very high fairness among different flows. This is because there is not much unfairness for these scenarios, since the HSDPA channel quality for all the flows are the same and there is no error for IEEE 802.11 links. However, for the 4-hop scenario, the fairness still is only about 0.98, which is similar in the scenario when round robin scheduling scheme is used. This indicates that  $\alpha$  values lower than 0.2 still introduces lesser weight for the 4-hop flow. We can see that the best  $\alpha$  for

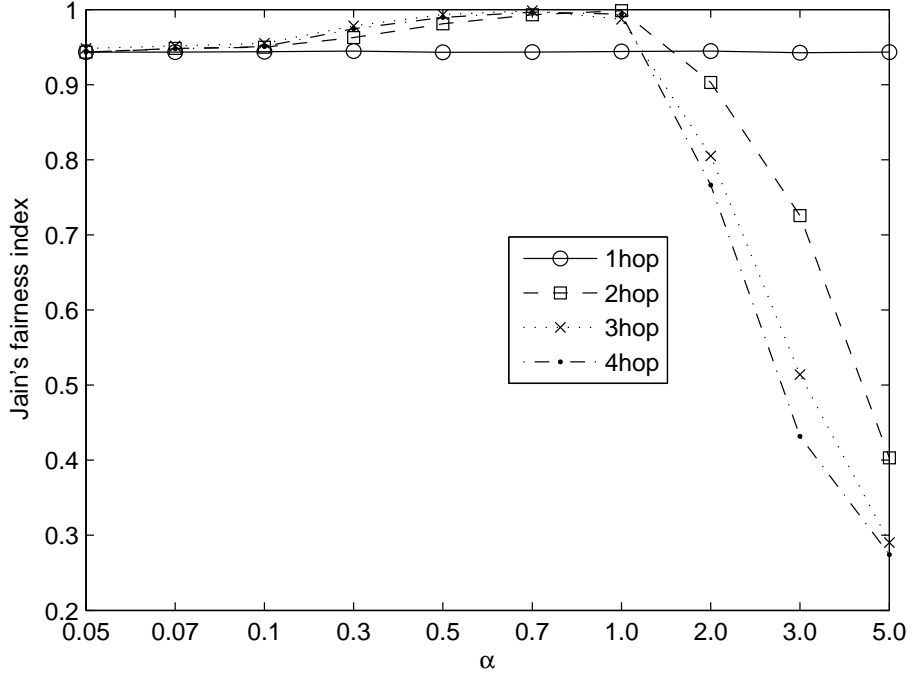


Figure 7.12: The  $\alpha$  selection in Group3.

this scenario is 0.3, wherein all the flows achieves fairness index higher than 0.99.

In Group3 scenario, since the HSDPA channel quality is quite different between Flow 1 and other flows, round robin will cause more unfairness result for Flow 1 (see Fig. 7.10). After using new scheduling mechanism, all scenarios except the 1-hop scenario showed performance enhancement. The 1-hop scenario did not improve due to the fact that all the flows are one hop connection with gateway and  $\alpha$  does not affect the performance of 1-hop. For other hops scenarios, the fairness index reaches 1 when the  $\alpha$  is 1.0. Also, too large  $\alpha$  will further decrease the fairness index to the lowest point 0.25 when  $\alpha$  is 5.0 for the 4hop scenario.

For the Group2 and Group4 scenarios, since there are errors in IEEE 802.11 links, we have to select the best  $\alpha$  and  $\beta$  combinations. We used 100 different  $\alpha$  and  $\beta$  combinations in Eq. 7.2 and plot the fairness index for Group2 and Group4 in Fig. 7.13 and Fig. 7.14. Only the 4-hop scenario's result is plotted in both figures. For Group2' 4-hop scenario, the best  $\alpha$  and  $\beta$  combination is 0.2 and 0.25 respectively. We can also clearly see that larger or smaller  $\alpha$  and  $\beta$  will result in very low fairness for the system. For the

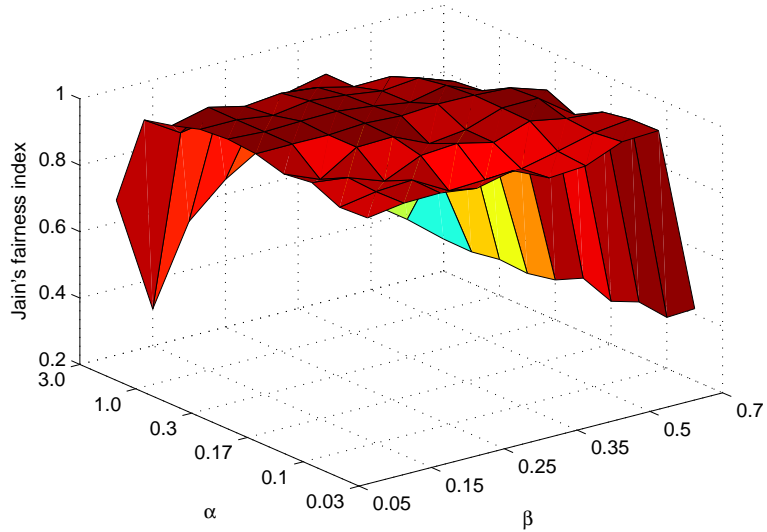


Figure 7.13: The  $\alpha$  and  $\beta$  selection in Group2.

Group4's 4hop scenario, we get into similar conclusion and the best  $\alpha$  and  $\beta$  combination is 0.07 and 0.3 respectively.

Based on the result from Fig. 7.11 and Fig. 7.14, we see that the rule for selecting the best  $\alpha$  and  $\beta$  are different for different Groups, which suggest scheduling mechanism have to be adaptive for different scenarios. However, the difference in result between optimal and suboptimal  $\alpha$  or  $\beta$  is not very large, which suggests that for a certain topology combination, we only need one group of  $\alpha$  or  $\beta$  to achieve good performance.

#### 7.5.4 Fairness index improvement

In the previous section, we have selected the best  $\alpha$  and  $\beta$  for all the simulation groups. We use the groups' scenarios as in Fig. 7.10 and apply our Eq. 7.2, for the Group2 and Group4. We used the best  $\alpha$  or  $\beta$  achieved for the 4-hop scenario to the other hop scenarios. We get the following result as shown in Fig. 7.15. We can see that almost for all the scenarios, the fairness index increases, especially for the Group4, 4-hop scenario, the fairness index increases from 0.88 to 0.987.

We also list the throughput result for the Group4 scenario in Table 7.4. We can see that for all the scenarios, the Flow1's throughput increases and shares the resources more fairly among other flows.

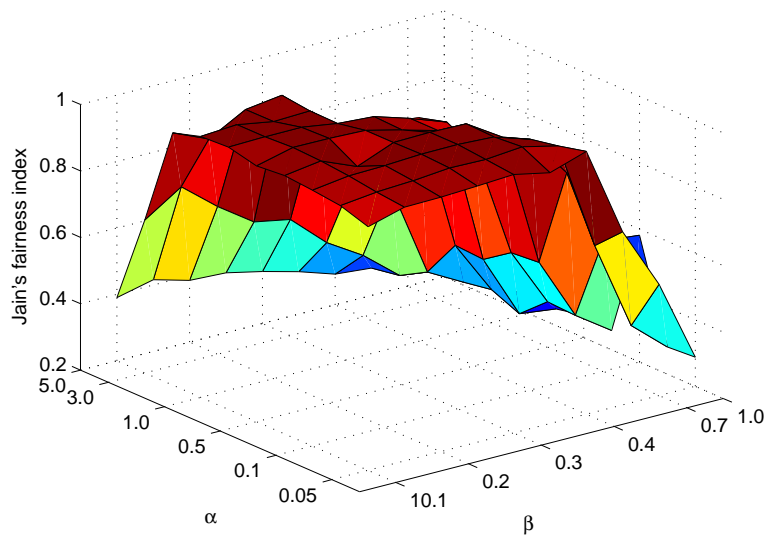


Figure 7.14: The  $\alpha$  and  $\beta$  selection in Group4.

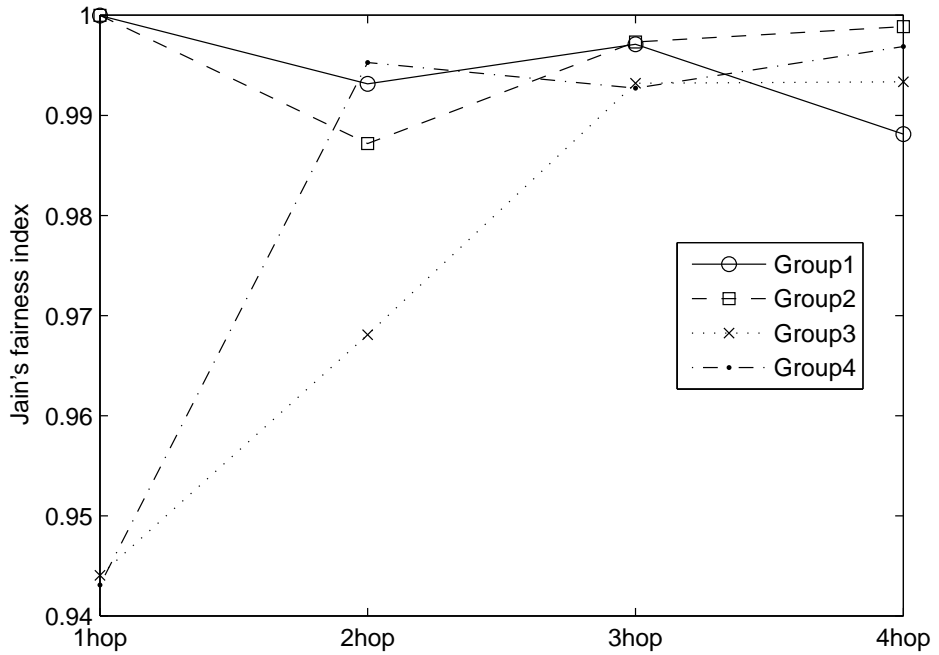


Figure 7.15: Fairness index with the new multi-hop aware scheduling.

Table 7.4: Throughput for all the flows in Group4 simulation with new scheduling scheme.

	1hop	2hop	3hop	4hop
Flow1 (Mbps)	0.412079	0.589823	0.481410	0.455753
Flow2 (Mbps)	0.795520	0.655644	0.546789	0.431752
Flow3 (Mbps)	0.794990	0.659287	0.550830	0.428043
Flow4 (Mbps)	0.849219	0.717423	0.614155	0.491479
Improvement (Flow1)	36%	123%	92%	95%

## 7.6 Chapter Summary and Discussion

In this chapter, we first introduced the idea of integrated network, which involves two types of wireless radio technologies: UMTS/HSDPA and IEEE 802.11. We were motivated by the question that why we need to investigate the performance of this network. This is because investigating this network can help us to optimize the network settings and achieve better performance. We used the simulations to investigate the performance of integrated network's transport layer. Single TCP flow is used to study the end-to-end throughput, the retransmission scheme of HSDPA. Then we used multiple flows and multiple gateways to study the fairness issue in this new network. New method for calculate the weight for the weighted scheduling mechanism is proposed and its effectiveness were validated by large number of simulation results.



# Chapter 8

## Application Layer Evaluation

### 8.1 Introduction

In previous chapter, we have discussed the integrated network performance in transport layer. In this chapter, we shall discuss its performance in application layer.

There are still new challenges that exist for different traffic types transmitting over this resource limited channel sharing network. The HSDPA uses the shared downlink channel which may be used by lots of users with higher bandwidth demand. Meanwhile, the link quality of HSDPA is also dynamic. How to ensure the quality of the content that is delivered to each user is an open question. Video streaming is a potential application of the cellular ad hoc network. In this chapter, we use our simulation tools with realistic simulation environment to simulate single and multi MPEG-4 video streams over cellular multi-hop network. The impacting factors which affect the end-to-end performance of single flow is analyzed and we show the possibility of solving the challenges for single flow performance optimization. In the multi flow simulations, we also show how much unfairness can be caused by different network topology for each flow, and we have also proposed a solution for this challenge.

To the best of our knowledge, this is the first work in the study of the end-to-end performance of MPEG-4 over the multi-hop cellular ad hoc network with HSDPA channel model. A tool-set for evaluating the performance optimization of MPEG-4 traffic over integrated network is introduced. The rest of the chapter is organized as follows; the related works have been discussed in Section 8.2, Section 8.3 introduces the background technology. Our simulation model is described in Section 8.4 and in Section 8.5 we present the simulation results. The chapter is summarized in Section 8.6.

## 8.2 Related Work

In Section 7.2, we introduce the related work for integrated network architecture, we do not repeat them in this chapter, we only introduce the works that are related to the video streaming over wireless networks.

The special traffic characteristics and strictly delay constraint of video traffic have different requirements for 3G cellular networks compared to other traffic, e.g., TCP [1]. The work [65] evaluates the performance of single MPEG-4 flow transmitted over UMTS network simulations. The paper [97] evaluates the MPEG-4 traffic over a live UMTS network and concludes that if the video coding rate is lower than channel rate, the video is not impaired much. However, the end-to-end performance evaluation of the MPEG-4 video source over multi-hop cellular network with HSDPA channel is still missing. This heterogenous network has more impacting factors which affects the end-to-end performance. Lots of optimization work has been done to improve the performance of MPEG-4 over cellular network. The work [76] proposes to use adaptive coding rate to compress the MPEG-4 video and based on the channel quality the system chooses appropriate video data rate to be transmitted over the HSDPA network. However, the video quality can be dynamic due to the link quality variance in certain links. Also the ad hoc network is not considered in this work.

Previous work has also discussed the problem of multi flows over the resource limited cellular network. The work [82] uses the simulation method to compare the performance of multiple video users sharing the HSDPA down-link channel. Different HSDPA scheduling mechanisms are used to compare with the best effort scheduling mechanism and can be concluded that by using QoS service scheduling the number of users in the system can be increased. However, the fairness issue for different users has not been discussed and the users with bad channel quality in HSDPA network or ad hoc network will not be performed well. The paper [81] proposed a normalized rate. They considered different QoS classes or user groups and studied resource allocation among those user groups using HSDPA MAC-layer scheduling. They have proposed a Normalized Rate Guarantee (NRG) scheduler, which is an extension of a previous QoS scheduler by Hosein (2002). Our work assumes that all the flows use best effort priority, none of the previous works have discussed the problem of factors in the ad hoc network.

## 8.3 Multi-hop Cellular Networks and MPEG-4

In this section, we give an overview of multi-hop cellular networks and MPEG-4.

### 8.3.1 System architecture

Fig. 1.4 depicts the architecture of the multi-hop cellular network. The Internet is connected to a host and the UMTS network. In this work, the host is represented by a video server. A node which has both UMTS and IEEE 802.11 interfaces acts as a gateway between the UMTS network and the ad hoc network. The gateway includes protocols for gateway-discovery, gateway selection, address allocation, routing, session negotiation, which were addressed in [114].

To be able to realize our newly integrated network, we have proposed the following network protocol stacks as depicted in Fig. 8.1 and it is very similar to the architecture as we described in Chapter 7. The only difference is that the MPEG-4 is used as application traffic. The MPEG-4 sender and receiver is set at the application layer.

### 8.3.2 MPEG-4

MPEG-4 is a collection of methods defining compression of audio and visual (AV) digital data and standardized by ISO/IEC. This standard defines tools to create, represent and distribute individual audiovisual objects, both natural and synthetic. MPEG-4 provides the advanced video coding (AVC) compression process that consumes smaller bandwidth. As a result, it is likely to become the preferred approach for the next-generation digital image distribution. An MPEG-4 encoder generates three types of frames, Intra-frames (I-frames), Predictive frames (P-frames) and Bi-directional frames (B-frames). The P, B frames have higher compression and I frame can be encoded and decoded faster.

## 8.4 Simulation Models

### 8.4.1 Integrated network module in ns-2

EURANE [23] was extended to support the multi-hop networks and generate the UMTS/HSDPA channel input trace file to realize the end-to-end IP

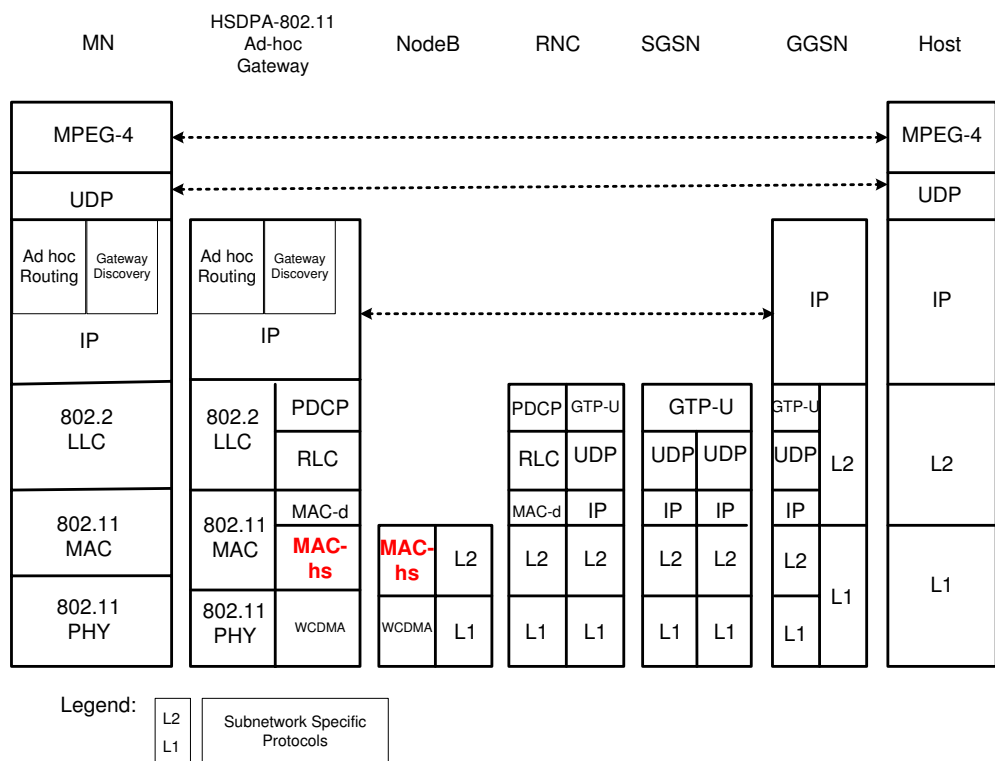


Figure 8.1: Multi-hop cellular protocol Stacks.

packet transmission over UMTS/HSDPA. The detailed description of this integrated network can be found in [112].

The UMTS and HSDPA have two major differences. Firstly, the UMTS system uses power adaption to maintain a fixed error rate. In the simulation, the packet error rate was set to 0% - 50% on the dedicated channels. However, HSDPA system uses a shared channel that has constant transmission power. Thus, users can experience different channel conditions. In the simulation, the HSDPA used a pre-generated trace file that models channel behavior [112]. To compensate for the random effect introduced by the channel model, all simulations with HSDPA channel were repeated 10 times with different trace files and the average result was used. Using different distances between Node B and UE, eight different types of HSDPA channel quality files (0-700 m) were generated. The average SNR value was used for representing the HSDPA channel quality levels. Secondly, in the method of retransmitting lost frames, UMTS system uses the RLC layer for retransmission, which is between the RNC node and the UE while HSDPA uses MAC for retransmission which is between Node B and UE. The retransmission scheme of HSDPA is faster due to smaller TTI.

#### 8.4.2 MPEG-4 video evaluation tool-set

EvalVid [49] is a tool-set for evaluating video quality transmitted over a simulated communication network. The work [44] further extended this tool-set to include ns-2. We integrated EURANE into the tool-set. The integrated environment is depicted in Fig. 8.2. The raw video with YUV format is encoded into the MPEG-4 format with a certain coding rate. The raw video source used in the simulation is the Common Intermediate Format (CIF) format ( $352 \times 288$  pixels). The *MPEG-4 encoder* supports different coding rates according to the user requirement. The encoded MPEG-4 video is segmented into UDP packets based on maximum segmentation packet size and captured in a *trace file*, which contains the information of the transmitted packet departure time. The trace file is fed into the EURANE traffic generator agent which in turn is segmented and encapsulated in the UDP datagrams. The received video frames in the simulation is recorded by the simulator into the *Log file*. The program reconstructs the video using the compressed video and the received log file. This transmitted video is decoded again and is compared with the original raw video frames.

Two metrics, namely, the end-to-end delay of video packets and Mean Opinion Score (MOS) were used to evaluate the performance. MOS is the human impression of the video quality, which is given on scale from 1 to 5 [65]. During the simulation, erroneous video packet due to impairment of

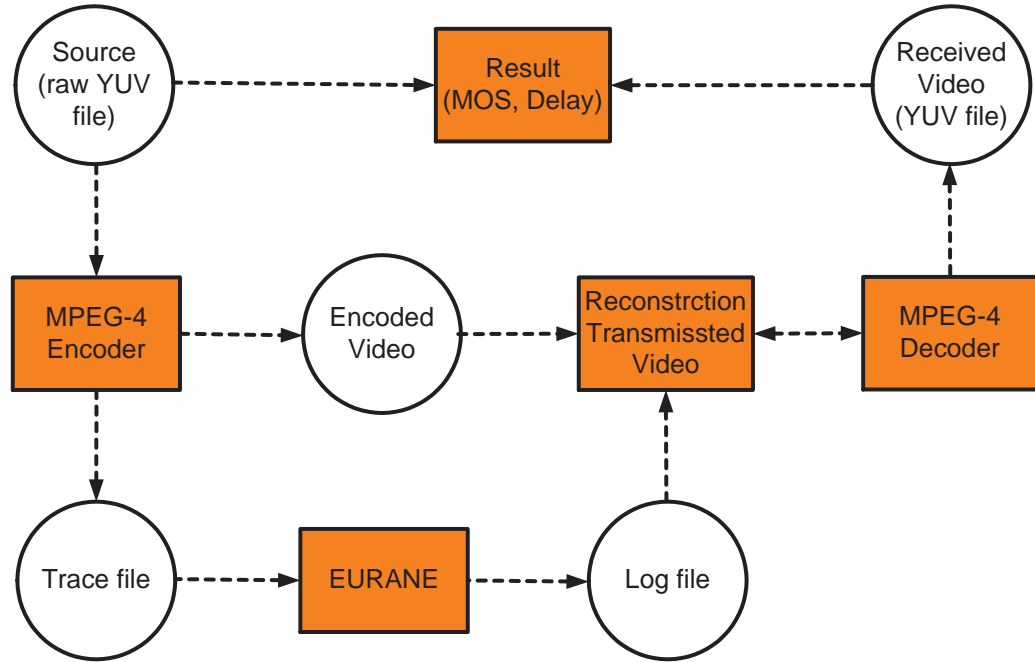


Figure 8.2: MPEG-4 video stream evaluation tool-set.

cellular radio channels will be recovered by the link layer. We assume that IEEE 802.11b links are ideal and no packets will be lost. MPEG-4 video streaming is a delay constraint application, packets arrived later than the buffer time will be dropped. This leads to quality degradation, and thus, lowers the MOS.

### 8.4.3 Simulation setup

The simulations were carried out using the topology shown in Fig. 8.3. We used the SGSN as our MPEG-4 traffic source. In the ad hoc network, a chain topology was used to connect the 802.11 nodes, the MPEG-4 receiver can be the mobile gateway, MN1 and MN2, which corresponded to 0-hop, 1-hop and 2-hop. The configuration of wired link is shown in Fig. 8.3. The configuration of the wireless link, MPEG-4 video streaming parameters are in Table 8.1. In the simulation, the IEEE 802.11b's highest data rate was used. This is because we assume our applications are outdoor and the transmission distance between IEEE 802.11 nodes is 130m. Some references in the literature indicates that 802.11g radio performs badly in those conditions [6].

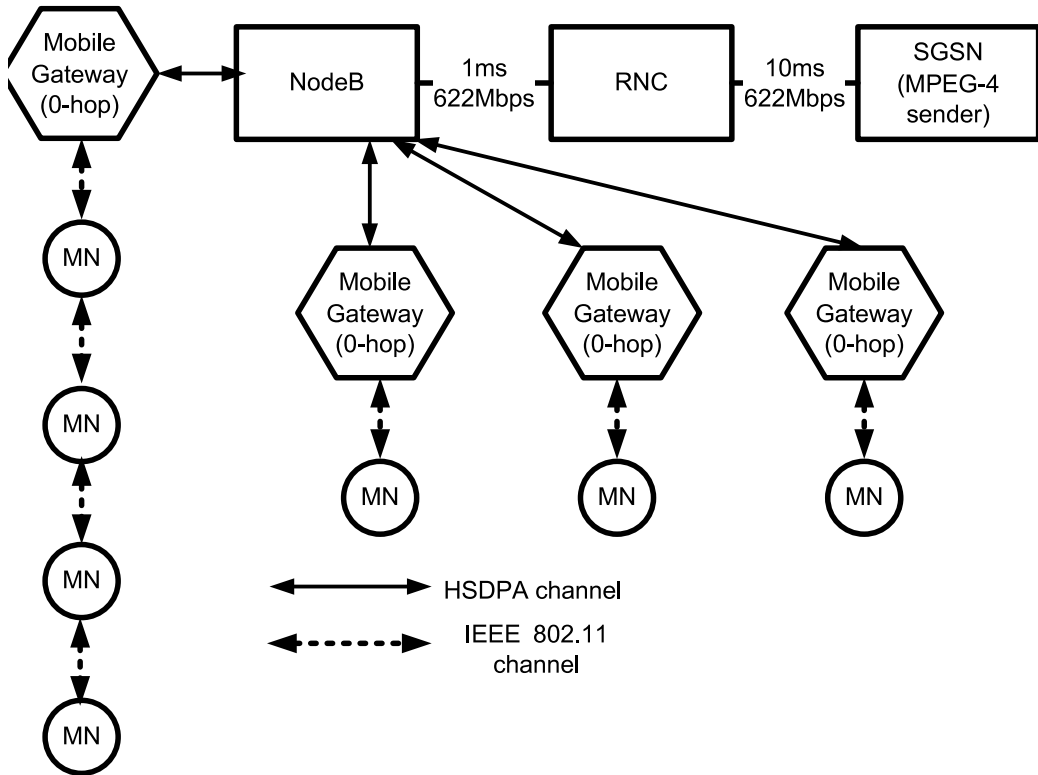


Figure 8.3: Simulation Topology.

#### 8.4.4 Video contents

The video source that we use are the "waterfall" and "flower" scenarios shown in Fig. 8.4. One picture of the video content of this scenario is shown in Fig. 8.4(a) and Fig. 8.4(b). The raw video rate of "waterfall" and "flower" is 3 Mbps and 4 Mbps, respectively. We coded them into 1 Mbps mp4 file for network transmission for single flow scenarios and 0.8 Mbps for multi flow scenarios.

## 8.5 Simulation Results

We divide the simulations into two different types. Single MPEG-4 flow and multi MPEG-4 flows.

Table 8.1: Simulation parameters

HSDPA	Values
Distance from NodeB	0-700 m
Path loss component (n)	3.52
Mobile gateway speed	3 km/h
Mobile gateway move pattern	circle
Standard deviation in shadow fading (N)	8 dB
Maximum buffer size at NodeB	1000 Kbytes
UPlink TTI	10 ms
Downlink TTI	2 ms
Uplink bandwidth	384 Kbps
UMTS	Values
UPlink TTI	10 ms
Downlink TTI	10 ms
Uplink bandwidth	384 Kbps
Downlink bandwidth	384 or 2084 Kbps
IEEE 802.11	Values
IEEE 802.11 error rate	10-50%
IEEE 802.11 bandwidth	11 Mbps
RTS/CTS Threshold	3000 Bytes
MPEG-4	Values
Video Coding rate	0.8 or 1 Mbps
Video buffer time	1 s
Number of frames per second	25
Maximum segmentation packet size	1000 Bytes

### 8.5.1 Single MPEG-4 flow

For the single MPEG-4 flows, we assume that only one MPEG-4 flow exists in the system, so the problem is to select the best path that delivers the video content with the best quality.

#### Impact of Video Sources

Each video source will have different packet distribution. The video with high temporal information produces larger P and B frames and the video with more stationary contents produce larger I frames. Fig. 8.4(c) and Fig. 8.4(d) depict the segmentation packet sizes with frame numbers of these two video streams. We can see that the "flower" video stream has larger P, B frames and "waterfall" video stream has larger I frames at the start of the video

stream.

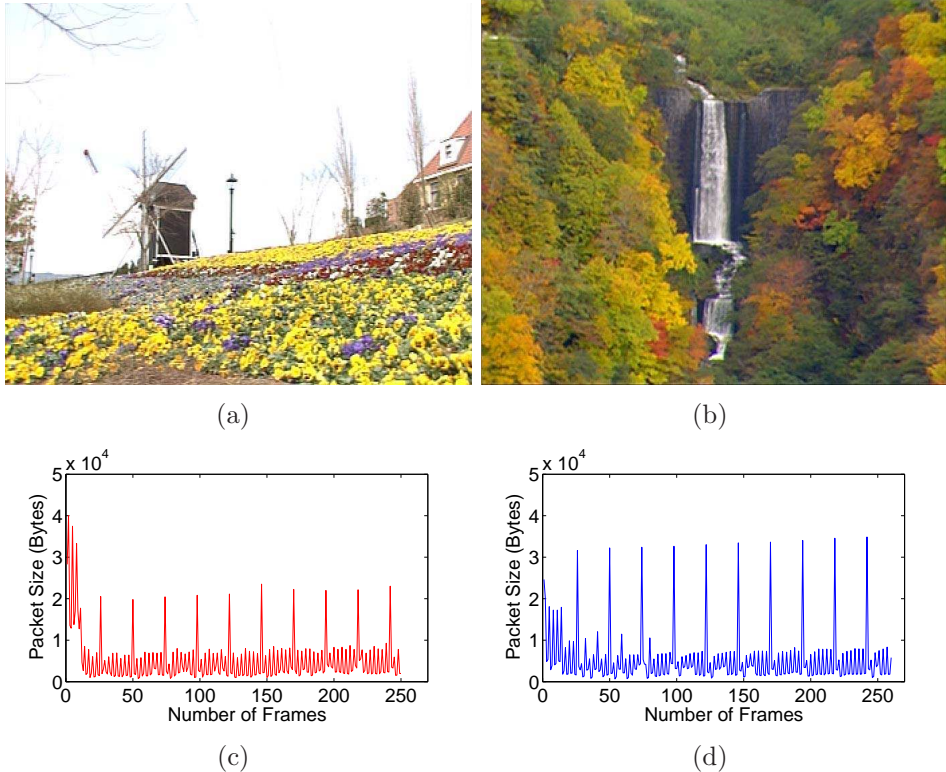


Figure 8.4: Different video source comparison: (a) flower video, (b) waterfall video, (c) flower video, segmentation packets size vs time, (d) waterfall video, segmentation packets size vs time.

We use 1-hop scenario with HSDPA channel to evaluate the performance difference caused by different video sources. In Fig. 8.5, we depict the average MOS value with different channel conditions. We can see that the average MOS value for the flower scenario begins to decrease when the average SNR decreases to 5.43 dB. The average MOS value further drops to 2.8, when the channel quality becomes worse. The MOS value drops to 1 when the channel quality is 0.18 dB. However, for the waterfall scenario, the MOS value only begins to decrease when the average SNR is 2.58 dB. The MOS value of waterfall video is always higher than the flower video even when the channel quality is the same. Video source packet distribution deviation causes the difference.

The end-to-end delay cumulative distribution function shows the network performance for delivery of a certain video source. We depict the delay when the HSDPA channel has an average SNR of 22.37 dB. Fig. 8.6 depicts the

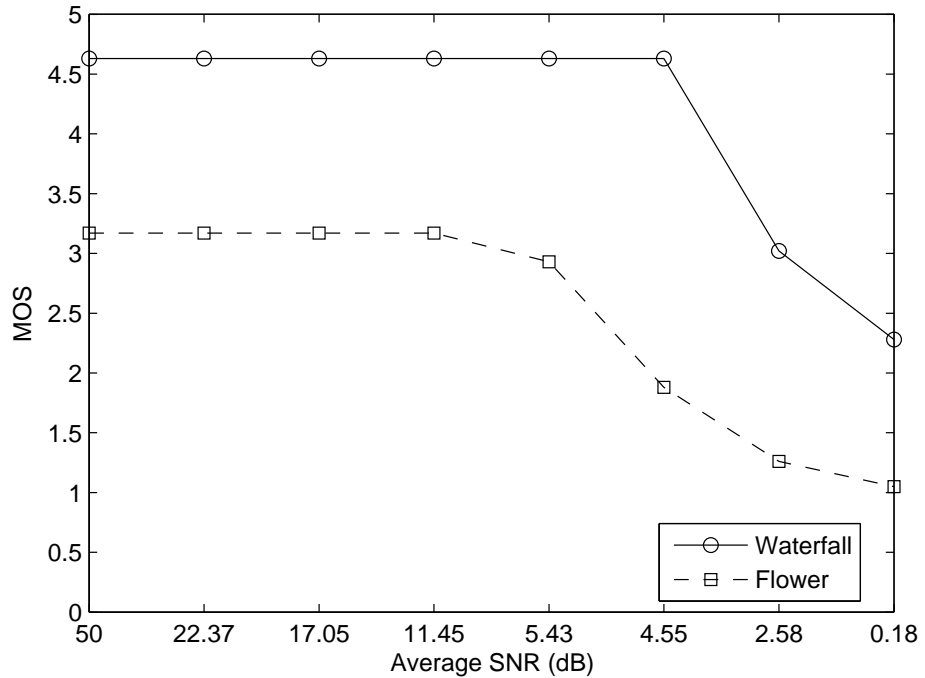


Figure 8.5: Different MPEG-4 video sources over HSDPA channel: MOS compare.

end-to-end delay cumulative distribution function of the two video streams. In this network setting, all packets have a delay less than the buffer time (1s). We can observe that about 70% of the packets of the two video streams have the same delay distribution. For the other 30%, the packets from video source flower have larger delay than the packets from the waterfall video source.

As shown in Fig. 8.5, the MOS of flower is lower than the waterfall even under the ideal HSDPA channel conditions. This is due to lossy MPEG-4 encoding. The flower video source has consecutively several big packets at the beginning of the video. Thus, at beginning of video transmission the delay for flower scenario keeps on increasing, reaches the maximum of 0.45s, then decreases to the normal level again. The flower video uses larger P, B frames<sup>1</sup> which results in more transmission delay in HSDPA MAC layer. The result shows that the video source difference can cause large performance difference under the same network conditions.

---

<sup>1</sup>The "flower" and "waterfall" scenario have the same compressing data rate, 1 Mbps. It is obviously the "waterfall" that has larger I frames, so the "flower" has larger P, B frames.

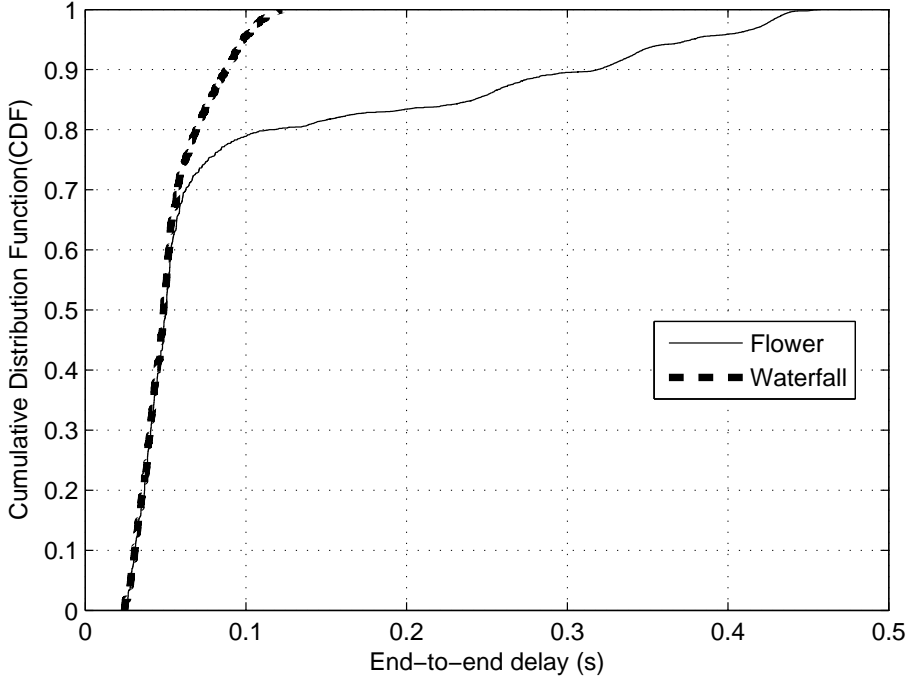


Figure 8.6: Different MPEG-4 video sources over HSDPA channel: Delay compare.

### Impact of HSDPA and UMTS transmission strategy

As described in Section 8.4.1, HSDPA and UMTS system uses different retransmission strategies. The UMTS uses the RLC layer to retransmit the lost frames. In the RLC layer, two timers, namely, the status prohibit timer and poll timer, are used to control the retransmission process. The status prohibit timer and the poll timer located at both UE and RNC dictates when the retransmission takes place. Larger timer value will slow down the retransmission process while the smaller timer may trigger unnecessary retransmission which costs bandwidth.

We carried out experiments with UMTS channel with the downlink bandwidth of 384 Kbps. The performance comparison of different RLC timer values is depicted in Fig. 8.7. We used four different timer values and the poll timer and the status prohibit timer were set to be the same. It is obvious that too large (100 ms) or small (40 ms) will not result in optimal performance. It is interesting to see that no single timer value achieves the best performance for all channel conditions. Generally the 60 ms configuration achieves the best performance for most of the scenarios. A smaller value (40ms) per-

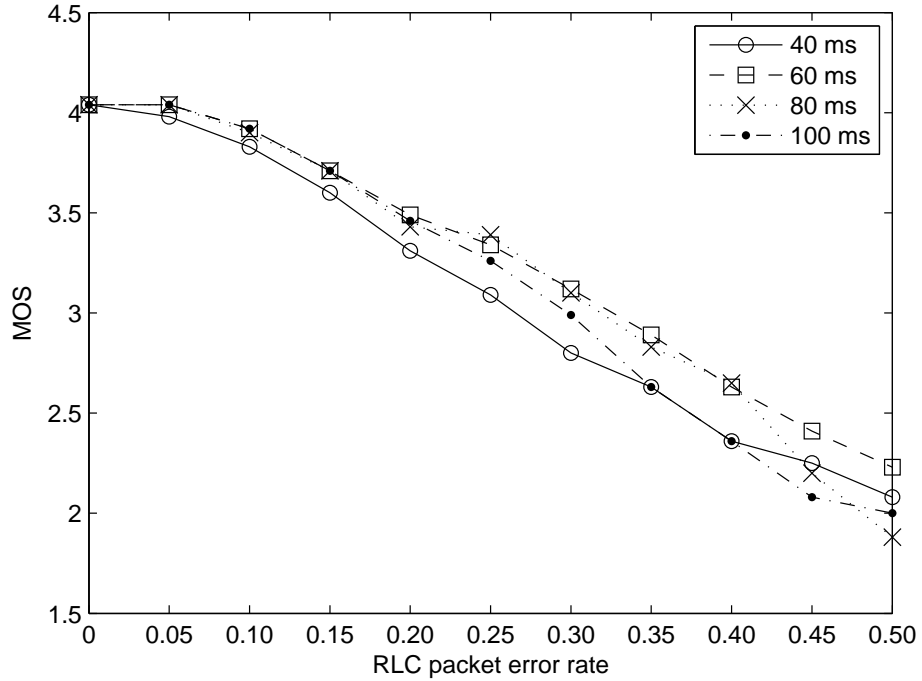


Figure 8.7: MPEG-4 video over UMTS channel with different retransmission timer values.

forms slightly worse than the larger value when the channel quality or packet error rate is from 0% to 35%, which indicates that small timer values result in the redundant retransmissions that decreases the performance. When the channel becomes very bad (packet error rates of 35% to 50%), smaller values (40ms) outperform larger ones due to faster retransmission. The result indicates that for the UMTS channel, the optimal timer value for video transmission should be adaptive based on the channel conditions.

The HSDPA system uses the fixed interval to retransmit the lost MAC Frames and no timer is employed. However, the variance of the channel quality can have an impact on the video transmission quality. In Fig. 8.8, we show the end-to-end delay cumulative distribution function of video packet delivery for HSDPA transmission with different channel conditions. We can see that, when the average SNR value is higher than 17.05 dB, the end-to-end delay is always within 150ms. When the quality of the channel deteriorates, end-to-end delay increases.

Now, we compare the performance of MPEG-4 over these two transmission strategies. For a fair comparison, we select a set of parameters for both

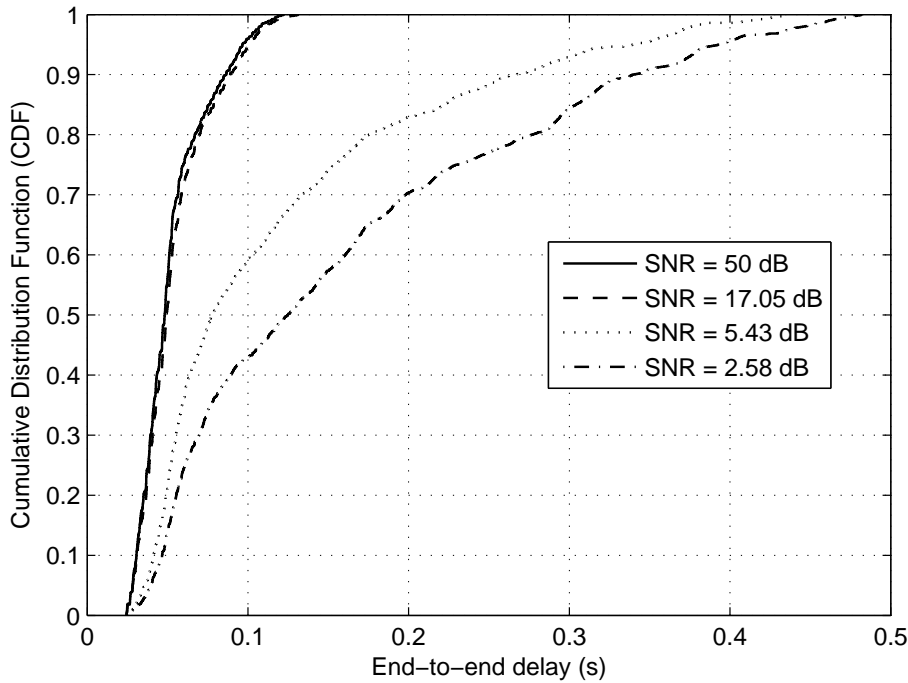


Figure 8.8: MPEG-4 video over HSDPA channel with different channel conditions.

HSDPA and UMTS, which gives the same maximum TCP throughput. For UMTS, the settings for the downlink channel were 2048 Kbps and a fixed packet error rate of 5%. For HSDPA, the setting is the average SNR which was 2.58 dB. Fig. 8.9 plots the end-to-end delay of video packets for HSDPA and UMTS. We can observe that the delay distribution is different, the delay in UMTS system has less deviation. For HSDPA, 85% of the packets have lower delays compared to UMTS due to the faster retransmission mechanism. However, the other 15% of the packets have even longer delays than UMTS. This result is due to the fact that UMTS has fixed error rates which leads to more stable performance, while HSDPA channel variance has strong effect on the end-to-end delay.

### **Impact of the network configuration in multi-hop cellular network**

Different configurations will result in different minimum bandwidth for cellular and ad hoc networks. The integrated multi-hop cellular network will have different network bottleneck under different configurations [112]. As we have described in Section 8.4.2, if the encoded MPEG-4 video bit rate is higher

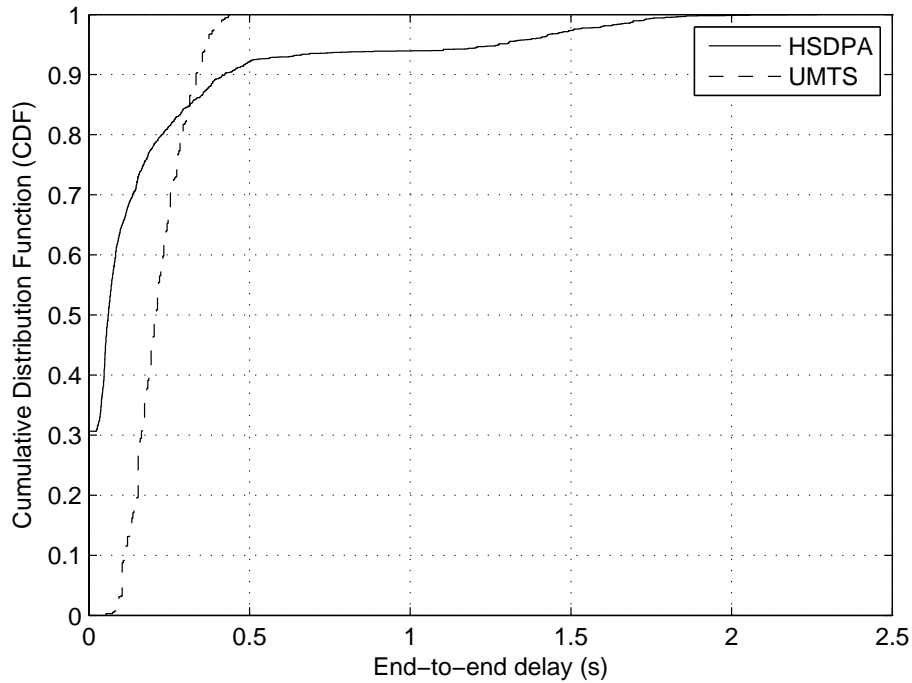


Figure 8.9: Delay compare between UMTS and HSDPA channel for MPEG-4 video stream.

than this bottleneck, packets delay may be higher than the buffer level and cause the MOS value to decrease.

Traffic contention and the number of hops will impact the video quality. In this section, we have two different scenarios, one is with different number of hops in a multi-hop ad hoc network. The other scenario is where two flows are used, one is MPEG-4 video traffic with 1 Mbps bit rate and the other one is Constant Bit Rate (CBR) traffic in the shared channels. The CBR traffic share the two different channels with MPEG-4 flow. The HSDPA channel is used. The factors' that impact the MOS value is depicted in Fig. 8.11 and Fig. 8.10 respectively. As discussed in Section 8.4, we used 0, 1 and 2-hop topology in the multi-hop network for Fig. 8.10 and three different contention traffic levels with 1-hop topology are used in Fig. 8.11. It is obvious to see that the MOS value is the same for the 0 and 1-hop scenario, and the MOS value in 2-hop begins to decrease when the HSDPA channel is bad, which indicates that with more hops in the multi-hop ad hoc network, the increased end-to-end delay can decrease the MPEG-4 video stream quality when HSDPA channel quality is bad.

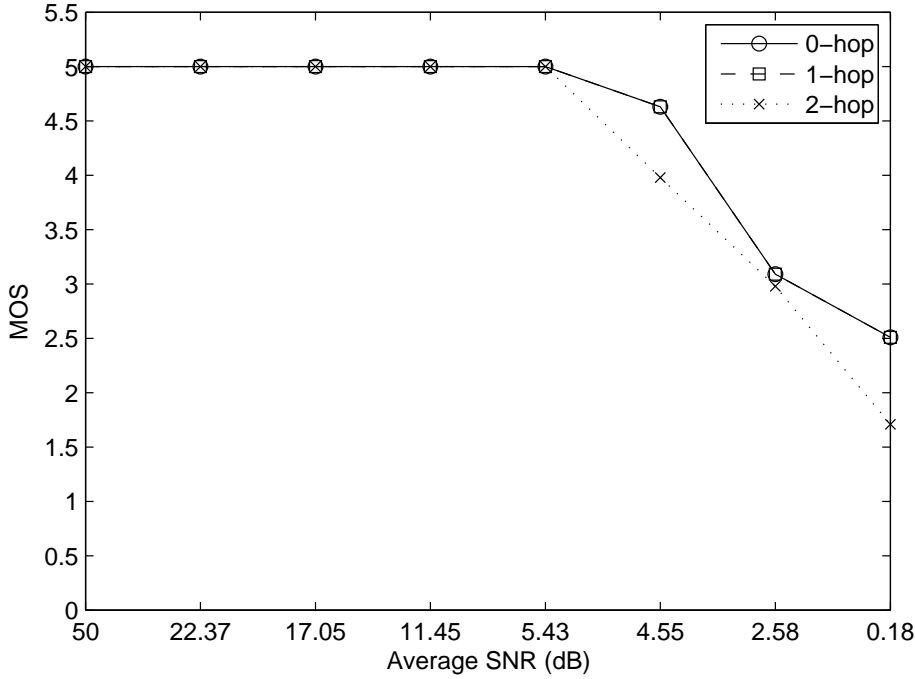


Figure 8.10: Number of hops extension.

It is interesting to observe that, although the MPEG-4 bit rate is 1 Mbps and the contention traffic load is 1 Mbps i.e., maximum and the maximum HSDPA channel bandwidth is 3.36 Mbps, the MOS value still begins to decrease when the channel becomes worse. We can see that with different CBR traffic intensity, the MOS values decrease differently when the channel's SNR decreases. When the average SNR is 5.43 dB, the MOS value with 500 Kbps has a MOS value of 4.52 and 1000 Kbps scenario has only 4.3. When the average SNR is 4.55 dB, the average MOS value drops to 3 which means the video quality is very bad and unacceptable. The simulation results demonstrate the QoS provision should be provided based on the precise knowledge of the network configuration and status. When the channel quality is bad (average SNR lower than 2.58 dB), the video transmission performance also varies a lot based on our result.

Same as in Section 8.5.1, we still use the end-to-end delay result when the HSDPA channel has an average SNR = 22.37 dB. We used 5 different contention traffic levels in the simulation and plot the delay in Fig. 8.12. We can see that when there is no contending traffic and with 500 Kbps CBR contending traffic, the performance is similar. When there is higher contention

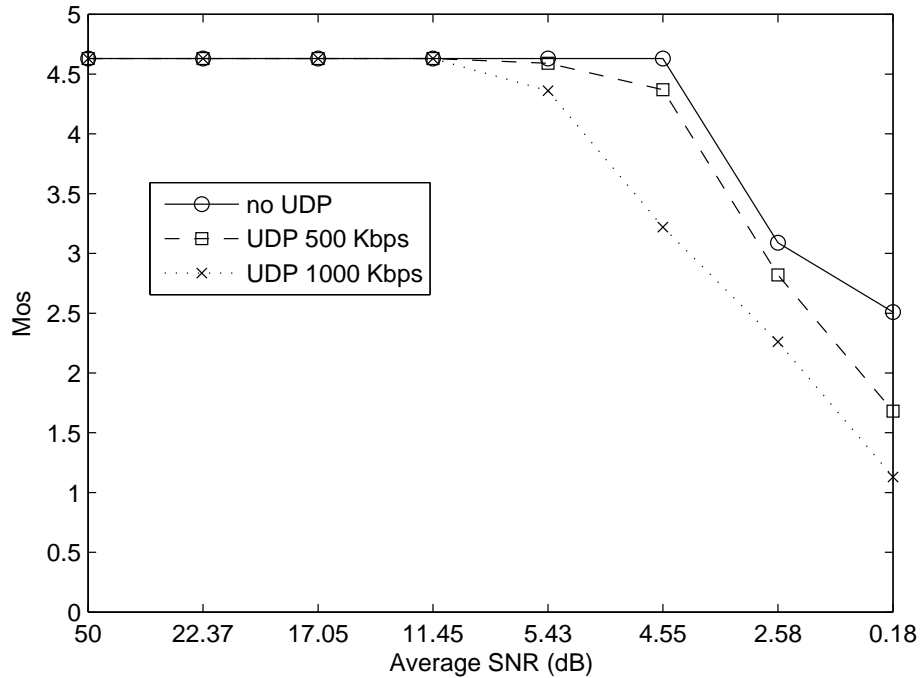


Figure 8.11: Different contention traffic levels.

traffic passing the channel, the end-to-end delay increases much more and can reach up to 0.3s.

### Impact of errors on IEEE 802.11 channels

With the retransmission scheme in our cellular network simulation model, there will be no UDP packet loss during the transmission in the cellular network. In the previous section, we assume that there is no error in IEEE 802.11 links. Therefore, the MOS value decrease is only caused by the delayed packets. The impact of IEEE 802.11 links on the end-to-end performance is not obvious due to its short delay. In this section, we also set uniform distributed errors in the IEEE 802.11 channel. We used four error rates in our simulation, 10%, 20%, 30% and 50%. For the 802.11 channel, we set the maximum number of retransmission for data packet to be 7.

We first use the one hop topology in the 802.11 channel, same as in Fig. 8.8. We use different HSDPA channel traces with different average SNR value. The MOS value is shown in Fig. 8.13. We can see that for all the scenarios, the MOS value decreases when the HSDPA channel has a lower average SNR. When the error rate in IEEE 802.11 increases, the MOS value

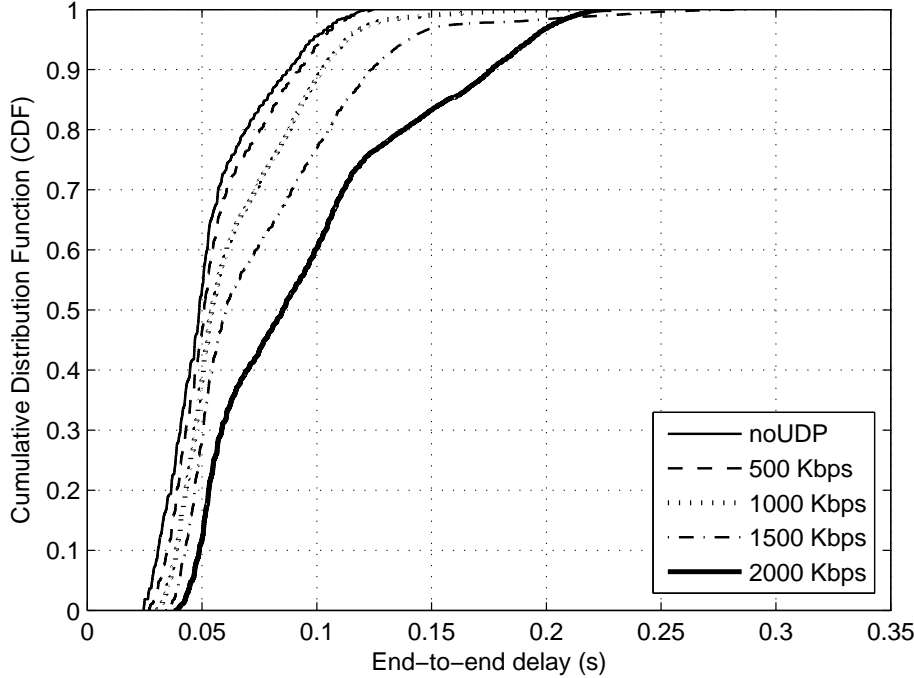


Figure 8.12: End-to-end packet delay with multiple flows.

decreases dramatically. For 50% error rate, the MOS value decreases to 1 which means the video can not be seen at all. It is interesting to notice that up to 20% error, the video quality starts to decrease when the HSDPA channel is still in good quality ( $SNR > 4.55 dB$ ). In the situation where HSDPA has very low average SNR, ( $SNR < 4.55 dB$ ), the HSDPA channel causes the MOS value to be further decreased. This MOS value result indicates that the bottleneck effect (see Fig.6 in [112]) will be more obvious when there is error in IEEE 802.11 channel. The end-to-end video quality can be influenced easily by the channel quality variance in cellular network or ad hoc network.

It is also interesting to look at the end-to-end delay in Fig. 8.14. We can see that with higher error rates in IEEE 802.11, the average delay decreases. We analyze the trace file and find that this is due to the factor that more packets are lost and their delay count is 0.

We also did the simulations with different number of hops extension in ad hoc network with the same IEEE 802.11 error rate, all the simulations use the same HSDPA channel trace which have an average SNR 50 dB. From Fig. 8.15, we can see that when the number of hops increase, the MOS value further decreases dramatically. When the error is higher than 20 percent, the

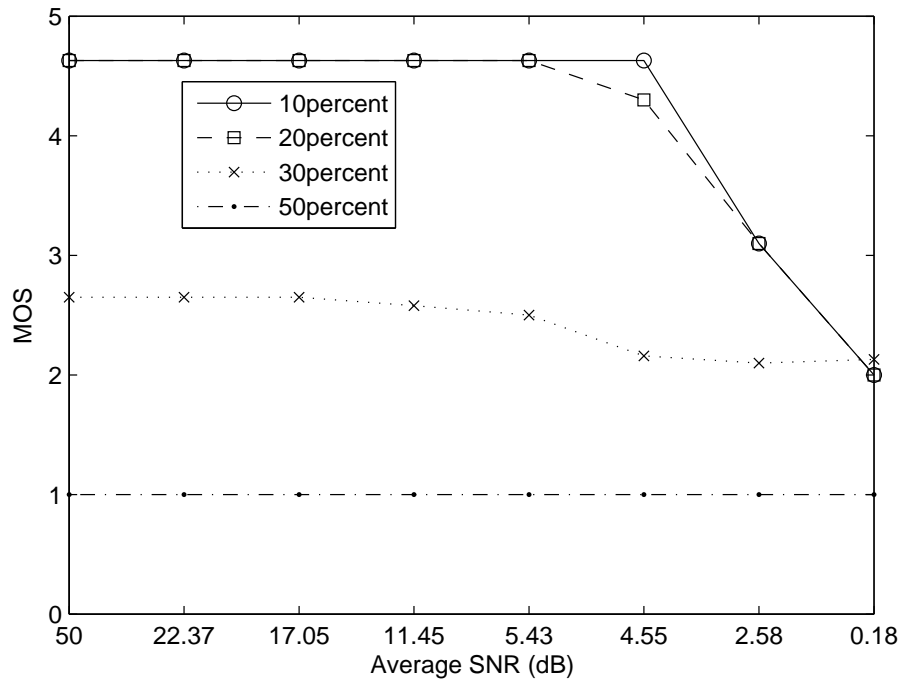


Figure 8.13: The MOS value decrease in different error rate.

MOS value for the 2-hop scenario is lower than 1.5, which means the 2-hop topology can not be used at all when the error rate is higher than 20%.

### Challenges for single MPEG-4 over cellular multi-hop network

The simulation results shown in this section indicate that both networks, cellular and 802.11 ad hoc network can cause MPEG-4 video performance degradation on the receiver side. The cellular network uses the ARQ mechanism to prevent packet loss but also results in a longer delay for the video packet which causes the video quality to decrease. The IEEE 802.11 MAC layer also has the retransmission attempts which can prevent parts of packet loss, but still can cause packet delay and reduce the MPEG-4 video quality due to packet losses. In the scenarios which have several gateways for a large scale ad hoc network, the end users' experience can be affected by both networks. In order to achieve the best end-to-end video quality, the mechanism for selecting the best gateway and relaying node need to be designed. The mechanism should consider the effect of delay in cellular network and packet losses in 802.11 ad hoc network, which make the best combination during the route selection.

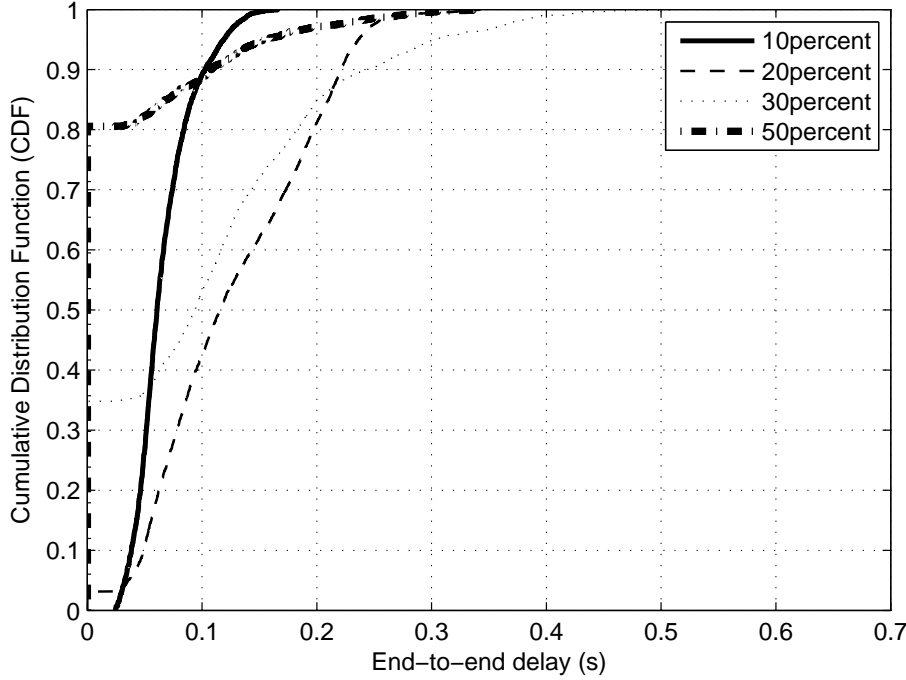


Figure 8.14: The delay distribution in different error rate.

We have carried out another simulation with the following configuration. For the HSDPA trace file, we assume different distances between the NodeB and UE, each distance corresponds to a trace file and we use the average SNR to represent this trace file. Now we assume that one MPEG-4 receiver uses the HSDPA channel that has 700m between the UE and NodeB. Other MPEG-4 receiver can be with different configurations. We assume the distance between each IEEE 802.11 node to be 100m. Therefore, we can make an assumption that if we want to have a connection between a receiver which is located 700m away from a certain NodeB, we have several combination choices. It can be 700m with only HSDPA channel, or 600m HSDPA channel with 1-hop ad hoc relay, or with 500m HSDPA channel with 2-hop ad hoc relay. However, due to the environmental differences, the error rates in ad hoc network may also vary. We still assumed four different error rates in our simulation and the result is plotted in Fig. 8.16. The simulation results indicate that ad hoc relay indeed can improve the end-to-end quality compared to the HSDPA channel. However, this depends on the channel quality of IEEE 802.11 also, which is determined by lots of factors in IEEE 802.11 channels.

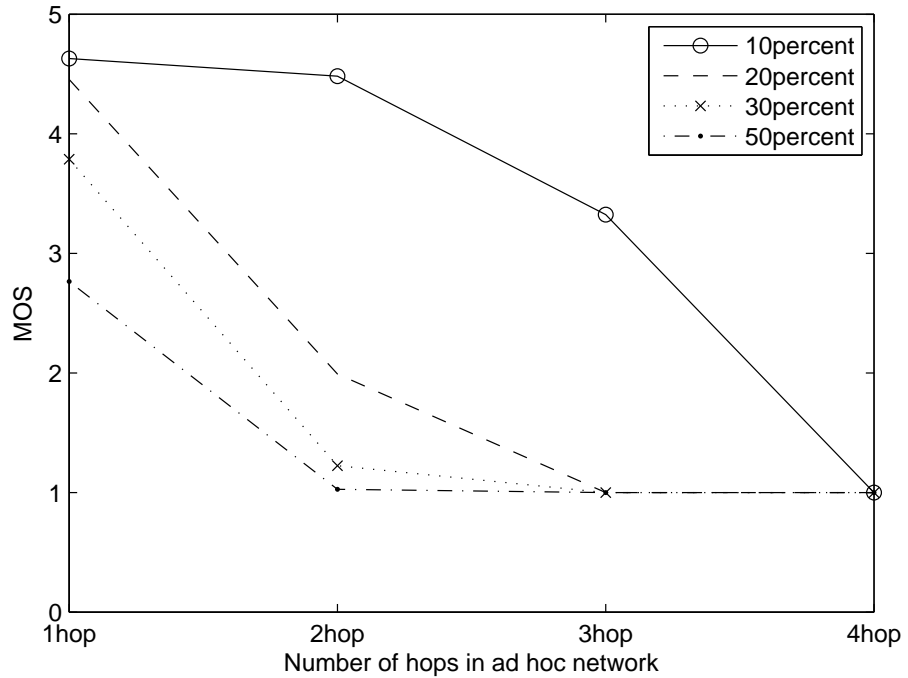


Figure 8.15: The MOS value decrease in multi-hop network.

The results in Fig. 8.16 indicate that a smart self-selecting algorithm is necessary to achieve the optimal performance for single flow. However, this is a selection problem over two different networks. Different factors should be considered in the path selection. Our MPEG-4 simulation tool-set can be used for designing and evaluating this new mechanism. The cellular network uses the channel model based on the distance between user node and base station. The IEEE 802.11 can also use the distance to decide the channel quality. Based on the measurement result from [111], the average SNRs for error rates 0.5, 0.3, 0.2 and 0.1 is 20, 24, 26 and 28 dB. The ns-2 simulator can calculate the SNR between two nodes based on their distance. We can use the SNR to error rate mapping achieved from the measurement to predict the corresponding error rates between these two ad hoc nodes. Therefore, we can achieve quite realistic simulation environment and with our simulation tool-set, we can validate the performance of the special gateway and route selection protocol which selects the best relaying nodes and gateway combination for the MPEG-4 traffic.

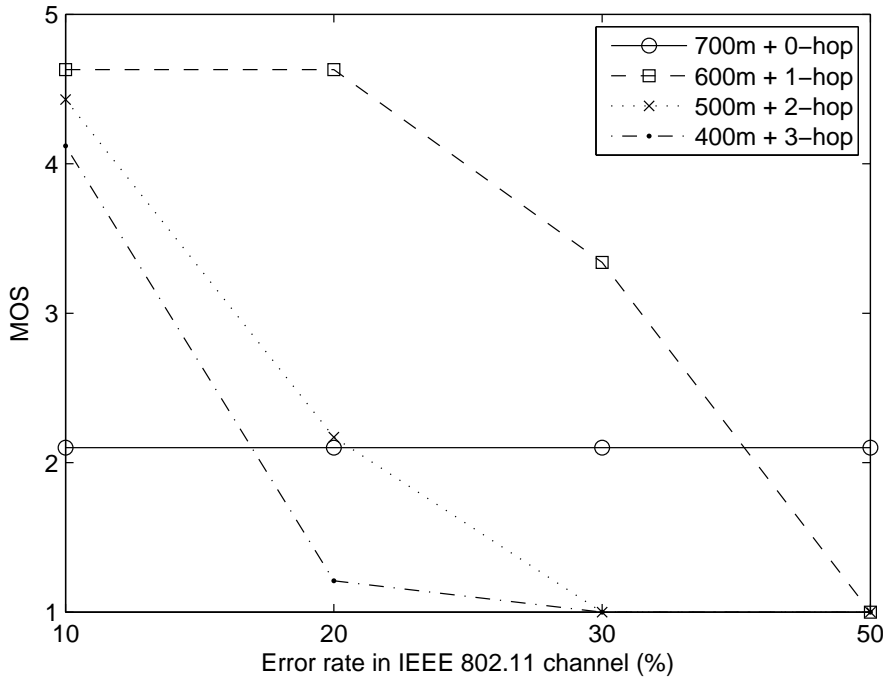


Figure 8.16: The MOS value tradeoff with different network topology configurations.

### 8.5.2 Multiple MPEG-4 flows

For single flow, the main problem is to find the optimal route which delivers the best end-to-end performance. When there are multiple flows in the system, the fairness problem will emerge. Different flows may experience different channel quality due to the difference of destinations of each flow. The flows which have more number of hops and bad channel quality may be suppressed by the flows that have less number of hops and better channel quality. The end-to-end performance can be quite different due to the unfairness. How to let different flows sharing the limited resources more fairly and do not affect the system performance is going to be a challenge for this integrated network. We are going to demonstrate this unfairness via the simulation result and propose our solution. In this section, we use four flows in our simulation. As the maximum bandwidth for HSDPA is 3.36 Mbps, we encoded the MPEG-4 video source "waterfall" to be 0.8 Mbps to suit the HSDPA channel. The HSDPA default scheduling mechanism round robin is used.

### Unfairness caused by HSDPA channel quality variance

We first examine the performance difference caused by the cellular channels. We set the simulation topology as follows: Flow1, Flow2, Flow3 and Flow4 all use one hop connection to the gateway. Flow1, Flow3 and Flow4 always assume the best HSDPA channel quality, which get the average SNR as 50. Flow2 will experience different HSDPA channel quality as shown in Fig. 8.17. We can see that MOS value of Flow2 is quite different from other flows when the channel decreases to 17.05 dB.

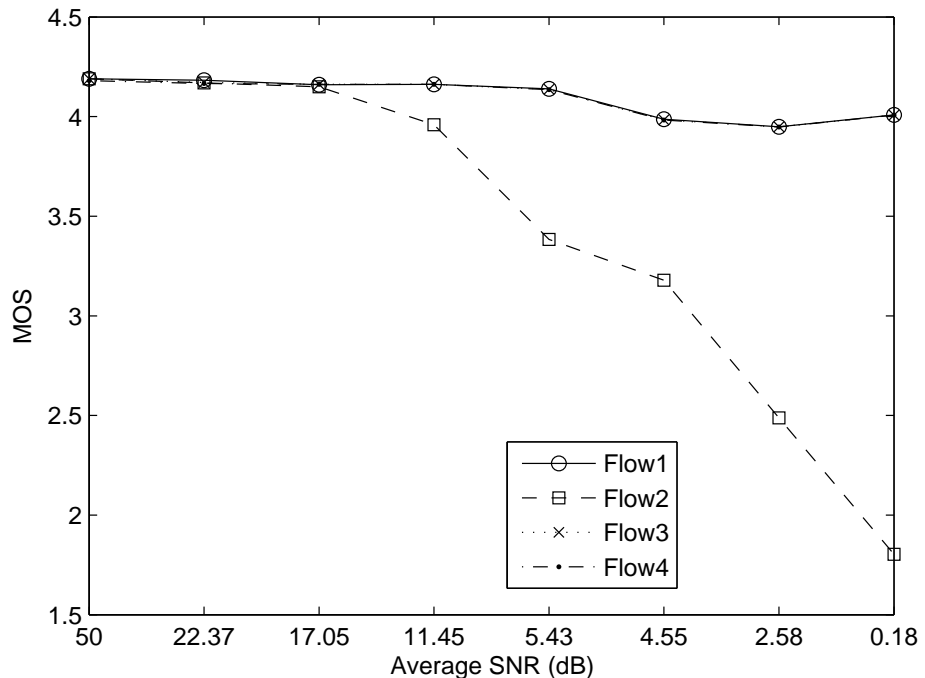


Figure 8.17: The MOS value for different flows when HSDPA channel quality is different.

We use the same fairness index [37] as in Section 7.5 as our system fairness performance evaluation metric. The performance is shown in Fig. 8.18 and the unfairness can be as low as 0.93.

### Unfairness caused by ad hoc topology

In this section, all the flows assume the same HSDPA channel, with perfect quality( $SNR = 50$ ).

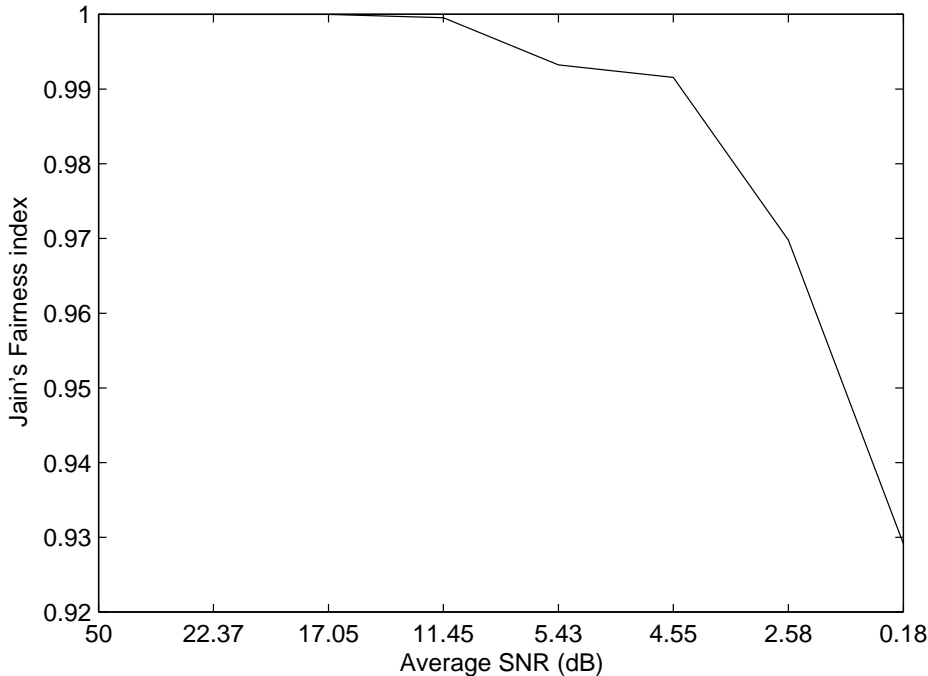


Figure 8.18: The fairness of the MOS value between different flows when HSDPA channel quality is different.

**Error free IEEE 802.11** We first assume that there is no error in the IEEE 802.11 channel. We assume that three flows use the same one-hop connection to the gateway, and the other flow uses 1-hop, 2-hop, 3-hop and 4-hop connections to the gateway. We use two different coding rates to compress the MPEG-4 video namely 0.8 Mbps and 3 Mbps. With different number of hops, there is no clear performance degradation. The average MOS values are 4.16 and 2.85 for the two coding rate despite the number of hops between the MPEG-4 receiver and the gateway. This result can be explained by the same reason described in Section 8.5.1 that IEEE 802.11 has very little delay when no packet is lost.

**Erroneous IEEE 802.11** Our next step is to set different error rate in IEEE 802.11 channels. We let three flows use 1hop topology and the other flow use 2hop topology. The MOS value is plotted in Fig. 8.19. We can see very obviously that the flow which has 2-hop topology will experience much higher performance degradation with high errors. All the flows will have the same performance when the channel is too bad, 50% error in 802.11 channel.

We also computed the fairness index for all the scenarios in Fig. 8.20. The index can be as low as 0.88 which indicates quite unfair situation.

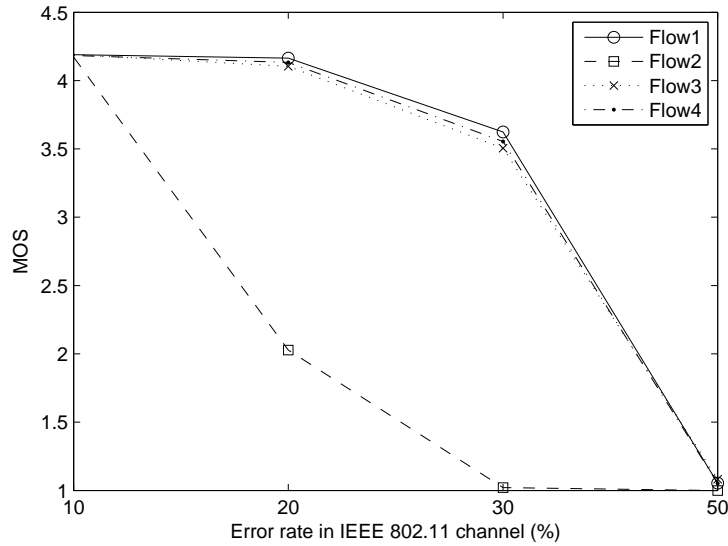


Figure 8.19: The MOS value for different flows with different IEEE 802.11 ad hoc error rate.

### Challenges for multiple MPEG-4 flows over cellular multi-hop network

We have showed some unfairness in terms of the end-to-end performance for multi flows over cellular multi-hop network. If some flow is with bad HSDPA channel and large number of hops away from the gateway, it will experience even worse performance. How to ensure the performance for the flows that have bad channel quality is going to be a big challenge. The problem is that two different networks have many factors that can impact the performance of a video flow. A weight mechanism can be used in HSDPA scheduling system to tune the transmission probability of each flow and give more weight for the "weak" flows. How to use one metric computed out of several factors to determine the weight would be an interesting problem.

## 8.6 Chapter Summary and Discussion

In this chapter, we evaluated the performance of MPEG-4 video transmission over the next generation UMTS/HSDPA and IEEE 802.11 integrated

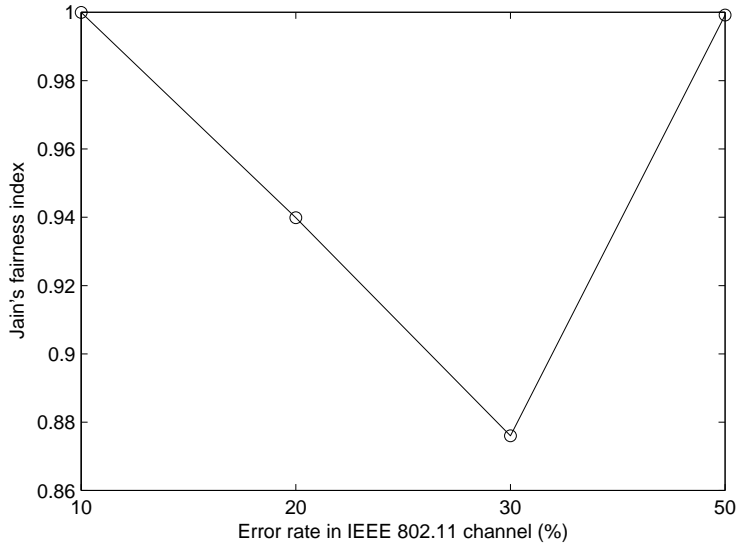


Figure 8.20: The fairness of the MOS value between different flows with different IEEE 802.11 ad hoc error rate.

network by simulation. From the simulation results, we conclude that for this new multi-hop cellular network, high quality MPEG-4 video streaming with compressing bit rate of 1 Mbps is feasible for single flow situation. Using an integrated MPEG-4 tool-set, we analyzed the impact of several factors on the MPEG-4 video streaming performance over the network. We demonstrate that the integrated network can also enhance the performance of cellular network itself using the relaying ad hoc nodes. Unfairness is showed in multi flow scenarios and solution for this challenge is proposed.



# **Chapter 9**

## **Conclusion**

### **9.1 How Far We Have Gone**

With the rapid development of the modern communication technology, especially the wireless technology, there is no doubt that more and more electronic devices will appear in our life and we can envisage that they will be connected via the communication networks in the future. Different communication radios and technologies will create tremendous wireless links with various link quality. How to efficiently gather, transfer and utilize the link quality information in different OSI layers and between different nodes will be an interesting topic. In this thesis, we have analyzed the importance of this trend and have showed our results in the previous chapters.

Recalling the thesis, in Chapter 1, we introduced the motivation for this thesis. All kinds of link quality issues for three different radios are discussed in Chapter 2. We proposed two different link quality estimation methods and did an analytical comparison with different estimation indicators in Chapter 3. In Chapter 4, we demonstrated the first application of the link quality in MAC layer for power saving and interference reduction. Chapter 5 discussed how to use link quality information to achieve better data rate selection in the MAC layer. The achievement in Chapter 3 and Chapter 5 is further applied in routing layer and result is presented in Chapter 6. The link quality affecting the higher layers are discussed in Chapter 7 and Chapter 8.

Previous works have already demonstrated the importance of utilizing information from different communication layers. However, the information they are using itself is far from accurate. Especially, we proved that traditional link quality estimation is inaccurate and responds very slowly to the link changes in the mobile scenarios. We proposed different methods based on different conditions and we showed the performance enhancement based on

our new proposals in all the layers. Also, huge amount of measurement and simulation results give us an indication about the performance enhancement that can be achieved.

The goal of this thesis to research the impact of the wireless link quality to all the communication layers which is broad research area and of high standard. We have achieved this goal to some extent. We now summarize our achievements in the next section and discuss the directions for future research in Section 9.3.

## 9.2 Main Results and Contributions

This thesis has been structured in three major parts, each one addresses one type of research topic, they are described in the following subsections. Each of the topic itself is a complete and independent work under the general assumptions and scenarios. We summarize the conclusions we make for each topic. Here we list the work to its corresponding chapters.

1. Link quality based optimization of the end-to-end performance, mainly in Chapter 2, Chapter 3, Chapter 5 and Chapter 6.
2. Link quality based optimization for the power saving and interference reduction, mainly in Chapter 4.
3. Cellular multi-hop network, mainly in Chapter 7 and Chapter 8.

### 9.2.1 Link quality based optimization for the end-to-end performance

In this thesis, we have identified the importance of knowing wireless link quality. We used the preliminary measurement result to show that the wireless link quality's characteristics are very dynamic and different for different links. We did many experiments and observed the IEEE 802.11 and IEEE 802.15.4's link quality in plenty of wireless links. We investigated all possible wireless link quality indicators and got to the conclusion that the SNR will be a good indicator compared to the other current available ones.

We have discussed the methods of using SNR to predict the link quality. We have proposed two methods for IEEE 802.11 radio and one method for IEEE 802.15.4 radio. In the linearization method we use the correlation between SNR and PDR evaluated from the preliminary measurement and found the best linearization rate to describe this correlation. Also, the linearization methods combine the hello packet counting information. SNR map is a profile for each data rate of IEEE 802.11b/g obtained by counting the received packets for each observable SNR value. The combination can be

used with the broadcast packet delivery ratio. Even in the absence of traffic on a particular link the SNR map allows accurate LQE. In order to create SNR maps we use passing data traffic instead of probing packets. We conclude that the linearization method is good for static environment while the SNR mapping method would achieve good performance even when the environment is changed. To identify the potential of different LQE indicators, we present a simple analytical model to compare all important LQE methods outlined in this thesis. In some scenarios, the experiments indicate that our proposed method can have 50% of performance enhancement in accurately without introducing overhead in the network.

Further, we also propose a novel rate adaptation algorithm for IEEE 802.11b/g networks using our proposed LQE method to improve the route adaptation performance. We have first compared the performance using different smoothing factors for a widely used rate adaption mechanism. Then, we used our link quality estimation in the rate adaptation mechanism. We showed that our proposed mechanism outperforms the traditional mechanism in all the scenarios and we can achieve maximum 100% enhancement in certain scenarios.

At last, we implement our proposed LQE, rate adaptation and route selection algorithms, in hardware and compare its performance. Using different test-beds and in diverse scenarios, with the traditional beacon packet-based LQE, we show over 50% improvement in rate adaptation and throughput obtained at the routing layer for both LQE methods. To the best of our knowledge, our work is the first to use this approach to improve the end-to-end system performance.

Our methods are validated by real measurement results and can be used in all IEEE 802.11 and IEEE 802.15.4 radio systems. The methods can be also used in other short range radio technologies.

### 9.2.2 Link quality based optimization for the power saving

Energy consumption is a key challenge for wireless networks. In this thesis, we have proposed to select the transmission power by using accurate link quality information in order to reduce the energy consumption. We have proposed five methods for the best transmission power level selection for the initialization phase to get a good transmission power level to start. We proposed to use an EWMA method to update the PDR and transmission power level correlation during the updating phase and use this to adapt the transmission power. Furthermore, we investigated the optimal parameters for

this correlation in order to achieve minimum energy consumption. Different impacting factors were also analyzed. We carried out our measurement in two types of real test-bed and showed that significant energy can be saved for the transmitter in typical scenarios. Meanwhile, we showed that the energy emission to the environment can also be greatly reduced, which means the interference towards other communication nodes are greatly reduced.

The same as previous section, we also used the measurement results to validate our mechanism and we showed that the power can be saved to as much as 10% and the interference can be reduced as much as 90% in certain scenarios.

### 9.2.3 Cellular multi-hop network with different link quality

As we have introduced in Chapter 1, the integrated UMTS/HSDPA and IEEE 802.11 network can provide seamless Internet access for end users and can also help the operators to balance the load between the cellular network cells. By the method of simulation we analyzed the performance of TCP over this integrated network. Based on our simulation result, we draw the conclusion that the IEEE 802.11 network affects the end-to-end TCP performance due to the bottleneck effect, the bottleneck changes based on different network topology and configuration. The HSDPA radio channel usage and end user experience is also affected by the different channel conditions and configurations. Meanwhile, the IEEE 802.11 network increases the RTT of the TCP flow, thus, based on the number of extended hops, the file download performance can also vary. System performance and route selection decisions can be optimized based on our simulation results.

Further, we have revealed that due to complex topology and link quality differences between different traffic flows, a fair sharing of radio resources among all the users became a new problem. Simulation results reveal that the Jain's fairness index can be as low as 0.88 in certain scenarios. Traditional scheduling algorithms in HSDPA considered only the HSDPA channel quality to allocate resources in different flows, which can not reach the fairness sharing and some users in the ad hoc network can hardly access the Internet. We proposed a novel scheduling mechanism which can consider the HSDPA channel quality, number of hops and channel quality of IEEE 802.11 links. Using the proposed scheduler, the fairness among the flows could be improved by 14% and the throughput for the unfair flow can be increased by as high as 123%.

Further, if the multiple traffic flows exist in this network, the fairness

issue will be an important aspect. Our model can be used for analyzing the fairness amongst different flows and modify the system to reserve and allocate the resources more efficiently.

Finally, we evaluated the performance of MPEG-4 video transmission over the next generation cellular multi-hop network by simulation. From the simulation results, we conclude that for the novel multi-hop cellular network, high quality MPEG-4 video streaming with compressing bit rate of 1 Mbps is feasible for single flow situation. Using an integrated MPEG-4 tool-set, we analyzed the impact of several factors on the MPEG-4 video streaming performance over the novel integrated multi-hop UMTS/HSDPA and IEEE 802.11 network. We demonstrate that the integrated network can also enhance the performance of cellular network itself using the relaying ad hoc nodes. Unfairness is showed in multi flow scenarios and solution for this challenge is proposed. The link quality variance in both network will result in dynamic network bottleneck, which suggests that the selection of relaying node and gateway should consider those factors and dynamically make the selection.

### 9.3 Future Work

After describing all the research we have done till now, one question will appear. Can we estimate the channel accurately enough for different type of scenarios and radios? Can the system always select the best data rate, transmitting power level or route? Is the packet transmission over the cellular multi-hop network evaluated completely and the system performance is optimized? Unfortunately, the answer is no. Our work is just the beginning of investigation over iceberg above the sea and further work has to be done to answer those questions.

Based on the chapters in thesis, we list the possible research directions for the future research.

#### Link quality estimation

More advanced link quality estimation method which may incorporate more factors and information sources can be proposed. The improvement from the hardware system will provide us more information, such as Bit Error Rate (BER). An appropriate weight system could be proposed to enable the combination of different impacting factors for different higher layer applications.

#### Rate adaptation

Better rate adaptation methods can be proposed if more accurate LQE could be done. Meanwhile, better performance can be achieved via more cross layer design, e.g, application layer information can be useful to the rate adaptation mechanism to decide whether the rate adaptation should be throughput optimization oriented or have a delay limited target.

#### Power saving

The next step for power saving and interference reduction is to evaluate the power saving amount with the best combination of data rates, packet sizes and transmission power levels. That is in a certain channel condition, based on available link quality. Further, combined with current link quality information, selection of the route that consumes the least energy would be an interesting subject.

#### Link quality based routing

An interesting area for further exploration is to use the link quality information to select the route in multi-radio, multi-channel environment. Also, power saving can be achieved if accurate link quality information is used for minimum power consumption route selection. We can envisage that in future, the best route selection will be a trade off mechanism, based on accurate link quality information and all the requirement, the system selects the optimal route that can satisfy all the requirements from different aspects to a certain extent.

#### Performance of integrated network transport layer

For future work, other network topologies instead of a chain topology, varying channel quality for each link in the multi-hop ad hoc networks can be considered in performance evaluation in the integrated network. Mathematical methods need to be used instead of simulations to determine the weights in our weighted scheduling mechanism for fairly allocate resources among different traffic flows can be done.

#### Performance of integrated network application layer

For the application layer, future work can be how to incorporate the lower layers information to this layer for performance optimization. For example, good data rate adaptation can be helpful in video streaming applications. Using the mathematical model for best route selection for single video stream and resource application for multiple video streams can be also an interesting and promising topic.

The above topics are my suggestions to the future research, I believe the contents of the thesis will be helpful for further investigation of more interesting results in the above areas.

Let me use a Chinese old saying from a famous poet (Yuan Qu) who came out from my birth province 2000 years ago to end this thesis: There is still a long way to go, and I shall look for all opportunities to investigate the truth deeper!

路漫漫其修远兮，  
吾将上下而求索



# Appendix A

## IEEE 802.11 Test-bed

The IEEE 802.11 based experiment indoor test-bed is build partly for the prototype of PN. The outdoor test-bed is build at University of California, Davis for wireless mesh network research. Both test-beds use the off-shelf devices and build their own architecture. Now we start to introduce both test-bed in detail.

### A.1 Indoor test-bed

#### A.1.1 Hardware

The hardware prototype consisted of laptops, each equipped with 3Com OfficeConnect 108Mb 11g PC IEEE 802.11b/g card. The card contains Atheros chip which is supported by the open source Madwifi driver version 0.9.4 [57].

#### A.1.2 Software

The basic structure of test-bed is depicted in Fig. A.1, we explain each part as following.

- MAC

The Madwifi driver is used in the MAC layer to control the packet sending, information gathering and data rate control. We adapted the driver and let it as in Fig. A.1(b) for information transferring in both direction. Packet SNR values were obtained from the driver by Linux's iwspy interface [91] every time a beacon or data packet was received. To make sure that data traffic does not delay beacon packets, a priority queue was used on each of the interfaces that gives beacons the highest priority. A lost data or beacon packet is assigned the SNR value of

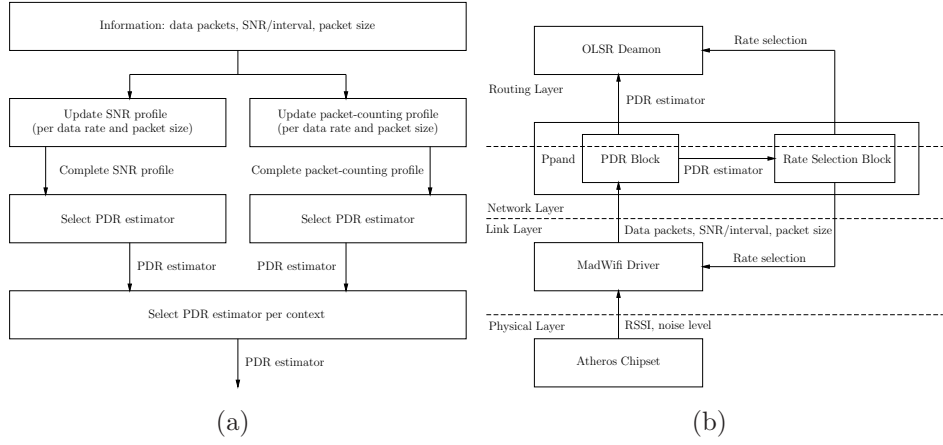


Figure A.1: Proposed IEEE 802.11b/g system: (a) LQE system (PDR block), and (b) software implementation of the complete IEEE 802.11b/g network node.

the previous packet, while the first non-received packet is assigned the minimum receivable signal strength of  $-95$  dBm. With every received beacon a new optimal transmit data rate and route is computed. To obtain information on the retransmissions of data packets necessary to evaluate, retrieve the current noise floor (used in computing SNR), and the selected data rate for each node, the Madwifi driver was modified. We note here that the noise floor reported by the Madwifi driver was relatively stable and varied in the range  $\approx [-94, -98]$  dBm. The transmission power level was set to default 15 dBm.

- Ppand

We adapted the routing daemon and parameters to get the link quality information from Ppand instead of using the daemon's own packet delivery ratio estimation method. OLSRD then uses its topology control messages to share the link quality information with the rest of the network. The topology control message interval is modified to 1s instead of 5s in our test-bed, this is due to the daemon is designed for stationary scenario in which link quality may not change much in this interval. However, in our mobile scenario, link quality is quite dynamic, so the default values reduce the improvement introduced by accurate link quality information. A smaller interval will cause very little overhead, but trade off for faster route selection decisions.

The software implementation architecture is depicted in Fig. A.1(b). Ppand [36], developed for PN, maintains a neighbor list, i.e. creates

and splits PN clusters, and combines all the cross-layer information providing an abstraction of multiple link layers to the network layer. As shown in Fig. A.1(b), it operates between the network interfaces and the rest of the networking stack. Its purpose is to discover neighbors, handle departures and arrivals of the nodes, authenticate nodes, secure communication, and monitor PDR of the links to those neighbors using methods described in Chapter 2. Ppand generates and processes unicast packets for the purpose of authentication and authorization and beacon packets for the purpose of link maintenance. Unicast packets are sent by Ppand depending on the network situation, while beacon packets are sent every second. If the beacon has been lost fifty consecutive times then the neighbor is removed from the neighbor list.

- Routing layer

In the routing layer the OLSR [15] was implemented using GNU/Linux open source OLSR daemon [90] version 4.10.0. A packet delivery ratio aware extension was added to in the routing daemon that made the route decisions based on PDR instead of number of hops. We adapted the routing daemon to get the link quality information from Ppand instead of the daemon's own PDR estimation. The TC message interval was set to 1 s from 5 s. The original daemon was designed for the stationary scenario in which link quality does not change much over a 5 s interval. However, in a mobile scenario, described below, link quality is quite dynamic, so the original interval would limit the potential performance improvement with accurate link quality information. The shorter interval caused very little additional overhead, but resulted in slower route selection decisions. Though the OLSR protocol was used in our test-bed, the results obtained in our experiments should apply to other routing protocols as well since the gains were due to improved route selection and not through improved route signaling.

- Traffic generator

We write our own traffic generator, which can generate UDP and TCP traffic as the measurement demand. For the UDP traffic, the packets are generated with uniform distribution and number of packets per interval is set for experiment.

- Operational system

The laptops ran the GNU/Linux 2.6.24 kernel.

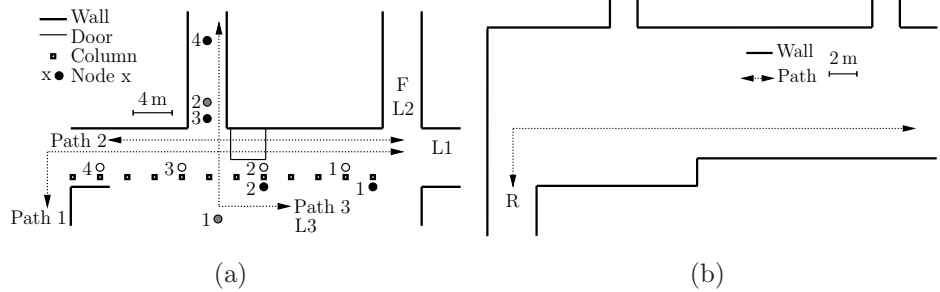


Figure A.2: Different topologies used in the evaluation of the proposed network for experiments T1–T6 in (a) cafeteria, and (b) aula.

### A.1.3 Scenarios

The proposed link quality aware rate and route adaptation IEEE 802.11b/g ad hoc network has been evaluated for different measurement scenarios using five nodes. We have evaluated the LQE process, rate adaptation and routing independently for different scenarios. All of them are described below.

In evaluating proposed link quality aware IEEE 802.11b/g network we have set up six different scenarios referred as T1–T6. Scenarios T1–T5 were setup at the cafeteria of Electrical Engineering, Mathematics and Computer Science department of Delft University of Technology. This environment was chosen purposefully, since it contained many walls, pillars, doors, etc., which presents a challenging propagation environment. In all but one scenario, described below with the help of Fig. A.2, one pair communicated on channel 7, which was least affected by other transmissions. Finally, all experiments were performed during late afternoon and night to reduce the probability of interference on that channel. For T6 we set up the experiment in the aula of Delft University of Technology, which had a different structure, e.g., bigger size, thicker walls and less pillars, than the cafeteria and had more background IEEE 802.11b/g traffic on the selected channel 7.

- T1 The sender was located at L1 while the mobile node moved along path 1 with the speed of  $\approx 1$  m/s. This scenario was needed to evaluate the proposed method in a mobile environment and to observe the SNR mapping table for a broad range of SNR values. For 80% of path 1 the link had LOS and for the remaining 20% was shadowed by the wall. The shadowed portion of the path was needed to obtain very low values of SNR. In LOS portion we could not obtain a SNR lower than 15 dB.
- T2 The sender was located at L1 while the receiver moved along path 2, in stop-and-go fashion, i.e., the receiver resides in one location for

1 min and then moves 1 m away from the sender (in the case of LQE measurements), and waits 3 min, then moves 4 m away from the sender (in the case of rate adaptation measurements). The whole process took about 50 min.

- T3 The same as T2, except the sender moved along path 2 and the receiver was located at L2.
- T4 The same as T3, with a third node located at F separated 20 cm from L2 and not involved in the same network. Node F broadcasted a large amount of traffic, i.e., 500 packets/s, at the same data rate and packet size as the sender at L1, but on a channel two away from that of the sender and receiver. This scenario served the purpose of evaluating the impact of adjacent channel interference on the proposed LQE method.
- T5 The same as T4, except the interfering node transmitted packets on the same channel as the sender and receiver. This scenario served the purpose of evaluating the impact of co-channel interference on the proposed LQE method.
- T6 The topology for this rate adaptation experiment is the same as in T1, compare Fig. A.1.3 and Fig. A.1.3. The nodes had SNR profiles created in the cafeteria. This experiment was set up to show the ease of adaptability of the proposed LQE to different types of environments and to evaluate the process given by (3.5).

Finally, in case of routing process evaluation we have set up the following three scenarios, called as R1–R3.

- R1 The sender and receiver were located close to each other at L3, see Fig. A.1.3. The sender followed path 3 away from receiver and returned. For this path two nodes, marked as grey circles in Fig. A.2, forwarded the traffic. The movement was repeated 10 times and lasted 90 s. Before each movement along path 3 the sender waited 30 s at L3, to let the rate adaptation mechanism stabilize to de-correlate each movement from the previous.
- R2 The sender located at L1, see Fig. A.2, sent traffic to each of its four neighbors one by one, marked as white circles in Fig. A.2. The sender send a constant flow of UDP traffic for 5 min to one receiver before it targeted the next node. Nodes were allowed to forward the traffic.

R3 The same as R2, but the receiving nodes were located differently, marked as the black circles in Fig. A.2. This was the non-LOS communication scenario in a ad hoc network.

It is important to discuss why we decided to limit ourselves to the line (tandem) topology with five nodes. First, in real life, large scale ad hoc networks, where dozens of nodes are actively transmitting is rare. Second, due to the IEEE 802.11 transmission medium characteristics end-to-end throughput decreases dramatically with increasing hop count [60], especially for very high data rates, i.e.  $R \gtrsim 11$  Mbps. Thus for many hops (greater than five) random routing and contention effects will invalidate the throughput comparison of different methods.

## A.2 Outdoor test-bed

### A.2.1 Hardware

All nodes used in the outdoor experiments were running IEEE 802.11b/g. Each device was equipped with two radios using the Atheros chipset, the same as used in the indoor test-bed described in Section A.1.2.

### A.2.2 Software

The operating system was a modified GNU/Linux kernel version 2.6.28 using the modified Madwifi driver version 0.9.4. Because no rate and route adaptation experiments were performed outdoors, Ppand was not needed. Instead a socket-based application that created SNR profiles was developed based on Madwifi. Note, that just like in the indoor experiments noise floor oscillated around  $-95$  dBm.

### A.2.3 Scenarios

The outdoor experiments were performed on the Quail Ridge Wireless Mesh Network [103]. The network was located in Napa County, California, on a southern peninsula of Lake Berryessa and consisted of hilly and densely forested terrain. There were 34 nodes at the time of testing, all placed at varying elevations due to the terrain spanning 2000 acres. Distances between nodes ranged from 1 mile to a few hundred meters. Directional antennas were used for point-to-point links on top of the hills, while omnidirectional antennas were used for lower elevations. The following experiment was performed.

- T7 A randomly selected sender sent a data to a randomly selected receiver for about 30 minutes in all available data rates. This experiment was needed to obtain an SNR profile for outdoor scenario.



# Appendix B

## IEEE 802.15.4 Test-bed

The IEEE 802.15.4 test-bed is build for testing the performance of this short range radio. All the experiments described in this thesis are one-hop communication, therefore, the routing function in the device is not used.

### B.1 Hardware

We used a IEEE 802.15.4 complaint device in the 2.4GHz ISM band from Moteiv, called Tmote sky. During the experiment, the USB is used as power supply. The Tmote is shown in Fig. B.1.

### B.2 Software

As in IEEE 802.11, we also wrote a one-hop communication program for these devices. We used three different payloads, they were 20, 50 and 100 Bytes. IEEE 802.15.4 has a packet header, which consists of a 11 Bytes of PHY header and 6 Bytes MAC header. The standard data rate (250 kbps) was used during all experiments. We used 15 different transmission power levels for Tmote. Since there are 31 possible levels, we only used the odd levels between 3 and 31. Based on [10], they correspond to the dBm as follow: [-25 to 0] All the experiments were done in a channel that did not interfere with any IEEE 802.11 radio. We also did experiment in a channel that was impacted by IEEE 802.11 radio interference and found that the result was not impacted much. We used broadcast packets in the same way as in IEEE 802.11. The receiver side recorded the number of received packets and the used transmition power level.



Figure B.1: Tmote.

### B.3 Scenario

The IEEE 802.15.4 experiments were done in the same location as for IEEE 802.11, however, different distances were used. The channel was NLOS and the distances were 12, 14, 16, 18m respectively. We call these experiment scenarios as T-scenario1 to T-scenario4. The experiments with different packet sizes were done with 17m between sender and receiver with NLOS channel.

## Appendix C

### UMTS/HSDPA Simulator Structure

As described in Chapter 7 and Chapter 8. We use the simulations instead of test-bed to investigate the performance of UMTS and IEEE 802.11 integrated network due to some constraints. The basic architecture of UMTS/HSDPA and IEEE 802.11 cellular multi-hop network in NS-2 is described in [113]. The work in this thesis further extends this simulation module and enables HSDPA for this simulation. In this part of the thesis we describe the simulator in detail.

In our implementation, the NS-2 version is ns-2.29. It supports the TCP/IP protocol suite, several ad hoc routing protocols and the basic IEEE 802.11 ad hoc and infrastructure functionality. The UMTS modules which were developed in Eurane [23] were used since NS-2 does not support UMTS. In order to implement the integrated network architecture, the UMTS UE and the MN's protocol stacks are modified and the mobile gateway is added as a new entity in NS-2. In order to connect the MN to the mobile gateway, two new protocols are also added. Fig. C.1 depicts the schematic diagram of the integrated network implementation in NS-2. Each network node is represented by the rectangular block. UMTS and IEEE 802.11 radio channels are represented by the hexagonal block. The arrows show the packet flow during simulation. The gateway block implements the mobile gateway node which contains two different network interfaces. The two new protocols, namely routing agent and gateway discovery are implemented in the elliptical block in figure. In the following part, we introduce the simulator architecture in detail.

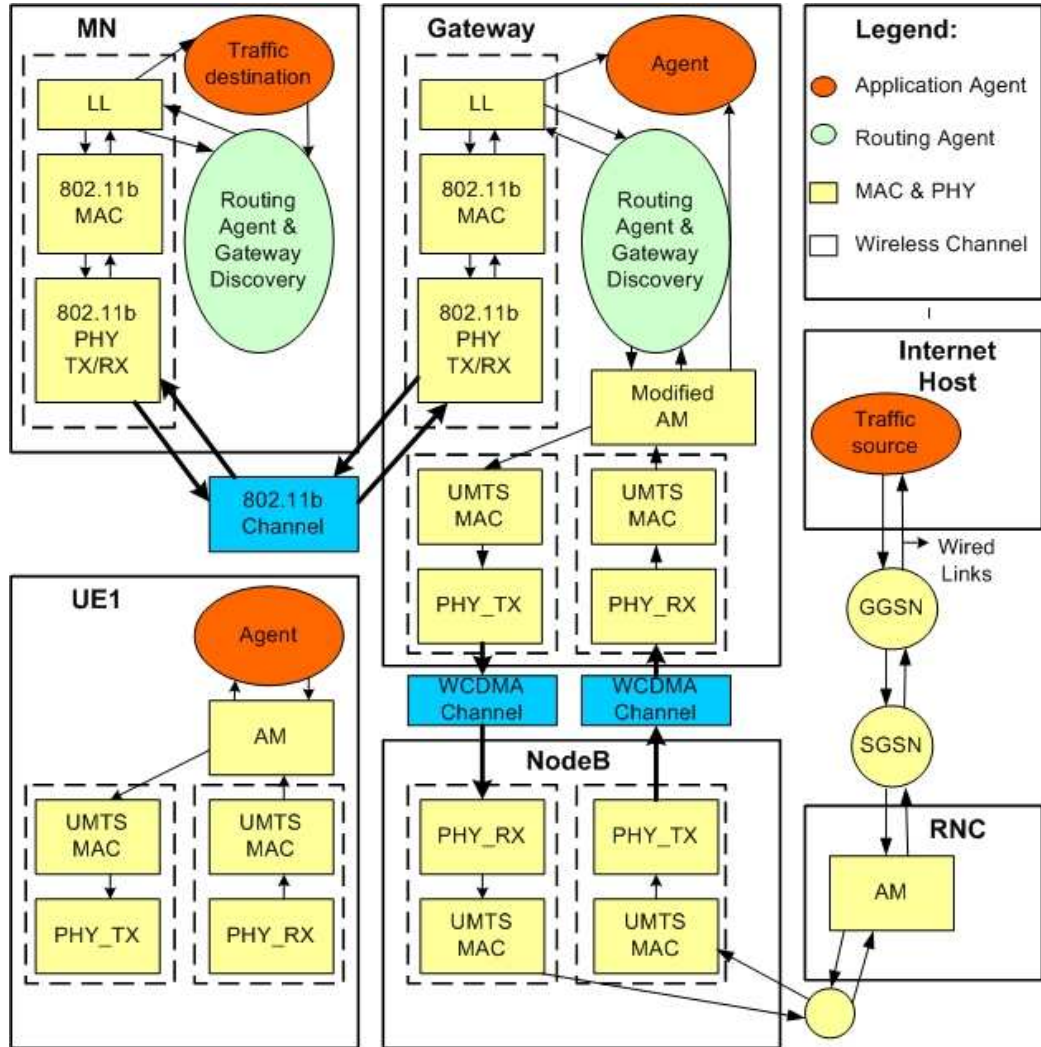


Figure C.1: Simulation Model Overview.

## C.1 IEEE 802.11 Model

The IEEE Medium Access Control (MAC) and Physical models are provided by NS-2. The MAC model implements the basic Carrier Sense Multiple Access with Collision Avoidance (CSMA/CA) mechanism, and an optional CSMA/CA plus RTS/CTS mechanism which is used to reserve the IEEE 802.11 radio channel and prevent data packet collisions. The physical model realizes a simple radio propagation model which combines a free space propagation model and a two-ray ground reflection model. In the simulation, the IEEE 802.11b has been considered.

## C.2 UMTS Model

On the UMTS interface, TCP/IP header compression is not supported in the Packet Data Convergence Protocol (PDCP) layer. The RLC model is configured to use acknowledged mode for TCP-based applications. It implements the complete functionality which includes piggybacking, in-sequence delivery of upper layer data (e.g., TCP segments), segmentation, reassembly and concatenation of the upper layer data. The Selective-Repeat ARQ mechanism was configured to retransmit erroneous RLC blocks until they are correctly received by the receiver. In this case, TCP would perceive a reliable link with variable transfer delay. The MAC model schedules and delivers a set of transport blocks to the physical layer at every TTI. In UMTS, a MAC protocol data unit is referred to as a transport block. The physical model captures the erroneous transport block on the dedicated channel using an uniform error distribution model. It is valid to assume that the erroneous transport blocks perceived by RLC is independent and uniformly distributed as a result of interleaving and forward error-correction mechanisms at the physical layer. The functionality of UMTS SGSN and GGSN were abstracted out and modeled as traditional ns-2 nodes since they are wired nodes and, in many ways, mimic the behavior of IP router.

## C.3 New Mobile Gateway

As the gateway contains both the UMTS and the IEEE 802.11 protocol stacks, the UMTS node definition was redefined to accommodate these two protocol stacks. As a result, the UMTS nodes, viz., UE, Node B and RNC, were defined as Node/MobileNode/UmtsNode instead of Node/UmtsNode. In order to participate in the ad hoc nodes' topology monitoring system in NS-2 (i.e., "god"), the gateway must contain MobileNode properties. The gateway node type is defined as Node/MobileNode/UmtsNode/HYBUE. Fig. C.2 illustrates the schematic view of the main components of the gateway. Each functional block is represented by an uppercase letter. The gateway is extended from UE implementation which is in turn modified from the normal wired node in NS-2. Our extension added an IEEE 802.11 network interface and made modifications to the packet flow direction and routing agent, which enables the gateway to interconnect the UMTS and IEEE 802.11 ad hoc networks. The classifier is used for packet forwarding. Classifiers C, D, and E functions the same as in the normal wired node in NS-2. For the gateway, since the Protocol Data Unit (PDU) and the Service Data Unit (SDU) packets should also be differentiated, the classifier B is used to sepa-

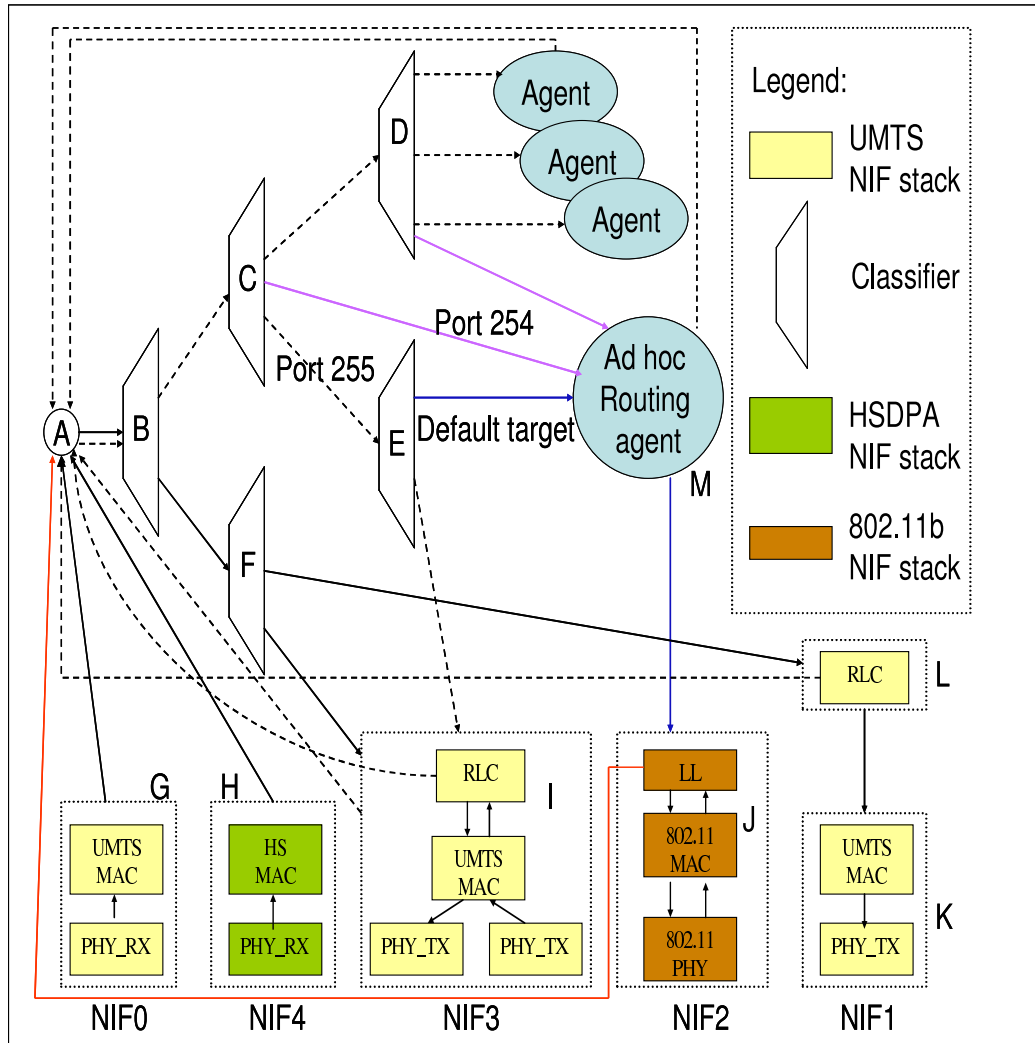


Figure C.2: New Mobile Gateway.

rate the IP layer packets (SDU) and RLC layer packets (PDU). Classifier C is modified such that it should be able to direct the IP packets to three different directions, the gateway itself (to D), the ad hoc network (to L) and the UMTS network (to E, default port). While the classifier F is the classifier for RLC packets which will direct PDU packets to the UMTS dedicated channel (to J) and the common channel (to L). The Network Interfaces (NIFs) in Figure 4 implement the UMTS and the IEEE 802.11 network interfaces. In the simulation, each NIF can be added to the gateway. With J and M, the IEEE 802.11 network interface and the ad hoc routing agent can be added to the gateway, which enables communication with the ad hoc network. If the

UMTS enhanced version High Speed Downlink Packet Access (HSDPA) is used, the NIF H can also be added to act as high speed downlink MAC and PHY. The other network interfaces (G, I, K and L) are for UMTS dedicated channel and common channel which can be instantiated for the integrated network before starting the simulation. The direction of different packet flows is marked by the arrow in Figure 4. We differentiate between IP packet flows and RLC packet flows at the gateway. Since the RLC layer is in charge of the segmentation of the IP packets into RLC packets and vice versa, the packet flowing in or out of the gateway consists of RLC or IP packets. The IP packet flows are indicated by the red, blue and purple arrows. In the original UMTS implementation, each NIF is sequentially assigned with a numeric value starting from "0". For instance, the FACH NIF (labeled G) and RACH NIF (labeled K) are assigned with "0" and "1", respectively, once a UMTS UE is instantiated. However, if a mobile gateway is instantiated, it contains an IEEE 802.11 NIF (labeled J) which is assigned with "2". If a UMTS DCH NIF (labeled I) is created, it will be assigned with "3" instead of "2" as in the original UMTS implementation. This numbering causes a problem in the ad hoc network configuration since the UMTS MAC class is derived from the parent MAC class in NS-2, which has a counter MacIndex to record the number of MAC instances created in the simulation. The instantiation of UMTS MAC increases the counter. This effect is counteracted by decrementing the assigned NIF value in the ad hoc configuration.

## C.4 Addressing and Routing

Once the mobile gateway has been designed to interconnect the IEEE 802.11b ad hoc networks and the UMTS networks, an addressing and routing solution is also required for the end-to-end communication. NS-2 supports two addressing modes, namely flat addressing and hierarchical addressing. In the flat addressing mode, the address space is organized into a single domain, while the latter is organized into sub-domains. The current implementation of the UMTS models only supports the flat addressing mode, while the IEEE 802.11 and wired network allow both addressing modes. Our special address system is depicted in Fig. C.3.

As for routing is concerned, the IEEE 802.11, UMTS and wired network have implemented different routing schemes. Ad hoc routing protocols are used in the IEEE 802.11 networks and the wired network uses static routing schemes, e.g., Dijkstra's. The UMTS implementation also uses the same routing schemes as the wired network with some modification. Since the UMTS UE, Node B and RNC are structurally different from the traditional

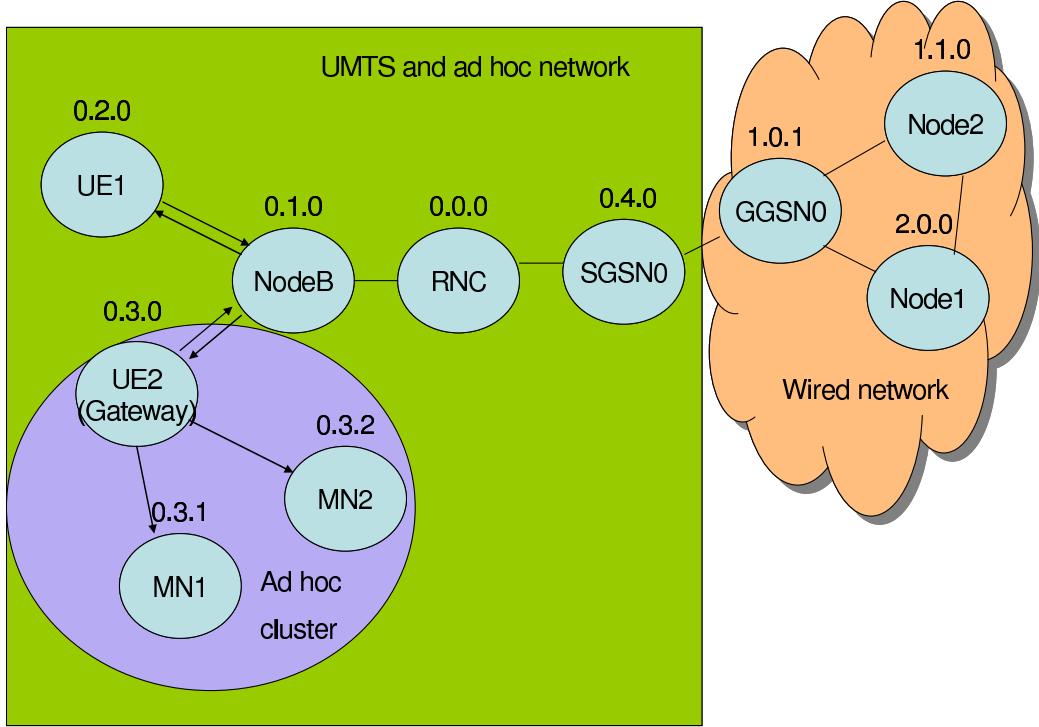


Figure C.3: Integrated Network Hierarchical Routing.

NS-2 nodes, the static routing schemes are unable to operate in these nodes. The UMTS implementation has alleviated this problem by constructing a default route. The default route is manually set at the beginning of the simulation using an Otcl command. Since the routing protocols used in UMTS, IEEE 802.11 and fixed networks are different, hierarchical addressing mode is suitable for the integration and has imposed the least modification to each individual network module. Hence, the UMTS implementation was modified to support hierarchical addressing mode. With hierarchical addressing, a node does not need to know the routing information of other networks, but it has to know the next hop neighbor to forward the packet. Figure 5 illustrates the integrated UMTS and IEEE 802.11 ad hoc which is organized into different sub-domains. The SGSN0 has the same address domain as the UMTS and the ad hoc networks. The GGSN0 and the other nodes in the wired network have another domain. Any packets destined for the UMTS UE or MN will be sent directly to SGSN0. The RNC node was modified so that it can direct packets to a particular ad hoc cluster to the corresponding mobile gateway in the ad hoc cluster.

## C.5 Gateway Discovery Protocol

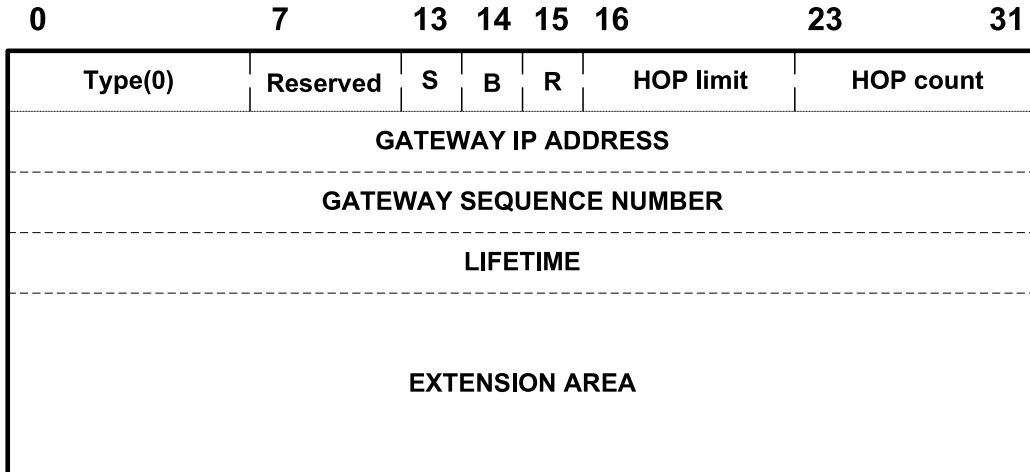


Figure C.4: Gateway Discovery Advertisement.

Before any MN in the ad hoc network can send or receive data packets from an external IP network, the MN needs to discover a gateway which can provide connectivity to the external IP networks. The gateway discovery protocol enables the MN to discover the mobile gateway even if the MN is several hops away from the mobile gateway. We have chosen to implement a proactive gateway discovery protocol in which the mobile gateway periodically broadcasts gateway advertisement messages to all MNs. The format of the gateway advertisement message is shown in Fig. C.4. The type field identifies the type of gateway discovery protocols. Presently, only the proactive gateway discovery protocol is implemented and it is set to "0" by the mobile gateway. The hop limit field sets the number of hops. The advertisement message can be traversed while the hop count field indicates the number hops the advertisement message has already traversed. The gateway IP address field identifies the mobile gateway. The sequence number field is used by MNs to detect and drop duplicate gateway advertisement messages. The S, B and R bits are used to indicate the additional information included in the extension area. Additional information can include service providers, price, quality of service, etc.



# Appendix D

## Abbreviations

3GPP	Third Generation Partnership Project
AODV	Ad Hoc On-Demand Distance Vector
ARQ	Automatic Repeat Request
AVC	advanced video coding
BS	Base Station
CIF	Common Intermediate Format
CHARM	Channel-Aware Rate Adaptation Algorithm
CTS	Clear to Send
CSMA/CA	Carrier sense multiple access with collision avoidance
DCF	Distributed Coordination Function
DHCP	Dynamic Host Configuration Protocol
DNS	Domain Name System
DSDV	Destination-Sequenced Distance-Vector Routing
DSR	Dynamic Source Routing
DSSS	Direct Sequence Spread Spectrum
ENT	Effective Number of Transmissions
ETX	Expected Transmission Count
ETT	Estimated Transmission Time
EURANE	Enhanced UMTS Radio Access Network Extensions for ns-2

EWMA	Exponentially Weighted Moving Average
FEC	Forward Error Correction
FIFO	First In First Out
GGSN	Gateway GPRS Support Node
GPS	Global Positioning System
GSM	Global System for Mobile Communication
HSDPA	High-Speed Downlink Packet Access
ICMP	Internet Control Message Protocol
IEEE	Institute of Electrical and Electronic Engineers
IP	Internet Protocol
IrDA	Infrared Data Association
LQA	Link Quality Assessment
LQE	Link Quality Estimation
MAC	Medium Access Control
MANET	Mobile Ad Hoc Network
mETX	Modified Expected Transmission Count
MN	Mobile Node
MPDU	MAC Protocol Data Unit
MPEG-4	Moving Picture Experts Group-4
MTM	Medium Time Metric
NAT	Network Address Translation
NLOS	Non Line Of Sight
NS-2	Network Simulator-2
OLSR	Optimized Link State Routing Protocol
PAN	Personal Area Network
PC	Personal Computer
PDA	Personal Digital Assistant
PDPCP	Packet Data Convergence Protocol
PDU	Packet Data Unit
PFS	Prioritized Flooding with Self-Pruning
PNP2008	Personal Network Pilot 2008
PN	Personal Network
P-PAN	Private Personal Area Network
QoS	Quality of Service
RLC	Radio Link Control
RNC	Radio Network Controller
RSSI	Received Signal Strength Indication
RTS	Request to Send
RTT	Round Trip Time

SACK	Selective Acknowledgment
SDU	Service Data Unit
SIM	Subscriber Identity Module
SGSN	Serving GPRS Support Node
SMS	Short Message Service
SNR	Signal to Noise Ratio
SSA	Signal Stability-Based Adaptive Routing
TC	Topology Control
TCP	Transmission Control Protocol
TTI	Transmission Time Interval
UE	User Equipment
UCAN	A Unified Cellular and Ad-Hoc Network Architecture
UDP	User Datagram Protocol
UMTS	Universal Mobile Telecommunications System
UPN	Universal Personal Networking
USB	Universal Serial Bus
UWB	Ultra-Wide Band
VoIP	Voice over IP
WAN	Wide Area Network
WCETT	Weighted Cumulative ETT
WiMAX	Worldwide Interoperability for Microwave Access
WLAN	Wireless Local Area Network
WMN	wireless mesh network
WPAN	Wireless Personal Area Network
WSN	Wireless Strategic Network
ZRP	Zone Routing Protocol



# Bibliography

- [1] A. Alexiou, D. Antonellis, and C. Bouras, “Adaptive and reliable video transmission over UMTS for enhanced performance,” *International Journal of Communication Systems*, vol. 1, no. 1, pp. 65–81, 2007.
- [2] M. Assaad, B. Jouaber, and D. Zeghlache, “TCP Performance over UMTS-HSDPA System,” *Telecommunication Systems*, vol. 27, no. 2, pp. 371–391, 2004.
- [3] M. H. Alizai, O. Landsiedel, K. Wehrle, and A. Becher, “Challenges in short-term wireless link quality estimation,” in *Proc. GI/ITG KuVS Fachgespräch “Drahtlose Sensornetze”*, Berlin, Germany, Sept. 25–26, 2008.
- [4] D. Aguayo, J. Bicket, S. Biswas, G. Judd, and R. Morris, “Link-level measurements from an 802.11b mesh network,” *ACM SIGCOMM Computer Communication Review*, vol. 34, no. 4, pp. 121–123, Oct. 2004.
- [5] S. Agarwal, R. Katz, S. Krishnamurthy, and S. Dao, “Distributed power control in ad-hoc wireless networks,” in *Proc. IEEE PIMRC’01*, vol. 2, San Diego, California, October 2001.
- [6] G. Bianchi, F. Formisano, and D. Giustiniano, “802.11 b/g Link Level Measurements for an Outdoor Wireless Campus Network,” in *Proc. IEEE WoWMoM’06*. Washington, DC, USA, 2006, pp. 525–530.
- [7] G. Breed, “Bit error rate: Fundamental concepts and measurement issues,” *High Frequency Electronics*, vol. 2, no. 1, pp. 46–47, Jan. 2003.
- [8] J. Bicket, “Bit-rate selection in wireless networks,” Master’s thesis, Massachusetts Institute of Technology, Cambridge, MA, USA, 2005.
- [9] J. Bicket, D. Aguayo, S. Biswas, and R. Morris, “Architecture and evaluation of an unplanned 802.11b mesh network,” in *Proc. ACM MobiCom*, Cologne, Germany, Aug. 28 – Sep. 2, 2005.

- [10] *CC2240: 2.4GHz IEEE 802.15.4 / ZigBee-ready RF Transceiver*, Chipcon. [Online]. Available: <http://www.chipcon.com>
- [11] M. Chan and R. Ramjee, “TCP/IP performance over 3G wireless links with rate and delay variation,” *Wireless Networks*, vol. 11, no. 1, pp. 81–97, 2005.
- [12] M. Chatterjee, G. Mandyam, and S. Das, “MAC layer retransmissions in 1XTREME,” in *Proc. PIMRC’02*. Atlantic Pavilion, Lisbon, Portugal: Citeseer, September 15-18 2002, pp. 1452–1456.
- [13] J. Choi, Y. Ko, and J. Kim, “Enhanced power saving scheme for IEEE 802.11 DCF based wireless networks,” *Lecture notes in computer science*, pp. 835–840, 2003.
- [14] C.-C. Chen, H. Luo, E. Seo, N. H. Vaidya, and X. Wang, “Rate-adaptive framing for interfered wireless networks,” in *Proc. IEEE INFOCOM*, Anchorage, AK, USA, May 6–12, 2007.
- [15] T. Clausen and P. Jacquet, “Optimized link state routing protocol (OLSR),” RFC 3626, Oct. 2003.
- [16] T. Clausen, P. Jacquet, A. Laouiti, P. Muhlethaler, A. Qayyum, and L. Viennot, “Optimized link state routing protocol,” in *Proc. IEEE INMIC’01*, Lahore, Pakistan, Dec. 28–30, 2001.
- [17] L. Correia, D. Macedo, D. Silva, A. Santos, A. Loureiro, and J. Noqueira, “Transmission Power Control in MAC Protocols for Wireless Sensor Networks,” in *Proc. ACM MSWiM’05*, Montreal, Canada, October 2005.
- [18] S. Colin. (ed.), “Implementation of Enhanced WAF Versions,” IST 6-hop Project,” Deliverable D3.1.
- [19] D. S. J. De Couto, D. Aguayo, J. Bicket, and R. Morris, “A high-throughput path metric for multi-hop wireless routing,” in *Proc. ACM MobiCom’03*, San Diego, CA, USA, Sept. 14–19, 2003.
- [20] D. S. J. De Couto, D. Aguayo, J. Bicket, and R. Morris, “A high-throughput path metric for multi-hop wireless routing,” *Wireless Networks*, vol. 11, no. 4, pp. 419–434, July 2005.
- [21] O. De Mey, L. Schumacher, and X. Dubois, “Optimum Number of RLC Retransmissions for Best TCP Performance in UTRAN,” in *Proc. PIMRC’05*, Berlin, Germany, 2005.

- [22] R. Draves, J. Padhye, and B. Zill, “Routing in multi-radio, multi-hop wireless mesh networks,” in *Proc. ACM MobiCom*, Philadelphia, PA, USA, Sep. 26 – Oct. 1, 2004.
- [23] *Eurane*, <http://www.ti-wmc.nl/eurane/>.
- [24] Z. Fu, H. Luo, P. Zerfos, S. Lu, L. Zhang, and M. Gerla, “The Impact of Multihop Wireless Channel on TCP Performance,” *IEEE Trans. Mobile Comput.*, pp. 209–221, 2005.
- [25] R. Fonseca, O. Gnawali, K. Jamieson, and P. Levis, “Four-bit wireless link estimation,” in *Proc. ACM HotNets-VI*, Atlanta, GA, USA, Nov. 14–15, 2007.
- [26] M. Folke and S. Landström, “An NS module for simulation of HSDPA,” Lulea University of Technology, Tech. Rep., 2006.
- [27] M. Gudmundson, “Correlation model for shadow fading in mobile radio systems,” *Electronics Letters*, vol. 27, no. 23, pp. 2145–2146, 1991.
- [28] J. Gutierrez, M. Naeve, E. Callaway, M. Bourgeois, V. Mitter, and B. Heile, “IEEE 802.15.4: a developing standard for low-power low-cost wireless personal area networks,” vol. 15, no. 5, pp. 12–19, Sept. 2001.
- [29] A. Haider, R. Harris, and H. Sirisena, “Simulation-based performance analysis of HSDPA for UMTS networks,” *Australian Telecommunication Networks and Application Conference*, pp. 204–208, 2006.
- [30] I. Haratcherev, K. Langendoen, R. Lagendijk, and H. Sips, “SNR-based rate control in WaveLAN,” in *Proc. ASCI*, Ouddorp, the Netherlands, June 2–4, 2004.
- [31] J. Harris and M. Airy, “Analytical model for radio link protocol for IS-95 CDMA systems,” in *Proc. VTC 2000-Spring*, vol. 3, Tokyo, Japan, 2000.
- [32] R. Hekmat, “Fundamental properties of wireless mobile ad-hoc networks,” Ph.D. dissertation, Delft University of Technology, Delft, the Netherlands, 2005.
- [33] G. Holland, N. H. Vaidya, and P. Bahl, “A rate-adaptive MAC protocol for multi-hop wireless networks,” in *Proc. ACM MobiCom*, Rome, Italy, July 16–21, 2001.

- [34] H. Hsieh and R. Sivakumar, “On using peer-to-peer communication in cellular wireless data networks,” *IEEE Trans. Mobile Comput.*, pp. 57–72, 2004.
- [35] “HSDPA overall description (rel.5),” *3GPP TS 25.308*, vol. 5.2.0, 2002/03.
- [36] M. Jacobsson, “Personal networks: An architecture for self-organized personal wireless communications,” Ph.D. dissertation, Delft University of Technology, Delft, the Netherlands, 2008.
- [37] R. Jain, *The Art of Computer Systems Performance Analysis*. John Wiley and Sons, 1991.
- [38] A. Jardosh, K. Ramachandran, K. Almeroth, and E. Belding-Royer, “Understanding link-layer behavior in highly congested IEEE 802.11b wireless networks,” in *Proc. E-WIND (ACM SIGCOMM’05 Workshop)*, Philadelphia, PA, USA, Aug. 22, 2005.
- [39] M. Jeruchim, P. Balaban, and K. Shanmugan, *Simulation of communication systems*, second edition ed. Kluwer Academic/Plenum, 1992.
- [40] E. Jung and N. Vaidya, “A power control MAC protocol for ad hoc networks,” *Wireless Networks*, vol. 11, no. 1, pp. 55–66, 2005.
- [41] G. Judd, X. Wang, and P. Steenkiste, “Low-overhead channel-aware rate adaptation,” in *Proc. ACM MobiCom*, Montreal, QC, Canada, Sept. 9–14, 2007.
- [42] G. Karbaschi and a. B. W. A. Fladenmuller, “Link-quality measurement enhancement for routing in wireless mesh networks,” in *Proc. IEEE WoWMoM*, Newport Beach, CA, USA, June 23–26, 2008.
- [43] A. Keshavarzian, E. Uysal-Biyikoglu, D. Lal, and K. Chintalapudi, “From experience with indoor wireless networks: A link quality metric that captures channel memory,” *IEEE Commun. Lett.*, vol. 11, no. 9, pp. 729–731, Sept. 2007.
- [44] C. Ke, C. Lin, C. Shieh, and W. Hwang, “A novel realistic simulation tool for video transmission over wireless network,” in *Proc. IEEE SUTC’06*, Taichung, Taiwan, June 2006.
- [45] K. Kim and K. Shin, “On accurate measurement of link quality in multi-hop wireless mesh networks,” in *Proc. ACM MobiCom*, Los Angeles, CA, USA, Sept. 24–29, 2006.

- [46] J. Kim and J. Huh, "Link Adaptation Strategy on Transmission Rate and Power Control in IEEE 802.11 WLANs," in *Proc. IEEE VTC-2006 Fall*, 2006, pp. 1–5.
- [47] J. Kim, S. Kim, S. Choi, and D. Qiao, "CARA: Collision-Aware Rate Adaptation for IEEE 802.11 WLANs," in *Proc. IEEE INFOCOM'06*, Barcelona, Spain, 2006, pp. 23–29.
- [48] K.-H. Kim and K. G. Shin, "On accurate and asymmetry-aware measurement of link quality in wireless mesh networks," *IEEE/ACM Trans. Networking*, vol. 17, no. 4, pp. 1172–1185, Aug. 2009.
- [49] J. Klaue, B. Rathke, and A. Wolisz, "Evalvid - a framework for video transmission and quality evaluation," in *Proc. 13th International Conference on Modelling Techniques and Tools for Computer Performance Evaluation*, Urbana, Illinois, September 2003.
- [50] M. Kubisch, H. Karl, A. Wolisz, L. Zhong, and J. Rabaey, "Distributed algorithms for transmission power control in wireless sensor networks," in *Proc. IEEE WCNC'03*, vol. 1, New Orleans, Louisiana, March 2003.
- [51] C. E. Koksal and H. Balakrishnan, "Quality-aware routing metrics for time-varying wireless mesh networks," *IEEE J. Select. Areas Commun.*, vol. 24, no. 11, pp. 1984–1994, Nov. 2006.
- [52] K. Kowalik, M. Bykowski, B. Keegan, and M. Davis, "An evaluation of a conservative transmit power control mechanism on an indoor 802.11 wireless mesh testbed." 2008. [Online]. Available: <http://arrow.dit.ie/commcon/7>
- [53] M. Lacage, M. Manshaei, and T. Turletti, "IEEE802.11 rate adaptation: a practical approach," in *Proc. ACM/IEEE MSWiM*, Venice, Italy, Oct. 4–6, 2004.
- [54] D. Lal, A. Manjeshwar, F. Herrmann, E. Uysal-Biyikoglu, and A. Kesavarzian, "Measurement and characterization of link quality metrics in energy constrained wireless sensor networks," in *Proc. IEEE GLOBECOM*, San Francisco, CA, USA, Dec. 1–5, 2003.
- [55] F. Lefevre and G. Vivier, "Optimizing UMTS link layer parameters for a TCP connection," in *Proc. IEEE VTC'01*, vol. 4. IEEE; 1999, 2001, pp. 2318–2322.

- [56] J. Lei, L. Greenstein, and H. Liu, “Mapping link SNRs of real-world wireless networks onto an indoor testbed,” *IEEE Trans. Wireless Commun.*, vol. 8, no. 1, pp. 157–165, Jan. 2009.
- [57] S. Leffler. (2009) The MadWifi project. [Online]. Available: <http://madwifi-project.org>
- [58] X. Li, P. Kong, and K. Chua, “Analysis of TCP throughput in IEEE 802.11 based multi-hop ad hoc networks,” in *Computer Communications and Networks, 2005. ICCCN 2005. Proceedings. 14th International Conference on*, 2005, pp. 297–302.
- [59] Q. Li, J. Aslam, and D. Rus, “Online power-aware routing in wireless ad-hoc networks,” in *Proc. IEEE Mobicom’01*. New York, NY, USA: ACM, July 2001, pp. 97–107.
- [60] F. Y. Li, A. Hafslund, M. Hauge, P. Engelstad, O. Kure, and P. Spilling, “Dilemma of using high data rate in IEEE 802.11b based multihop ad hoc networks,” in *Proc. IASTED CIIT*, St. Thomas, US Virgin Islands, Nov. 22–24, 2004.
- [61] P. Liaskovitis, C. Schurgers, Energy consumption of multi-hop wireless networks under throughput constraints and range scaling, ACM SIGMOBILE Mobile Computing and Communications Review 13 (2009) 1–13.
- [62] H. Lin and S. Das, “Performance study of link layer and MAC layer protocols to support TCP in 3G CDMA systems,” *IEEE Transactions on Mobile Computing*, vol. 4, no. 5, pp. 489–501, 2005.
- [63] S. Lin, J. Zhang, G. Zhou, L. Gu, J. Stankovic, and T. He, “ATPC: Adaptive transmission power control for wireless sensor networks,” in *Proc. Sensys’06*, Boulder, Colorado, 2006, pp. 223–236.
- [64] H. Luo, R. Ramjee, P. Sinha, L. Li, and S. Lu, “UCAN: a unified cellular and ad-hoc network architecture,” in *Proc. ACM Mobicom’03*, 2003, pp. 353–367.
- [65] A. Lo, G. Heijenk, and I. Niemegeers, “Performance evaluation of MPEG-4 Video Streaming over UMTS Networks using an Integrated tool Environment,” in *Proc. SPECTS’05*, Philadelphia, PA, July 2005.
- [66] A. Mäder and D. Staehle, “A flow-level simulation framework for hsdpa-enabled umts networks,” in *Proceedings of the 10th ACM Symposium*

- on Modeling, analysis, and simulation of wireless and mobile systems.* ACM New York, NY, USA, 2007, pp. 269–278.
- [67] D. Moltchanov, Y. Koucheryavy, and J. Harju, “Simple, Accurate and Computationally Efficient Wireless Channel Modeling Algorithm,” in *Proc. WWIC’05*, Xanthi, Greece, May 11-13, 2005, pp. 234-245.
  - [68] D. Moltchanov, “State Description of Wireless Channels Using Change-Point Statistical Tests,” in *Proc. WWIC’06*, Bern, Switzerland, May 10-12, 2006, pp. 275-286.
  - [69] D. Moltchanov, Y. Koucheryavy, and J. Harju, “Performance response of wireless channels for quantitatively different loss and arrival statistics,” *Performance Evaluation*, vol. 67, Issue 1, 2009.
  - [70] J. Monks, V. Bharghavan, and W. Hwu, “A power controlled multiple access protocol for wireless packetnetworks,” in *Proc. IEEE INFOCOM’01*, vol. 1, Anchorage, Alaska, April 2001.
  - [71] C. Newport, D. Kotz, Y. Yuan, R. S. Gray, J. Liu, and C. Elliott, “Experimental evaluation of wireless simulation assumptions,” *SIMULATION*, vol. 83, no. 9, pp. 643–661, Sept. 2007.
  - [72] I. G. Niemegeers and S. H. M. Heemstra de Groot, “From personal area networks to personal networks: A user oriented approach,” *Wireless Personal Communications*, vol. 22, no. 2, pp. 175–186, Aug. 2004.
  - [73] I. G. Niemegeers and S. H. de Groot, “Research Issues in Ad-Hoc Distributed Personal Networking,” *Wireless Personal Communications*, vol. 26, pp. 149–167, 2003.
  - [74] *N2Nsoft*. [Online]. Available: <http://www.n2nsoft.com/index.php?page=network-simulation>
  - [75] P. Ng and S. Liew, “Throughput analysis of IEEE802. 11 multi-hop ad hoc networks,” *IEEE/ACM Transactions on Networking (TON)*, vol. 15, no. 2, p. 322, 2007.
  - [76] K. Psannis, “MPEG-based Video over High Speed Downlink Packet Access Wireless Networks,” *ICGST International Journal on Computer Networks and Internet Research*, vol. 5, no. 2, pp. 45–51, 2006.
  - [77] I. Richardson, *H. 264 and MPEG-4 video compression: video coding for next-generation multimedia*. John Wiley & Sons Inc, 2003.

- [78] G. Hackmann., O. Chipara., and C. Lu, “Robust Topology Control for Indoor Wireless Sensor Networks,” in *Proc. SenSys’08*, Raleigh, North Carolina, November 2008.
- [79] B. Sadeghi, V. Kanodia, A. Sabharwal, and E. Knightly, “Opportunistic media access for multirate ad hoc networks,” in *Proc. ACM Mobicom’02*, Atlanta, Georgia, USA, 2002.
- [80] M. Senel, K. Chintalapudi, D. Lal, A. Keshavarzian, and E. Coyle, “A Kalman filter based link quality estimation scheme for wireless sensor networks,” in *IEEE GLOBECOM*, Washington, DC, USA, Nov. 26–30, 2007.
- [81] K. Singh and D. Ros, “Normalized Rate Guarantee Scheduler for High Speed Downlink Packet Access,” in *IEEE Global Telecommunications Conference, 2007. GLOBECOM’07*, Washington, DC, USA, November 2007, pp. 576–580.
- [82] K. Singh, J. Orozco, D. Ros, and G. Rubino, “Streaming of H. 264 Video over HSDPA: Impact of MAC-Layer Schedulers on User-Perceived Quality,” *Collection des rapports de Recherche de NST Bretagne*, 2007.
- [83] V. Shrivastava, D. Agrawal, A. Mishra, S. Banerjee, and T. Nadeem, “Understanding the limitations of transmit power control for indoor wlans,” in *Proc. ACM SIGCOMM’07*. NY, USA: ACM New York, October 2007, pp. 351–364.
- [84] D. Son, B. Krishnamachari, and J. Heidemann, “Experimental study of the effects of transmission power control and blacklisting in wireless sensor networks,” in *Proc. IEEE SECON’04*, Santa Clara, California, October 2004, pp. 289–298.
- [85] M. Souryal, L. Klein-Berndt, L. Miller, and N. Moayeri, “Link assessment in an indoor 802.11 network,” in *Proc. IEEE WCNC*, Las Vegas, NV, USA, Apr. 3–6, 2006.
- [86] K. Sohaib, N. Cuong, and J. Nordberg, “HSDPA System Simulation.” School of Engineering Department of Applied Signal Processing Blekinge Institute of Technology, 2005.
- [87] K. Srinivasan, P. Dutta, A. Tavakoli, and P. Levis, “Understanding the causes of packet delivery success and failure in dense wireless sensor networks,” in *Proc. ACM SenSys*, Boulder, CO, USA, Oct. 31 – Nov. 3, 2006.

- [88] K. Srinivasan, P. Dutta, A. Tavakoli, and P. Levis, "Some implications of low power wireless to IP networking," in *Proc. ACM HotNets-V*, Irvine, CA, USA, Nov. 29–30, 2006.
- [89] W. Stevens, *TCP/IP illustrated (vol. 1): the protocols*. Addison-Wesley Longman Publishing Co., Inc. Boston, MA, USA, 1993.
- [90] A. Tonnesen, T. Lopatic, H. Gredler, B. Petrovitsch, A. Kaplan, S.-O. Tücke, and others, "OLSRD: An adhoc wireless mesh routing deamon," 2008. [Online]. Available: <http://www.olsr.org>
- [91] J. Tourrilhes. (2009) Wireless tools for Linux. [Online]. Available: [http://www.hpl.hp.com/personal/Jean\\_Tourrilhes/Linux/Tools.html](http://www.hpl.hp.com/personal/Jean_Tourrilhes/Linux/Tools.html)
- [92] H. Tsai, N. Wisitpongphan, and O. Tonguz, "Link-quality aware ad hoc on-demand distance vector routing protocol," in *Proc. IEEE ISWPC*, Phuket, Thailand, Jan. 16–18, 2006.
- [93] L. Verma, S. Kim, S. Choi, and S. Lee, "Reliable, low overhead link quality estimation for 802.11 wireless mesh networks," in *Proc. IEEE WiMesh (IEEE SECON'08 Workshop)*, San Francisco, CA, USA, June 16, 2008.
- [94] A. Vlavianos, L. Law, I. Broustis, S. Krishnamurthy, and M. Faloutsos, "Assessing link quality in IEEE 802.11 wireless networks: Which is the right metric?" in *Proc. IEEE PIMRC*, Cannes, France, Sept. 15–18, 2008.
- [95] Y. Wang, M. Martonosi, and L. Peh, "A supervised learning approach for routing optimizations in wireless sensor networks," in *Proc. REALMAN (ACM MobiHoc'06 Workshop)*, Florence, Italy, May 26, 2006.
- [96] R. Wattenhofer, L. Li, P. Bahl, and Y. Wang, "Distributed topology control for power efficient operation in multihop wireless ad hoc networks," in *Proc. IEEE INFOCOM 2001*, vol. 3, Anchorage, Alaska, 2001, pp. 1388–1397.
- [97] R. Weber, M. Guerra, S. Sawhney, L. Golovanevsky, and M. Kang, "Measurement and Analysis of Video Streaming Performance in Live UMTS Networks," in *Proc. WPMC 2006*. SAN DIEGO, CA, USA: Citeseer, September 2006, pp. 1–5.
- [98] H. Wei and R. Gitlin, "Two-hop-relay architecture for next-generation WWAN/WLAN integration," *Wireless Communications, IEEE*, vol. 11, no. 2, pp. 24–30, 2004.

- [99] Williamson.C, “Internet traffic measurement,” *IEEE Internet Comput.*, vol. 5, no. 6, pp. 70–74, 2001.
- [100] *WCDMA HSPA Simulations Possibilities to use WinProp for HSPA network planning*. [Online]. Available: <http://www.awe-communications.com/Network/3G/Applications/HSDPA.html>
- [101] C. Williamson, “Internet traffic measurement,” *IEEE Internet Comput.*, vol. 5, no. 6, pp. 70–74, Nov./Dec. 2001.
- [102] S. H. Y. Wong, H. Yang, S. Lu, and V. Bharghavan, “Robust rate adaptation for 802.11 wireless networks,” in *Proc. ACM MobiCom*, Los Angeles, CA, USA, Sept. 24–29, 2006.
- [103] D. Wu, D. Gupta, and P. Mohapatra, “Quail ridge reserve wireless mesh network: Experiences, challenges and findings,” in *Proc. IEEE/Create-Net TridentCom*, Orlando, FL, USA, May 21–23, 2007.
- [104] S. Xiao, V. Sivaraman, and A. Burdett, “Adapting radio transmit power in wireless body area sensor networks,” in *Proc. the ICST BodyNets’08*, Tempe, Arizona, March 2008.
- [105] S. Xiao, A. Dhamdhere, V. Sivaraman, A. Burdett, Transmission power control in body area sensor networks for healthcare monitoring, *IEEE Journal on Selected Areas in Communications* 27 (1) (2009) 37–48.
- [106] Y. Xu and W. Lee, “Exploring spatial correlation for link quality estimation in wireless sensor networks,” in *Proc. IEEE PerCom*, Pisa, Italy, Mar. 13–17, 2006.
- [107] H. Zhang, A. Arora, and P. Sinha, “Link estimation and routing in sensor network backbones: Beacon-based or data-driven?” *IEEE Trans. Mobile Comput.*, vol. 8, no. 5, pp. 653–667, May 2009.
- [108] J. Zhang, K. Tan, J. Zhao, H. Wu, and Y. Zhang, “A practical SNR-guided rate adaptation,” in *Proc. IEEE INFOCOM Mini-Conference*, Phoenix, AZ, USA, Apr. 15–17, 2008.
- [109] J. Zhou, M. Jacobsson, and I. G. Niemegeers, “Cross layer design for enhanced quality routing in personal wireless,” in *Proc. PerNets (IEEE/Create-Net MobiQuitous 2007 Workshop)*, Philadelphia, PA, USA, Aug. 10, 2007.

- [110] J. Zhou, M. Jacobsson, E. Onur, and I. G. Niemegeers, “A novel link quality assessment method for mobile multi-rate multi-hop wireless networks,” in *Proc. IEEE CCNC*, Las Vegas, NV, USA, Jan. 10–13, 2009.
- [111] J. Zhou, C. Guo, P. Pawełczak, and I. G. Niemegeers, “Adaptable link quality estimation for multi data rate communication networks,” in *Proc. IEEE VTC2009-Spring*, Barcelona, Spain, Apr. 26–29, 2009.
- [112] J. Zhou, A. Lo, Z. Liu, and I. Niemegeers, “TCP Performance Evaluation Over Multi-hop Cellular Network: HSDPA and IEEE 802.11,” in *Proc. ISWCS’08*, Reykjavik, Iceland, October 2008.
- [113] A. Lo, J. Zhou, and I. Niemegeers, “Simulation-Based Analysis of TCP Over Beyond 3G Cellular Multi-Hop Networks,” in *Proc. IEEE PIMRC’06*, Helsinki, Finland, September 2006.
- [114] A. Lo, J. Zhou, and I. Niemegeers., “Multi-hop Cellular Networks: Integrated IEEE 802.11 Ad hoc and Universal Mobile Telecommunications System (UMTS) Networks,” in *Proc. ERCIM eMobility Workshop 2008*, Tampere, Finland, May 2008, pp. 37–48.
- [115] M. Zuniga and B. Krishnamachari, “Analyzing the transitional region in low power wireless links,” in *Proc. IEEE SECON*, Santa Clara, CA, USA, Oct. 4–7, 2004.



# Publications by the Author

## Journal and Magazine Publications

- J.1 J. Zhou, M. Jacobsson and I. G.M.M. Niemegeers, “Link Quality-Based Transmission Power Adaptation for Reduction of Energy Consumption and Interference”, accepted in *Eurosip Wireless Communications and Networking*, Hindawi
- J.2 J. Zhou, V.S. Rao, P. Pawelczak, D. Wu and P. Mohapatra, “Practical Rate and Route Adaptation with Efficient Link Quality Estimation for IEEE 802.11b/g Multi-Hop Networks”, submitted to *Computer Communications*, Elsevier
- J.3 J. Zhou, M. Jacobsson, E. Onur and I. G.M.M. Niemegeers, “An Investigation of Link Quality Assessment for Mobile Multi-hop and Multi-rate Wireless Networks”, submitted to *Wireless Personal Communications*, Springer
- J.4 J. Zhou, R.V. Prasad, Y. Lu and I.G.M.M. Niemegeers, “Analysis of a Multi-hop Integrated UMTS and WLAN Network”, submitted to *Telecommunication Systems*, Springer
- J.5 J. Zhou, P. Pawelczak, V.S. Rao, S. Joshi and D. Cabric, “Link Quality in Wireless Sensor and Mesh Networks: Estimation and Applications”, submitted to *IEEE Communications Magazine*, IEEE

## Peer-Reviewed Conference Publications

- C.1 J. Zhou, A. Lo, J. Hao and I.G.M.M. Niemegeers, “A Novel Multi-hop Aware scheduling mechanism for Cellular multi-hop network”, in *Proc. WWIC 2010*, Lulea, Sweden, 1–3 June 2010.

- C.2 J. Zhou, A. Lo and I.G.M.M. Niemegeers, “MPEG-4 evaluation over Cellular multi-hop network”, in *Proc. Simutools 2010*, Malaga, Spain, March, 2010.
- C.3 J. Zhou, X. Zhang, M. Jacobsson, and I. G.M.M. Niemegeers, “Link Quality-based Transmission Power Adaptation for Energy Saving in IEEE 802.11”, in *Proc. IEEE PIMRC'09*, Tokyo, Japan, 13–19 Nov. 2009.
- C.4 J. Zhou, C. Guo, P. Pawelczak and I.G.M.M. Niemegeers, “Adaptable Link Quality Estimation for Multi Data Rate Communication Networks”, in *Proc. IEEE VTC2009-Spring*, Barcelona, Spain, 26-29 April, 2009.
- C.5 J. Zhou, E. Onur, M. Jacobsson and I. G.M.M. Niemegeers, “On the smoothing factor for rate adaptation in IEEE 802.11b/g mobile multi-hop networks”, *Proc. SIU 2009*, pp.237-240, 9-11 Antalya, Turkey, April 2009.
- C.6 J. Zhou, M. Jacobsson, E. Onur and I. G.M.M. Niemegeers, “Novel Link Quality Assessment Method for Mobile Multi-Rate Multi-Hop Wireless Networks”, in *Proc. IEEE CCNC 2009*, Las Vegas, NV, USA. 10-13 January, 2009. (**Best Student Paper Award, out of 450 submissions**)
- C.7 C. Guo, J. Zhou, P. Pawelczak and I.G.M.M. Niemegeers, “Improving Packet Delivery Probability Estimation for Indoor Ad Hoc and Wireless Sensor Networks”, in *Proc. IEEE CCNC 2009*, Las Vegas, NV, USA. 10-13 January, 2009.
- C.8 M. Ibrohimovna, S. Heemstra de Groot and J. Zhou “Secure and dynamic cooperation of personal networks in a Fednet”, in *Proc. IEEE CCNC 2009*, Las Vegas, NV, USA. 10-13 January, 2009.
- C.9 J. Zhou, Z. Liu, A. Lo and I.G.M.M. Niemegeers, “TCP Performance Evaluation Over Multi-hop Cellular Network: HSDPA and IEEE 802.11”, in *Proc. ISWCS 2008*, Reykjavik, Iceland, 21-24 Oct, 2008.
- C.10 J. Zhou, M. Jacobsson, E. Onur and I. G.M.M. Niemegeers, “Factors that Impact Link Quality Estimation in Personal Networks”, in *Proc. ISCN 2008*, Istanbul, Turkey , June 18-20, 2008.

- C.11** A. Lo, J. Zhou and I.G.M.M. Niemegeers, “Multi-hop Cellular Networks: Integrated IEEE 802.11 Ad hoc and Universal Mobile Telecommunications System (UMTS) Networks”, in *Proc. WWIC 2010*, Tampere, Finland, May 30, 2008.
- C.12** J. Zhou, M. Jacobsson and I.G.M.M. Niemegeers, “Cross Layer Design for Enhanced Quality Routing in Personal Wireless”, in *Proc. MobiQuitos 2007*, Philadelphia, USA, 10 August 2007.
- C.13** J. Zhou, M. Jacobsson and I.G.M.M. Niemegeers, “Cross Layer Design for Enhanced Quality Personal Wireless Networking”, in *Proc. Med-Hoc-Net 2007*, Corfu, Greece, June 13-15, 2007.
- C.14** A. Lo, J. Zhou and I.G.M.M. Niemegeers, “Beyond 3G cellular multi-hop networks”, in *Proc. Chinacom 2006*, Beijing, China, November, 2006
- C.15** A. Lo, J. Zhou, M. Jacobsson and I.G.M.M. Niemegeers, “NS-2 Models for simulating a novel beyond 3G cellular multi-hop network”, in *Proc. ValueTools 2006*, Pisa, Italy, October, 2006
- C.16** A. Lo, J. Zhou and I.G.M.M. Niemegeers, “Simulation-based analysis of TCP interaction over next-generation mobile networks”, in *Proc. MSWIM 2006*, Malaga, Spain, October, 2006
- C.17** A. Lo, J. Zhou and I.G.M.M. Niemegeers, “Simulation-based analysis of TCP over beyond 3G cellular multi-hop networks”, in *Proc. PIMRC 2006*, Helsinki, Finland, September, 2006

## Relations to This Dissertation

This dissertation is based on the previously published or submitted papers. Table D.1 provides a relation between papers and chapters of this dissertation.

Table D.1: Relation between chapters of the dissertation and the list of publications by the author; ●: major relation, ○: minor relation

Publication	Ch. 1	Ch. 2	Ch. 3	Ch. 4	Ch. 5	Ch. 6	Ch. 7	Ch. 8
J.1	○	○		●				
J.2	○	●	●	○	●	●		
J.3	○	●	●			●		
J.4	○						●	○
J.5	●	●	○	○	○	○		
C.1	○						●	○
C.2	○						○	●
C.3	○	○			●			
C.4	○	○		●				
C.5	○				●			
C.6	○	●	●		○	●		
C.7	○	●	●					
C.8	○							
C.9	○						●	○
C.10	○	○	●					
C.11	○						●	○
C.12	○	○	●			●		
C.13	○	●	○	○	○	○		
C.14	○						●	○
C.15	○						●	○
C.16	○						●	○
C.17	○						●	○

# **Curriculum Vitae**

Jinglong Zhou was born in Wuhan, Hubei Province in China on August 20, 1982. He received his B.Sc. degree in Electrical Information Engineering department from HuaZhong University of Science and Technology, Wuhan, China, in 2004. In April 2006, he received his M.Sc degree in Electrical Engineering, graduated with honors (Cum Laude), from Delft University of Technology, the Netherlands. After graduating, he started as a Ph.D student in the Wireless and Mobile Communications group (WMC) of Delft University of Technology and worked on the Dutch National project "Free-band Personal Network Pilot 2008 (PNP2008)". During his Ph.D study, he won the best student paper award in IEEE CCNC 2009 conference. From March 2010, he worked on the Hand Hygiene Management System (HHMS) project as a Post-doc researcher for six months and he is currently working in the Vodafone company in Netherlands.

